January 2015

Anticancer Effects of Vitamin E Forms and Their Long-chain Metabolites via Modulation of Sphingolipid Metabolism

Yumi Jang
Purdue University

Graduate School Form 30
Updated 1/15/2015

PURDUE UNIVERSITY
GRADUATE SCHOOL
Thesis/Dissertation Acceptance

This is to certify that the thesis/dissertation prepared

By Yumi Jang

Entitled

Anticancer Effects of Vitamin E Forms and Their Long-chain Metabolites via Modulation of Sphingolipid Metabolism

For the degree of Doctor of Philosophy

Is approved by the final examining committee:

Qing Jiang
Chair

Dorothy Teegarden

John R. Burgess

Yava Jones-Hall

To the best of my knowledge and as understood by the student in the Thesis/Dissertation Agreement, Publication Delay, and Certification Disclaimer (Graduate School Form 32), this thesis/dissertation adheres to the provisions of Purdue University's "Policy of Integrity in Research" and the use of copyright material.

Approved by Major Professor(s): Qing Jiang

Approved by: Connie M. Weaver 9/2/2015

Head of the Departmental Graduate Program Date

ANTICANCER EFFECTS OF VITAMIN E FORMS AND THEIR LONG-CHAIN METABOLITES VIA MODULATION OF SPHINGOLIPID METABOLISM

A Dissertation

Submitted to the Faculty

of

Purdue University

by

Yumi Jang

In Partial Fulfillment of the

Requirements for the Degree

of

Doctor of Philosophy

December 2015

Purdue University

West Lafayette, Indiana

ACKNOWLEDGEMENTS

I owe a debt of gratitude to many people who have made this dissertation possible.

My deepest gratitude goes first to my advisor, Dr. Qing Jiang for her invaluable guidance and continued support throughout my Ph.D. study. I have been amazingly fortunate to have her as my advisor. Without her help, I could not have imagined the possibility of this achievement. I appreciate her mentorship, immense knowledge, enthusiasm, motivation and encouragement. I have learned a lot from her about experimental techniques, scientific critical thinking skills, professional knowledge, and so forth, which benefit me both for my graduate research and for my future career development as a scientist. She has been a tremendous mentor for me. I would also like to express my appreciation to my committee members, Dr. Dorothy Teegarden, Dr. John Burgess and Dr. Yava Jones-Hall for their insightful advice and help on my research and their precious time.

I would like to thank the past and current Jiang lab members, Yun Wang, Ziying Jiang, Xiayu Rao, Agnetha Linn Rostgaard-Hansen, Na Young Park, Chao Yang, Tianlin Xu, Kilia Liu for their help, support, and companionship over the years. Many thanks go to my friends inside and outside of Purdue, who have supported me with constant friendship and encouragement. Special thanks to my coworker, Amber S. Jannasch in

Bindley Bioscience Center of Purdue for her expertise and technical support in doing liquid chromatography tandem mass spectrometry.

Last but not least, my great thanks go to my beloved family. Words cannot express how grateful I am to my parents and parents-in-law for their endless love. I would like to thank my son to be born soon, my lovely sunshine, who brought me happiness and energy when I felt sad and tired. I am especially grateful to my husband, my best friend, and my soulmate, Hyun Sung. Without his love and support, this journey would not have been possible. To him I dedicate this thesis.

TABLE OF CONTENTS

Page

Page

Page

Page

LIST OF TABLES

LIST OF FIGURES

Figure Page

ABSTRACT

Jang, Yumi. Ph.D., Purdue University, December 2015. Anticancer Effects of Vitamin E Forms and Their Long-chain Metabolites via Modulation of Sphingolipid Metabolism. Major Professor: Qing Jiang.

Cancer is one of the leading causes of death. Studies have shown that vitamin E forms including gamma-tocopherol (γT), delta-tocopherol (δT), and gamma-tocotrienol (γTE) exhibited potent anticancer activities in various types of cancer cells. But molecular mechanisms underlying anticancer actions of γTE are not completely understood. 13'-carboxychromanols (13'-COOHs), major fecal excreted long-chain metabolites of vitamin E, have recently been shown to induce apoptosis in liver cancer cells. However, it is not clear whether 13'-COOHs have anticancer effects on other types of cancer. In the current study, we investigated the anticancer effects and mechanisms of γTE and 13'-COOHs; δT-13'-COOH and δTE-13'-COOH, which are metabolites of δT or delta-tocotrienol (δTE), respectively. Like γTE, 13'-COOHs inhibited the growth and induced apoptosis and autophagy in human colon, breast, and pancreatic cancer cells in a time- and dose-dependent manner. In these activities, 13'-COOHs were similar or more potent than γTE, both of which were much stronger than γT and δT. Since we have previously shown that γTE and γT induce prostate cancer cell death by modulation of sphingolipid metabolism, we investigated whether γTE and 13'-COOHs have effects on

the levels of sphingolipids in cancer cells using liquid chromatography tandem mass spectrometry. Treatment of human colon cancer HCT-116 cells with γTE or δT-13'-COOH significantly increased in intracellular dihydroceramides (dhCers) and dihydrosphingosine (dhSph), sphingoid bases in *de novo* synthesis pathway of sphingolipids, but decreased in $C_{16:0}$-ceramide (Cer) during shorter treatment. During longer treatment, γTE or δT-13'-COOH increased in $C_{16:0}$- and $C_{18:0}$-Cers while decreased in SMs. To investigate potential effects on *de novo* synthesis of sphingolipids, we used $^{13}C_3$, ^{15}N-labeled L-serine, which condensed with palmitoyl-CoA to form the first sphingolipid intermediate in the *de novo* synthesis pathway. We found that compared with controls, γTE or δT-13'-COOH treatment increased labeled dhCers and dhSph, but led to decrease in labeled Cers. These results strongly suggest that γTE or δT-13'-COOH inhibit dihydroceramide desaturase (DEGS)-catalyzed reactions and may activate sphingomyelin hydrolysis to enhance Cer levels. Consistently, we found that γTE or δT-13'-COOH inhibited the DEGS activity, while they did not affect DEGS expression. The importance of sphingolipid modulation was further supported by blocking the increase of these sphingolipids, which resulted in a partial counteraction of γTE or 13'-COOHs-induced cell death. In agreement with these cell-based studies, δTE-13'-COOH showed anticancer activities in a preclinical model in mice. In addition, we found that various phytochemicals including curcumin, resveratrol, and epigallocatechin gallate, etc. also modulated sphingolipid metabolism in cancer cells. Overall, our studies demonstrate that γTE and 13'-COOHs have potent anticancer effects by modulating enzyme activities in sphingolipid metabolism.

CHAPTER 1. LITERATURE REVIEW

1.1 Vitamin E

1.1.1 Vitamin E Forms and Food Sources

Vitamin E is an important nutrient and is a well-known lipophilic chain-breaking antioxidant. In 1922, Evans and Bishop first discovered vitamin E as an essential dietary factor for reproduction in rats (Evans and Bishop, 1922). Since the discovery, many researchers have focused on the potential health benefits of vitamin E for various diseases. Natural forms of vitamin E consist of eight structurally related molecules that can be further divided into two major groups, which are tocopherols and tocotrienols. Tocopherols and tocotrienols are composed of the same basic chemical structure characterized by a 16-carbon phytyl chain which is attached at the 2-position of a chromane ring. However, the difference between tocopherols and tocotrienols is that tocopherols have a saturated phytyl chain whereas tocotrienols have an unsaturated phytyl chain with three double bonds. Individual tocopherols and tocotrienols, which are α-, β-, γ- and δ-tocopherol (αT, βT, γT and δT) and α-, β-, γ- and δ-tocotrienol (αTE, βTE, γTE and δTE), are differ from each other based on the number and position of

methyl groups in the chromane ring. The structures of tocopherols and tocotrienols are illustrated in Figure 1.1.

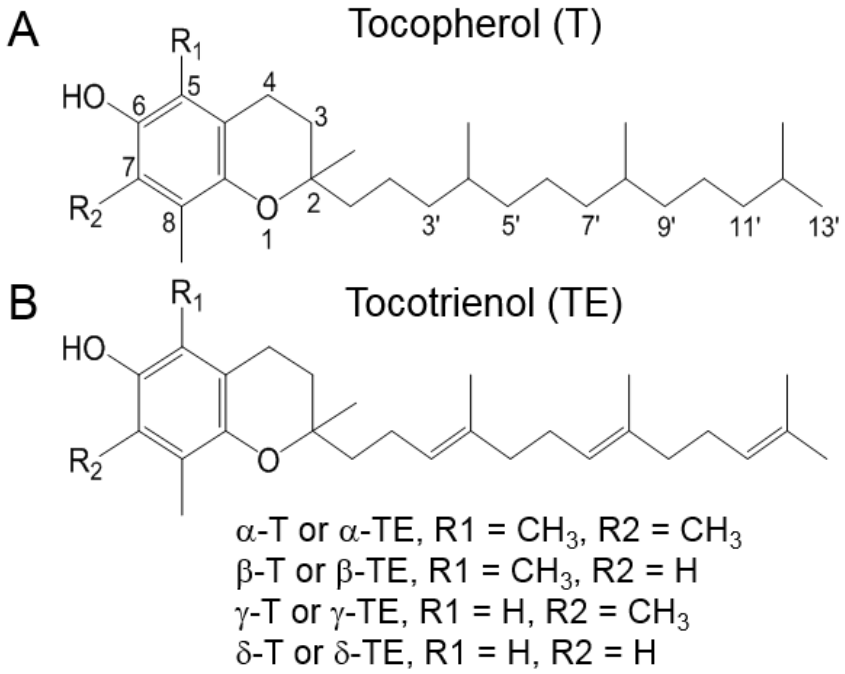

Figure 1.1 Structures of natural forms of vitamin E. (A) Tocopherols and (B) tocotrienols. All vitamin E forms contain a 16-carbon phytyl chain which is attached at the 2-position of a chromane ring. The difference between tocopherol and tocotrienol is that tocotrienol has an unsaturated phytyl chain with three double bonds.

Furthermore, vitamin E is found in both natural and synthetic forms. Natural forms of tocopherol have the RRR configuration at the 2, 4', and 8'-positions of the phytyl tail, and natural forms of tocotrienol have the R configuration at the 2-position of the phytyl tail. Both natural single stereoisomeric form of α-tocopherol (RRR, formerly *d*-α-tocopherol) and synthetic form of α-tocopherol are available commercially for the use as a dietary supplement. When α-tocopherol is synthesized chemically, this synthetic form consists of an approximately equimolar mixture of all eight possible stereoisomers (*all-racemic* α-tocopherol, formerly *dl*-α-tocopherol): RRR, RRS, RSS, RSR, SRR, SSR, SRS, and SSS (Brigelius-Flohe and Traber, 1999; Burton et al., 1998). Although they have similar structures, the different stereoisomers of vitamin E have different bioavailability and bioacitivity, which will be discussed in the next section. In addition, as the free forms of vitamin E are easy to be oxidized, more stable forms of vitamin E as a dietary supplement have been produced. Since ester forms are very stable, α-tocopherol is usually sold either as acetate esters (RRR α-tocopheryl acetate or *all-rac* α-tocopheryl acetate) or as succinate esters (RRR α-tocopheryl succinate or *all-rac* α-tocopheryl succinate). Among them, the acetate ester of *all-rac* α-tocopherol is the most common form of vitamin E supplementation due to the cost and the stability (Vagni et al., 2011).

Since humans and animals do not make vitamin E, they acquire natural forms of vitamin E from plants. Vitamin E is found in various types of foods such as some fruits, vegetable oils, green leafy vegetables, plant seeds, corn, barley, oats, and wheat germ. Natural sources of tocopherols include vegetable oils, plant seeds and nuts. For instance, peanuts, almonds, and sunflower seeds are major sources of αT, whereas γT is rich in walnuts, pecans, corn oil, soybean oil and sesame oil. δT is found in soybean oil and rice

germ. As the corn and soybean oils are widely used, γT accounts for about 70% of the vitamin E in the US diet. On the other hand, tocotrienols are mainly found in palm oil, barley, oats and some cereal grains, but in much smaller amounts than tocopherols (Jiang et al., 2001; McLaughlin and Weihrauch, 1979; Slover, 1971).

1.1.2 Bioavailability and Metabolites

Vitamin E is a lipophilic (fat-soluble) vitamin, and similar to other lipids, all vitamin E forms are absorbed equally into the intestine along with dietary fat, and incorporated into chylomicrons. The chylomicron-bound vitamin E is transported through lymphatic system to peripheral tissues such as skin, adipose, muscle or brain with the help of lipoprotein lipase. The chylomicron remnants are taken up by the liver for metabolism or further distribution. In the liver, αT is preferentially incorporated into very-low-density lipoproteins due to the high affinity of α-tocopherol transfer protein (α-TTP) together with ATP-binding cassette transporter A1 (ABCA1), and re-distributed throughout the body. Therefore, αT is the predominant form in most human and animal tissues and plasma as it is protected by α-TTP from being metabolized (Brigelius-Flohe and Traber, 1999; Jiang, 2014; Jiang et al., 2001; Manor and Morley, 2007; Traber, 2007).

In contrast, α-TTP has much lower affinity toward other forms of vitamin E. Thus, non-αT forms of vitamin E such as β-, γ-, δ-T and α-, β-, γ-, δ-TE are relatively low in tissues as they are preferentially catabolized in the liver via cytochrome P450 (CYP4F2)-mediated ω-hydroxylation to 13’-hydroxychromanol (13’-OH). 13’-OH is

then further oxidized to 13'-carboxychromanol (13'-COOH), followed by β-oxidation of the phytyl chain to generate various shorter chain length of carboxychromanols including 11'- and 9'-COOHs, and the terminal product 3'-COOH or (2'-carboxyethyl)-6-hydroxychromans (CEHCs), which is the water-soluble metabolite of vitamin E, and then primarily excreted out of the body by the urine (Fig. 1.2) (Jiang, 2014; Sontag and Parker, 2002; Swanson et al., 1999). In parallel with β-oxidation, conjugation such as sulfation and glucuronidation of the phenolic on the chromane ring in the intermediate metabolites takes place when the intake of vitamin E forms is high (Jiang et al., 2007). Therefore, despite γT is the major form of vitamin E in the US diet, αT is the predominant form of vitamin E in the body. The plasma concentrations of αT are about 20~30 μM, but γT is 5-10 times lower than αT in the plasma (Behrens and Madere, 1986; Jiang et al., 2001). Also, the bioavailability of γT is suppressed by increased intake of αT (Handelman et al., 1985), but γT supplementation increased the levels of both tocopherols (Clement and Bourre, 1997).

In addition to the different bioavailability of each natural vitamin E form, the different stereoisomers of vitamin E have different bioavailability as well as biopotencies. Both natural form of vitamin E and synthetic vitamin E are absorbed in the body. However, after absorption, RRR-αT, a natural form of vitamin E has a greater bioavailability and activities than the *all-rac* forms due to the higher affinity of RRR-αT toward the liver protein named α-TTP over the synthetic forms. Thus, synthetic forms of vitamin E are preferentially excreted. The bioavailability of natural vitamin E is about twice as high compared with synthetic forms, thus intake of twice more amount of

synthetic forms of vitamin E are required to match the bioavailability of the natural forms (Brigelius-Flohe and Traber, 1999; Burton et al., 1998; Vagni et al., 2011).

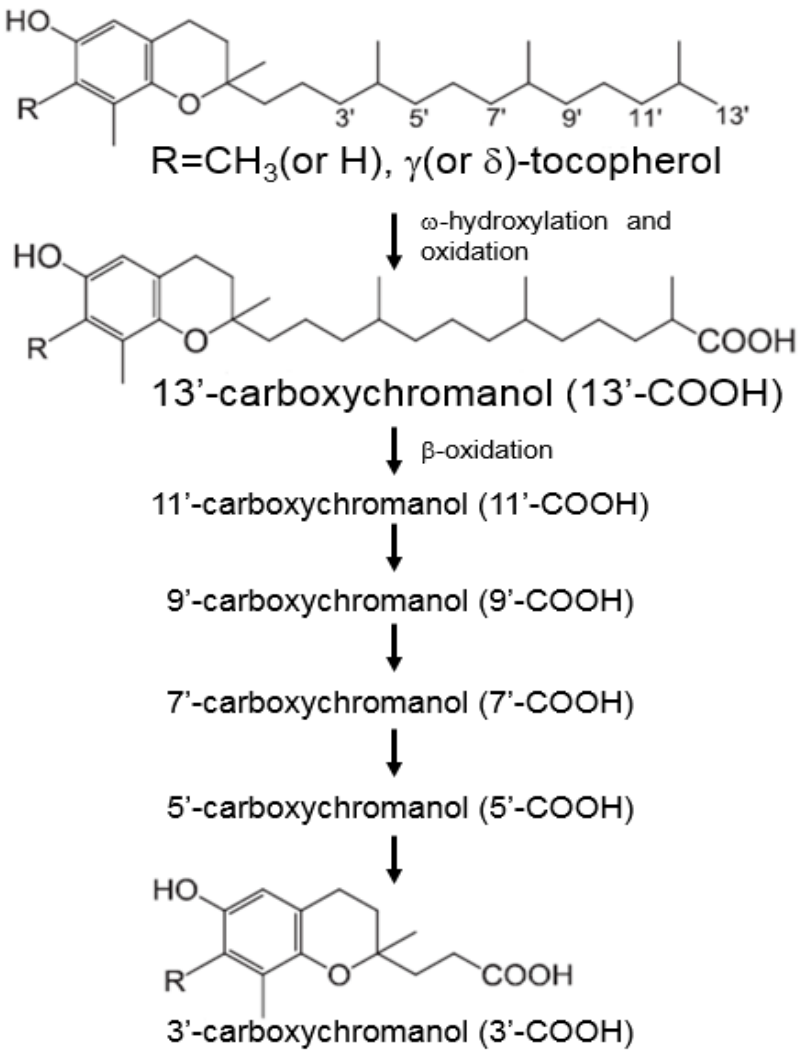

Figure 1.2 Metabolism of vitamin E forms and their metabolites. Vitamin E forms are metabolized via ω-hydroxylation and β-oxidation

1.1.3 Bioactivities of Vitamin E

The biological activity of vitamin E compounds has historically been assessed by the rat fetal resorption assay. In this assay, the biological activity of vitamin E is measured based on its ability to prevent or reverse the symptoms of vitamin E deficiency such as fetal resorption, encephalomalacia and muscular dystrophy, followed by embryo death. Among natural forms of vitamin E, αT has been shown to have the highest biological acitivity measured by this assay. Studies have also demonstrated that α-TTP is present in pregnant rodent uterus, and αT is important during pregnancy (Bieri and Evarts, 1974). However, this difference in activity between vitamin E forms appears to be caused by the lower concentrations of non-αT forms of vitamin E in tissues and plasma due to its shorter retention time, not because of their actual differences in biological activity.

Antioxidant function

Free radicals generated by oxidative stress exert an important role in the development of numerous diseases including cancer, atherosclerosis, and neurodegenerative diseases. All vitamin E forms have been well recognized as one of the most important antioxidants. It has been known to be a potent, lipophilic peroxyl radical scavenger that protects biological molecules from oxygen toxicity. In vitamin E studies, most researches have primarily focused on αT until recently, because αT is the predominant form of vitamin E in tissues and plasma, and due to its highest biological activities as well as the relationship between its low intake and the higher incidence of

vitamin E deficiency-associated ataxia. Moreover, among tocopherols, αT has been shown to have the highest antioxidant activities against peroxyl radical (LOO·) and delta-tocopherol is the least active (alpha > beta = gamma > delta). αT terminates the chain reaction of free radical mediated lipid peroxidation by donating hydrogens from the phenolic group on the chromane ring to lipid radicals. Therefore, αT protects lipid membrane from lipid radical damage (Kamal-Eldin and Appelqvist, 1996). After αT becomes a free radical itself, it can be recycled back to antioxidant form by vitamin C (ascorbic acid) (Traber and Stevens, 2011). In contrast, γT has its unique ability to change highly reactive nitrogen back into safe NO, thereby protection against oxidation damage by reactive nitrogen species. αT lacks this ability (Cooney et al., 1993; Jiang et al., 2001).

On the other hand, tocotrienols also show antioxidant effects by scavenging the chain-propagating peroxyl radical. It has been demonstrated that αTE has a more potent antioxidant activity than αT for the scavenging peroxyl radicals in liposomes as it is distributed more evenly in the phospholipid bilayer of the plasma membrane, and it shows more efficient collision with radicals (Packer et al., 2001; Wong and Radhakrishnan, 2012).

In addition to tocopherols and tocotrienols, 13'-carboxychromanols from δT and δTE, which are long-chain metabolites of vitamin E, have been shown to exert stronger antioxidative activities compared with *dl*-αT (Jiang, 2014; Terashima et al., 2002).

Non-antioxidant functions

Besides antioxidant activities of vitamin E, vitamin E isoforms have other biological functions independent of their antioxidant properties such as anti-inflammatory, anticancer, cardioprotective, and antidiabetic effects. Chronic inflammation has been recognized to contribute to the development of other chronic diseases including cardiovascular diseases and cancer (Balkwill and Mantovani, 2001; Libby et al., 2002). Eicosanoids derived from arachidonic acid via cyclooxygenases (COX) and 5-lipoxygenase (LOX)-catalyzed reaction play important roles in regulation of inflammation and cancer (Vane, 1976; Wang and Dubois, 2010). Mechanistic studies have shown that vitamin E forms such as γT, δT, and γTE exert anti-inflammatory activities by inhibiting COXs and 5-LOX activities and suppressing nuclear factor κB (NF-κB) and Janus kinase (JAK)-signal transducer and activator of transcription (STAT) 6 or JAK-STAT3 signaling pathways in various types of cells (Jiang, 2014; Jiang et al., 2000; Wang and Jiang, 2013; Wong and Radhakrishnan, 2012). In particular, recent studies in our group found novel mechanisms of anti-inflammatory effects of γTE in which γTE inhibited TNFα-stimulated NF-κB, TAK1 and JNK activation by modulation of sphingolipids, induction of ER stress followed by up-regulation of A20 (Wang et al., 2015). In addition, our group have also demonstrated that δT-13'-COOH, a long-chain carboxychromanol from δT, competitively inhibited COX-1 and -2 activities, and it was much stronger than short-chain carboxychromanols and unmetabolized vitamin E forms in these effects (Jiang et al., 2008). δT-13'-COOH also inhibited 5-LOX activity (Jiang et al., 2011), indicating that δT-13'-COOH is a unique dual inhibitor of COX-1/COX-2 and 5-LOX.

In addition to the anti-inflammatory activities of vitamin E forms, αT, γT, and δT have been demonstrated to prevent the development of atherosclerosis by inhibiting protein kinase C activity and proliferation of smooth muscle cell (Chatelain et al., 1993; Tasinato et al., 1995). Several studies have been shown that the plasma concentrations and the intake of γT are inversely associated with increased risk of cardiovascular disease (CVD), suggesting that γT is important in the defense against CVD (Ohrvall et al., 1996). Moreover, tocotrienols have been shown to have cardioprotective effects, which may be stem from their blood-pressure-lowering, cholesterol-lowering, and antiatherogenic effects of tocotrienols (Wong and Radhakrishnan, 2012). In the cholesterol-lowering activities of tocotrienols, tocotrienols affected on the mevalonate pathway by post-transcriptionally suppressing the 3-hydroxyl-3-methyl-glutaryl CoA reductase (Parker et al., 1993).

Vitamin E forms also showed antidiabetic effects. For example, γT, but not αT, partially protected insulin-secreting cells from the nitric oxide-induced functional inhibition (Sjoholm et al., 2000) and palm vitamin E (tocotrienol-rich diet; TRF) decreased advanced glycosylation end-points in non-diabetic rats and improved glycemic control in streptozotocin-induced diabetic rats (Wan Nazaimoon and Khalid, 2002).

Independent of its antioxidant activity, vitamin E forms also have shown to prevent cancer by inhibition of cell-cycle, suppression of DNA synthesis and by inducing apoptosis (Wong and Radhakrishnan, 2012). The anticancer activities of each vitamin E form will be more discussed in the following section.

1.2 Vitamin E Forms in Cancer Prevention

1.2.1 Cancer

Cancer, also known as a malignant tumor and a complex disease caused by abnormal and uncontrolled cell proliferation, is one of the leading causes of death worldwide. Over the past 60 years, death rates from heart diseases and stroke have dropped significantly, but the death from cancer has changed little since the 1950s. According to World Health Organization (WHO), cancer now accounts for more than 14 million new cases and 8.2 million deaths per year worldwide (World Cancer Report 2014). Cumulative cancer risk is estimated to be 30% and 22% in men and women, respectively, by age 75 in developed area worldwide (Jemal et al., 2011). Therefore, cancer is a growing health problem around the world. Among various cancer types, lung, colon, breast, and pancreatic cancers are the major leading causes of cancer-related death in the United States (Siegel et al., 2015). However, there is still no effective therapy for late-stage cancer as many cancer therapeutic agents have side effects or due to high rates of cancer recurrence. Since cancer is a result of a multistep process, which takes years or decades to develop, chemoprevention that prevents or delays the onset of late-stage cancer can be an attractive strategy for reducing cancer-related death.

In this regard, natural forms of vitamin E are potentially good chemoprevention agents as they are known to be safe and specific forms of vitamin E have been shown to have cancer prevention effects. Among them, αT, which is the predominant vitamin E form in tissues and the primary form in vitamin E supplements, and shows ataxia, muscle

degeneration, and infertility when it has deficiency, is the most extensively studied vitamin E form in relation to prevention of chronic diseases such as cardiovascular diseases and cancer. However, the human clinical studies as well as numerous animal studies of αT in cancer prevention resulted in inconsistent and disappointing outcomes (Moya-Camarena and Jiang, 2012). In this section, we review the several studies of vitamin E forms including αT and non-αT forms of vitamin E in cancer prevention so far. In addition, potential mechanisms of the actions by vitamin E metabolites are briefly discussed.

1.2.2 α-Tocopherol

Despite eight different forms of vitamin E, most studies have focused on αT for the last couple of decades due to its abundance in the body and antioxidant properties. Especially, all the human intervention studies for the vitamin E in cancer prevention have exclusively focused on αT. Since 1993, eight large randomized clinical trials (RCTs) to examine the effect of αT or combinations of αT with other nutrients on cancer incidence and cancer mortality have been reported; Linxian study (Blot et al., 1993), the α-Tocopherol, β-Carotene Cancer Prevention Study (ATBC) (Heinonen et al., 1998), Heart Protection Study (HPS) (Heart, 2002), *Supple' mentation en Vitamines et Miéraux Antioxydants* (SUVIMAX) (Hercberg et al., 2004), Women's Health Study (WHS) (Lee et al., 2005), The Heart Outcomes Prevention Evaluation and The HOPE-The Ongoing Outcomes (HOPE and HOPE-TOO) (Lonn et al., 2005), Selenium and vitamin E Cancer Prevention Tiral (SELECT) (Lippman et al., 2009), Physician's Health Study II (PHSII)

(Gaziano et al., 2009). However, results from eight large intervention studies that tested the anticancer effects of αT have been inconsistent and disappointing. Only three studies including the Linxian study, the ATBC study, and the SUVIMAX study have found that αT or its combination with other antioxidants reduced total cancer incidence and mortality or a risk of prostate cancer. Importantly, these three studies have something in common with their population characteristics that they were not general healthy populations. Specifically, the Linxian study in China had population with moderate micronutrients deficiency, and the ATBC study was conducted in male heavy smokers, and the subjects of the SUVIMAX study included men who have low plasma levels of antioxidant levels.

Beside these human clinical studies, several animal studies to test the beneficial effects of αT on cancer have also yielded inconsistent and disappointing outcomes. On the other hand, recent mechanistic studies and studies using preclinical animal models have demonstrated that other forms of vitamin E appear to have different and stronger biological properties compared with αT for the prevention and therapy against cancer.

1.2.3 Non-αT Forms of Vitamin E

Despite most studies in the cancer prevention focused exclusively on the αT form of vitamin E in the past, recent studies by others and us have shown that other forms of vitamin E appear to have unique and stronger anticancer activities.

γT, the major form of vitamin E in many plant seeds and in the US diet, and the second most common tocopherol in human serum, has unique and important properties

for cancer prevention and therapy that are not shared by αT. First of all, as we already mentioned in section 1.1.3, γT exerts anti-inflammatory activities, which are known to play important roles in cancer prevention. Specifically, our previous studies have shown that γT and γ-CEHC, but not αT, exert anti-inflammatory activities by inhibition of prostaglandin E_2 (PGE_2) synthesis, which occurred through COX-catalyzed reaction, in activated macrophages and epithelial cells and by inhibition of 5-LOX-catalyzed synthesis of leukotriene B_4 (LTB_4) in carrageenan-induced inflammation in rats (Jiang and Ames, 2003; Jiang et al., 2000). We also showed that γT, but not αT, inhibited proliferation and induced apoptosis in human prostate cancer cells, but not in normal prostate epithelial cells by interrupting sphingolipid metabolism, specifically by accumulating dihydrosphingosine and dihydroceramides (Jiang et al., 2004). Follow-up studies also reported that γT induced apoptosis in human breast cancer cells by the induction of increases in cellular ceramides and dihydroceramides levels and activating c-Jun N-terminal kinase (JNK)/CCAAT/enhancer-binding protein homologous protein (CHOP)/death receptor-5 (DR5) proapoptotic signaling (Gopalan et al., 2012; Yu et al., 2008b). Moreover, RRR-γT, but not RRR-αT induced apoptosis in multiple colon cancer cell lines, but not in normal colon cells (Campbell et al., 2006). In addition to a number of cancer cell studies, several animal studies were conducted to investigate whether these anticancer effects of γT are also translated into *in vivo* animal models. Yu *et al.* reported that γT supplementation, but not αT, significantly reduced breast tumor growth compared with control diet group in xenograft mouse models (Yu et al., 2009; Yu et al., 2008a). γT, but not αT, also suppressed tumor progression, along with activation of caspase-3 and -7 in the ventral lobe in a transgenic prostate cancer rat model (Takahashi et al., 2009). Our

group recently demonstrated that γT significantly attenuated moderate colitis and suppressed inflammation-promoted colon tumorigenesis (Jiang et al., 2013). Furthermore, several studies investigated the anticancer effects of γT *in vivo* using γT-rich mixed tocopherols (γ-TmT). γ-TmT supplementation as well as γT or δT produced a significant inhibition of azoxymethane (AOM)-induced aberrant crypt foci (ACF; a precancer lesion) in the colon of rats (Guan et al., 2012; Newmark et al., 2006). Another study was conducted to test the effects of γ-TmT against colon cancer, and in this study, γ-TmT suppressed AOM/DSS-induced tumorigenesis in CF-1 mice (Ju et al., 2009). Besides colon cancer, γ-TmT was also effective in suppression of breast tumorigenesis in preclinical rat models (Lee et al., 2009; Smolarek et al., 2012; Suh et al., 2007). Moreover, in a human study, Helzlsouer *et al.* conducted a nested case-control study to investigate the associations of αT, γT, and selenium with incidence of prostate cancer. They observed that higher plasma γT concentrations were associated with a statistically significant lower risk of developing prostate cancer. Interestingly, this protective association against prostate cancer was found with only γT, not with αT or selenium (Helzlsouer et al., 2000).

Besides tocopherols, recent studies suggested that tocotrienols, especially γTE and δTE, appear to have potent anticancer effects in various cancer cells. γTE, which is an abundant vitamin E form in palm oil, has been shown to have strong anti-inflammatory activities by inhibition of TNFα-stimulated NF-κB, TAK1 and JNK activation via sphingolipid modulation, ER stress induction, and A20 upregulation (Wang et al., 2015). γTE inhibited cell proliferation and induced apoptosis in human colon cancer cells, by the mechanisms of cell cycle arrest, an increase of Bax/Bcl-2 ratio, and

activation of caspase-3 (Xu et al., 2009). Our group also showed that γTE induced apoptosis and autophagy by interrupting sphingolipid modulation in prostate and breast cancer cells (Gopalan et al., 2012; Jiang et al., 2012). Several studies have shown that γTE and δTE significantly inhibited cell proliferation and induced apoptosis in both estrogen receptor-negative MDA-MB-435 and estrogen receptor-positive MCF-7 human breast cancer cells (Guthrie et al., 1997; Loganathan et al., 2013; Park et al., 2010; Yu et al., 1999b). Consistent with the results in cancer cell culture studies, γTE and δTE showed effective anticancer properties in several *in vivo* animal studies. For instance, several studies have shown that γTE supplementation significantly inhibited prostate tumor growth in xenograft models (Jiang et al., 2012; Kumar et al., 2006; Yap et al., 2010). γTE also showed these anticancer properties against pancreatic cancer, which generally shows resistance to chemotherapy, by inhibition of tumor growth and sensitization it to gemcitabine (Kunnumakkara et al., 2010). Interestingly, Hiura *et al.* reported that both γTE and δTE supplementation significantly delayed liver tumor growth, by particularly being accumulated in tumors, not in normal tissues (Hiura et al., 2009). In addition, δTE was observed to show potent tumor antiangiogenic potential compared with αT (Shibata et al., 2009).

1.2.4 13’-Carboxychromanol, a Long-chain Vitamin E Metabolite

13’-carboxychromanol (13’-COOH) is a long-chain metabolite of vitamin E (Fig. 1.2). Sontag and Parker first discovered cytochrome P450 ω-hydroxylase pathway of tocopherol catabolism and identified all key intermediates including long- and short-

chain carboxychromanols and final metabolite, 3'-carboxychromanol in human hepatocyte (Sontag and Parker, 2002). Consistently, our group identified these intermediates after treatment with γT and δT in human A549 cells, and first discovered that in parallel with β-oxidation, sulfation of intermediate metabolites takes place. Importantly, these sulfated or non-sulfated long-chain carboxychromanols were found in rat plasma and liver upon vitamin E supplementation (Jiang et al., 2007). We also observed the similar metabolism of γTE in human A549 cells and in rats (Freiser and Jiang, 2009). Bardowell *et al.* revealed the presence of all six carboxychromanol metabolites and 13'-OH in fecal samples from mice fed with 800 mg/kg body weight γT and δT for 12 weeks. They also found similar findings in fecal material from an adult male supplemented with 400 mg/kg/day γT for 14 days (Bardowell et al., 2012a).

Recently, our group began to investigate the biological activities of these vitamin E metabolites and demonstrated that long-chain carboxychromanols have stronger anti-inflammatory activities than their unmetabolized vitamin E forms. Particularly, δT-13'-COOH, a long-chain carboxychromanol from δT, has been shown to exert anti-inflammatory effects by showing much more potent inhibiting actions on COX-1/COX-2 and 5-LOX activities than short-chain carboxychromanols and unmetabolized vitamin E precursors (Jiang et al., 2008; Jiang et al., 2011). Moreover, Birringer *et al.* investigated the biological activities of long-chain carboxychromanols synthesized from garcinoid acid, a δTE derivative extracted from the African bitter nut *Garcinia kola*, in human HepG2 hepatocellular liver carcinoma cells. 13'-COOHs from αT and δT have shown to induce mitochondria-mediated apoptosis with increased mitochondrial ROS formation and reduced mitochondrial membrane potential (Birringer et al., 2010). Although, the

results of these studies show that vitamin E metabolites, especially 13'-COOHs exert potential anticancer properties, thus may contribute to beneficial effects of vitamin E forms *in vivo*, the effects and the underlying mechanisms by which 13'-COOHs exert these beneficial effects are not completely understood yet, thus warranting further investigation.

1.3 Phytochemicals in Cancer Prevention

1.3.1 Overview of Phytochemicals

Cancer is the second leading cause of death worldwide, and now many researchers have been focusing on the prevention as well as the treatment to overcome cancer. The World Health Organization (WHO) indicates that at least one-third of all cancer deaths are preventable and that the diet is closely associated with this cancer prevention (Bode and Dong, 2009). Epidemiological studies have consistently shown that populations consuming high levels of fruits and vegetables have low incidence rates of various cancers (Block et al., 1992; Steinmetz and Potter, 1996). Therefore, numerous cell culture and animal model studies have been conducted to find biologically active compounds from edible plants and evaluate their protective effects against various diseases including cancer. This group of plant bioactive compounds now called as phytochemicals. Phytochemicals are non-nutritive plant chemicals expressed as secondary metabolites ('phyto' means 'plant' in the Greek word), which have protective or disease-preventing properties in humans and animals. The National Cancer Institute

(NCI) has identified that to date, greater than 1,000 different phytochemicals from plant sources have cancer preventive activities. Since phytochemicals are natural products, they have been used for the prevention and treatment of cancer for a long time due to their safety and general availability, and became important research targets for cancer research (Surh, 2003). Phytochemicals are generally classified as phenolics, carotenoids, alkaloids, nitrogen-containing compounds, and organosulfur compounds (Liu, 2004). They are typically divided into two distinct classes depending on their chemical structure, solubility, and physiological absorption properties; water-soluble dietary phytochemicals: phenolics and polyphenols, lipid-soluble dietary phytochemicals: carotenoids, tocochromanols (vitamin E derivatives), and curcuminoids. Among them, the most studied phytochemicals are the phenolics and carotenoids. This review will briefly introduce a general classification of phytochemicals and their key phytochemicals from each group with their dietary sources and health beneficial properties. Figure 1.3 illustrates the chemical structures of representative dietary phytochemicals that have been known to possess chemopreventive potential.

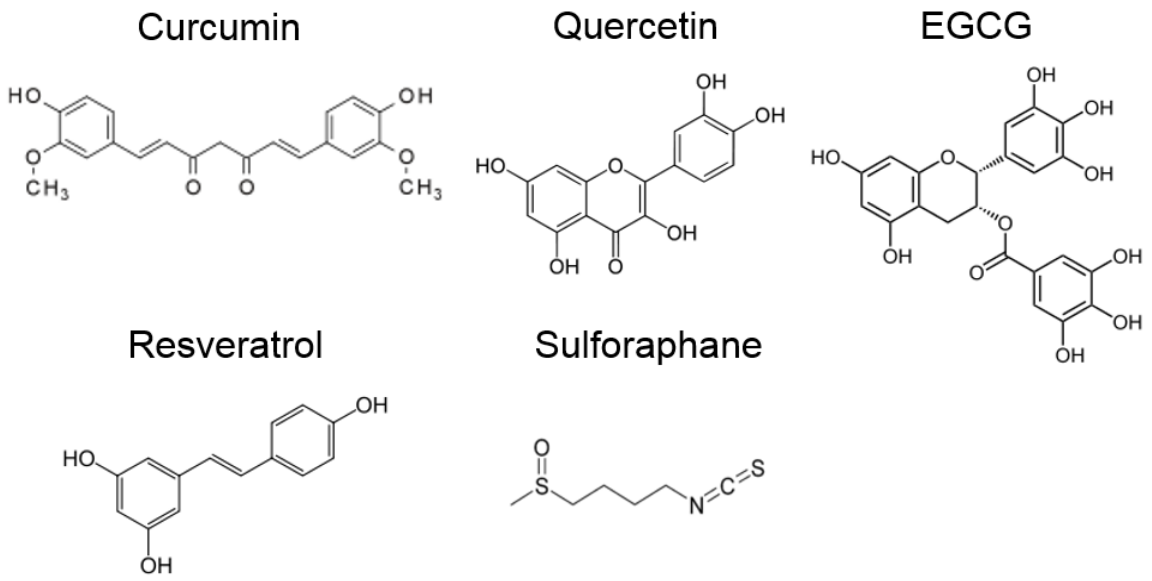

Figure 1.3 Chemical structures of representative dietary phytochemicals. Structures of curcumin, quercetin, epigallocatechin gallate (EGCG), resveratrol, and sulforaphane.

Phenolics

Phenolics (also known as polyphenols) are compounds that contain one or more hydroxyl groups attached to one or more aromatic rings in their chemical structure. They are generally categorized as flavonoids, phenolic acids, stilbenes, curcuminoids, coumarins, and tannins, and numerous epidemiological studies have been demonstrated that phenolics showed beneficial properties against cancer, CVD, neurodegenerative diseases, diabetes, and osteoporosis (Gonzalez-Vallinas et al., 2013).

Flavonoids represent the 60% of dietary phenolics with more than 4,000 varieties. Their chemical structure consists of two benzene rings linked by three carbons that are usually in an oxygenated heterocycle ring. Based on the differences in the heterocycle ring, they are classified into six groups: flavonols (quercetin and kaempferol), flavanols (catechin, epicatechin, epigallocatechin, and epigallocatechin gallate), flavones (luteolin

and apigenin), flavanones (naringenin), anthocyanidins, and isoflavonoids (genistain) (Liu, 2004).

Quercetin. Quercetin is the most abundant flavonoids in fruits and vegetables. It is a flavonol and the major sources are onion, apple, and broccoli. Quercetin has shown a free radical-scavenging activity and health benefits against many diseases including CVD, cancer, and neurodegenerative diseases. Quercetin exerts its anticancer effects by its antioxidant and antiproliferative activities and by regulating various cell-signaling pathways, cell cycle, and apoptosis (Murakami et al., 2008; Okamoto, 2005).

(-)-Epigallocatechin-3-gallate (EGCG). EGCG is the major catechin and an antioxidant polyphenol flavonoid found mostly in green tea. It has been shown to exert health beneficial properties for cancer, atherosclerosis, and neurodegenerative diseases (Khan et al., 2006).

Stilbenes are a family of plant secondary metabolites produced in a small number of plant species including grapevine in response to environmental stresses which are biotic and abiotic stresses. The bioactive stilbenes such as resveratrol and pterostilbene possess several health benefits such as antioxidant, cardioprotective, and cancer preventive properties (Rimando and Suh, 2008).

Resveratrol. Among stilbenes, in particular, resveratrol, which is mainly present in grapes and red wine, has received much attention because of its anticancer, antioxidant, cardioprotective, and lifespan extending properties (Agarwal and Baur, 2011; Bishayee, 2009).

Curcuminoids are components of the cherished Indian spice known as rhizome of turmeric, and produce a pronounced yellow color and flavor, which allow it to be used as

spice blends, such as curry. Curcumin is the primary curcuminoid and several studies in recent years have shown that it has several biological activities, including antioxidant, anti-inflammatory, anti-microbial, anti-mutagen and anticancer properties (Shehzad et al., 2010).

Carotenoids

Carotenoids are naturally occurring fat-soluble pigments, and about 600 different carotenoids have been identified and they are particularly plentiful in the red, orange, and yellow colored fruits and vegetables, and dark leafy green vegetables. There are two categories of carotenoids, which are provitamin A carotenoids that the body can turn into vitamin A such as β-carotene and β-cryptoxanthin, and non-provitamin A carotenoids such as lutein, lycopene, and zeaxanthin. Carotenoids are powerful antioxidant and have been implicated in many beneficial effects on human health with anticancer, cardioprotective, and immune system enhancing properties (Britton, 1995; Maiani et al., 2009; Tan et al., 2010)

Organosulfur compounds

Organosulfur compounds are naturally occrurring organic compounds that contain sulfur in their structure. Dietary organosulfur compounds are commonly found in garlic and cruciferous vegetables such as broccoli, cabbage, and cauliflower. These compounds have been demonstrated that they possess a number of biological activities such as antioxidant, antimicrobial, and anticancer effects. Moreover, several epidemiological

studies have suggested that comsumption of organosulfur compounds can decrease the incidence of different types of cancer (Moriarty et al., 2007).

Sulforaphane. Sulforaphane is a compound in the isothiocyanate group of organosulfur compounds. It is obtained from cruciferous vegetables such as broccoli and cabbage. For example, when fresh broccoli is chopped or chewed, it releases enzyme myrosinase, and myrosinase-catalyzed hydrolysis of glucosinolate glucoraphanin occurs to produce sulforaphane. It has shown antioxidant and anticancer activities against various types of cancer (Clarke et al., 2008).

1.3.2 Molecular and Cellular Targets of Phytochemicals for Cancer Prevention

Carcinogenesis is a multistep process and it consists of three closely linked stages that are tumor initiation, promotion and progression. Moreover, as cancer is a multifactor disease, it may require treatment with compounds that can alter this multiple process and target multiple intracellular components with greater effectiveness and less toxicity. In this regard, a large variety of phytochemicals are potential chemopreventive reagents due to its safety and numerous recent studies have demonstrated that several phytochemicals have anticancer properties by targeting various cellular signaling molecules. These chemopreventive phytochemicals can block, reverse or retard the development and progression of the cells in premalignant stage into malignant ones. The cellular mechanisms that phytochemicals elicit anticancer effects are multi-faceted, thus various cellular molecules and signalings could be potential targets of chemopreventive phytochemicals including regulation of cell signaling cascades by affecting several

kinases and transcription factors that decide the expression of genes involved in cell survival or death (Surh, 2003). During the past decades, there has been remarkable advances in identifying the molecular and cellular targets that mediate chemopreventive effects of specific phytochemicals, but despite this progress, the identification of clear mechanisms and targets of these phytochemicals are still incomplete. This section will review several identified key cellular signaling pathways and molecular targets by which representative phytochemicals exert their chemopreventive effects. Representative cellular signaling molecules and pathways targeted by various phytochemicals include the NRF/KEAP1 complex, NF-κB and AP1 with MAPK pathways, oncogenic AKT/protein kinase B (PKB) signaling pathway, β-catenin, and proteins involved in apoptosis induction.

1.3.2.1 NRF-KEAP1 Complex and Activation of NRF

One of the important ways to prevent cancer development is to block the initiation stage of carcinogenesis. The exposure to toxic environmental insults which cause DNA damage can be blocked and detoxified by phase II enzymes such as glutathione S-transferase (GST), NAD(P)H:quinone oxidoreductase (NQO) and heme oxygenase-1 (HO-1), resulting in the removal of toxicants from the cells before they are able to damage the DNA (Hayes and McMahon, 2001). The nuclear factor-erythroid 2p45 (NF-E2)-related factor 2 (NRF2) is a transcription factor that regulates expression of phase II enzymes. A cytosolic actin-binding protein called Kelch-like ECH-associated protein 1

(KEAP1) is a negative regulator of NRF2 which inhibits its translocation to the nucleus (Itoh et al., 1999). These two proteins interact with each other, but phase II enzyme inducers or prooxidants break the link, resulting in the releasement of NRF2 from KEAP1. In addition, phosphorylation of NRF2 by several kinases such as phosphatidylinositol 3-kinase (PI3K), protein kinase C (PKC), c-Jun NH2-terminal kinase (JNK) and extracellular-signal-regulated kinase (ERK) are known to facilitate the dissociation of NRF2 and KEAP1 (Huang et al., 2002). The released and translocated NRF2 in nucleus binds to the antioxidant-responsive element (ARE) to express genes that encode phase II detoxification or antioxidant enzymes.

Several phytochemicals have been demonstrated to activate NRF. For instance, Chen *et al.* found that EGCG, a major green tea polyphenol, showed potent activation of ARE, MAPKs including ERK, JNK and p38, and caspase-3-mediated cell death (Chen et al., 2000). Sulforaphane from cruciferous vegetables also activated MAPKs and upregulated ARE-dependent phase II detoxifying enzymes (Yu et al., 1999a).

1.3.2.2 Suppressing NF-κB and AP1 Activation

Several chemopreventive agents elicit anticancer effects by modulating cell-signaling pathways that regulate cell proliferation and differentiation. One of the components that play important roles in these pathways is the mitogen-activated protein kinases (MAPKs). Abnormal regulation of this MAPK pathway and its downstream transcription factor can cause uncontrolled cell proliferation and growth, leading to

conversion to malignancy (Zhang and Liu, 2002). These MAPKs and other kinases such as PKC and PI3K activate several transcription factors, including nuclear factor κB (NF-κB) and activator protein 1 (AP1) (Li and Verma, 2002). NF-κB and AP1 are ubiquitous eukaryotic transcription factors that regulate various target gene expression and mediate pleiotropic effects, thus they are targets of several chemopreventive phytochemicals. Overexpression or aberrant activation of NF-κB has been associated with over-proliferation and malignant transformation. Inactive NF-κB resides in the cytoplasm as a complex with the regulatory protein IκB. The activation of NF-κB pathway starts from the phosphorylation of IκB by IκB kinase (IKK), leading to IκB phosphorylation, ubiquitination and degradation by the 26S proteasome. The released NF-κB from IκB is then translocated to the nucleus, and it binds to specific promoter regions of genes, which are involved in the regulation of cell proliferation, differentiation, apoptosis and inflammation (Li and Verma, 2002). Recent studies have shown that activation of NF-κB is also regulated by AKT signaling pathway. PI3K activates AKT via phosphorylation, and this leads to NF-κB activation by stimulating IKK activity (Das et al., 2003; Li and Sarkar, 2002). AP1 is another transcription factor that is also regulated by the MAPK signaling cascade and regulates gene expressions that are involved in cell proliferation and differentiation, leading to tumor promotion and malignant transformation (Li and Verma, 2002).

A number of chemopreventive phytochemicals have been shown to suppress NF-κB and AP1 activation, leading to prevent abnormal cell proliferation and growth. Curcumin inhibits TNF-α-induced COX-2 gene transcription and NF-κB activation (Plummer et al., 1999). Genistein inhibits AKT activation and NF-κB activation (Gong et

al., 2003; Li and Sarkar, 2002). EGCG inhibits the activities of PI3K and AKT (Pianetti et al., 2002). In addition, IKK has shown to be inhibited by several chemopreventive phytochemicals, including curcumin (Bharti et al., 2003; Plummer et al., 1999), resveratrol (Holmes-McNary and Baldwin, 2000) and EGCG (Yang et al., 2001).

1.3.2.3 Downregulation of β-Catenin-mediated Signaling Pathway

β-Catenin is one of the important targets of numerous chemopreventive phytochemicals. It functions as a transcription factor and involves in the regulation of cell proliferation and tumorigenesis. Growth factors and WNT proteins stimulate β-catenin-mediated signaling pathway. The interaction of a WNT protein with its transmembrane receptor inactivates glycogen synthase kinase-3β (GSK-3β) by phosphorylation. The interaction of a growth factor with receptor kinase (RTK) activates PI3K, leading to AKT phosphorylation. Phosphorylated AKT also inactivates GSK-3β by phosphorylation. GSK-3β forms a multiprotein complex with adenomatous polyposis coli (APC), axin and conductin, and this complex regulates the fate of β-catenein. In the presence of a growth factor or WNT signal, the phosphorylated and inactivated GSK-3β stabilizes β-catenin in the cytoplasm. The β-catenin translocates to the nucleus and acts as a transcription factor, resulting in the activation of gene transcription involved in the cellular proliferation and growth. On the other hand, in the absence of stimuli, GSK-3β phosphorylates cytosolic β-catenin, which is in turn targeted for ubiquitylation followed by proteasomal degradation (MacDonald et al., 2009).

Some chemopreventive phytochemicals have been shown to target and downregulate the β-catenin-mediated signaling pathway and exert subsequent anticancer activities. For instance, curcumin reduced the cellular levels of β-catenin through caspase-mediated degradation of the protein (Mahmoud et al., 2000). Resveratrol has also shown to attenuate the expression of β-catenin in human colon cancer cells (Joe et al., 2002). Inhibition of β-catenin activity and reduction of its protein expression has been shown by EGCG treatment (Dashwood et al., 2002).

1.3.2.4 Induction of Apoptosis

Despite the regulation of abnormal cell proliferation and growth may retard or block tumor development, the induction of programmed cell death via apoptosis can completely remove abnormal cells from a tissue. In contrast to necrosis, apoptosis is a tightly regulated mechanism of cell death that can be induced by a variety of signals and stimuli.

Several dietary phytochemicals have been shown to induce apoptosis in cancer cells. Sulforaphane, a molecule in the isothiocyanate group of organosulfur compounds, induces apoptosis and inhibition of proliferation of human bladder cancer cells (Tang et al., 2006). EGCG treatment also inhibits cell growth and induces apoptosis in human epidermoid carcinoma cells, but not in normal human epidermal keratinocytes (Ahmad et al., 1997). Curcumin was also reported to induce apoptosis by up-regulating pro-

apoptotic proteins such as Bim, Bax, and Bak, and down-regulating the anti-apoptotic proteins such as Bcl-2 and Bcl-xL (Shankar and Srivastava, 2007).

1.4 Sphingolipids Metabolism and Their Biological Activities

1.4.1 Overview of Sphingolipids

Over the past twenty years, several groups of lipids and their metabolites have started to receive more attention, as they serve as biologically active molecules exerting a wide range of biological functions and providing health benefits through modification of tissue composition or induction of several cell-signaling pathways. Among a broad variety of bioactive lipids, evidences suggested that the polyunsaturated fatty acids (PUFAs) and eicosanoids are the most important bioactive lipids. Another well-known group of bioactive lipids is the sphingolipids. Sphingolipids were first identified in brain extracts at the end of the 19th century and were named after the Greek mythological creature, the Sphinx, on the basis of the nature of their enigmatic molecular structure (Thudichum, 1884).

Sphingolipids are a class of natural lipids that primarily have sphingosine as their structural backbone, amide-linked long-chain fatty acids, and one of various polar head groups. Thus, they are the most structurally diverse class of membrane lipids depending on their head groups. Among them, since sphingomyelin (SM) is an essential component in the outer leaflet of the plasma membrane and provides a barrier to the extracellular environment, sphingolipids were thought to act only as structural roles. However, current

evidence also suggests that they are pleiotropic molecules playing important roles in the regulation of numerous functions including cell survival, apoptosis, senescence, and differentiation. Indeed, sphingolipid metabolism has proved to be a dynamic process, and several sphingolipid metabolites are now recognized as second messengers playing essential roles in various cell functions (Hannun et al., 1986; Hannun and Obeid, 2008; Spiegel and Merrill, 1996).

The levels of endogenous sphingolipid metabolites are controlled by *de novo* synthesis and dynamic metabolisms involving synthesis of complex sphingolipids and catabolic pathways of complex sphingolipids or ceramides (Fig. 1.4) (Gault et al., 2010; Hannun and Obeid, 2008). Therefore, this review section will focus on the dynamic sphingolipid metabolism and enzymes involved in this pathway.

1.4.1.1 *De novo* Sphingolipids Biosynthesis

The *de novo* sphingolipid biosynthesis starts in the endoplasmic reticulum from condensation of palmitoyl-CoA and serine into 3-keto-dihydrosphingosine by serine palmitoyltransferase (SPT). The intermediate 3-ketosphinganine is rapidly reduced to dihydrosphingosine (dhSph) by a NADPH dependent 3-ketosphinganine reductase. An acylation by a family of (dihydro)ceramide synthases (CerSs) using fatty acyl-CoAs generates dihydroceramide (dhCer) subspecies. Dihydroceramide desaturase (DEGS) introduces a 4,5-*trans* double bond in dhCers to make the final product, Ceramide (Cer) (Merrill, 2002).

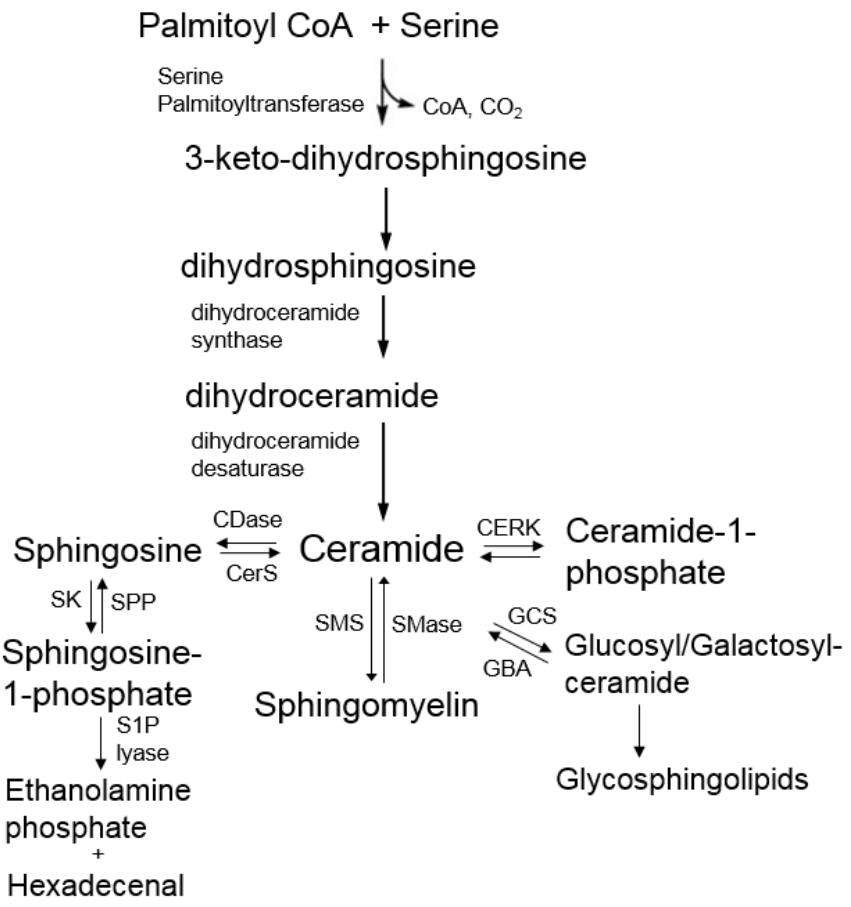

Figure 1.4 Sphingolipid metabolism. *De novo* biosynthesis pathway of sphingolipids, the production of complex sphingolipids from ceramide, the degradation of ceramide to sphingosine, the formation of sphingosine-1-phosphate (S1P), and the clearance of S1P by S1P lyase. SMS, sphingomyelin synthase; SMase, sphingomyelinase; CERK, ceramide kinase; GCS, glucosylceramide synthase; GBA, acid glucocerebrosidase; SK, sphingosine kinase; SPP, S1P phosphatase

Serine Palmitoyltransferase (SPT)

The first step in the sphingolipid biosynthesis is the condensation of cytosolic serine and palmitoyl-CoA, a reaction catalyzed by SPT to produce 3-keto-dihydrosphingosine. SPT is encoded by the genes *SPTLC1, SPTLC2,* and *SPTLC3*.

However, *SPTLC3* has been identified in yeast, but not in mammals (Gable et al., 2000). SPT is a member of a pyridoxal 5′-phosphate-dependent α-oxoamine synthases family. Mammalian SPT has LCB1 and LCB2 subunits, and each SPT subunit contains several transmembrane domains and displays type I topology. Although little is known about SPT regulation, many factors have been reported to regulate SPT activity and its activity is regulated transcriptionally and post-transcriptionally. The most widely known factor that affects SPT activity is the availability of serine and palmitoyl-CoA pool. SPT is inhibited by several synthetic and natural products. The selective inhibitors of this enzyme are L-cycloserine and beta-chloroalanine. More potent and selective natural inhibitors of SPT have been isolated from microorganisms which include sphingofungins, lipoxamycin and ISP-1/myriocin. The myriocin is a potent inhibitor of SPT and is widely used to block and identify the role of *de novo* sphingolipid biosynthesis (Hanada, 2003; Wadsworth et al., 2013).

(Dihydro)ceramide Synthase (CerS)

Dihydrosphingosine is further acylated by the action of CerS. Recently, human CerS 1-6 have been discovered as yeast homologues of the longevity assurance gene 1-6 (LASS1-6), and are encoded by six distinct genes, resulting in the generation of huge dhCer and Cer profiles (Pewzner-Jung et al., 2006). Each CerS has substrate preference for different lengths of fatty acyl-CoAs, thus producing distinct dhCers with different acyl-chain lengths. For example, whereas CerS1 prefer stearoyl-CoA as a substrate and mainly generate C18-Cer species (Venkataraman et al., 2002), CerS5 and CerS6 both prefer palmitoyl-CoA as substrates and produce predominantly C16-Cer species

(Riebeling et al., 2003). On the other hand, CerS2 prefer C20-C26 acyl-CoA species and form long chain Cer species (Laviad et al., 2008). CerS3 utilizes middle and long chain acyl-CoA and makes the corresponding Cer species (Mizutani et al., 2006) (Fig. 1.5). These CerS proteins are localized mainly to the ER and its activity is inhibited by a number of fungal inhibitors such as fumonisin B1 (FB1), a mycotoxin produced by *Fusarium verticillioides*. The nature of the inhibition of CerS by FB1, which contains an aminoeicosapentol backbone, is that CerS recognizes the aminopentol moiety of this compound, which competes with the binding sites for dhSph and fatty acyl-CoA (Merrill et al., 2001).

Dihydroceramide Desaturase (DEGS)

The last step of the *de novo* biosynthesis of Cer is the insertion of a 4,5-*trans*-double bond into dhCer by dihydroceramide Δ4-desaturase (DEGS) to generate Cer. Michel *et al*. first reported the biochemical characterization of the DEGS reaction in 1997 using rat liver microsomes (Michel et al., 1997). They have shown that the DEGS uses molecular oxygen as electron acceptor to have a hydroxyl group in the C4-position of the dhSph, and then with NADP or NADPH as an electron donor, a dehydration reaction occurs to produce a double bond in the C4-C5 position of dhCer. Therefore, they confirmed that the conversion of dhCer to Cer was occurred by a desaturase and not by a dehydrogenase. Two different DEGSs, DEGS1 and DEGS2, have been so far reported. In bioinformatics approach, Ternes *et al.* identified a family of sphingolipid Δ4-desaturases (homologs of the *Drosophila melanogaster* degenerative spermatocyte gene 1 (*des-1*)) (Ternes et al., 2002). DEGS-1, the human homolog of *des-1*, exhibits high dhCer Δ4-

desaturase and very low C-4 hydroxylase activities, whereas DEGS2, another ortholog identified in mouse and human, is similarly active as both sphinglipid C-4 hydroxylase and Δ4-desaturase activities, resulting in the production of either phytoceramide or ceramide. Like the previous two enzymes in the *de novo* sphingolipid biosynthesis pathway, DEGS is localized in the ER membrane where it can access to dhCer species. DEGS1 activity is largely influenced by a number of factors including the length of the alkyl chain of the sphingoid base (C18 > C12 > C8) and fatty acid (C8 > C18), the stereochemistry of the dhSph moiety of the substrate (D-erythro-isomer > L- or D-threo-isomers), and the nature of the headgroup (dhCer: the highest activity, dhSM: some (~20%) activity). The activity of DEGS is inhibited by several compounds, including cyclopropene-containing ceramide, GT-11 (C8-cyclopropenylceramide; C8-CPPC) (Triola et al., 2003; Triola et al., 2004) which is a competitive inhibitor of DEGS, and XM462.

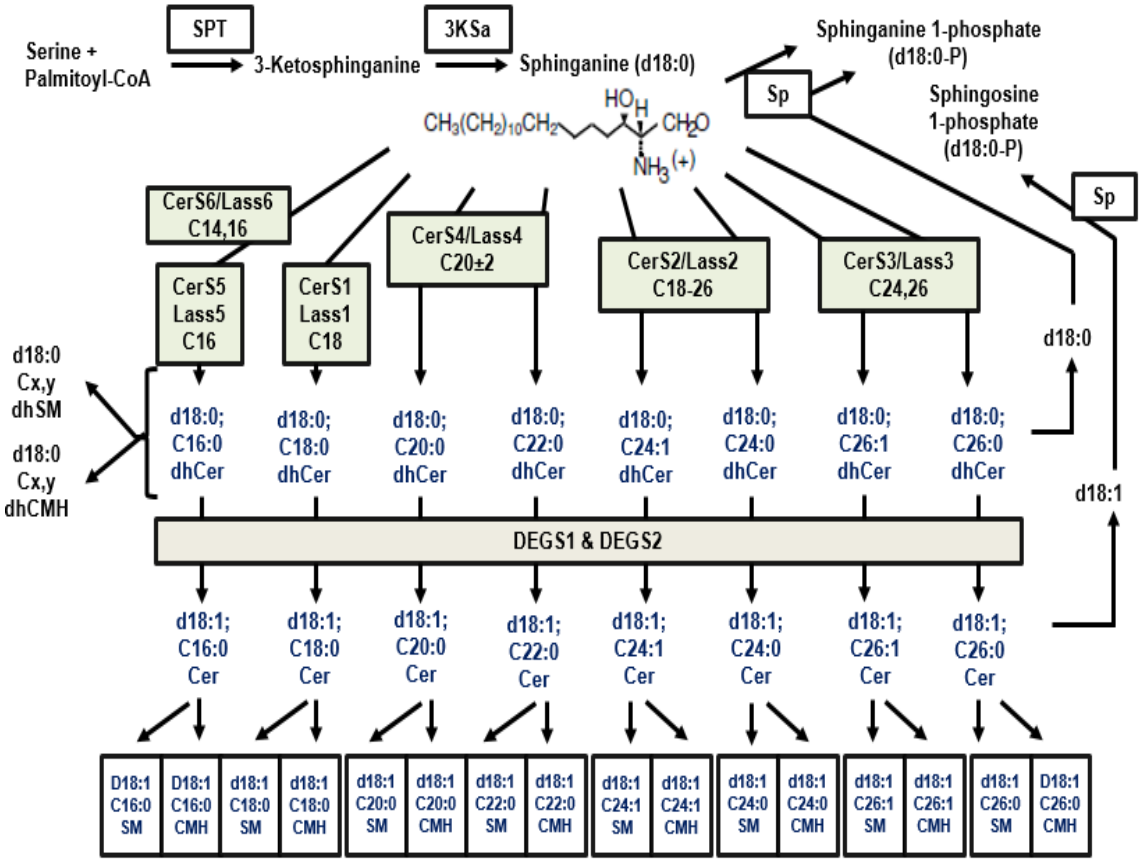

Figure 1.5 *De novo* biosynthesis of sphingolipids highlighting the synthesis of many ceramides with different fatty acid chain length. Biosynthesis of sphinganine, which can be acylated by the CerS/Lass gene products with their specific fatty acyl-CoA preference. Each dhCer can be desaturased to the corresponding Cer species, followed by the production of more complex sphingolipids. Cer, ceramide; CerS, ceramide synthase; dhCer, dihydroceramide; DEGS, dihydroceramide desaturase; SM, sphingomyelin

1.4.1.2 Synthesis of Complex Sphingolipids

Cer formed via the *de novo* sphingolipid biosynthesis pathway in the ER is transported to the Golgi to generate more complex sphingolipids (Hannun and Obeid,

2008). Since Cer is a lipophilic molecule, it needs to be transported either by vesicular transport for the delivery of Cer to synthesize glucosyl-Cer (Watson and Stephens, 2005) or by the protein Cer transfer protein (CERT), which is a cytosolic protein and specifically delivers Cer for SM synthesis (Hanada et al., 2003). In addition, transfer of glucosyl-Cer for complex glycosphingolipids synthesis requires FAPP2 transfer protein (D'Angelo et al., 2007). Therefore, in the Golgi apparatus, more complex sphingolipids such as glucosyl-, or galactosyl-Cers and sphingomyelin (SM) are generated from Cers. Glucosyl-Cer and galactosyl-Cer are synthesized by the actions of enzymes glucosyl-Cer synthase and Cer galactosyltransferase, respectively. Meanwhile, SM, which is the most abundant sphingolipids in mammalian cells, is produced by the action of SM synthases (SMS). There are at least two members of the SMS family and SMS1 and 2 are localized to the *trans*-Golgi, but SMS2 is also present in the plasma membrane. The synthesis of SM is catalyzed by the SMS enzyme, which transfers the phosphocholine headgroup from phosphatidylcholine to Cer yielding the products SM and diacylglycerol (DAG). The activity of SMS enzyme is inhibited by tricyclodecan-9-xanthogenate (D609) (Amtmann, 1996). The produced SM and complex glycosphingolipids are delivered to the plasma membrane by vesicular transport. A majority of the total SM resides at the plasma membrane, where it plays important roles structurally and functionally (Huitema et al., 2004).

Moreover, although Cer is mainly converted into complex sphingolipids in the Golgi, it can also be Cer-1-phosphate through phosphorylation by Cer kinase (Gault et al., 2010).

1.4.1.3 Catabolism of Complex Sphingolipids and Ceramides

SM is the most abundant complex sphingolipid in mammalian cells, and it can be broken down to maintain cellular homeostasis, which occurs by the action of sphingomyelinase (SMase) family. The SMase family hydrolyzes phosphocholine headgroups in the SM to produce Cer and phosphocholine. The SMase family has two major categories based upon their pH optimum, which are the acid and neutral SMases. Acid SMases that are present in lysosomes and the outer membrane leaflet or neutral SMases in the inner leaflet of the bilayer can metabolize SMs to Cers and other bioactive lipids (Marchesini and Hannun, 2004). Although the functions and regulatory mechanisms of SMases are not well characterized, some studies have been investigated the factors and mechanisms that control the SMases activation. Acid SMases has been shown to be activated by the TNF receptor, oxidants, and UV radiation (Henry et al., 2013; Zhang et al., 2001). Neutral SMases activation has also been investigated that serum starvation (Jayadev et al., 1995), oxidative stress (Marchesini and Hannun, 2004), treatment of vitamin D (Okazaki et al., 1994), and curcumin (Abdel Shakor et al., 2014) activate the enzyme. Neutral SMase activation was also a necessary signaling event for the TNF-induced human MCF-7 breast cancer cell death (Luberto et al., 2002). A number of compounds that inhibit SMases were also found. Desipramine, which is a member of the tricyclic antidepressant family, has been used as a selective acid SMase inhibitor by acting on the proteolytic degradation of acid SMase. SR33557 is also a specific acid SMase inhibitor, and NB6 is another inhibitor of the SMase gene transcription. GW4869 is a noncompetitive inhibitor of neutral SMase.

Catabolism of Cer occurs by the action of ceramidases (CDases) to form sphingosine. There are two major CDases, which are acid CDase localized in the lysosomes and neutral CDase localized in the ER and the mitochondria. After Cer is deacylated into sphingosine, sphingosine-1-phosphate (S1P) is synthesized from sphingosine and ATP by the action of one of the sphingosine kinases (SphK); SphK1 or SphK2. Meanwhile, the sphingosine produced from Cer hydrolysis by acid CDase in lysosome may exit the lysosome and salvaged into Cer and sphingolipid pathways. The last step of the sphingolipid catabolic pathway is the degradation of S1P by S1P lyase, a microsomal enzyme to produce 2-hexadecenal and phosphoethanolamine (Gault et al., 2010).

1.4.2 Bioactive Sphingoid Bases and Their Roles in Cell Growth, Survival, and Death

Sphingolipids are diverse groups of lipids that play a variety of essential roles as components of cell membrane structure and cell signaling molecules, thus affecting on the mammalian development and physiology. Moreover, dysregulated sphingolipids metabolism is known to occur in some diseases such as cancer, diabetes, atherosclerosis, and neurodegenerative diseases. Over the past two decades, several sphingolipids metabolites, such as sphingosine, Cer, and S1P were defined as bioactive lipid messengers and regulatory molecules, and many researchers have begun to investigate their various roles and functions. These metabolites are now clearly known to play critical roles in regulating various cellular events including differentiation, proliferation, apoptosis, and autophagy (Ryland et al., 2011; Zheng et al., 2006). However, as the

sphingolipid metabolism is complex and dynamic processes, and the produced metabolites have different or opposite functions, their relative levels and balance between each other are important for the regulation of survival and death within the cells. For instance, while Cer has antiproliferative and proapoptotic properties, S1P involves in cellular proliferation and survival. Thus, a model has been previously proposed in which the equilibrium between these two molecules, the 'Cer/S1P rheostat', could determine cell fate (Cuvillier, 2002). Besides this model, recent studies have suggested that sphingolipid metabolites are interconvertible and each metabolite has its distinct functions. For example, Cer can be further metabolized to sphingosine by ceramidase, which has been shown to induce apoptosis in many cell types. This sphingosine can be further phosphorylated to form S1P by sphingosine kinase. In addition, Cer can be generated from SM via SMases. Therefore, now it is important to understand this complexity of sphingolipid metabolism and specific enzymes that are involved in the pathway, and define the roles and regulation of each metabolite by the application of the comprehensive 'sphingodynamic' model. This present review will focus on the roles of several bioactive sphingolipid metabolites and their regulation.

1.4.2.1 Sphingosine

The first sphingolipid identified that exerts pleiotropic effects on protein kinase C and other targets was sphingosine (Hannun et al., 1986; Merrill et al., 1986; Wilson et al., 1986). Sphingosine is generated from Cer by CDase, and it, in turn, can be

phosphorylated by sphingosine kinase to form S1P. Sphingosine has been shown to be produced during the early stages of apoptosis, and the exogenously added sphingosine itself also induced apoptosis in many cell types (Ahn and Schroeder, 2002; Cuvillier, 2002). Although the role of sphingosine in apoptosis was not extensively studied compared with that of Cer, there are several defined mechanisms that could account for sphingosine to mediate apoptosis. Treatment of sphingosine has been shown to inhibit MAPKs, Erk-1 and Erk-2 activities, and activate JNK and p38, which are stress-activated protein kinases. Moreover, several studies have revealed that caspases, cysteine proteases, are activated during sphingosine-induced apoptosis. In addition, sphingosine induces apoptosis by the mitochondrial pathway, particularly by down-regulating the PI3K-Akt pathway (Cuvillier, 2002).

1.4.2.2 Ceramide

After sphingosine was recognized as a second messenger, Cer also became another candidate for the sphingolipid metabolite, which may act as bioactive cellular signaling molecule (Goldkorn et al., 1991). Cer has a variable length of fatty acid chain attached at the carbon 2 position of long-chain sphingosine by an amide bond. It is either synthesized via *de novo* synthesis by condensation of serine and palmitoyl-CoA or generated by sphingomyelin catabolism by the action of sphingomyelinases. Now, due to its diverse roles including the regulation of cell death and senescence, even more emphasis has been placed on the Cer. Although there are many signaling pathways that

are influenced by Cer, interest has focused on defining the direct targets of Cer. Several proteins such as Cer-activated protein phosphatases (CAPPs), various protein kinases and cathepsin D, have been identified that interact directly with Cer. The CAPPs which are serine/threonine phosphatase, such as PP1 and PP2A, are bound and activated by Cer and induce growth arrest or apoptosis. Targets of these CAPPs for dephosphorylation include the retinoblastoma gene product (Rb), PKCα, protein kinase B (PKB or AKT) and Bcl-2 (Hannun and Obeid, 2008; Kolesnick, 2002; Ohanian and Ohanian, 2001). Moreover, kinase suppressor of ras (KSR), which is a Cer-activated protein kinase (CAPK), has also been identified. KSR is a serine/threonine kinase that phosphorylates and activate Raf to initiate MAPK signaling cascade. In addition, PKCζ and the protease cathepsin D have been shown to be direct targets for Cer. Activation of PKCζ by Cer has been linked cytokines to NFκB signaling (Ohanian and Ohanian, 2001) and implicated in proapoptotic functions. Cathepsin D has been proposed as a specific target for acid SMase-generated Cer in lysosome and implicated in subsequent induction of mitochondrial apoptosis.

While Cer has been proposed as an important cell-signaling messenger for the regulation of diverse events such as differentiation, proliferation and senescence, it has received much attention as a potential mediator of apoptosis. Intensive investigation in the past decade has firmly established that Cer could play a key role in apoptosis signaling in response to cytokines, anticancer drugs, or environmental stresses. Treatment of cells with Cer has been shown to induce apoptosis by the mitochondria-mediated pathway and down-regulation of the PI3K-Akt pathway (Ahn and Schroeder, 2002; Radin, 2001). In addition, Cer has shown to be accumulated in the mitochondrial

membranes after chemotherapeutic drugs or TNFα treatment and caused mitochondrial outer membrane permeabilization by making pore, resulting in the induction of mitochondrial apoptosis (Siskind, 2005). Recent studies have shown that addition of exogenous Cer also induced autophagy, and the autophagy was induced by compounds treatment such as tamoxifen, a chemotherapeutic drug, and 4-HPR in which endogenous Cer increase was involved (Scarlatti et al., 2004; Zheng et al., 2006). In addition to the proapoptotic and proautophagic effects of Cer, it has been implicated in the inhibitory properties of inflammation. Treatment of Cer has been found to inhibit phosphorylation of pro-inflammatory kinases and production of cytokines, and also decrease the inflammatory interleukin 6 (Kitatani et al., 2009; Sun et al., 2008).

Recently, emerging results suggest that endogenous Cers with different fatty acyl-chain lengths appear to have distinct bioactivities. Thus, many researchers have been investigating the role of CerS family that makes Cers as well as specific functions of individual Cer species. These researches were enabled by the development of mass spectrometry (MS)-based approaches for the direct quantitation of Cers over the past 15 years, instead of using a variety of indirect assays, such as enzymatic assays or TLC separations. With the highly sensitive and specific MS-based method, each individual Cer species with different mass could be effectively quantified even in a mixture at low nM concentrations. Watts *et al*. applied this technique to investigate the changes of individual Cer levels during apoptosis in cells for the first time, and observed specific elevations of $C_{16:0}$-Cer (Watts et al., 1999). One study found that B-cell receptor-triggered cell death was associated with an elevation in $C_{16:0}$-Cer in Ramos B-cells. The increase of this Cer was inhibited by FB1, an inhibitor of CerS, which also inhibited several apoptotic

hallmarks such as activation of caspases, mitochondrial damage followed by induction of cell death, suggesting that *de novo* generated $C_{16:0}$-Cer is involved in mitochondrial apoptosis (Kroesen et al., 2001). More recently, numerous studies have been revealed the changes of individual Cer levels in specific cancers, and reported the distinct functions of each individual Cer species in the regulation of tumor growth and therapy using the sphingolipidomic analysis. Koybasi *et al.* first found that only one specific Cer, $C_{18:0}$-Cer was selectively down-regulated in human head and neck squamous cell carcinoma (HNSCC) tissues, and this Cer involved in the inhibition of cancer cell growth and may play an important role in the regulation of cell fate (Koybasi et al., 2004). Consistently, Karahatay *et al.* also found the significantly decreased levels of $C_{18:0}$-Cer in HNSCC tumors. (Karahatay et al., 2007). In contrast, this group found an increase in the levels of $C_{16:0}$-, $C_{24:0}$- and $C_{24:1}$-Cers in the same cancer patients. The increased levels of these Cer species were also observed in malignant breast cancer tissues compared with benign and normal tissues (Schiffmann et al., 2009a). One study has shown that SW620 colon cancer cells had lower expression levels of CerS6 and significantly decreased $C_{16:0}$-Cer which resulted in the resistance to the tumor necrosis factor-related apoptosis-inducing ligand (TRAIL)-induced apoptosis. Moderate elevation in CerS6 expression reversed the apoptotic response to TRAIL in this cell line (White-Gilbertson et al., 2009). Schiffmann *et al.* also implicated an increase of $C_{16:0}$-Cer by CerS6 activation from the salvage pathway in a selective COX-2 inhibitor, celecoxib-induced toxic effects in HCT-116 colon cancer cells (Schiffmann et al., 2009b). Recent study has found that the accumulation of long-chain Cers by CerS5 and 6 through the salvage pathway play important role in ultraviolet light-C-induced programmed cell death of MCF-7 breast

cancer cells (Mullen et al., 2011). However, interestingly, another recent study by Senkal *et al*. revealed novel prosurvival role of $C_{16:0}$-Cer against ER stress-induced apoptosis in HNSCCs. They found that whereas $C_{18:0}$-Cer showed proapoptotic roles, $C_{16:0}$-Cer showed antiapoptotic and prosurvival roles, suggesting that $C_{16:0}$-Cer and $C_{18:0}$-Cer generated by CerS1 or CerS5, respectively, play opposite roles in determining cancer cell survival or apoptosis (Senkal et al., 2010). In addition to the proapoptotic roles of $C_{18:0}$-Cer, it has been shown to mediate lethal autophagy induction, independent of apoptosis in HNSCC cell lines (Sentelle et al., 2012). Taken together, although there is still controversy in the roles of each individual Cer species, recent studies have demonstrated the distinct roles of individual Cer species, and Cers with different fatty acyl chain lengths may contribute to tumor growth and therapy.

1.4.2.3 Dihydrosphingosine and Sphingosine-1-phosphate

Although sphingosine and Cer have been recognized and studied as pivotal apoptosis-inducing molecules for a long time, emerging evidence suggests that other sphingolipid intermediates in the *de novo* synthesis of sphingolipid pathway also play important roles in cell survival and death.

First, dihydrosphigosine (dhSph or sphinganine), an intermediate upstream of CerS an enzyme sensitive to fumunosin B1, has been shown to induce apoptosis in human colon cancer cells (Ahn and Schroeder, 2002), activation-induced T cells (Solomon et al., 2003), and undifferentiated HL-60 and U937 leukemic cells (Jarvis et al.,

1996; Ohta et al., 1995). Moreover, our group found that the treatment of γT, the predominant form of vitamin E in US diet, or mixed vitamin E forms induced huge accumulation of dhSph, resulting in the induction of human prostate cancer cell death (Jiang et al., 2004). We also found that γTE enhanced the intracellular levels of dhSph and inhibited PI3K-mediated Akt phosphorylation followed by induction of apoptosis and autophagy in human prostate cancer cells (Jiang et al., 2012). In addition, safingol, the synthetic L-*threo*-stereoisomer of endogenous (D-erythro-) dhSph, has been shown to induce autophagy through inhibition of PKCs and PI3K in various cancer cells (Coward et al., 2009). Interestingly, fumonisin B1, an inhibitor of CerS, caused the accumulation of dhSph in tissues, serum, and urine, which appear to be responsible for the toxicity of this mycotoxin (Merrill et al., 2001).

Sphingosine and Cer are representative sphingolipid metabolites, which are typically associated with induction of cell death, while S1P is involved in opposite roles such as cell proliferative, mitogenic, survival, antiapoptotic and drug resistant actions. S1P is produced through the action of SphK from sphingosine, which is generated via deacylation of Cer. SphK activity is increased by a number of stimuli such as growth factors, cytokines and G protein-coupled receptors (GPCRs), but the mechanisms regulating the activity of SphK are not yet clearly understood. The increased S1P by the action of SphK interacts with GPCRs as extracellular signals. S1P signaling through these GPCRs has been implicated in various cellular responses including differentiation, migration, and mitogenesis. S1P has also been proposed to play as an intracellular second messenger, which activate calcium release, MAPKs, phospholipase D, and $p125^{FAK}$ phosphorylation, resulting in the regulation of differentiation and migration, and

increases in proliferation of cancer cells (Pyne and Pyne, 2000). Several studies suggest that the levels of S1P are closely linked to resistance to the cancer cell death induction, and the apoptosis-inducing action of Cer is antagonized by S1P. S1P also increased platelet-derived growth factor and vascular endothelial growth factor which are associated with angiogenesis and metastasis of tumor (Catarzi et al., 2007; Heo et al., 2009). Interestingly, S1P has been shown to induce COX-2 expression, which activates inflammatory response and has been recognized to be linked to the cancer progression (Snider et al., 2010).

1.4.2.4 Dihydroceramide

Dihydroceramide (DhCer) is another sphingolipid metabolite which is converted to Cer via DEGS. The only structural difference between Cer and dhCer is the presence or absence of a 4, 5-*trans*-double bond, respectively. Whereas Cer is well known sphingolipid involved in cell death, dhCer was thought to be an inactive precursor of Cer and a non-signaling molecule. In the early 1990's, a study demonstrated that dhCers were inactive in inhibition of cell growth and induction of apoptosis, in which Cers were active in HL-60 cells (Bielawska et al., 1993). Ahn *et al.* also have shown that sphingosine, dhSph, and C2-Cer inhibited growth, caused apoptosis and death of colon cancer cells, whereas dhCer had no effect on these (Ahn and Schroeder, 2002). Several other previous studies also have revealed and confirmed that dhCers have not been found to mimic the effects of Cer, and they are inert compounds as compared with their potent Cer.

However, these studies used unnatural C2 or C6 short-chain analogs instead of natural long-chain Cer and dhCer. Stiban *et al.* first investigated the effects of their long-chain analogs, and found that dhCer are not ineffective. In this study, dhCer hindered Cer channel formation in mitochondria, resulting in the inhibition of apoptotic cell death (Stiban et al., 2006).

On the other hand, technology used in the previous studies showing the important roles of Cer in the induction of cell death was limited in that it could not distinguish between Cer and dhCer. The potential effects of dhCer were recognized with the use of liquid chromatography tandem mass spectrometry (LC-MS/MS) technology, which can identify even different species of Cer and dhCer. For example, 4-hydroxy phenylretinamide (4-HPR or fenretinide), a synthetic retinoid, had been thought to cause large elevation of Cer to induce growth arrest and apoptosis in numerous cancer cells (Erdreich-Epstein et al., 2002; Wang et al., 2003; Wang et al., 2001). However, the LC-MS/MS analysis revealed that 4-HPR did not increase in Cer, but rather accumulate dhCer by inhibiting DEGS.

DhCers are now considered as one of the bioactive sphingolipid metabolites and have shown to be involved in important cellular responses such as cell cycle arrest (Kraveka et al., 2007), apoptosis (Gopalan et al., 2012; Jiang et al., 2012; Jiang et al., 2004), autophagy (Jiang et al., 2012; Signorelli et al., 2009; Zheng et al., 2006), and oxidative stress (Idkowiak-Baldys et al., 2010). Recently, several compounds including natural bioactives such as vitamin E forms, resveratrol, and cancer chemotherapeutic agents have been shown to inhibit DEGS and induce subsequent increases in dhCer levels followed by the regulation of cellular responses. Among them, our group found that γT is

the first natural compound that has been shown to induce apoptotic cell death by increasing intracellular dhCer and dhSph in human prostate cancer cells (Jiang et al., 2004). Since then, subsequent studies have reported several compounds that can modulate intracellular levels of dhCer. Fenretinide, a vitamin A analog with chemotherapeutic properties, also enhanced intracellular dhCer by inhibition of DEGS activity, leading to cell cycle arrest and inhibition of cell growth in human neuroblastoma cells (Kraveka et al., 2007). Following studies from this group found that fenretinide, which bears a structural resemblance to dhCer, directly and irreversibly inhibited DEGS activity (Rahmaniyan et al., 2011). Moreover, resveratrol treatment showed an increase in dhCers levels, which resulted in the induction of autophagy in gastric cancer cells. Importantly, XM462, an inhibitor of DEGS, caused the accumulation of dhCer and it was sufficient to have autophagy (Signorelli et al., 2009). Consistently, in the earlier studies, Zheng *et al.* also showed the induction of autophagy in C2-dhCer-treated prostate cancer cells (Zheng et al., 2006). Celecoxib, a selective COX-2 inhibitor, induced various cancer cell death by promoting dhCer and dhSph accumulation through the inhibition of DEGS and activation of sphingolipid biosynthesis, while depleting cells of Cers. DEGS activity was also found to be inhibited by oxidative stress (Idkowiak-Baldys et al., 2010) or hypoxic environment (Devlin et al., 2011), resulting in significant elevation in dhCer levels and inhibition of cell proliferation. Again, our group has recently shown that γTE, an analog of γT, also enhanced dhCer as well as dhSph, which lead to the induction of apoptosis and autophagy in human cancer cells (Gopalan et al., 2012; Jiang et al., 2012). On the other hand, γTE did not significantly affect Cer or sphingosine levels, and γTE was much more potent than γT in these activities. Our very recent studies implicated the

importance of dhCer increase in the γTE-mediated NFκB inhibition through increase of ER stress and up-regulation of A20 (Wang et al., 2015).

CHAPTER 2. SPHINGOLIPID METABOLISM IS THE INITIAL PRIMARY TARGET OF GAMMA-TOCOTRIENOL AND PLAYS A ROLE IN CELL DEATH INDUCTION

2.1 Abstract

Our previous studies suggest that gamma-tocotrienol (γTE) has potent anticancer activities in cancer cells via modulation of sphingolipid metabolism. Here, by employing liquid chromatography tandem mass spectrometry, we investigated temporal changes in levels of sphingolipids by γTE treatment in human colon cancer HCT-116 cells. Incubation with γTE for 16 h resulted in accumulation of dihydrosphingosine (dhSph) and dihydroceramides (dhCer), and these changes intensified during prolonged treatment. In contrast, γTE treatment led to a significant decrease in $C_{16:0}$-ceramide (Cer) levels at 8 h, but showed no difference at 16 h or increase at 24 h, compared with controls. Meanwhile, γTE led to a decrease in $C_{24:1}$-Cer and $C_{24:0}$-Cer from 8 to 24 h, but an increase in $C_{18:0}$-Cer from 16 h. Interestingly, sphingomyelins (SM) declined from 8 h but cells showed obvious apoptosis (PARP cleavage) or autophagy (LC3 increase) only at 16 h or longer treatment with γTE. Using $^{13}C_3$, ^{15}N-labeled L-serine, we further evaluated the effect of γTE on *de novo* synthesis of sphingolipids. We observed that γTE had no effect on total *de novo* sphingolipid biosynthesis, but induced increases in labeled dhCers and dhSMs, but decreases in labeled Cers, between 2-6 h. These data indicate that γTE may

inhibit dhCer desaturase (DEGS). Consistent with these results, γTE inhibited the DEGS activity as indicated *in situ* assay and *in vitro* assay with microsomes. The importance of sphingolipids modulation in γTE-induced cancer cell death such as the accumulation of dhCers and dhSph during the initial phase, and the increase of Cers and decrease of SMs during the prolonged treatment period was supported by blocking these enhancements using each individual enzyme inhibitors, myriocin and desipramine, respectively. Co-treatment of cells with myriocin or desipramine partially but significantly reversed the γTE-induced cancer cell death. These results indicate that γTE exerts anticancer effects by modulating enzyme activities in sphingolipid metabolism, specifically, by inhibition of DEGS and activation of SM hydrolysis.

2.2 Introduction

Natural forms of vitamin E consist of α-, β-, γ- and δ-tocopherols (αT, βT, γT and δT) and α-, β-, γ- and δ-tocotrienols (αTE, βTE, γTE and δTE). Although these forms share the similar structures, different forms of vitamin E appear to have distinct activities and metabolism. Among them, αT, which is the predominant vitamin E form in tissues and plasma, and the form that is the least catabolized, is the most extensively studied. However, the human clinical studies as well as numerous animal studies of αT in cancer prevention resulted in inconsistent and disappointing outcomes. On the other hand, other forms of vitamin E, although they are low in tissues due to the extensive catabolism, appeared to have unique and strong anticancer activities. Especially, γTE has been shown to have potent anticancer effects in various types of cancer cells (Jiang, 2014; Moya-

Camarena and Jiang, 2012). However, the molecular mechanism by which γTE exerts its anticancer effects are not understood yet.

Recently, our group has shown that γT and γTE induced apoptosis and autophagy through mechanisms involving dhCer and dhSph accumulation in prostate and breast cancer cells, and this modulation of sphingolipid played an important role in γT and γTE-induced cell death (Gopalan et al., 2012; Jiang et al., 2012; Jiang et al., 2004). Sphingolipids constitute an essential component of cell membrane and also are important signaling molecules that regulate cell growth, differentiation, senescence and apoptosis (Hannun and Obeid, 2008; Ryland et al., 2011; Zheng et al., 2006). The levels of endogenous sphingolpids are controlled by *de novo* synthesis pathway and dynamic metabolisms involving catabolic pathways and synthetic pathways of complex sphingolipids. Briefly, *de novo* sphingolipid synthesis begins in the endoplasmic reticulum from condensation of palmitoyl-CoA and serine into 3-keto-dihydrosphingosine by serine palmitoyltransferase (SPT). The intermediate 3-ketodihydrosphingosine is rapidly reduced to dihydrosphingosine (dhSph), followed by acylation by a family of (dihydro)ceramide synthases (CerSs) using fatty acyl-CoAs to generate the corresponding dihydroceramide (dhCer) subspecies. In mammals, there are six identified genes that encode CerS, and each CerS has substrate preference for different lengths of fatty acyl CoAs, thus producing distinct dhCers with different acyl-chain lengths. Dihydroceramide desaturase (DEGS) inserts a 4,5-*trans* double bond in dhCers to make the final product, ceramide (Cer). In the Golgi apparatus, more complex sphingolipids such as glucosyl- or galactosyl-Cers and sphingomyelin (SM) by the actions of glucosyl-Cer synthase, Cer galactosyltransferase, and SM synthases (SMS),

repectively, can be generated from Cers (Fig. 2.3A). As for the degradation pathways, Cer is broken down by ceramidases into sphingosine (Sph), which may be salvaged into sphingolipid pathways or can be phosphorylated to form sphingosine-1-phosphate (S1P). Also, Cer can be generated by breakdown of SM through the action of acid or neutral SMases, which operate at different pH optima (Hannun and Obeid, 2008; Hannun and Obeid, 2011; Kitatani et al., 2008; Marchesini and Hannun, 2004).

Among different species of sphingolipids, only Cers and S1P have been focused to be bioactive molecules. On the other hand, dhCers were thought to be an inactive precursor of Cer, which is a well-known sphingolipid metabolite involved in cell death (Zheng et al., 2006). However, technology used in the previous studies showing the important roles of Cer in the induction of cell death was limited in that it could not distinguish between Cer and dhCer. Recent studies, using liquid chromatography tandem mass spectrometry (LC-MS/MS) technology which can identify even different species of Cer and dhCer, have shown dhCers to be involved in important cellular responses such as cell cycle arrest (Kraveka et al., 2007), apoptosis (Gopalan et al., 2012; Jiang et al., 2012; Stiban et al., 2006), autophagy (Jiang et al., 2012; Signorelli et al., 2009; Zheng et al., 2006), and oxidative stress (Idkowiak-Baldys et al., 2010).

Therefore, we hypothesize that the sphingolipid pathway may be also an important target for the anti-proliferative effects of γTE in other cancer cells. In this study, we investigated the anticancer effects and mechanisms of γTE in human cancer cells and our study revealed that modulation of sphingolipid was the primary target of γTE in the induction of cancer cell death.

2.3 Materials and Methods

2.3.1 Materials and reagents

γTE (97-99%), a gift from BASF (Ludwigshafen, Germany), was dissolved in DMSO at 100 mM and then diluted to 5 mM in fatty acid-free BSA (10 mg/ml). Sphingolipid standards were obtained from Avanti Polar Lipids (Alabaster, AL). CHAPS was purchased from Thermo Fisher Scientific. C8-cyclopropenylceramide (C8-CPPC) was purchased from Matreya LLC (Pleasant Gap, PA). Myriocin from *Mycelia Sterilia*, desipramine, GW4869, $^{13}C_3$, ^{15}N-labeled L-serine, N-acetyl cysteine (NAC), dimethyl sulfoxide (DMSO), [3-(4,5)-dimethylthiazol-2-yl]-2,5-diphenyl tetrazolium bromide] (MTT), and all other chemicals were from Sigma (St Louis, MO).

2.3.2 Cell culture and treatment

Human colon cancer HCT-116 and breast cancer MCF-7 cells were obtained from American Type Culture Collection (Manassas, VA). Cells were routinely cultured in growth media containing 10% fetal bovine serum (FBS) at 37 °C in 5% CO_2. HCT-116 cells were cultured in McCoy's 5A modified medium. MCF-7 cells were incubated in Dulbecco's modified eagle medium (DMEM) supplemented with 0.1% insulin. At the time of experiments, cells were seeded in each medium with 10% FBS either at a density of 4 x 10^4 cells/well in 24-well plates or at a density of 7-8 x 10^5 cells in 10-cm dishes. Unless otherwise indicated, for experiment, cells were seeded in 10-cm dishes except MTT assay. After overnight attachment, media were replaced with fresh DMEM

containing 1% FBS and γTE or other compounds. All the treatment solutions were freshly prepared for each experiment.

2.3.3 MTT assay

Cell viability was examined by MTT assay to estimate mitochondrial dehydrogenase activity. In living cells, the enzyme reduces MTT to form formazan which was dissolved in DMSO and measured the absorbance at 570 nm by using a microplate reader (SpectraMax 190, Molecular Devices, Sunnyvale, CA).

2.3.4 Lipid extraction

Total lipids were extracted as previously described (Merrill et al., 2005). Briefly, cell pellets were resuspended in methanol/chloroform/water (10:5:1 [v/v/v]) after the addition of internal standard mixture containing 0.5 nmol $C_{12:0}$/$C_{25:0}$-Cers, $C_{12:0}$-SM, and C17-Sph/dhSph (Avanti Polar Lipids, Alabaster, AL). The suspension was dispersed fully by tip sonication for 20 sec and then incubated overnight at 48 °C. 100 µL of solvent was used to determine the amount of total choline-containing phospholipids by an enzymatic colorimetric assay (Wako chemicals, Osaka, Japan) (Jiang et al., 2004). 75 µL of 1 M KOH in methanol was added to the rest of the solvent and sonicated for 30 min. After sonication, samples were incubated at 37 °C for 2 h and dried in a nitrogen evaporator.

2.3.5 Measurement of sphingolipids using liquid chromatography tandem mass spectrometry (LC-MS/MS)

Samples for sphingolipids analysis were resolved again in methanol and sonicated to disperse, then centrifuged to clarify before transferring to test vials for quantification. The LC-MS/MS method was slightly modified based on the method of Merrill *et al.* (Merrill et al., 2005). Analyses were performed using the Agilent 6460 triple quadrupole mass spectrometer coupled with the Agilent 1200 Rapid Resolution HPLC (Agilent Technologies, Santa Clara, CA) with detection of sphingolipids in positive mode by multiple reaction monitoring (MRM) technique. The HPLC mobile phases consisted of methanol-H_2O-formic acid (74:25:1, v/v/v; RA) and methanol-formic acid (99:1, v/v; RB); both RA and RB contain 5 mM ammonium formate. For measurement of ceramides and sphingoid bases, Agilent column XDB-C18 (4.6 x 50 mm) with particle size of 1.8 μm, was used with isocratic run (100% B) or gradient (0-1 min, 20% B, 10-13 min, 100% B and 15-20 min at 20% B), respectively. For measurement of sphingomyelins, Agilent Zorbax XDB-C8 (2.1 x 50 mm) with particle size of 3.4 μm, was used with gradient (0-1 min, 20% B, 10-20 min, 100% B, 22-30 min, 20% B). The MS/MS parameters were as follows: gas temperature, 325-350 °C; gas flow rate, 7-10 L/min; nebulizer pressure, 45-50 psi; capillary voltage, 3500 V; The fragmentor voltage was 100 V and collision energy was 12-20 V. Precursor-to-product ion transitions for each sphingolipid were used according to the method of Merrill *et al.* (Merrill et al., 2005).

2.3.6 *De novo* sphingolipids analysis

HCT-116 cells were treated with either 400 μM $^{13}C_3$, ^{15}N-labeled L-serine alone or with a combination of 400 μM $^{13}C_3$, ^{15}N-labeled L-serine and 20 μM of γTE for 30 min, 2 h, 3 h and 6 h. Lipids were extracted and *de novo* synthesized sphingolipids were measured using LC-MS/MS.

2.3.7 *In Situ* dihydroceramide desaturase assay

$C_{8:0}$-dihydroceramide ($C_{8:0}$-dhCer) was used as the substrate for the DEGS. HCT-116 cells were pretreated with either γTE or C8-CPPC as a positive control, followed by 10 μM of $C_{8:0}$-dhCer incubation for 1 h. The cells were collected and lipids were extracted. The levels of products ($C_{8:0}$-ceramide and $C_{8:0}$-sphingomyelin) were detected by LC-MS/MS.

2.3.8 *In Vitro* dihydroceramide desaturase assay

Microsomes were prepared and used as the DEGS enzyme source for this assay (Rahmaniyan et al., 2011). Livers from male Wistar rats were rinsed in ice-cold PBS and homogenized in buffer (0.25 M sucrose, 10 mM HEPES, 1 mM EDTA, pH 7.4) with a homogenizer in ice. The homogenate was centrifuged at 800 x g for 10min first and the supernatant was re-centrifuged at 10,000 x g for 15 min followed by ultracentrifugation of the resulting supernatant at 104,000 x g for 1 h. The microsomal pellet was resuspended in potassium phosphate buffer (50 mM, pH 7.4) and aliquots were stored at -80 °C until use. Protein amount was quantified by using a bicinchoninic acid (BCA) protein assay kit (Pierce, Rockford, IL). For the assay, substrate ($C_{8:0}$-dhCer) and tested

compounds were dried under a stream of nitrogen, followed by resuspension in CHAPS (1.1 mg/10 μl of water). 500 μg of microsomal protein was mixed with reaction buffer (20 mM bicine, pH 8.5, 50 mM NaCl, and 50 mM sucrose) and then the tested compounds were added, followed by 30 min pre-incubation at room temperature. 2 mM of NADH and 10 μM of $C_{8:0}$-dhCer were added and the mixture was incubated for 20 min at 37 °C with shaking. Lipid extraction was conducted directly after reaction and the product ($C_{8:0}$-ceramide) was quantified by LC-MS/MS.

2.3.9 Transmission Electron Microscopy (TEM)

After treatment, cells were fixed with 2% glutaldehyde in 0.1 M cacodylate buffer (pH 7.4) for 1 h at room temperature. After primary fixation, the attached cells were scraped and pooled together with the floating cells. All the cells were then centrifuged and washed twice with cacodylate buffer and once with water. A secondary fixation in reduced osmium containing 1% OsO_4 and 1.5% agarose and then diced and dehydrated in ethanol with a concentration gradient. The ultrathin sections were stained with 2% uranylacetate in 70% methanol for 5 min and lead citrate for 3 min. Finally, the cell images were taken by a FEI/Philips CM-10 bio-twin transmission electron microscope (FEI Company, Hillsboro, OR) using an acceleration voltage of 80 kV. Cells and the inner ultrastructure were observed in different magnification.

2.3.10 Western Blotting

Cells were lysed in lysis buffer containing Tris-EDTA, 1% SDS, 2 mM Na_3VO_4 and protease inhibitor cocktails (Sigma). Total proteins which were quantified by BCA

protein assay kit were denatured by boiling in Laemmli buffer for 5 min at 95 °C. Equal amount of proteins (15-30 μg) were separated on acrylamide gels by SDS-electrophoresis and then transferred onto a polyvinylidene fluoride (PVDF) membrane (Millipore, Bilerica, MA, USA), and probed by antibodies. Membranes were exposed to chemiluminescent reagent (PerkinElmer) and visualized on Kodak film with an M35A X-Omat processor (Kodak). The antibodies used in the study were as follows: DEGS1 (Novus Biologicals, Littleton, CO), membrane bound microtubule-associated protein light chain 3 (LC3; MBL international, Woburn, MA), poly (ADP-ribose) polymerase-1 (PARP-1) and Actin (Santa Cruz Biotechnology, Santa Cruz, CA), phosphorylated JNK at Thr-183 and Tyr-185 (p-JNK), and total JNK (Cell Signaling Technology, Danvers, MA).

2.3.11 Statistics

Statistical significance was determined using a Student's t-test. p-values of < 0.05 were considered to be statistically significant.

2.4 Results

2.4.1 Temporal changes of sphingolipids induced by γTE

We investigated the effects of γTE on sphingolipid metabolism using LC-MS/MS in human colon HCT-116 cancer cells. During the initial 8 h treatment, γTE caused significant decreases of $C_{16:0}$-Cer, $C_{18:0}$-Cer, $C_{24:1}$-Cer and $C_{24:0}$-Cer, resulting in the significant decreases in total Cers. However, individual Cer, which have been shown to

have distinct bioactivities (Hannun and Obeid, 2011; Senkal et al., 2010; Sentelle et al., 2012), appeared to respond differently to γTE in the longer time treatment. For example, $C_{16:0}$-Cer in γTE-treated cells returned to the control levels at 16 h but exceeded the control at 24 h. Compared with controls, $C_{18:0}$-Cer was enhanced in γTE-treated cells at 16 h, whereas C_{24}-Cers remained lower than controls during the prolonged treatment period (Fig. 2.1A). Meanwhile, γTE induced significant increases of dhCers and dhSph starting at 16 h, thus cells accumulated high levels of dhCers and dhSph at 16 h and 24 h treatment with γTE (Figs. 2.1B and C). As to SM, while dhSMs increased during 16-24 h incubation, SMs declined at 8 h compared with controls (Figs. 2.1D and E; Table 2.1). Furthermore, we observed similar sphingolipid modulatory effects of γTE on human breast MCF-7 cancer cells (Fig. 2.2; Table 2.2).

These data suggest that the initial action of γTE is likely to inhibit DEGS, which is evident by the increase of dhSph and dhCers and decrease of Cers, similar phenomena reported with DEGS knockout model (Ruangsiriluk et al., 2012; Siddique et al., 2013). During prolonged treatment, γTE may induce $C_{16:0}$-SM hydrolysis, which explains the subsequent increase of $C_{16:0}$-Cer during prolonged incubation times. On the other hand, another possible explanation for increased $C_{16:0}$-Cer and decreased SM is that the conversion of Cer to SM may be inhibited.

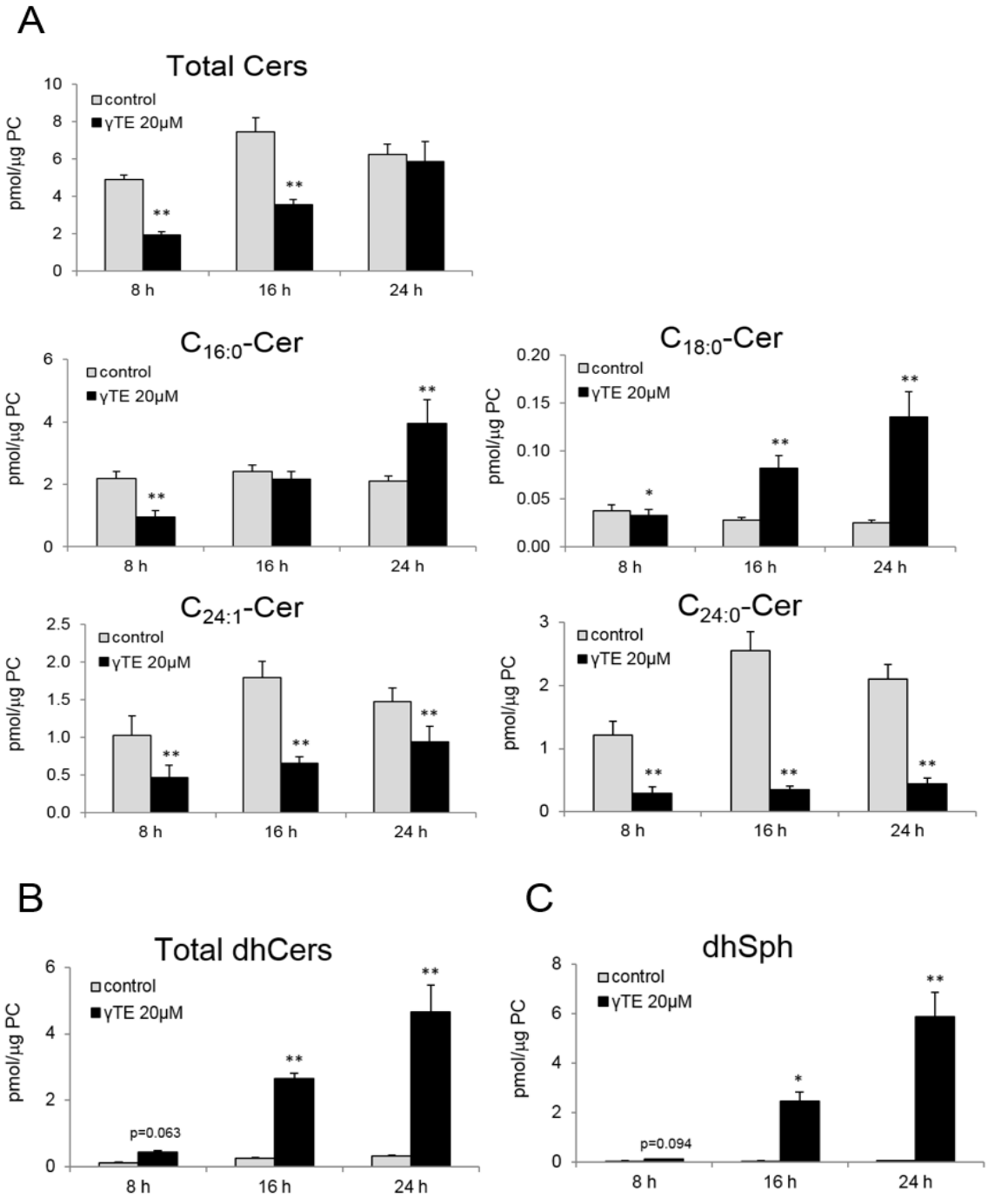
A
Total Cers
control
γTE 20μM
pmol/μg PC
8 h
16 h
24 h
C16:0-Cer
C18:0-Cer
C24:1-Cer
C24:0-Cer
B
Total dhCers
p=0.063
C
dhSph
p=0.094

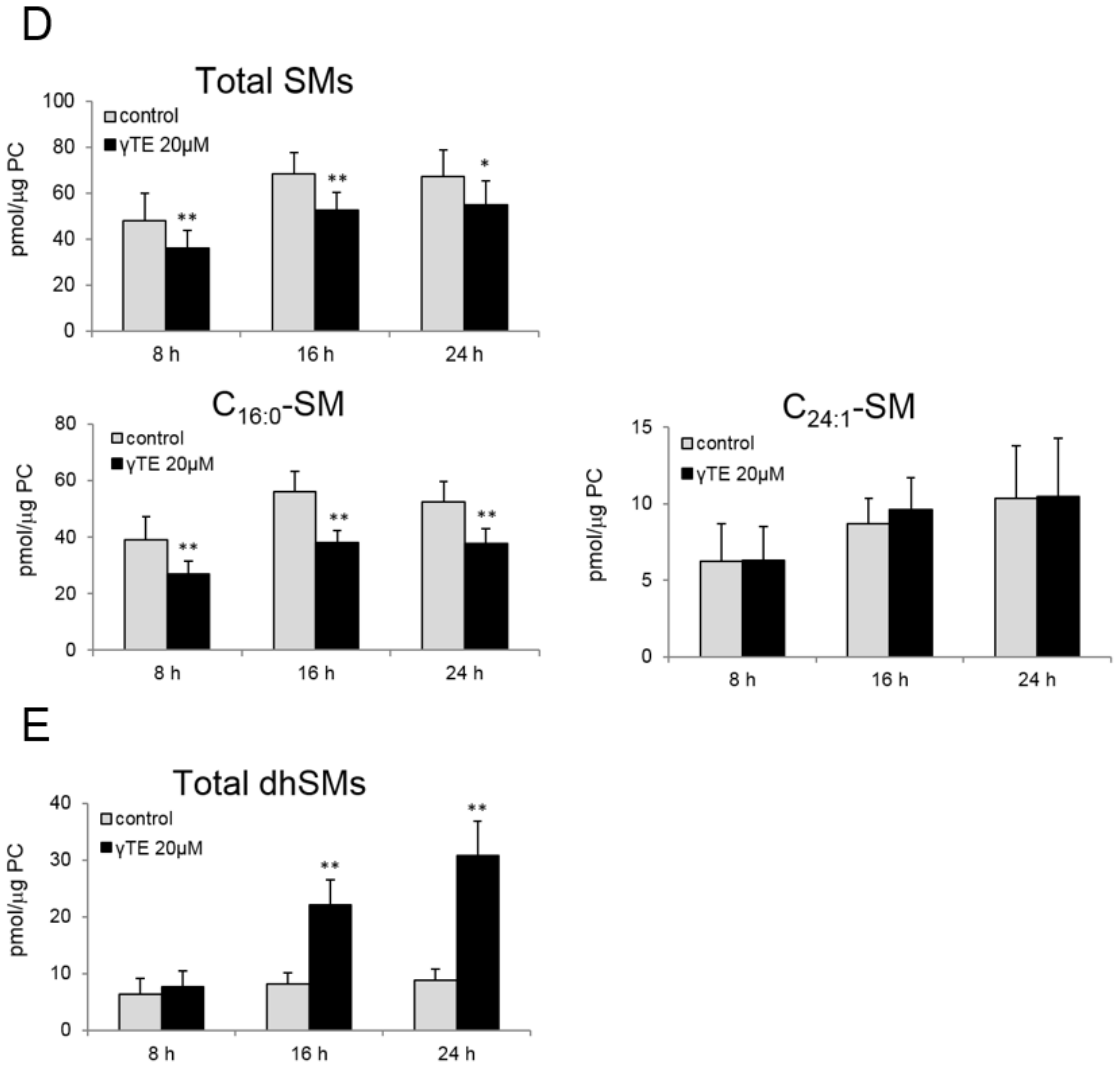

Figure 2.1 Effects of γTE on sphingolipid metabolism in HCT-116 cells. HCT-116 cells were treated with 20 μM of γTE for 8, 16, and 24 h. The sphingolipid levels including (A) total Cers, $C_{16:0}$-Cer, $C_{18:0}$-Cer, $C_{24:1}$-Cer, and $C_{24:0}$-Cer, (B) total dhCers, (C) dhSph, (D) total SMs, $C_{16:0}$-SM, and $C_{24:1}$-SM, and (E) total dhSMs were determined by LC-MS/MS. Results are shown as mean ± SEM for at least three independent experiments. *$p < 0.05$ and **$p < 0.01$ indicate a significant difference between treated and control cells.

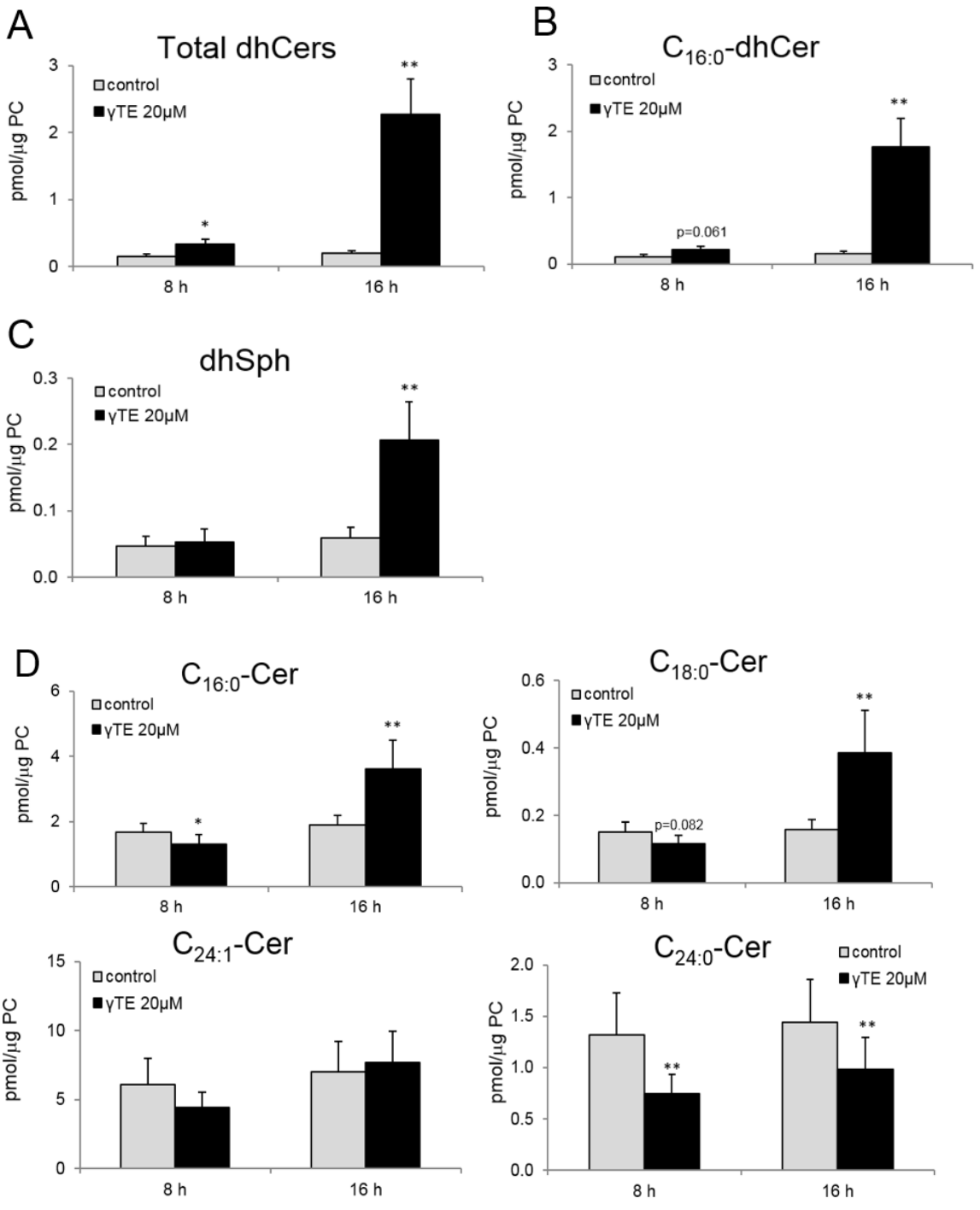
A
Total dhCers
control
γTE 20μM
pmol/μg PC
*
**
8 h
16 h
B
C16:0-dhCer
control
γTE 20μM
pmol/μg PC
p=0.061
**
8 h
16 h
C
dhSph
control
γTE 20μM
pmol/μg PC
**
8 h
16 h
D
C16:0-Cer
control
γTE 20μM
pmol/μg PC
*
**
8 h
16 h
C18:0-Cer
control
γTE 20μM
pmol/μg PC
p=0.082
**
8 h
16 h
C24:1-Cer
control
γTE 20μM
pmol/μg PC
8 h
16 h
C24:0-Cer
control
γTE 20μM
pmol/μg PC
**
**
8 h
16 h

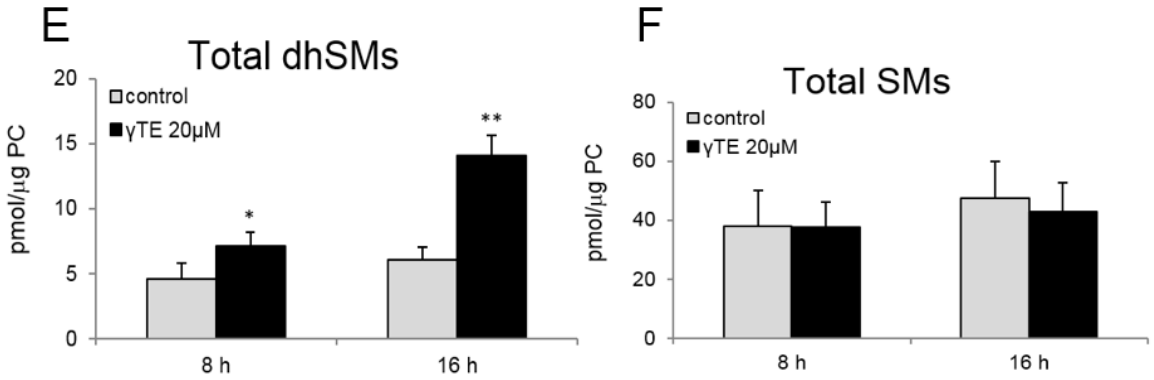

Figure 2.2 Effects of γTE on sphingolipid metabolism in MCF-7 cells. MCF-7 cells were treated with 20 μM γTE for 8 h or 16 h. The sphingolipid levels including (A) total dhCers, (B) $C_{16:0}$-dhCer, (C) dhSph, (D) $C_{16:0}$-Cer, $C_{18:0}$-Cer, $C_{24:1}$-Cer, and $C_{24:0}$-Cer, (E) total dhSMs, and (F) total SMs were determined by LC-MS/MS. Results are shown as mean ± SEM for five independent experiments. *$p < 0.05$ and **$p < 0.01$ indicate a significant difference between treated and control cells.

2.4.2 *De novo* synthesis of sphingolipids with labeled serine

To evaluate whether γTE has impact on *de novo* sphingolipid biosynthesis (Fig. 2.3A), $^{13}C_3$, ^{15}N- L-serine was added to culture media to trace only newly synthesized sphingolipids. Similar to those observed effects of γTE on sphingolipid metabolism above, γTE led to an increase of *de novo* synthesized dhCers and decrease in *de novo* Cers after 2 h, supporting the notion that DEGS is inhibited (Figs. 2.3B and C). Interestingly, compared with control cells, labeled dhSM and SM, which represented newly synthesized dhSM and SM, also significantly increased at 2 h in γTE-treated cells, while SMs returned to the control levels at 3 h (Figs. 2.3D and E). These results indicate that the conversion of $C_{16:0}$-Cer to $C_{16:0}$-SM was stimulated at the initial stage of treatment, despite the decrease of $C_{16:0}$-Cer in cells. As a result, the decrease of Cers due to inhibition of DEGS was intensified by increased SM synthesis. The continuous increase of *de novo* dhSM was probably a result of enhanced *de novo* dhCer, which led to limited accumulation of dhCer during the first few hours (Figs. 2.1B and E). On the other hand, we did not see significant difference between control and γTE-treated cells in total labeled sphingolipids (Fig. 2.1F), suggesting that the overall sphingolipid synthesis was not enhanced (Table 2.3).

Since labeled $C_{16:0}$-Cer is decreased, the increase of overall $C_{16:0}$-Cer in the subsequent time (24 h) and decrease of SM is likely due to hydrolysis of $C_{16:0}$-SM, which is obvious at 8 h incubation.

A *De novo* synthesis of sphingolipid

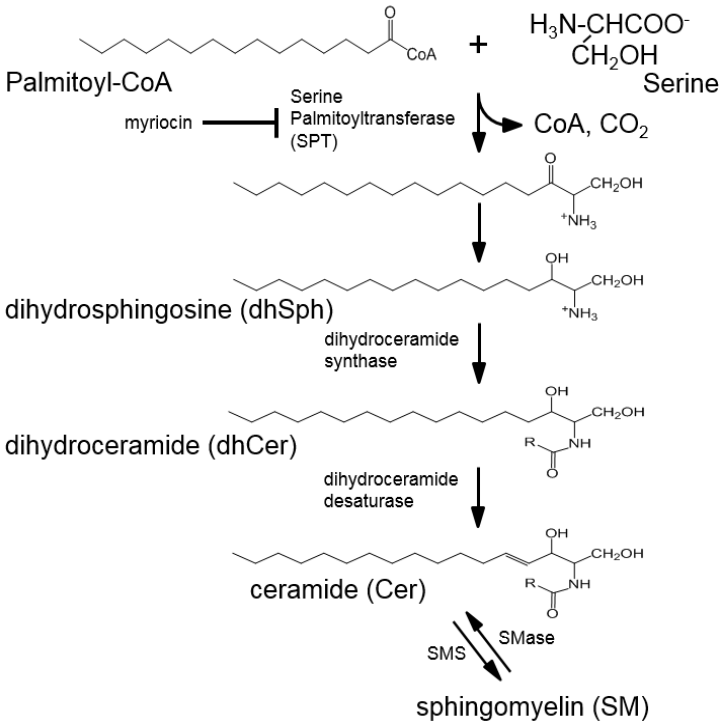

B

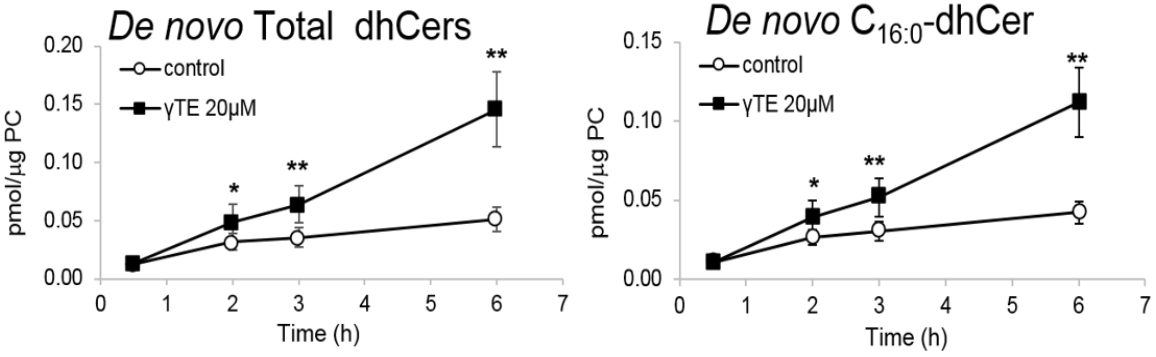

C

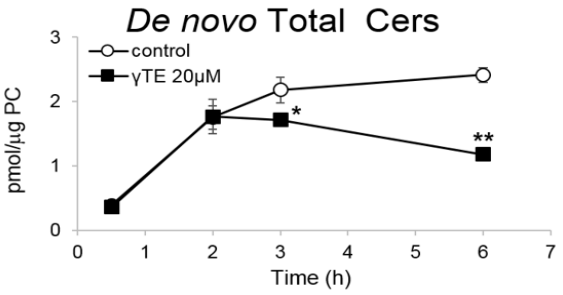
De novo Total Cers
control
γTE 20μM
pmol/μg PC
Time (h)
*
**

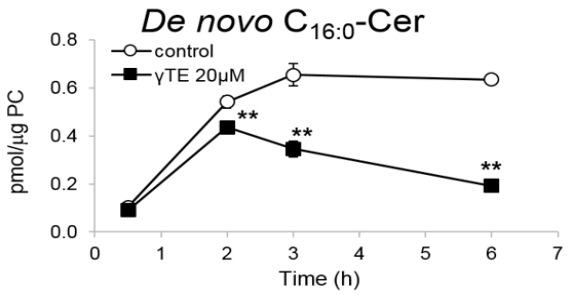
De novo C16:0-Cer
control
γTE 20μM
pmol/μg PC
Time (h)
**
**
**

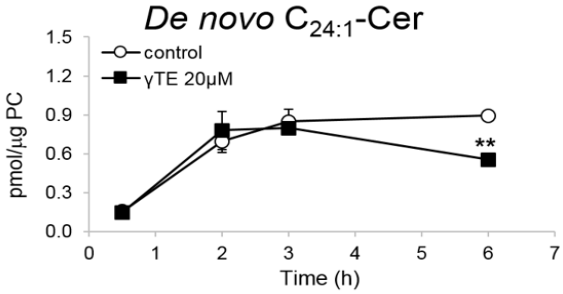
De novo C24:1-Cer
control
γTE 20μM
pmol/μg PC
Time (h)
**

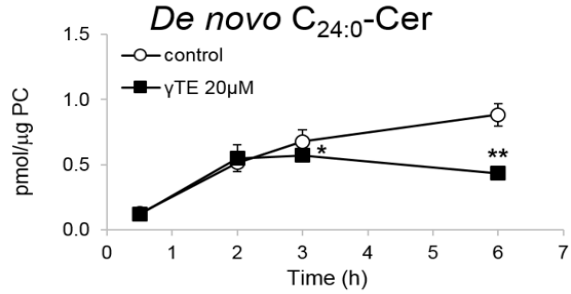
De novo C24:0-Cer
control
γTE 20μM
pmol/μg PC
Time (h)
*
**

D

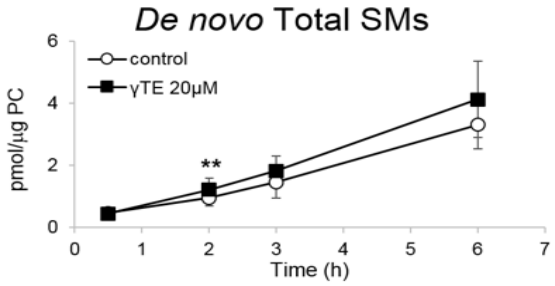
De novo Total SMs
control
γTE 20μM
pmol/μg PC
Time (h)
**

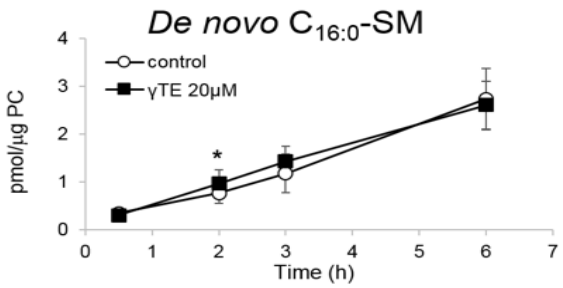
De novo C16:0-SM
control
γTE 20μM
pmol/μg PC
Time (h)
*

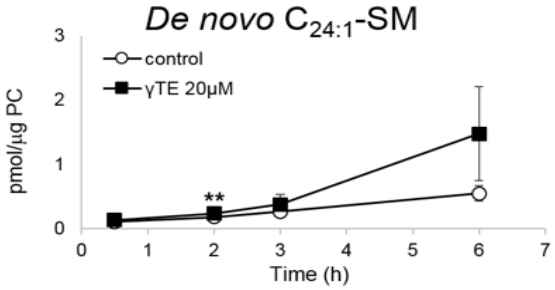
De novo C24:1-SM
control
γTE 20μM
pmol/μg PC
Time (h)
**

E

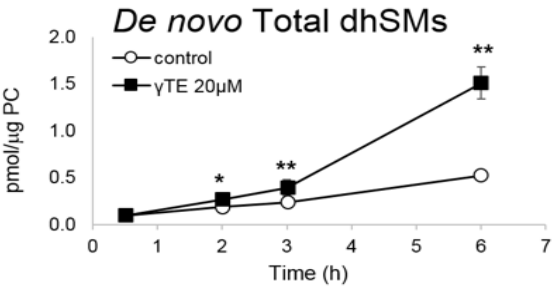
De novo Total dhSMs
control
γTE 20μM
pmol/μg PC
Time (h)
*
**
**

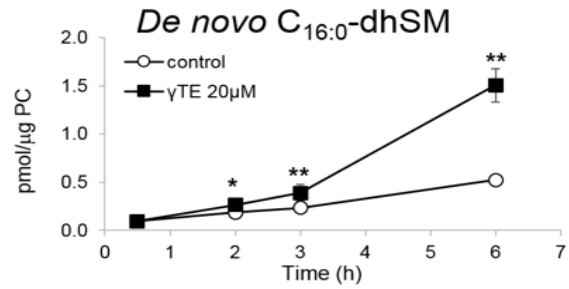
De novo C16:0-dhSM
control
γTE 20μM
pmol/μg PC
Time (h)
*
**
**

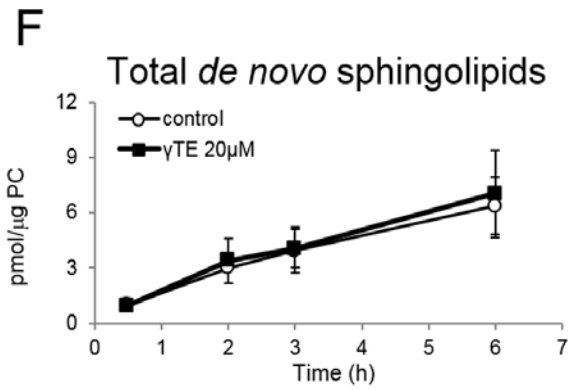

Figure 2.3 Effects of γTE on *de novo* sphingolipid biosynthesis in HCT-116 cells. (A) The *de novo* biosynthesis pathway of sphingolipids (SMS, sphingomyelin synthase; SMase, sphingomyelinase). HCT-116 cells were treated with either 400 μM $^{13}C_3$, ^{15}N-labeled L-serine alone as control or with a combination of 400 μM $^{13}C_3$, ^{15}N-labeled L-serine and 20 μM γTE for 0.5, 2, 3, and 6 h. The amount of each labeled *de novo* sphingolipid including (B) total and $C_{16:0}$-dhCers, (C) total, $C_{16:0}$-, $C_{24:1}$- and $C_{24:0}$-Cers, and (D) total, $C_{16:0}$- and $C_{24:1}$-SMs, and (E) total and $C_{16:0}$-dhSMs were determined by LC-MS/MS. (F) Total amounts of all the *de novo* synthesized sphingolipids were calculated. Results are shown as mean ± SEM for three independent experiments. *p < 0.05 and **p < 0.01 indicate a significant difference between treated and control cells.

2.4.3 Direct evidence that γTE inhibits DEGS

We found that γTE treatment increased *de novo* synthesized dhCers, but led to decrease in *de novo* Cers, suggesting that γTE decreases DEGS protein expression or inhibits DEGS-catalyzed enzyme reactions. γTE treatment did not affect the DEGS protein expression on HCT-116 cells as determined by western blotting (Fig. 2.4A). Next, to determine whether the observed sphingolipid change results from inhibition of DEGS enzyme activity, both *in situ* and *in vitro* assays were conducted. In the assays, the non-physiological $C_{8:0}$-dhCer was used as a substrate for the DEGS, and measured the $C_{8:0}$-sphingolipid products by LC-MS/MS; specifically $C_{8:0}$-Cer with $C_{8:0}$-SM or $C_{8:0}$-Cer for *in situ* and *in vitro* DEGS assays, respectively. *In situ* DEGS activity was evaluated in intact HCT-116 cells. C8-CPPC, a known competitive inhibitor of DEGS (Triola et al., 2003), inhibited DEGS activity, and showed ~75% reduction of the $C_{8:0}$-sphingolipids production. The relative inhibition of DEGS activity by 20 μM of γTE for 6 h and 8 h was ~40% and ~45%, respectively (Fig. 2.4B). In addition, the direct effect of γTE on DEGS activity was determined using rat liver microsomes. In this direct *in vitro* DEGS assay, γTE showed a modest DEGS activity inhibition by only ~10% at a concentration of 20 μM, and ~25% at 100 μM (Fig. 2.4C). The requirement of higher concentration of γTE for the DEGS inhibitory effects in *in vitro* assay could be due to limitation in permeability through the cell membrane of γTE. These results indicated that γTE inhibits DEGS activity, but not expression.

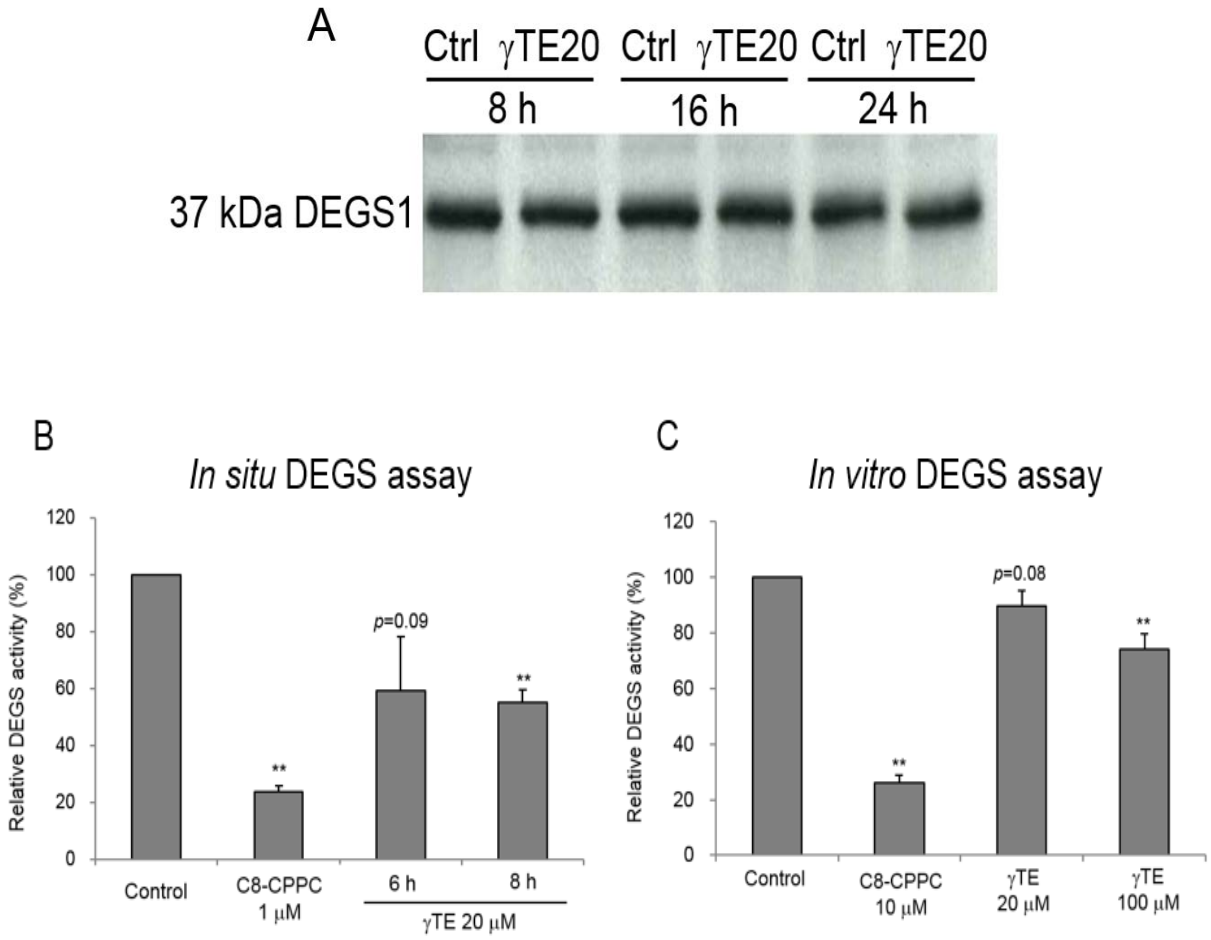

Figure 2.4 Effects of γTE on DEGS expression and activity. (A) HCT-116 cells were treated with 20 μM γTE for 8, 16, and 24 h and the protein levels of DEGS-1 were detected by western blotting. (B) *In situ* DEGS assay: HCT-116 cells were pretreated with either 20 μM γTE or 1 μM C8-CPPC as a positive control, followed by 10 μM $C_{8:0}$-dhCer incubation as a substrate for the enzyme for 1 h. The cells were collected and lipids were extracted. The levels of $C_{8:0}$-sphingolipid products were detected by LC-MS/MS. (B) *In vitro* DEGS assay using rat liver microsomes: Microsomes were used as the enzyme source for this assay. The microsomal proteins in reaction buffer were pre-mixed with either 20 or 100 μM γTE or 10 μM C8-CPPC for 30 min, followed by addition of 2 mM NADH and 10 μM $C_{8:0}$-dhCer and incubation for 20 min at 37 °C. Total lipids were extracted immediately after reaction, and the product was quantified by LC-MS/MS. The data are mean ± SD of three independent experiments. *$p < 0.05$ and **$p < 0.01$ indicate a significant difference between treated and control cells.

2.4.4 Temporal changes of cell death markers

γTE treatment caused PARP cleavage, as indicated by the appearance of the 89 kDa cleavage product from 16 h in HCT-116 cells. γTE treatment also increased levels of p-JNK, which is a stress marker, in HCT-116 cells, as consistent with the p-JNK upregulation by γTE in MCF-7 cells (Gopalan et al., 2012). The induction of autophagy in γTE-treated HCT-116 cells was first investigated by using LC3-II, a marker of autophagy. Interestingly, γTE treatment also led to an increase of LC3-II expression from 16 h (Fig 2.5A). It is important to note that the initial autophagy or apoptosis (at 16 h but not 8 h) is not due to decrease of $C_{16:0}$-Cer or C_{24}-Cers, but might be facilitated by increased dhSph, dhCer and increased $C_{18:0}$-Cer.

We further examined the morphological analysis using TEM. As shown in Fig. 2.5B, control HCT-116 cells appeared normal, displaying abundant microvilli at the cell surface, abundant organelles in the cytoplasm, and well-organized nuclei with clear nuclear membrane. However, cells treated with γTE for 21 h showed evidence of apoptosis characterized by cell shrinkage, loss of microvilli, loss of nuclear membrane and chromatin condensation. These data suggest that γTE treatment induced apoptosis and autophagy.

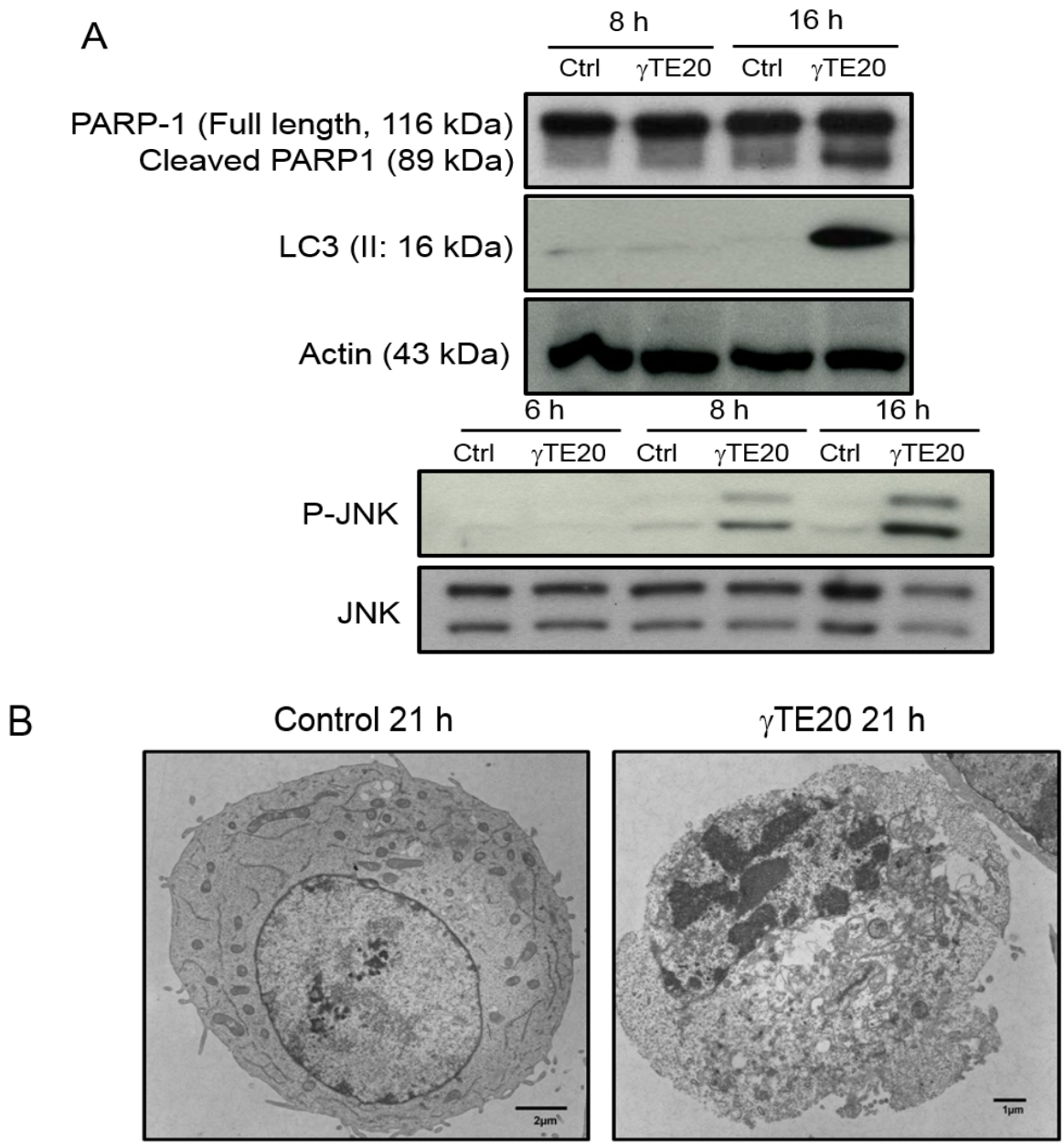

Figure 2.5 Induction of apoptosis and autophagy by γTE in HCT-116 cells. (A) HCT-116 cells were treated with 20 μM of γTE for 6, 8, and 16 h. Expression levels of full-length and cleaved PARP, LC3-II, Actin as a loading control, and levels of p-JNK and JNK were examined by western blotting. (B) HCT-116 cells were treated with 20 μM of γTE for 21 h. The morphology of HCT-116 cells was imaged by TEM. Representative TEM images of control group and γTE-treated group are shown in this figure.

2.4.5 The role of sphingolipid modulation in γTE-induced cell death

To evalulate the involvement and importance of *de novo* sphingolipid modulation in γTE-induced cancer cell death, we used two inhibitors of enzymes in sphingolipid biosynthesis pathway to block the specific effects of γTE on sphingolipid metabolism. Since the above results (Figs. 2.1B and C) have shown that γTE treatment induced accumulation of intracellular dhCers and dhSph, which are known to be toxic to cancer cells (Ahn and Schroeder, 2002; Jiang et al., 2004), we used myriocin, a specific inhibitor of serine palmitoyltransferase to inhibit the increase of these sphingoid bases. Interestingly, co-treatment of cells with myriocin showed partial but significant protection from the γTE-caused cancer cell death, as assayed by MTT assay. The importance of sphingolipid modulation in γTE-induced cell death was further confirmed by western blot experiments. Co-incubation of myriocin with γTE slightly but clearly prevented the γTE-induced PARP cleavage and LC3-II induction (Fig. 2.6A). These data suggest that the accumulation of dhSph and dhCers plays an important role in γTE-induced apoptosis, autophagy and subsequent cancer cell death.

During the prolonged treatment time, γTE led to an increase of Cers, but induced a significant decrease in SMs (Fig. 2.1) with the still lower *de novo* synthesized Cers compared with control (Fig. 2.2B), suggesting that γTE may induce SM hydrolysis by activating SMases. As Cers have been known to induce apoptosis, autophagy and cell death, we investigated the role of the increased Cers from SMs via SMases in γTE-induced cancer cell death by using desipramine and GW4869 to inhibit acid or neutral SMases, respectively. Co-treatment of cells with desipramine but not GW4869 (data not

shown) with γTE partially but significantly reversed γTE-induced cancer cell death (Fig. 2.6B), suggesting that the increase of Cers from SMs through the acid SMase activation may in part contribute to γTE-induced colon cancer cell death.

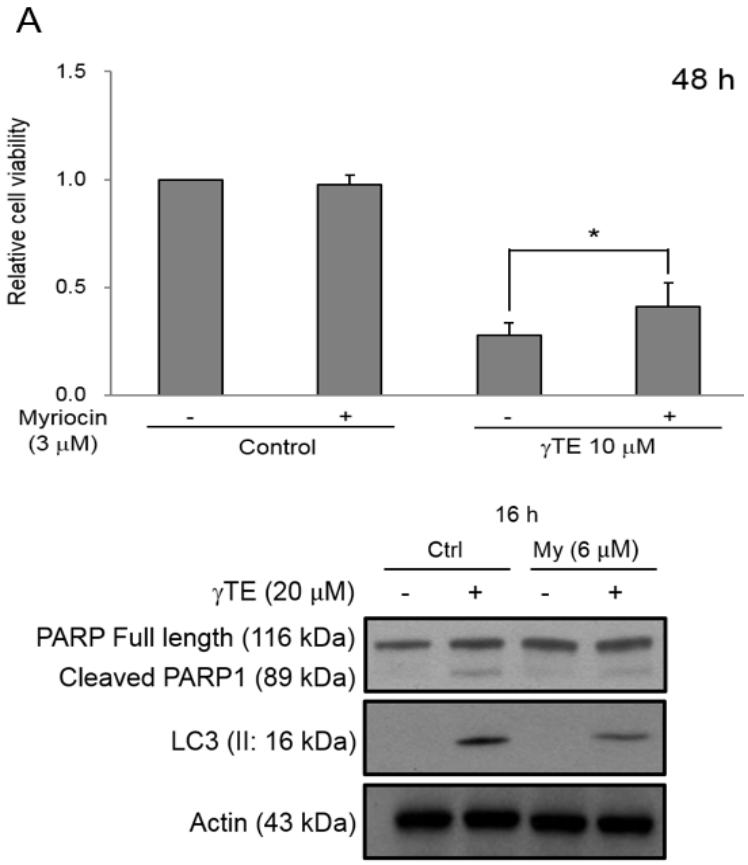

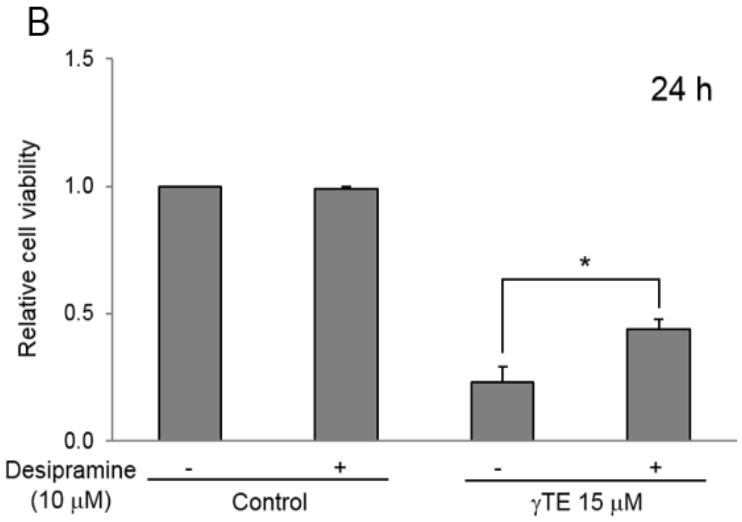

Figure 2.6 Protective effects of inhibitors of enzymes in sphingolipid metabolism on γTE-induced cancer cell death. (A) HCT-116 cells were treated with 10 or 20 μM of γTE with or without 3-6 μM of myriocin, a specific inhibitor of serine palmitoyltransferase to block the *de novo* sphingolipid pathway. After 48 h of treatment, relative cell viability was measured by MTT assay compared with control. In addition, after 16 h of treatment, the cells were collected and analyzed for detection of PARP cleavage and LC3-II expression. Western blots in this figure are representative of three or more independent experiments. (B) HCT-116 cells were treated with 15 μM of γTE with or without 10 μM of desipramine, an inhibitor of acid SMase for 24 h. Relative cell viability was measured by MTT assay compared with control. The data are mean ± SEM of at least three independent experiments. *$p < 0.05$ indicates a significant difference.

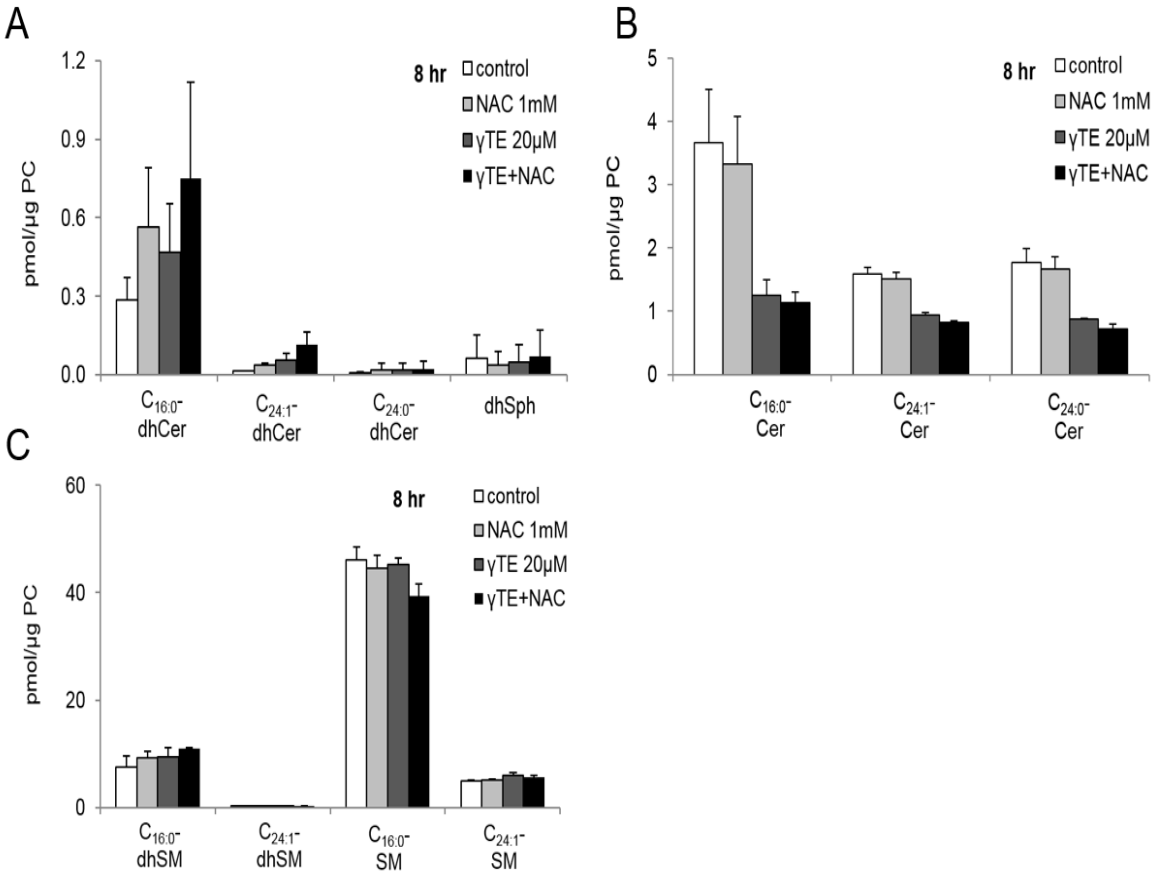

Figure 2.7 NAC, an antioxidant, did not reverse γTE-induced modulation of sphinoglipids in HCT-116 cells. HCT-116 cells were treated with either 20 μM γTE or 1 mM NAC alone or with a combination of γTE and NAC for 8 h. The sphingolipid levels including (A) $C_{16:0}$-dhCer, $C_{24:1}$-dhCer, $C_{24:0}$-dhCer, and dhSph, (B) $C_{16:0}$-Cer, $C_{24:1}$-Cer, and $C_{24:0}$-Cer, (C) $C_{16:0}$-dhSM, $C_{24:1}$-dhSM, $C_{16:0}$-SM, and $C_{24:1}$-SM were determined by LC-MS/MS. Results are shown as mean ± SD for two independent experiments.

Table 2.1 Effect of γTE on sphingolipid metabolism in HCT-116 cells. HCT-116 cells were treated with 20 μM γTE for 8, 16, and 24 h. The amount of each sphingolipid was determined by LC-MS/MS. Data are mean ± SEM of 5 independent experiments. *p < 0.05, **p < 0.01, significant difference between control and γTE-treated cells. Cer, ceramide; dhCer, dihydroceramide; Sph, sphingosine; dhSph, dihydrosphingosine; S1P, sphingosine-1-phosphate; SM, sphingomyelin; dhSM, dihydrosphingomyelin

Ceramides (pmol/μg PC)

$C_{16:0}$-Cer

Hours	**Control**	**γTE 20 μM**
8	2.19 ± 0.23	0.95 ± 0.22**
16	2.41 ± 0.22	2.17 ± 0.24
24	2.09 ± 0.17	3.96 ± 0.76**

$C_{18:0}$-Cer

Hours	**Control**	**γTE 20 μM**
8	0.038 ± 0.006	0.033 ± 0.006*
16	0.028 ± 0.003	0.082 ± 0.013**
24	0.025 ± 0.003	0.14 ± 0.027**

$C_{20:0}$-Cer

Hours	**Control**	**γTE 20 μM**
8	0.023 ± 0.004	0.017 ± 0.005*
16	0.020 ± 0.003	0.042 ± 0.009**
24	0.018 ± 0.003	0.065 ± 0.014**

$C_{22:0}$-Cer

Hours	**Control**	**γTE 20 μM**
8	0.20 ± 0.031	0.068 ± 0.010**
16	0.26 ± 0.086	0.095 ± 0.018**
24	0.21 ± 0.056	0.15 ± 0.030

$C_{24:1}$-Cer

Hours	**Control**	**γTE 20 μM**
8	1.02 ± 0.26	0.47 ± 0.16**
16	1.79 ± 0.22	0.66 ± 0.082**
24	1.47 ± 0.18	0.94 ± 0.20**

$C_{24:0}$-Cer

Hours	**Control**	**γTE 20 μM**
8	1.22 ± 0.22	0.30 ± 0.10**
16	2.56 ± 0.29	0.35 ± 0.057**
24	2.10 ± 0.24	0.44 ± 0.10**

$C_{26:1}$-Cer

Hours	**Control**	**γTE 20 μM**
8	0.096 ± 0.008	0.067 ± 0.013*
16	0.23 ± 0.036	0.11 ± 0.021**
24	0.18 ± 0.027	0.15 ± 0.040

$C_{26:0}$-Cer

Hours	**Control**	**γTE 20 μM**
8	0.090 ± 0.006	0.031 ± 0.015*
16	0.15 ± 0.046	0.043 ± 0.014**
24	0.13 ± 0.037	0.049 ± 0.018**

Total Cers

Hours	**Control**	**γTE 20 μM**
8	4.88 ± 0.25	1.93 ± 0.18**
16	7.44 ± 0.75	3.54 ± 0.29**
24	6.22 ± 0.56	5.88 ± 1.04

Dihydroceramides (pmol/μg PC)

$C_{16:0}$-dhCer

Hours	**Control**	**γTE 20 μM**
8	0.091 ± 0.030	0.31 ± 0.036
16	0.18 ± 0.027	2.22 ± 0.18**
24	0.21 ± 0.031	4.09 ± 0.78**

$C_{18:0}$-dhCer

Hours	**Control**	**γTE 20 μM**
8	0.0018 ± 0.0003	0.011 ± 0.003*
16	0.0010 ± 0.0001	0.1 ± 0.025**
24	0.0013 ± 0.0002	0.17 ± 0.034**

$C_{20:0}$-dhCer

Hours	**Control**	**γTE 20 μM**
8	0.00029 ± 0.0002	0.0066 ± 0.0026
16	0.00092 ± 0.0003	0.042 ± 0.013**
24	0.0011 ± 0.0003	0.06 ± 0.013**

$C_{22:0}$-dhCer

Hours	**Control**	**γTE 20 μM**
8	0.0038 ± 0.0014	0.018 ± 0.0046*
16	0.0074 ± 0.0037	0.033 ± 0.0077**
24	0.0090 ± 0.0034	0.042 ± 0.0082**

$C_{24:1}$-dhCer

Hours	**Control**	**γTE 20 μM**
8	0.010 ± 0.004	0.060 ± 0.010*
16	0.021 ± 0.006	0.14 ± 0.016**
24	0.031 ± 0.003	0.17 ± 0.026**

$C_{24:0}$-dhCer

Hours	**Control**	**γTE 20 μM**
8	0.010 ± 0.004	0.035 ± 0.007*
16	0.046 ± 0.011	0.075 ± 0.004*
24	0.059 ± 0.014	0.084 ± 0.015

$C_{26:1}$-dhCer

Hours	**Control**	**γTE 20 μM**
8	0.00063 ± 0.0004	0.0093 ± 0.002
16	0.0025 ± 0.001	0.037 ± 0.010**
24	0.0027 ± 0.001	0.034 ± 0.011*

$C_{26:0}$-dhCer

Hours	**Control**	**γTE 20 μM**
8	0.00069 ± 0.0007	0.0022 ± 0.0011
16	0.00092 ± 0.0007	0.011 ± 0.0060
24	0.0013 ± 0.0008	0.0063 ± 0.0054

Total dhCers

Hours	**Control**	**γTE 20 μM**
8	0.12 ± 0.035	0.45 ± 0.045
16	0.26 ± 0.029	2.66 ± 0.16**
24	0.32 ± 0.035	4.65 ± 0.82**

Sphingoid bases (pmol/μg PC)

Sph

Hours	**Control**	**γTE 20 μM**
8	0.42 ± 0.18	0.40 ± 0.11
16	0.30 ± 0.080	0.40 ± 0.053
24	0.30 ± 0.067	0.48 ± 0.048*

dhSph

Hours	**Control**	**γTE 20 μM**
8	0.046 ± 0.013	0.12 ± 0.015
16	0.043 ± 0.007	2.46 ± 0.39*
24	0.051 ± 0.007	5.89 ± 0.98**

S1P

Hours	**Control**	**γTE 20 μM**

8	0.021 ± 0.002	0.019 ± 0.004
16	0.0087 ± 0.001	0.012 ± 0.002
24	0.013 ± 0.005	0.016 ± 0.002

Sphingomyelins (pmol/μg PC)

$C_{16:0}$-SM

Hours	**Control**	**γTE 20 μM**
8	39.09 ± 8.17	26.99 ± 4.48**
16	56.18 ± 6.99	37.93 ± 4.40**
24	52.58 ± 7.07	37.78 ± 5.14**

$C_{18:0}$-SM

Hours	**Control**	**γTE 20 μM**
8	0.47 ± 0.19	0.44 ± 0.14
16	0.63 ± 0.15	1.12 ± 0.20**
24	0.53 ± 0.12	1.55 ± 0.32**

$C_{20:0}$-SM

Hours	**Control**	**γTE 20 μM**
8	0.43 ± 0.18	0.40 ± 0.17*
16	0.53 ± 0.12	0.81 ± 0.22*
24	0.51 ± 0.13	0.95 ± 0.25*

$C_{22:0}$-SM

Hours	**Control**	**γTE 20 μM**
8	1.62 ± 0.69	1.57 ± 0.66
16	2.17 ± 0.45	2.65 ± 0.72
24	2.64 ± 1.03	3.20 ± 1.29

$C_{24:1}$-SM

Hours	**Control**	**γTE 20 μM**
8	6.23 ± 2.44	6.32 ± 2.22
16	8.72 ± 1.66	9.65 ± 2.07
24	10.37 ± 3.44	10.50 ± 3.77

$C_{26:1}$-SM

Hours	**Control**	**γTE 20 μM**
8	0.29 ± 0.13	0.36 ± 0.16**
16	0.40 ± 0.094	0.76 ± 0.18**
24	0.60 ± 0.27	1.00 ± 0.44*

Total SMs

Hours	**Control**	**γTE 20 μM**
8	48.13 ± 11.76	36.09 ± 7.71**

16	68.62 ± 9.02	52.91 ± 7.62**
24	67.23 ± 11.73	54.99 ± 10.54*

Dihydrosphingomyelins (pmol/μg PC)

$C_{16:0}$-dhSM

Hours	**Control**	**γTE 20 μM**
8	5.25 ± 1.88	6.48 ± 2.13
16	7.32 ± 1.58	18.73 ± 3.42**
24	7.72 ± 1.62	26.29 ± 4.98**

$C_{18:0}$-dhSM

Hours	**Control**	**γTE 20 μM**
8	0.13 ± 0.074	0.19 ± 0.093
16	0.11 ± 0.032	1.13 ± 0.25**
24	0.12 ± 0.030	1.54 ± 0.37**

$C_{20:0}$-dhSM

Hours	**Control**	**γTE 20 μM**
8	0.24 ± 0.20	0.15 ± 0.092
16	0.10 ± 0.035	0.56 ± 0.14**
24	0.12 ± 0.038	0.74 ± 0.23**

$C_{22:0}$-dhSM

Hours	**Control**	**γTE 20 μM**
8	0.30 ± 0.20	0.35 ± 0.24
16	0.26 ± 0.11	0.82 ± 0.27**
24	0.34 ± 0.12	0.96 ± 0.38**

$C_{24:0}$-dhSM

Hours	**Control**	**γTE 20 μM**
8	0.41 ± 0.33	0.41 ± 0.32
16	0.37 ± 0.22	0.73 ± 0.27**
24	0.51 ± 0.21	0.94 ± 0.36*

$C_{26:0}$-dhSM

Hours	**Control**	**γTE 20 μM**
8	0.031 ± 0.027	0.032 ± 0.025
16	0.025 ± 0.013	0.15 ± 0.052**
24	0.034 ± 0.015	0.24 ± 0.094*

Total dhSMs

Hours	**Control**	**γTE 20 μM**
8	6.37 ± 2.72	7.61 ± 2.89
16	8.19 ± 1.92	22.13 ± 4.32**

24	8.84 ± 1.98	30.71 ± 6.19**

Table 2.2 Effect of γTE on sphingolipid metabolism in MCF-7 cells. MCF-7 cells were treated with 20 μM γTE for 8, and 16 h. The amount of each sphingolipid was determined by LC-MS/MS. Data are mean ± SEM of 5 independent experiments. *p < 0.05, **p < 0.01, significant difference between control and γTE-treated cells.

Ceramides (pmol/μg PC)

$C_{16:0}$-Cer

Hours	**Control**	**γTE 20 μM**
8	1.68 ± 0.28	1.32 ± 0.29*
16	1.90 ± 0.30	3.61 ± 0.89**

$C_{18:0}$-Cer

Hours	**Control**	**γTE 20 μM**
8	0.15 ± 0.030	0.12 ± 0.023
16	0.16 ± 0.029	0.39 ± 0.13**

$C_{20:0}$-Cer

Hours	**Control**	**γTE 20 μM**
8	0.039 ± 0.009	0.035 ± 0.009
16	0.039 ± 0.008	0.10 ± 0.031**

$C_{22:0}$-Cer

Hours	**Control**	**γTE 20 μM**
8	0.20 ± 0.040	0.16 ± 0.042
16	0.22 ± 0.057	0.34 ± 0.12*

$C_{24:1}$-Cer

Hours	**Control**	**γTE 20 μM**
8	6.08 ± 1.91	4.44 ± 1.11
16	6.98 ± 2.22	7.66 ± 2.29

$C_{24:0}$-Cer

Hours	**Control**	**γTE 20 μM**
8	1.32 ± 0.41	0.75 ± 0.18**
16	1.44 ± 0.42	0.99 ± 0.31**

$C_{26:1}$-Cer

Hours	**Control**	**γTE 20 μM**
8	0.12 ± 0.037	0.092 ± 0.022
16	0.18 ± 0.043	0.11 ± 0.036**

$C_{26:0}$-Cer

Hours	**Control**	**γTE 20 μM**
8	0.019 ± 0.011	0.018 ± 0.009
16	0.028 ± 0.015	0.017 ± 0.009

Total Cers

Hours	**Control**	**γTE 20 μM**
8	9.61 ± 2.41	6.93 ± 1.38
16	10.96 ± 2.70	13.21 ± 3.26

Dihydroceramides (pmol/μg PC)

$C_{16:0}$-dhCer

Hours	**Control**	**γTE 20 μM**
8	0.11 ± 0.030	0.22 ± 0.047
16	0.15 ± 0.036	1.76 ± 0.43**

$C_{18:0}$-dhCer

Hours	**Control**	**γTE 20 μM**
8	0.0036 ± 0.001	0.0056 ± 0.001
16	0.0033 ± 0.0005	0.10 ± 0.036*

$C_{20:0}$-dhCer

Hours	**Control**	**γTE 20 μM**
8	0.00058 ± 0.0001	0.0016 ± 0.0003*
16	0.00090 ± 0.0002	0.022 ± 0.0080**

$C_{22:0}$-dhCer

Hours	**Control**	**γTE 20 μM**
8	0.0017 ± 0.0003	0.0041 ± 0.001
16	0.0029 ± 0.0005	0.030 ± 0.009*

$C_{24:1}$-dhCer

Hours	**Control**	**γTE 20 μM**
8	0.025 ± 0.010	0.098 ± 0.026*
16	0.036 ± 0.016	0.33 ± 0.095*

$C_{24:0}$-dhCer

Hours	**Control**	**γTE 20 μM**
1	0.00093 ± 0.0009	0.0061 ± 0.0053
2	0.0019 ± 0.0012	0.028 ± 0.016

Total dhCers

Hours	**Control**	**γTE 20 μM**
8	0.14 ± 0.036	0.34 ± 0.064*
16	0.20 ± 0.042	2.28 ± 0.52**

Sphingoid bases (pmol/μg PC)

Sph

Hours	**Control**	**γTE 20 μM**
8	0.72 ± 0.14	0.40 ± 0.10*
16	0.80 ± 0.17	0.58 ± 0.11**

dhSph

Hours	**Control**	**γTE 20 μM**
8	0.047 ± 0.014	0.054 ± 0.019
16	0.059 ± 0.016	0.21 ± 0.058**

S1P

Hours	**Control**	**γTE 20 μM**
8	0.019 ± 0.004	0.021 ± 0.003
16	0.019 ± 0.005	0.017 ± 0.005

Sphingomyelins (pmol/μg PC)

$C_{16:0}$-SM

Hours	**Control**	**γTE 20 μM**
8	20.72 ± 7.15	19.42 ± 4.81
16	25.80 ± 7.59	20.93 ± 5.51**

$C_{18:0}$-SM

Hours	**Control**	**γTE 20 μM**
8	1.46 ± 0.34	1.51 ± 0.19
16	1.79 ± 0.21	1.70 ± 0.22

$C_{20:0}$-SM

Hours	**Control**	**γTE 20 μM**
8	1.02 ± 0.13	1.16 ± 0.030
16	1.37 ± 0.073	1.50 ± 0.088

$C_{22:0}$-SM

Hours	**Control**	**γTE 20 μM**
8	1.44 ± 0.67	1.54 ± 0.57
16	1.86 ± 0.67	2.05 ± 0.85

$C_{24:1}$-SM

Hours	**Control**	**γTE 20 μM**
8	10.15 ± 3.43	10.40 ± 2.67
16	12.38 ± 3.41	11.44 ± 2.94

$C_{26:1}$-SM

Hours	**Control**	**γTE 20 μM**

8	3.32 ± 0.53	3.84 ± 0.42
16	4.29 ± 0.89	5.23 ± 0.48

Total SMs

Hours	**Control**	**γTE 20 μM**
8	38.11 ± 12.10	37.86 ± 8.36
16	47.50 ± 12.38	42.85 ± 9.89

Dihydrosphingomyelins (pmol/μg PC)

$C_{16:0}$-dhSM

Hours	**Control**	**γTE 20 μM**
8	3.69 ± 1.00	5.66 ± 0.95**
16	4.81 ± 0.94	10.91 ± 1.51**

$C_{18:0}$-dhSM

Hours	**Control**	**γTE 20 μM**
8	0.29 ± 0.078	0.50 ± 0.067
16	0.36 ± 0.045	1.10 ± 0.037**

$C_{20:0}$-dhSM

Hours	**Control**	**γTE 20 μM**
8	0.29 ± 0.044	0.48 ± 0.078**
16	0.41 ± 0.064	1.09 ± 0.092**

$C_{22:0}$-dhSM

Hours	**Control**	**γTE 20 μM**
8	0.17 ± 0.048	0.23 ± 0.048
16	0.21 ± 0.042	0.43 ± 0.11*

$C_{24:0}$-dhSM

Hours	**Control**	**γTE 20 μM**
8	0.13 ± 0.031	0.21 ± 0.023
16	0.17 ± 0.011	0.41 ± 0.031**

$C_{26:0}$-dhSM

Hours	**Control**	**γTE 20 μM**
8	0.056 ± 0.014	0.069 ± 0.025
16	0.11 ± 0.057	0.17 ± 0.043

Total dhSMs

Hours	**Control**	**γTE 20 μM**
8	4.62 ± 1.16	7.14 ± 1.03*
16	6.07 ± 0.97	14.11 ± 1.52**

Table 2.3 Effect of γTE on *de novo* sphingolipid biosynthesis in HCT-116 cells. HCT-116 cells were treated with either 400 μM $^{13}C_3$, ^{15}N-labeled L-serine alone as control or with a combination of 400 μM $^{13}C_3$, ^{15}N-labeled L-serine and 20 μM γTE for 0.5, 2, 3, and 6 h. The amount of each labeled *de novo* sphingolipid was determined by LC-MS/MS. Data are mean ± SEM of 3 independent experiments. *p < 0.05, **p < 0.01, significant difference between control and γTE-treated cells.

Ceramides (pmol/μg PC)

***De novo* $C_{16:0}$-Cer**

Hours	**Control**	**γTE 20 μM**
0.5	0.10 ± 0.018	0.090 ± 0.015
2	0.54 ± 0.025	0.44 ± 0.023**
3	0.65 ± 0.045	0.35 ± 0.033**
6	0.64 ± 0.004	0.19 ± 0.008**

***De novo* $C_{24:1}$-Cer**

Hours	**Control**	**γTE 20 μM**
0.5	0.16 ± 0.024	0.15 ± 0.008
2	0.69 ± 0.087	0.78 ± 0.15
3	0.85 ± 0.096	0.80 ± 0.029
6	0.89 ± 0.029	0.55 ± 0.029**

***De novo* $C_{24:0}$-Cer**

Hours	**Control**	**γTE 20 μM**
0.5	0.13 ± 0.020	0.12 ± 0.003
2	0.52 ± 0.069	0.55 ± 0.10
3	0.68 ± 0.087	0.57 ± 0.049*
6	0.88 ± 0.086	0.43 ± 0.027**

***De novo* total Cers**

Hours	**Control**	**γTE 20 μM**
0.5	0.38 ± 0.058	0.36 ± 0.023
2	1.75 ± 0.18	1.77 ± 0.27
3	2.18 ± 0.20	1.71 ± 0.060*
6	2.41 ± 0.12	1.18 ± 0.050**

Dihydroceramides (pmol/μg PC)

***De novo* $C_{16:0}$-dhCer**

Hours	**Control**	**γTE 20 μM**
0.5	0.011 ± 0.002	0.010 ± 0.002

2	0.026 ± 0.005	0.039 ± 0.011*
3	0.030 ± 0.006	0.052 ± 0.012**
6	0.042 ± 0.007	0.11 ± 0.022**

***De novo* $C_{24:1}$-dhCer**

Hours	**Control**	**γTE 20 µM**
0.5	0.00094 ± 0.0003	0.0015 ± 0.0006
2	0.0025 ± 0.001	0.0062 ± 0.003
3	0.0025 ± 0.0009	0.0074 ± 0.002
6	0.0038 ± 0.0009	0.021 ± 0.004*

***De novo* $C_{24:0}$-dhCer**

Hours	**Control**	**γTE 20 µM**
0.5	0.0010 ± 0.001	0.0018 ± 0.001
2	0.0031 ± 0.002	0.0033 ± 0.002
3	0.0025 ± 0.001	0.0048 ± 0.003
6	0.0051 ± 0.003	0.012 ± 0.006

***De novo* total dhCers**

Hours	**Control**	**γTE 20 µM**
0.5	0.013 ± 0.003	0.014 ± 0.003
2	0.032 ± 0.007	0.049 ± 0.015*
3	0.035 ± 0.008	0.064 ± 0.016**
6	0.051 ± 0.010	0.15 ± 0.032**

Sphingoid bases (pmol/µg PC)

***De novo* Sph**

Hours	**Control**	**γTE 20 µM**
0.5	0.038 ± 0.024	0.022 ± 0.011
2	0.072 ± 0.021	0.062 ± 0.005
3	0.065 ± 0.008	0.054 ± 0.021
6	0.078 ± 0.008	0.034 ± 0.012**

Sphingomyelins (pmol/µg PC)

***De novo* $C_{16:0}$-SM**

Hours	**Control**	**γTE 20 µM**
0.5	0.35 ± 0.10	0.31 ± 0.071
2	0.77 ± 0.21	0.97 ± 0.29*
3	1.18 ± 0.40	1.43 ± 0.32
6	2.74 ± 0.64	2.61 ± 0.50

***De novo* $C_{18:0}$-SM**

Hours	**Control**	**γTE 20 µM**
0.5	0.011 ± 0.003	0.011 ± 0.002
2	0.013 ± 0.002	0.012 ± 0.004
3	0.012 ± 0.004	0.016 ± 0.005
6	0.024 ± 0.004	0.045 ± 0.014*

***De novo* $C_{24:1}$-SM**

Hours	**Control**	**γTE 20 µM**
0.5	0.11 ± 0.031	0.14 ± 0.029
2	0.18 ± 0.051	0.24 ± 0.077**
3	0.27 ± 0.090	0.38 ± 0.16
6	0.54 ± 0.12	1.47 ± 0.73

***De novo* total SMs**

Hours	**Control**	**γTE 20 µM**
0.5	0.47 ± 0.13	0.45 ± 0.10
2	0.96 ± 0.27	1.22 ± 0.37**
3	1.46 ± 0.50	1.83 ± 0.48
6	3.31 ± 0.76	4.13 ± 1.22

Dihydrosphingomyelins (pmol/µg PC)

***De novo* $C_{16:0}$-dhSM**

Hours	**Control**	**γTE 20 µM**
0.5	0.10 ± 0.020	0.10 ± 0.012
2	0.18 ± 0.029	0.27 ± 0.055*
3	0.24 ± 0.039	0.39 ± 0.084**
6	0.52 ± 0.045	1.51 ± 0.17**

2.5 Discussion

Our current study demonstrates that γTE induced apoptosis and autophagy in human colon cancer cells by modulating sphingolipids metabolism. γTE treatment caused huge accumulation of intracellular dhSph and dhCers, important sphingolipid intermediates in *de novo* biosynthesis pathway, which appear to mediate cell death (Ahn and Schroeder, 2002; Jiang et al., 2004). In particular, γTE led to increase in *de novo* dhCers and decrease in *de novo* Cers as early as after 2 h incubation and these changes intensified during prolonged treatment, supporting the notion that DEGS is inhibited by γTE. Consistently, γTE inhibited DEGS activity without affecting its protein expression. Importantly, the modulation of these sphingolipids by γTE occurred prior to any signs of cell death. Moreover, individual Cers, which appear to have distinct bioactivities (Hannun and Obeid, 2011; Senkal et al., 2010; Sentelle et al., 2012), showed different responses by γTE treatment. γTE treatment led to significant decrease in $C_{16:0}$-Cer at 8 h, but showed no difference at 16 h or increase at 24 h, compared with controls. On the other hand, while C_{24}-Cers decreased from 8 to 24 h, $C_{18:0}$-Cer increased from 16 h by γTE. Interestingly, SM decreased from 8 h but cells showed obvious apoptosis or autophagy only at 16 h or longer treatment with γTE. In addition, chemically blocking the increase of dhSph and dhCers, or the increase of Cers via SM hydrolysis by myriocin or desipramine, repectively, partially counteracted γTE-caused cell death, indicating that modulation of sphingolipids plays an important role in γTE-induced cancer cell death.

We showed that γTE led to marked accumulation of dhSph and dhCers in human colon and breast cancer cells. On the other hand, we did not observe a significant increase

of total Cers until the prolonged treatment with γTE. Although sphingosine and Cer have long been recognized and studied as pivotal apoptosis-inducing molecules (Woodcock, 2006), emerging evidence suggests that other sphingolipid intermediates in the *de novo* biosynthesis pathway also play important roles in determining cell fate (Ahn and Schroeder, 2002; Jarvis et al., 1996; Kraveka et al., 2007; Ohta et al., 1995; Signorelli et al., 2009; Solomon et al., 2003; Zheng et al., 2006). For instance, previous studies in our group found that γT, the predominant form of vitamin E in US diet, as well as γTE enhanced the intracellular levels of dhSph and dhCers which played significant roles in the induction of apoptosis and autophagy in human prostate and breast cancer cells (Gopalan et al., 2012; Jiang et al., 2012; Jiang et al., 2004). Consistent with these studies, co-treatment of cells with myriocin, a specific inhibitor of the first reaction in the *de novo* sphingolipid synthesis pathway to block the increase of these two sphingoid bases, partially but significantly reversed γTE-induced colon cancer cell death, indicating that the accumulation of dhSph and dhCers plays important roles in γTE-induced colon cancer cell death.

We identified that DEGS, an enzyme for the conversion of dhCer to Cers, is the initial target of γTE in its modulation of sphingolipid metabolism followed by cancer cell death. Specifically, in the serine-labeled study with γTE to only trace the effect of γTE on *de novo* biosynthesis pathway of sphingolipids, γTE caused rapid increase of *de novo* dhCers, but significant decrease of *de novo* Cers as early as after 2 h incubation, suggesting that DEGS-catalyzed reaction is likely to be inhibited as a result of γTE treatment (Fig. 2.3). Consistently, γTE inhibited DEGS activity in both *in situ* and *in vitro* assays, having no impact on its protein expression (Fig. 2.4). However, it is worth noting

that higher concentration of γTE was needed to have its inhibitory effect on DEGS activity when we used rat liver microsomes as an enzyme source. It may be due to limitation in permeability through the microsomal membrane of γTE under the cell-free environment.

DEGS is a key enzyme regulating the balance of dhCer and Cer as it catalyzes the insertion of a 4,5-*trans*-double bond into dhCer to generate Cer. Michel *et al.* first reported the biochemical characterization of the DEGS reaction in 1997 using rat liver microsomes (Michel et al., 1997). They have shown that the DEGS uses molecular oxygen as electron acceptor to have a hydroxyl group into the C4-position of the dhSph, and then with NADH or NADPH as electron donor, a dehydration reaction occurs to produce a double bond in the C4-C5 position of dhCer. Therefore, they confirmed that the conversion of dhCer to Cer was occurred by a desaturase, not by a dehydrogenase. Two different DEGSs, DEGS1 and DEGS2, have been so far reported. In bioinformatics approach, Ternes *et al.* identified a family of sphingolipid Δ4-desaturases (homologs of the *Drosophila melanogaster* degenerative spermatocyte gene 1 (*des-1*)). DEGS-1, the human homolog of *des-1*, exhibits high dhCer Δ4-desaturase and very low C-4 hydroxylase activities, whereas DEGS2, another ortholog identified in mouse and human, is similarly active as both sphinglipid C-4 hydroxylase and Δ4-desaturase activities, resulting in the production of either phyto-Cer or Cer. Recently, DEGS activity was also found to be inhibited by resveratrol (Signorelli et al., 2009), celecoxib (Schiffmann et al., 2009b), fenretinide (Rahmaniyan et al., 2011), hydrogen peroxide (Idkowiak-Baldys et al., 2010) or hypoxic environment (Devlin et al., 2011). Furthermore, as several phytochemicals are shown to induce oxidative stress as prooxidants (Babich et al., 2011;

Fujisawa et al., 2004; Galati et al., 2002) and oxidative stress can inhibit DEGS activity followed by dhCer accumulation (Idkowiak-Baldys et al., 2010), we investigated whether γTE also inhibits DEGS activity by acting as prooxidant. However, we found that N-acetylcysteine (NAC), an antioxidant, did not reverse γTE-induced modulation of sphingolipid metabolism (Fig. 2.7), suggesting that the inhibition of DEGS by γTE is not affected by NAC and these sphingolipid modulation did not caused by prooxidant effects of γTE.

In addition to the accumulation of dhSph and dhCers, γTE treatment had an impact on Cer species. Interestingly, the effects of γTE on specific Cer species were different. For instance, γTE treatment led to significant decrease in $C_{16:0}$-Cer during the initial phase, but increase in the longer time treatment. While γTE caused increase in $C_{18:0}$-Cer, it led to continuous decreases in $C_{24:1}$- and $C_{24:0}$-Cers. Interestingly, recent emerging results suggest that endogenous Cers with different fatty acyl-chain lengths appear to have distinct bioactivities. $C_{18:0}$-Cer generated by CerS1 has been found to induce apoptosis and lethal autophagy (Senkal et al., 2010; Sentelle et al., 2012). In contrast, $C_{16:0}$-Cer generated by CerS5/6 have been proposed to have opposed roles of anti-apoptosis to $C_{18:0}$-Cer (Senkal et al., 2010). However, several other studies found that this Cer also plays important roles in apoptotic cell death (Mullen et al., 2011; Schiffmann et al., 2009b; White-Gilbertson et al., 2009). Therefore, further investigation should be conducted to determine the role of individual Cer species and to characterize the effects of γTE on individual CerSs and Cers.

During prolonged treatment, γTE led to increase in Cers, especially $C_{16:0}$- and $C_{18:0}$-Cers, but decrease in SMs. Two main enzymes may contribute to the levels of Cers

and SMs, which are SMSs in the *de novo* synthesis pathway and SMases in the SM hydrolysis. In our *de novo* sphingolipids studies using $^{13}C_3$, ^{15}N- L-serine, we found that since labeled $C_{16:0}$-Cer is still decreased and the conversion of $C_{16:0}$-Cer to $C_{16:0}$-SM is stimulated at the initial stage of γTE treatment, we reason that the increase of Cers in the longer time treatment is likely caused by SM hydrolysis via the action of SMases. Co-treatment of cells with desipramine but not GW4869 partially but significantly counteracted γTE-induced cancer cell death, indicating that the increase of Cers from SMs through acid SMase-catalyzed SM hydrolysis may in part involved in γTE-induced colon cancer cell death.

In summary, our data strongly suggest that γTE-induced apoptosis, autophagy and cell death are mediated by modulation of sphingolipid metabolism as its primary target. The lipidomic analysis using LC-MS/MS reveals that γTE-exerted anticancer effects are caused by initial inhibition of DEGS activity and subsequent activation of SM hydrolysis via acid SMase.

CHAPTER 3. 13'-CARBOXYCHROMANOLS, LONG-CHAIN VITAMIN E METABOLITES, INDUCE APOPTOSIS AND AUTOPHAGY BY MODULATING SPHINGOLIPID METABOLISM IN DIFFERENT TYPES OF CANCER CELLS

3.1 Abstract

13'-Carboxychromanol (13'-COOH) is a major vitamin E metabolite excreted in feces. Here we investigated anticancer activities of δT-13'-COOH and δTE-13'-COOH, which are metabolites of delta-tocopherol (δT) or delta-tocotrienol (δTE), respectively. Both 13'-COOHs inhibited the growth and induced apoptosis and autophagy in human colon (HCT-116, HT-29), breast (MCF-7), and pancreatic (PANC-1, MiaPaca-2) cancer cells with the IC_{50} of 8-20 μM. In these activities, 13'-COOHs were much stronger than tocopherols. Using liquid chromatography tandem mass spectrometry, we found that δT-13'-COOH increased intracellular dihydrosphingosin and dihydroceramides but decreased $C_{16:0}$-ceramide within 2 h treatment. During longer treatment, δT-13'-COOH enhanced all sphingoid bases including ceramides while decreased sphingomyelins. Modulation of sphingolipids by 13'-COOHs was observed prior to or coinciding with appearance of cell death markers including PARP cleavage and LC3-II increase. The importance of sphingolipid modulation was supported by the observation that pharmaceutically blocking the increase of these sphingolipids partially counteracted 13'-

COOH-induced cell death. Further mechanistic studies indicated that 13'-COOH inhibited dihydroceramide desaturase without affecting its protein expression and may activate sphingomyelin hydrolysis to enhance ceramides. In agreement with these cell-based studies, δTE-13'-COOH significantly decreased colon tumor multiplicity induced by AOM with two cycles of 1.5% DSS without any apparent toxicity even when the dietary supplementation was started after AOM injection. Moreover, δTE-13'-COOH attenuated 1.8% DSS-induced colon inflammation, indicating that δTE-13'-COOH is able to attenuate colitis and its promoted tumorigenesis *in vivo*. Our mechanistic study demonstrates that 13'-COOHs have potent anticancer effects by modulating enzyme activities in sphingolipid metabolism in cancer cells.

3.2 Introduction

Cumulative cancer risk is estimated to be 30% and 22% in men and women, respectively, by age 75 in developed area worldwide (Jemal et al., 2011). Natural forms of vitamin E that consist of α-, β-, γ- and δ-tocopherol (αT, βT, γT and δT) and α-, β-, γ- and δ-tocotrienol (αTE, βTE, γTE and δTE), are potentially good cancer chemoprevention agents as they are known to be safe and specific forms of vitamin E have been shown to have cancer prevention effects. Specifically, γT, mixed tocopherols and tocotrienols have been demonstrated to inhibit the development of colon, prostate and breast cancer in various preclinical models (Jiang, 2014; Moya-Camarena and Jiang, 2012). Despite these exciting findings, the anticancer effects may not directly be rooted

in vitamin E *alone* because many forms of vitamin E are not highly bioavailable as a result of their extensive metabolism *in vivo*.

Tocopherols and tocotrienols, with exception for αT, are readily metabolized by cytochrome P450-catalyzed ω-hydroxylation and oxidation to 13'-carboxychromanols (13'-COOH), which are then further catabolized via β-oxidation to generate various shorter chain carboxychromanols or sulfation to form sulfated carboxychromanols (Jiang, 2014; Jiang et al., 2007; Sontag and Parker, 2002). Importantly, carboxychromanols and their sulfated counterparts have been detected in rodent plasma and liver upon supplementation of γT and γTE (Freiser and Jiang, 2009; Jiang et al., 2007). Recently, long-chain carboxychromanols are found at high levels in feces from mice fed diet supplemented with γT or δT, and 13'-COOHs appear to be major fecal excreted carboxychromanols (Bardowell et al., 2012a; Bardowell et al., 2012b; Jiang et al., 2013). Considering significant quantities of carboxychromanols *in vivo*, it is of importance to examine potential bioactivities of these metabolites.

Emerging studies have demonstrated that long-chain carboxychromanols have interesting bioactivities that are relevant to disease prevention and therapy (Jiang, 2014). In particular, we have demonstrated that δT-13'-COOH, a long-chain carboxychromanol from δT, competitively inhibits cyclooxygenase (COX-1 and COX-2) (Jiang et al., 2008) and is much stronger than short-chain carboxychromanols and unmetabolized vitamin E forms in these effects. δT-13'-COOH also inhibits 5-lipoxygenase (5-LOX) activity, whereas vitamin E forms do not inhibit the enzyme directly (Jiang et al., 2011). These results indicate that δT-13'-COOH is a unique dual inhibitor of COX-1/COX-2 and 5-LOX (Jiang, 2014; Jiang et al., 2008; Jiang et al., 2011), and is therefore useful as anti-

inflammatory and anticancer agents as both COXs and 5-LOX have been recognized to play significant roles in inflammation and cancer (Wang and Dubois, 2010). In addition, Birringer *et al.* (Birringer et al., 2010) demonstrated that 13'-COOHs metabolized from αT or δT induced apoptosis in human HepG2 cells. However, the anticancer study of 13'-COOHs was limited to this liver cell line and the underlying mechanism was not completely understood. In the present study, we investigated the effect of δT-13'-COOH and δTE-13'-COOH (a metabolite from δTE) (Fig. 3.1) on the proliferation of various types of cancer cells including colon, pancreas, and breast. Since vitamin E forms have been shown to exert anticancer effects via modulating sphingolipids (Jiang et al., 2012; Jiang et al., 2004), we further investigated whether 13'-COOHs are capable of altering sphingolipid metabolism and the role of modulation of sphingolipids in 13'-COOH-exerted anticancer activities. We also examined the anti-inflammatory effects and anticancer efficacy of δTE-13'-COOH supplementation against DSS-caused colon inflammation and AOM-induced and DSS-promoted colon tumorigenesis in male Balb/c mice, respectively.

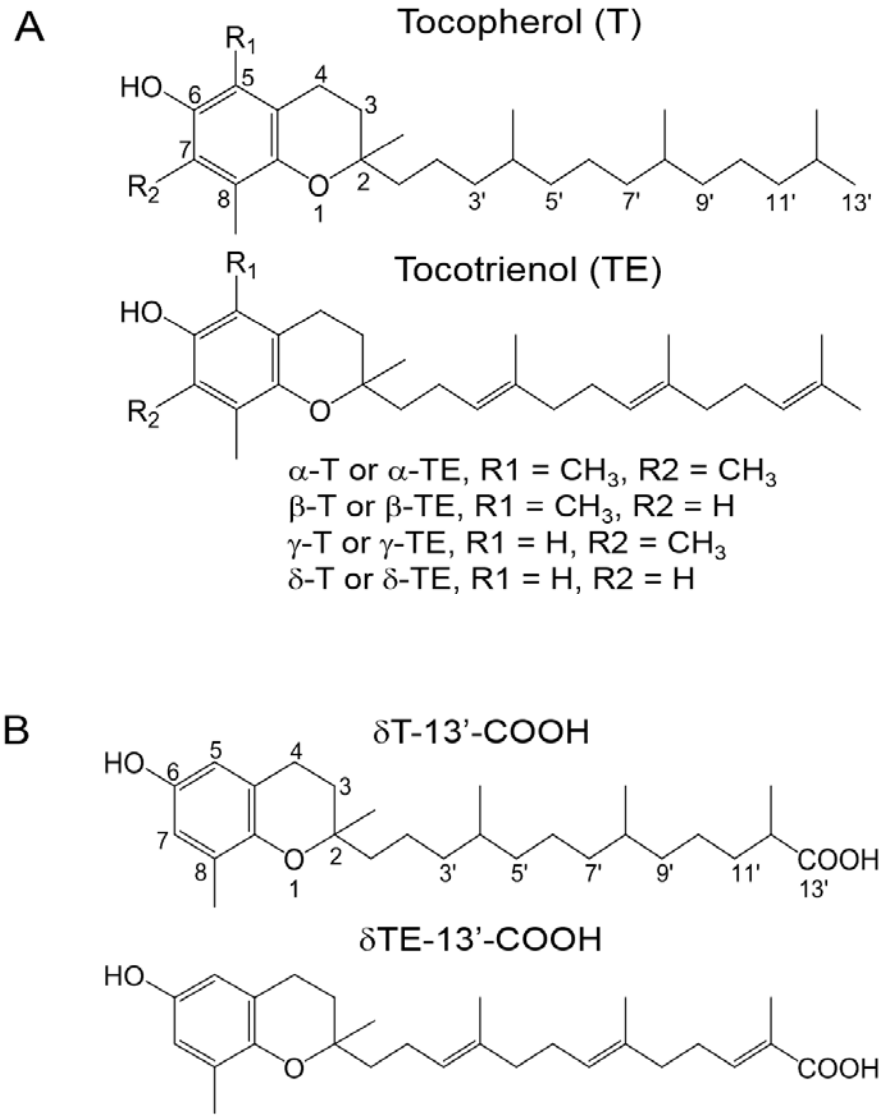

Figure 3.1 The structures of (A) natural forms of vitamin E and (B) 13'-COOHs, vitamin E metabolites of δT and δTE.

3.3 Materials and Methods

3.3.1 Materials and reagents

δT-13'-COOH and δTE-13'-COOH (>95% pure) were synthesized as previously described (Maloney and Hecht, 2005). γT (≥96%) and δT (93-97%) were purchased from Sigma (St Louis, MO) and Suppleco (Bellefonte, PA), and γTE (97-99%) was a gift from BASF (Ludwigshafen, Germany). C8-cyclopropenylceramide (C8-CPPC) was purchased from Matreya LLC (Pleasant Gap, PA). All sphingolipid standards were obtained from Avanti Polar Lipids (Alabaster, AL). CHAPS (3-((3-cholamidopropyl) dimethylammonio)-1-propanesulfonate) was purchased from Thermo Fisher Scientific. Myriocin from *Mycelia Sterilia*, $^{13}C_3$, ^{15}N-labeled L-serine, dimethyl sulfoxide (DMSO), [3-(4,5)-dimethylthiazol-2-yl]-2,5-diphenyl tetrazolium bromide] (MTT), and all other chemicals were from Sigma.

3.3.2 Cell culture and treatment

Human colon (HCT-116 and HT-29), breast (MCF-7), and pancreatic (PANC-1 and MiaPaCa-2) cancer cells, and human normal colonic epithelial CCD841CoN cells were obtained from American Type Culture Collection (Manassas, VA). Cells were routinely cultured in growth media containing 10% fetal bovine serum (FBS) at 37 °C in 5% CO_2. HT-29 and PANC-1 cells were cultured in Dulbecco's modified eagle medium (DMEM), and HCT-116 cells were cultured in McCoy's 5A modified medium. MCF-7 and MiaPaCa-2 cells were incubated in DMEM supplemented with 2.5% horse serum or 0.1% insulin, respectively. CCD841CoN cells were cultured in Eagle's minimum

essential medium (EMEM). For experiments, cells were seeded in the corresponding medium with 10% FBS either at a density of 4 x 10^4 cells/well in 24-well plates or at a density of 7-8 x 10^5 cells in 10-cm dishes. After overnight attachment, media were replaced with fresh DMEM containing 1% FBS and 13'-COOHs or other compounds. All the treatment solutions were freshly prepared for each experiment. Vitamin E forms were dissolved in DMSO at 100 mM and then diluted to fatty acid-free BSA (10 mg/ml).

3.3.3 MTT assay

Cell viability was examined by MTT assay to estimate mitochondrial dehydrogenase activity as previously described (Jiang et al., 2004).

3.3.4 Flow cytometry with Annexin V and Propidium Iodide staining

Both floating and attached cells were collected by trypsinization after treatment. Cells were stained with Annexin-V-Flous staining kit (Roche Applied Science, Indianapolis, IN), and apoptosis (Annexin V: Ex = 488 nm; Em = 518 nm) and necrosis (Propidium Iodide: Ex = 488-540 nm; Em = 617 nm) were evaluated by Beckman Coulter FC500 (Beckman Coulter, Miami, FL) and BD FACS Aria III cell sorter (BD Biosciences, San Jose, CA) with FlowJo software system.

3.3.5 Western Blotting

Cells were lysed in lysis buffer containing Tris-EDTA, 1% SDS, 2 mM Na_3VO_4 and protease inhibitor cocktails (Sigma). Total proteins were quantified by bicinchoninic acid (BCA) protein assay kit (Pierce, Rockford, IL) and were denatured by boiling in

Laemmli buffer (Bio-rad, Hercules, CA) for 5 min at 95 °C. Equal amount of proteins (15-30 μg) were separated on acrylamide gels by SDS-electrophoresis and then transferred onto a polyvinylidene fluoride (PVDF) membrane (Millipore, Bilerica, MA), and probed by antibodies. Membranes were exposed to chemiluminescent reagent (PerkinElmer, Waltham, MA) and visualized on Kodak film with an M35A X-Omat processor (Kodak, Rochester, NY). The antibodies used in the study were as follows: membrane bound microtubule-associated protein light chain 3 (LC3; MBL international, Woburn, MA), Caspase-9, poly (ADP-ribose) polymerase-1 (PARP-1) and Actin (Santa Cruz Biotechnology, Santa Cruz, CA), and DEGS1 (Novus Biologicals, Littleton, CO).

3.3.6 Lipid extraction

Lipid was extracted as previously described (Merrill et al., 2005). Briefly, cell pellets were resuspended in 500 μL of methanol, 250 μL of chloroform and 50 μL of water after the addition of 20 μL of internal standard mixture containing 25 μM of $C_{12:0}$-ceramide, $C_{25:0}$-ceramide, C_{17}-sphingosine, C_{17}-sphinganine, and $C_{12:0}$-sphingomyelin (Avanti Polar Lipids, Alabaster, AL). The suspension was dispersed fully by tip sonication for 20 sec and then incubated overnight at 48 °C. 100 μL of solvent was used to determine the amount of total choline-containing phospholipids by an enzymatic colorimetric assay (Wako chemicals, Osaka, Japan) (Jiang et al., 2004). 75 μL of 1M potassium hydroxide in methanol was added to the rest of the solvent and sonicated for 30 min. After sonication, samples were incubated at 37 °C for 2 h and evaporated under a stream of nitrogen.

3.3.7 Measurement of sphingolipids using liquid chromatography tandem mass spectrometry (LC-MS/MS)

Samples were resolved in methanol and sonicated to disperse, then centrifuged to clarify before transferring to test vials for quantification. The LC-MS/MS analyses were performed using the Agilent 6460 triple quadrupole mass spectrometer coupled with the Agilent 1200 Rapid Resolution HPLC (Agilent Technologies, Santa Clara, CA) with detection of sphingolipids in positive mode by multiple reaction monitoring (MRM) technique (Merrill et al., 2005). The HPLC mobile phases consisted of methanol-H_2O-formic acid (74:25:1, v/v/v; RA) and methanol-formic acid (99:1, v/v; RB); both RA and RB contain 5 mM ammonium formate. For measurement of Cers and sphingoid bases, Agilent column XDB-C18, particle size 1.8 μm, 4.6 x 50 mm was used with isocratic run (100% B) or gradient (0-1 min, 20% B, 10-13 min, 100% B and 15-20 min at 20% B), respectively. For measurement of SMs, Agilent Zorbax XDB-C8, particle size 3.5 μm, 2.1 x 50 mm was used with gradient (0-1 min, 20% B, 10-20 min, 100% B, 22-30 min, 20% B). The MS/MS parameters were as follows: gas temperature, 325-350 °C; gas flow rate, 7-10 L/min; nebulizer pressure, 45-50 psi; capillary voltage, 3500 V; The fragmentor voltage was 100 V and collision energy was 12-20 V. Precursor-to-product ion transitions for each sphingolipid were used according to the method of Merrill *et al.* (Merrill et al., 2005).

3.3.8 *De novo* sphingolipids analysis

HCT-116 cells were treated with either 400 μM $^{13}C_3$, ^{15}N-labeled L-serine alone or with a combination of 400 μM $^{13}C_3$, ^{15}N-labeled L-serine and 20 μM of δT-13'-COOH

for 0.5, 1, 1.5, 2 and 4 h. Lipid was extracted and *de novo* synthesized sphingolipids were measured using LC-MS/MS.

3.3.9 Dihydroceramide desaturase (DEGS) assay

For the *in vitro* assay of DEGS, HCT-116 cells were treated with either 20 μM δT-13'-COOH or 1 μM C8-CPPC for 1 or 2 h. Cells were collected and homogenized in a buffer (5 mM Hepes, pH 7.4, containing 50 mM sucrose) and kept on ice for 10 min. The cell homogenate was centrifuged at 250 x g for 5 min at 4 °C to remove unbroken cells. Reaction was started by addition of $C_{8:0}$-dhCer as a non-physiological substrate for DEGS and NADH for an hour at 37 °C.

In another *in vitro* assay, rat liver microsomes were prepared as described (Rahmaniyan et al., 2011). Briefly, livers from male Wistar rats were rinsed in ice-cold PBS and homogenized in buffer (0.25 M sucrose, 10 mM HEPES, 1 mM EDTA, pH 7.4) in ice. The homogenate was centrifuged at 800 x g for 10 min and the supernatant was centrifuged at 10,000 x g for 15 min. The resulting supernatant was ultracentrifuged at 104,000 x g for 1 h to obtain microsomal pellet, which was then resuspended in potassium phosphate buffer (50 mM, pH 7.4) and stored at -80 °C until use. In preparation for the assay, $C_{8:0}$-dhCer and tested compounds were dried under a stream of nitrogen, followed by resuspension in CHAPS (1.1 mg/10 μl of water). Microsomal fraction (500 μg of protein) was mixed with reaction buffer (20 mM bicine, pH 8.5, 50 mM NaCl, and 50 mM sucrose) and added with tested compounds, followed by 30 min pre-incubation at room temperature. 2 mM of NADH and 10 μM of $C_{8:0}$-dhCer were added and the mixture was incubated for 20 min at 37 °C with shaking. Lipid extraction

was conducted directly after reaction and the products ($C_{8:0}$-Cer and $C_{8:0}$-SM) were quantified by LC-MS/MS.

3.3.10 Animal studies

The animal use protocol was approved by the Animal Care and Use Committee at Purdue University. δTE-13'-COOH was isolated from the African Garcinia kola bitter nut according to the method described by Terashima *et al.* (Terashima et al., 1997), and modified δTE-13'-COOH-enriched AIN-93G purified diet was prepared by adding 0.22 g/kg δTE-13'-COOH.

In animal study 1 (AOM-DSS study), colon tumorigenesis was initiated by injection of azoxymethane (AOM; Sigma) and promoted by two cycles of dextran sodium sulfate (DSS; molecular weight of 36,000-50,000, MP Biochemicals, Solon, OH) at 1.5% in drinking water. Male Balb/c mice at 5-6 weeks of age from Harlan (Indianapolis, IN) were injected a dose of AOM (9.5 mg/kg body weight, i.p.) or the vehicle (sterile saline) after a week of acclimatization. A week later, AOM-injected mice were randomized into control or δTE-13'-COOH-supplemented groups, and they were given 1.5% DSS in drinking water for 1 week. The mice were started to be supplemented with either AIN-93G diet (for Non-AOM/DSS group; n=6, and AOM/DSS control diet group; n=17) or δTE-13'-COOH-enriched AIN-93G diet (for AOM/DSS δTE-13'-COOH supplementation group; n=15). Two weeks after first cycle of DSS administration, mice in AOM/DSS groups were again given the 2nd cycle of 1.5% DSS in drinking water for a week (Fig. 3.10A). Animals were observed and weighed daily and food intake was measured once a week. Fecal scoring as an indicator of colitis with combined scores of

rectal bleeding and stool consistency was evaluated daily and scored as follows (rectal bleeding: 0 = no blood, 0.5 = feces with tiny spots of bleeding, 1 = feces with blood less than 50% of area, 2 = feces with half-sized bleeding, and 3 = feces with blood more than 50% of area; stool consistency: 0 = normal, 1 = a little bit soft, 2 = soft, and 3 = very soft and diarrhea). During tissue harvest, colons were removed, rinsed with cold saline, cut open longitudinally from rectum to cecum. Lengths and weights of each colon tissue were measured and tumors were examined.

In animal study 2 (DSS study), to investigate the anti-inflammatory effects of δTE-13'-COOH against colitis, colon inflammation was induced by feeding mice with one cycle of 1.8% DSS in drinking water for 8 days in 5-6-week-old male Balb/c mice (Harlan). On the same day of DSS feeding started, the mice were supplemented with either AIN-93G diet (for Non-DSS group; n=8, and DSS control diet group; n=12) or δTE-13'-COOH-enriched AIN-93G diet (for DSS δTE-13'-COOH supplementation group; n=12; Fig 3.11A). During the study, animals were observed and weighed, and their fecal scorings were evaluated daily as described above, and food intake was measured once at the end of the study.

3.3.11 Statistics

Statistical significance was determined using a Student's t-test. $P < 0.05$ was considered statistically significant.

3.4 Results

3.4.1 13’-COOHs inhibited proliferation of various human cancer cells

We investigated the effect of δT- or δTE-13’-COOH on cell proliferation using MTT assays in various human cancer cell lines. We found that δT-13’-COOH inhibited the growth of human colon (HCT-116, HT-29), breast (MCF-7) and pancreatic (PANC-1, MiaPaCa-2) cancer cells in a time- and dose-dependent manner (Fig. 3.2A) with the IC_{50} values (estimated after 24 h incubation) of 8.9 μM, 8.6 μM and 13.5 μM in HCT-116, HT-29, and MCF-7 cells, respectively. In addition, δTE-13’-COOH also showed antiproliferative effects with IC_{50} values (at 24 h) of 16 μM, 17 μM and 19.7 μM in HCT-116, HT-29, and MCF-7 cells, respectively (Fig. 3.2B). In these activities, δT-13’-COOH was more potent than δTE-13’-COOH, and both 13’-COOHs were stronger than tocopherols (Fig. 3.2C). Interestingly, although human colon HT-29 cancer cells showed more resistance than HCT-116 cells to the treatment of γT and γTE (Fig. 3.2C), 13’-COOHs showed similar anticancer effects in both cell lines (Figs. 3.2A and B). In addition, human normal colonic epithelial cells, CCD841CoN, were used as a control cell line. δT-13’-COOH and δTE-13’-COOH showed about 2-fold higher IC_{50} values (at 24 h) in CCD841CoN cells compared with cancer cells (Fig. 3.2D).

A δT-13'-COOH

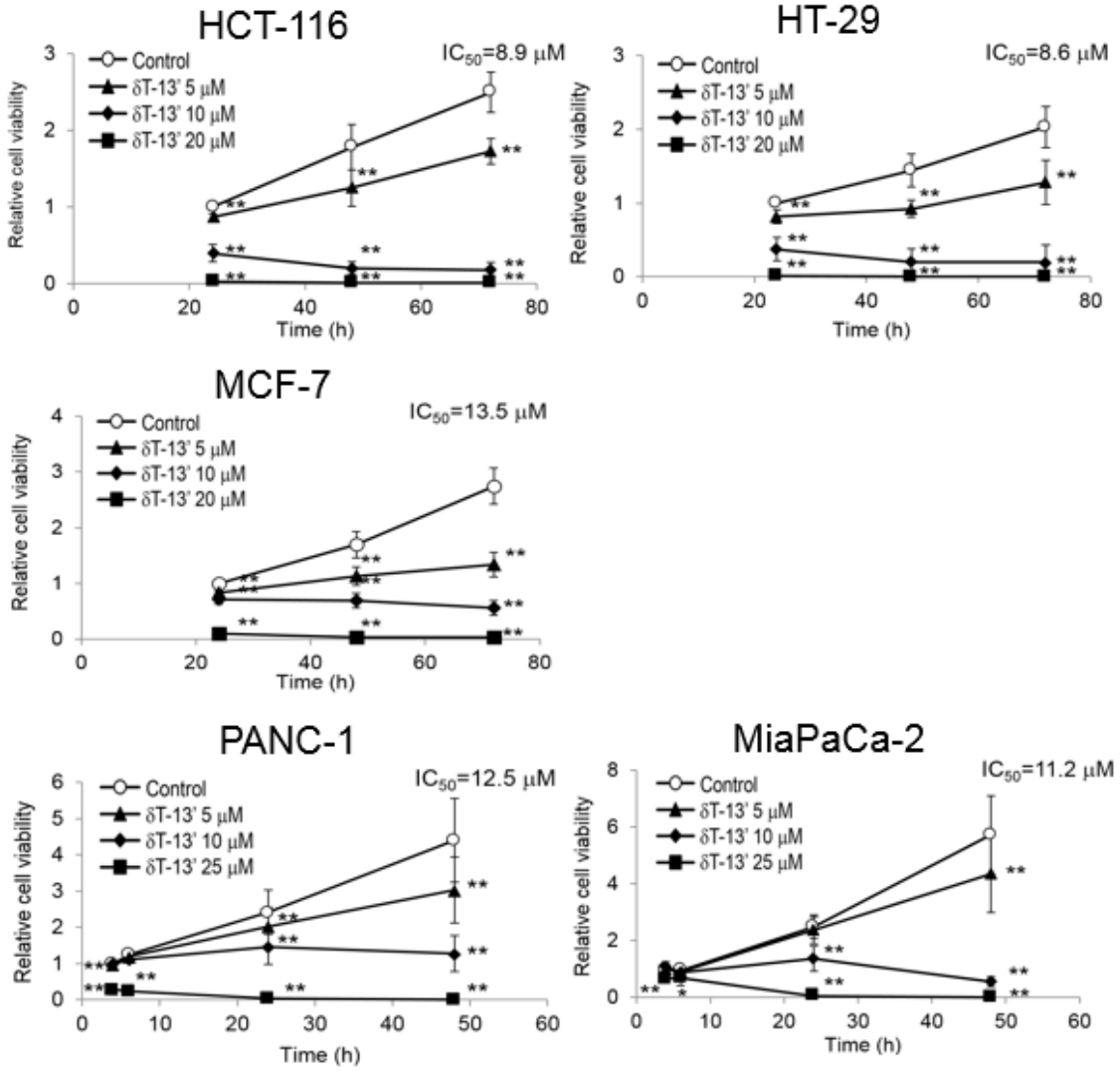

B δTE-13'-COOH

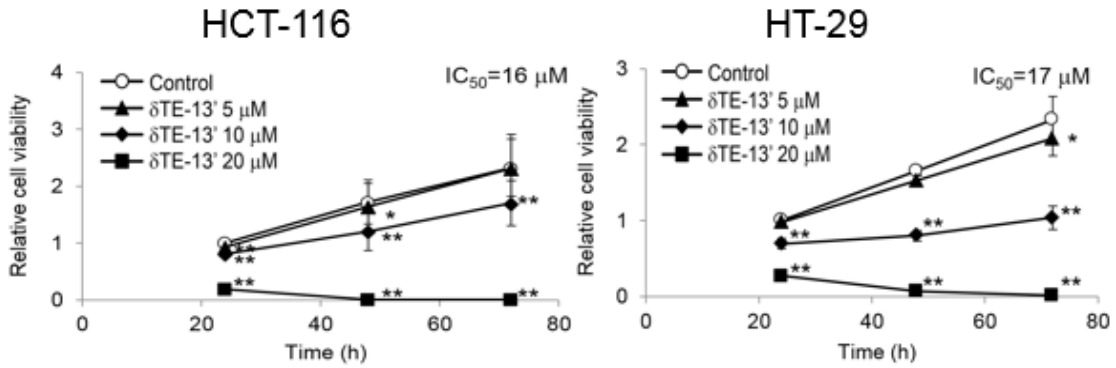

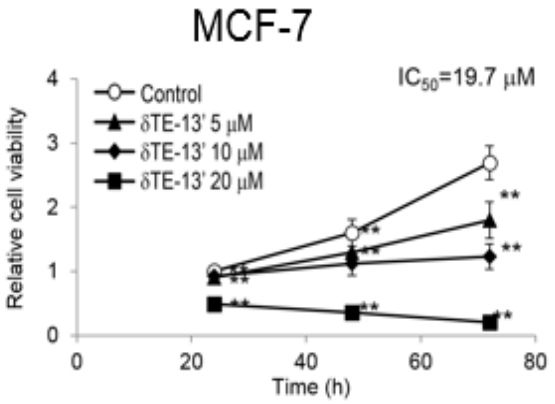

C Natural forms of vitamin E

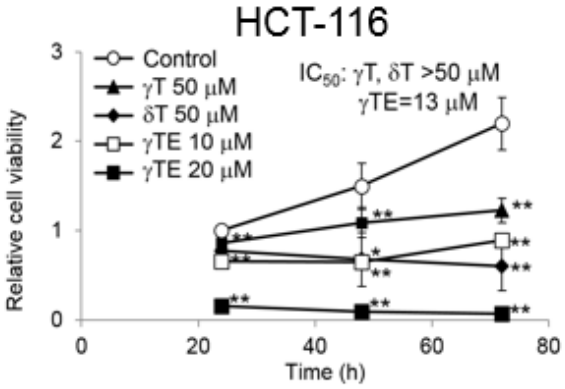

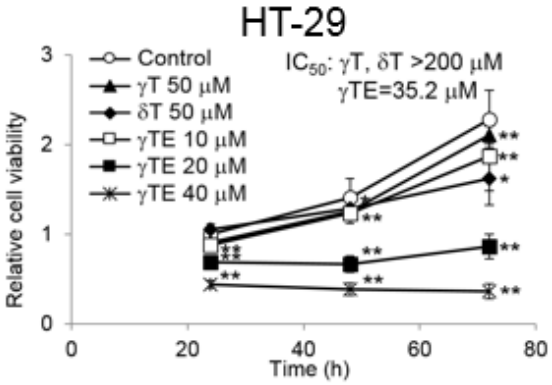

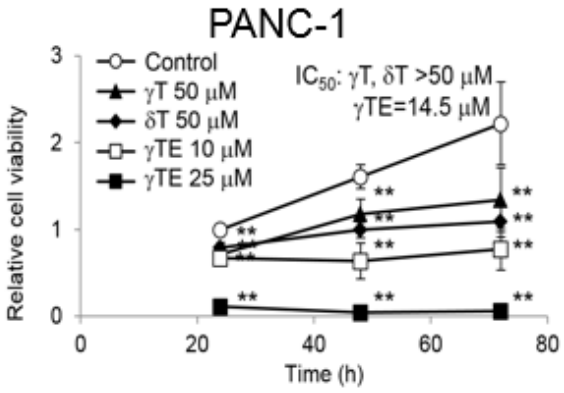

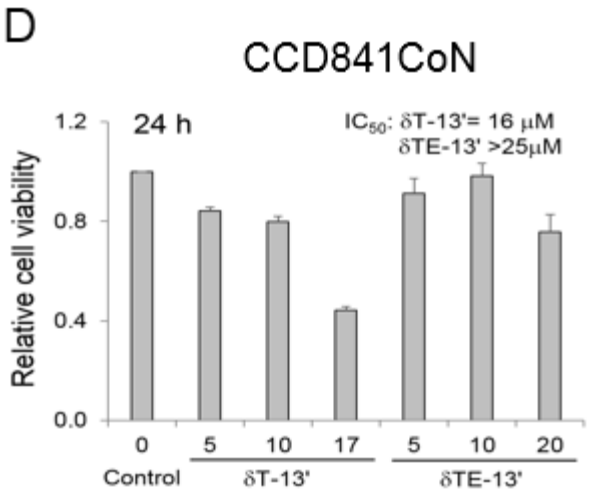

Figure 3.2 Anti-proliferative effects of 13'-COOHs derived from δT or δTE on various cancer cells. (A) The effects of δT-13'-COOH on human colon (HCT-116, HT-29), breast (MCF-7) and pancreatic (PANC-1, MiaPaCa-2) cancer cells. (B) The effects of δTE-13'-COOH on human colon (HCT-116, HT-29) and breast (MCF-7) cancer cells. (C) The effects of natural forms of vitamin E on human colon (HCT-116, HT-29) and pancreatic (PANC-1) cancer cells. (D) The effects of δT-13'-COOH and δTE-13'-COOH on human normal colonic epithelial (CCD841CoN) cells. Relative cell viability was measured after treatment with 13'-COOHs or natural forms of vitamin E at the stated concentrations and time by MTT assay compared with control. IC_{50} of 24 h is shown. The data are mean ± SD for at least three independent experiments, each performed in duplicate. *$p < 0.05$ and **$p < 0.01$ indicate a significant difference between treated and control cells.

3.4.2 13'-COOHs induced apoptosis and autophagy in various types of cancer cells

Based on microscopic examination, 13'-COOHs appeared to induce cell death as indicated by detachment and shrinkage of cells during prolonged treatment. Consistently, both δT-13'-COOH and δTE-13'-COOH induced early and late-stage apoptosis in HCT-116 cells compared with controls, as indicate by enhanced annexin V staining that is associated with externalization of phosphatidylserine to the cytoplasmic membrane (Fig. 3.3A). Furthermore, 13'-COOHs caused PARP cleavage and caspase-9 activation (Fig. 3.3B). Similar to the results from MTT assays, δT-13'-COOH appeared to be stronger

than δTE-13'-COOH in the induction of apoptosis. In addition to apoptosis, δT- and δTE-13'-COOHs treatment led to an increase of LC3-II, a marker of autophagy (Fig. 3.3C). We also observed similar biochemical changes in MCF-7 cells (data not shown). These results demonstrated that δT- and δTE-13'-COOH induced apoptosis and autophagy in human cancer cells.

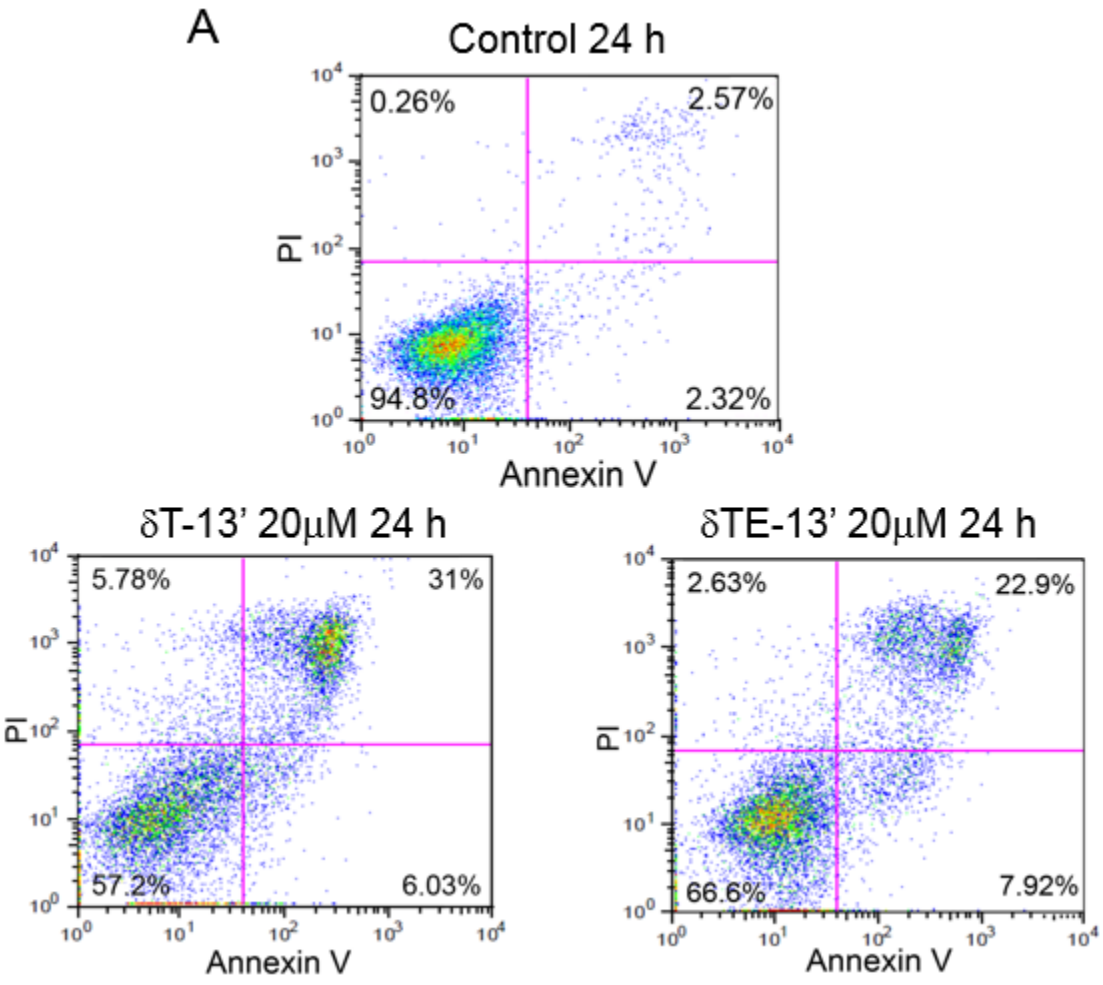

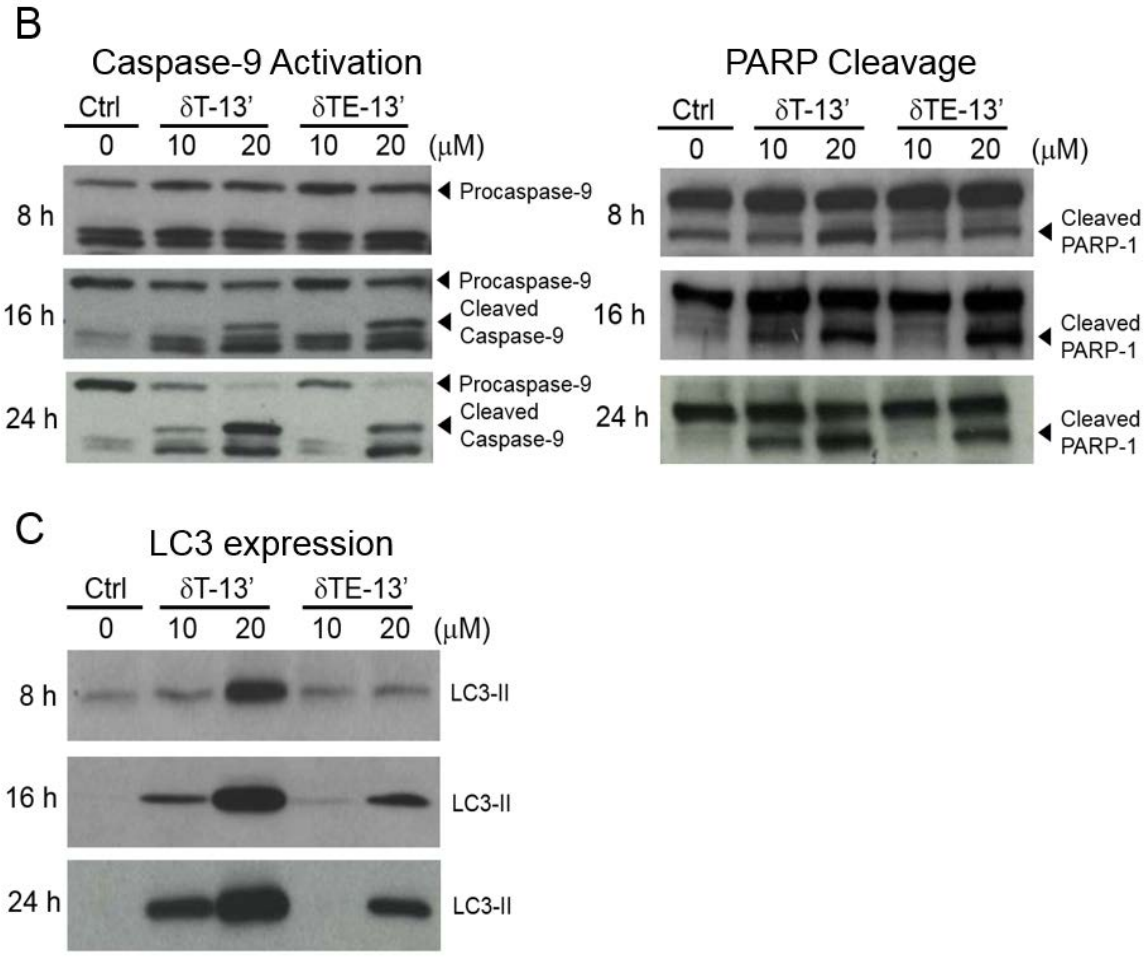

Figure 3.3 Induction of apoptosis and autophagy by 13'-COOHs in cancer cells. (A) HCT-116 cells were treated with 20 μM δT-13'-COOH or δTE-13'-COOH for 24 h. Induction of apoptosis and necrosis was quantified by annexin V and PI staining. Representative diagrams of FACS are shown here. Expression levels of (B) full-length and cleaved caspase-9 and PARP, and (C) LC3-II in HCT-116 cells after treatment with 10 or 20 μM of δT-13'-COOH or δTE-13'-COOH were examined by western blotting. Western blots in this figure are representative of three or more independent experiments.

3.4.3 13’-COOHs modulated sphingolipids in HCT-116 and MCF-7 cells

We have demonstrated that modulation of sphingolipid pathway plays a role in γT and γTE-induced death in human prostate and breast cancer cells (Gopalan et al., 2012; Jiang et al., 2012; Jiang et al., 2004). Here we investigated effects of 13’-COOHs on sphingolipid metabolism using LC-MS/MS. Compared with controls, δT-13’-COOH dose-dependently increased total dihydroceramides (dhCers) (Fig. 3.4A), individual dhCer including $C_{16:0}$- (Fig. 3.4B), $C_{18:0}$-, $C_{24:1}$- and $C_{24:0}$-dhCers (data not shown), and dihydrosphingosine (dhSph) (Fig. 3.4C). Interestingly, δT-13’-COOH (20 μM) enhanced $C_{16:0}$-dhCer and dhSph at 1 h after incubation, which was prior to any signs of cell morphological changes. Consequently, cells accumulated high levels of dhCers and dhSph after incubation for 8-16 h. In contrast to dhCer, the effect of 13’-COOHs on individual ceramides (Cer) varied with treatment time, concentrations, and specific ceramide species. Specifically, compared with controls, δT-13’-COOH induced a significant decrease of $C_{16:0}$-Cer after 2 h incubation, but enhanced this sphingoid base during longer treatment (8 h or 16 h incubation). δT-13’-COOH at 20 μM increased $C_{18:0}$-Cer after 4 h treatment, while treatment of δT-13’-COOH at 10 and 20 μM caused opposite effects on C_{24}-Cers (Fig. 3.4D). For sphingomyelin (SM), δT-13’-COOH led to persistent decrease in all types of SM species starting at 2 h (Fig. 3.4E; Table 3.1). Besides HCT-116 cells, we observed similar modulatory effects of δT-13’-COOH on MCF-7 cells (Fig. 3.5; Table 3.2). Furthermore, δTE-13’-COOH at 20 μM induced similar modulation of sphingolipids to that by δT-13’-COOH (Fig. 3.6; Table 3.3), although less potent than its δT analog.

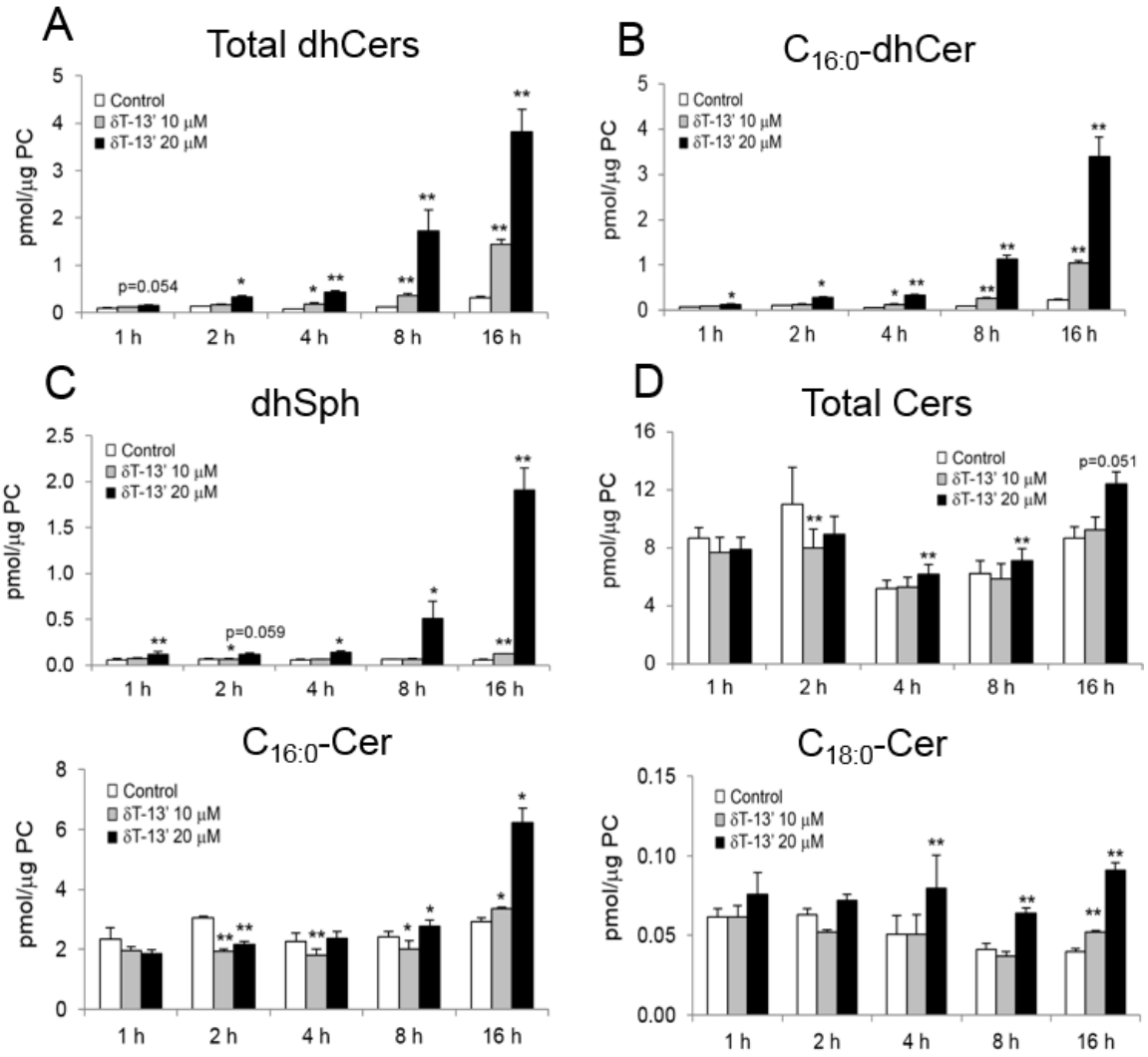
A
Total dhCers
B
C16:0-dhCer
C
dhSph
D
Total Cers
C16:0-Cer
C18:0-Cer
Control
δT-13' 10 μM
δT-13' 20 μM
pmol/μg PC
p=0.054
p=0.059
p=0.051
1 h
2 h
4 h
8 h
16 h

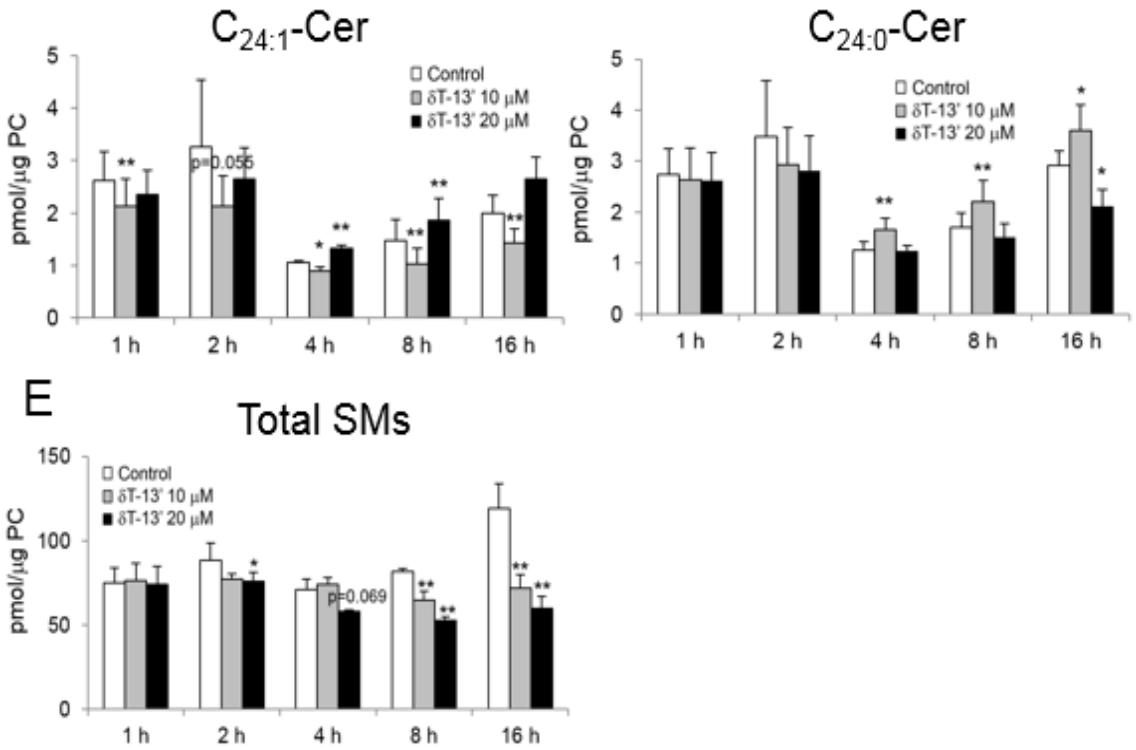

Figure 3.4 Effects of δT-13'-COOH on sphingolipid metabolism in HCT-116 cells. HCT-116 cells were treated with 10 or 20 μM δT-13'-COOH with increasing treatment times as indicated (1, 2, 4, 8, or 16 h). The sphingolipid levels including (A) total dhCers, (B) $C_{16:0}$-dhCer, (C) dhSph, (D) total, $C_{16:0}$-, $C_{18:0}$-, $C_{24:1}$-, and $C_{24:0}$-Cers and (E) total SMs were determined by LC-MS/MS. Results are shown as mean ± SEM for at least three independent experiments. *$p < 0.05$ and **$p < 0.01$ indicate a significant difference between treated and control cells.

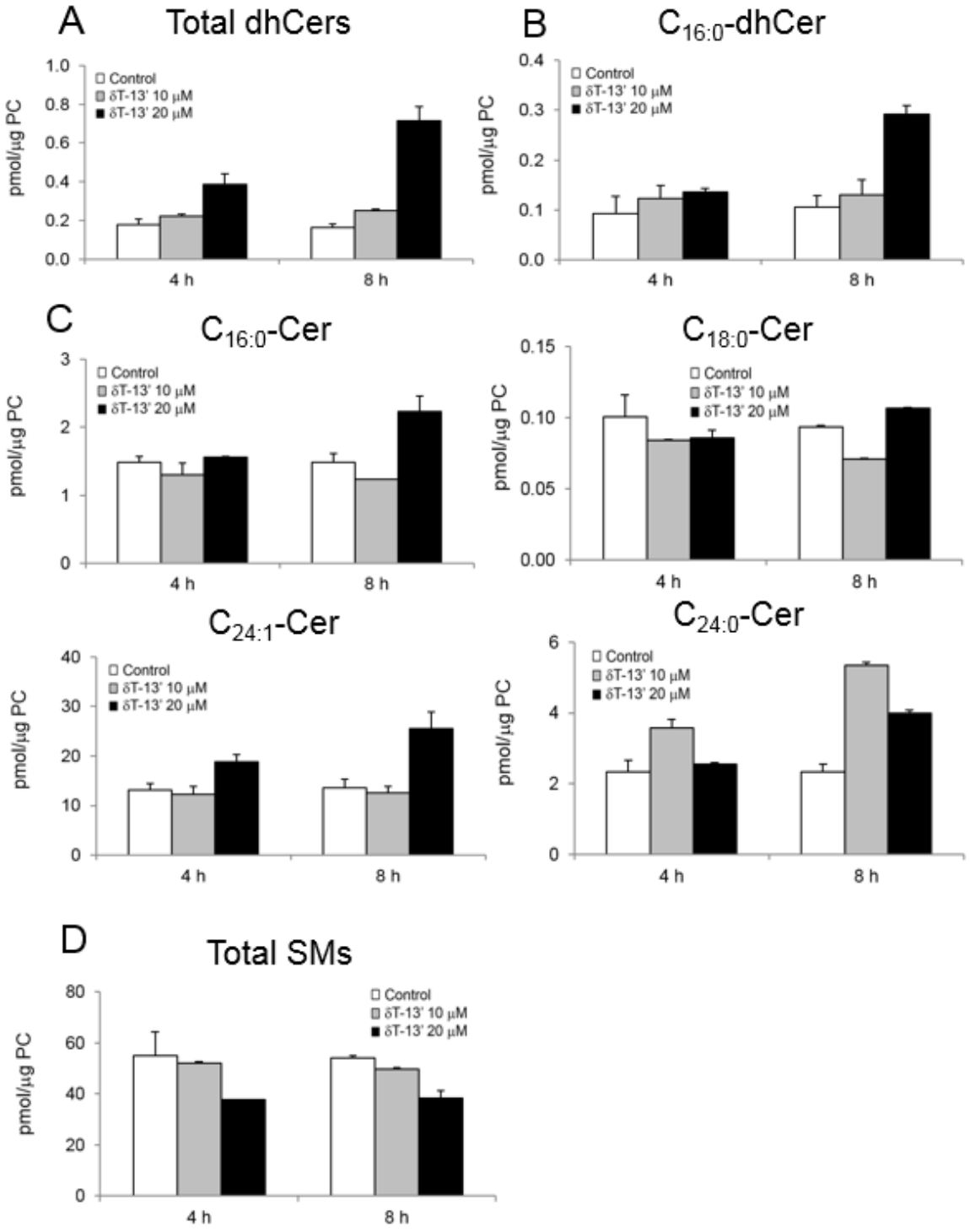

Figure 3.5 Effects of δT-13'-COOH on sphingolipid metabolism in MCF-7 cells. MCF-7 cells were treated with 10 or 20 μM δT-13'-COOH for 4 h or 8 h. The sphingolipid levels including (A) total dhCers, (B) $C_{16:0}$-dhCer, (C) $C_{16:0}$-Cer, $C_{18:0}$-Cer, $C_{24:1}$-Cer, and $C_{24:0}$-Cer and (D) total SMs were determined by LC-MS/MS. Results are shown as mean ± SD for two independent experiments.

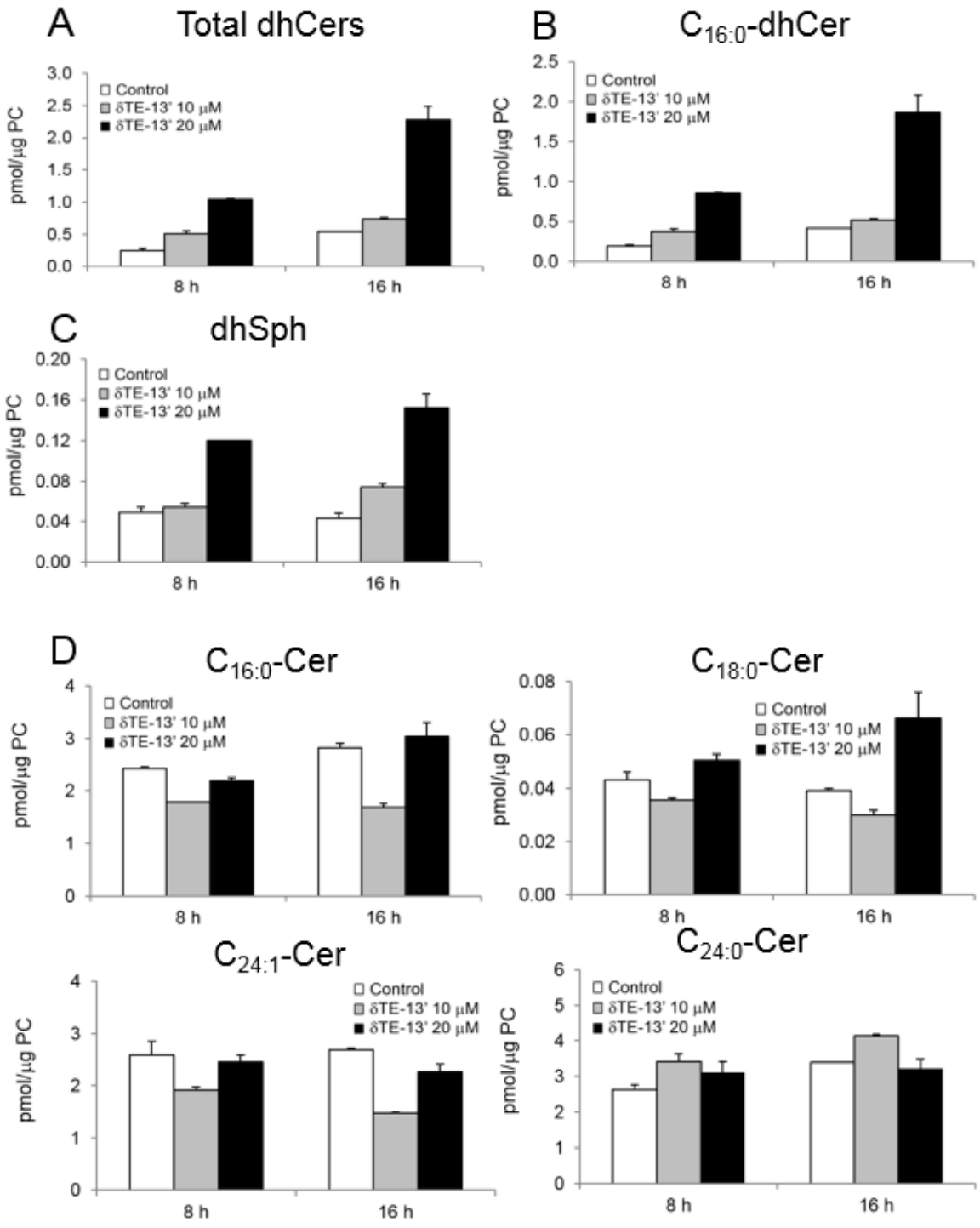
A
Total dhCers
pmol/µg PC
Control
δTE-13' 10 µM
δTE-13' 20 µM
8 h
16 h
B
C16:0-dhCer
C
dhSph
D
C16:0-Cer
C18:0-Cer
C24:1-Cer
C24:0-Cer

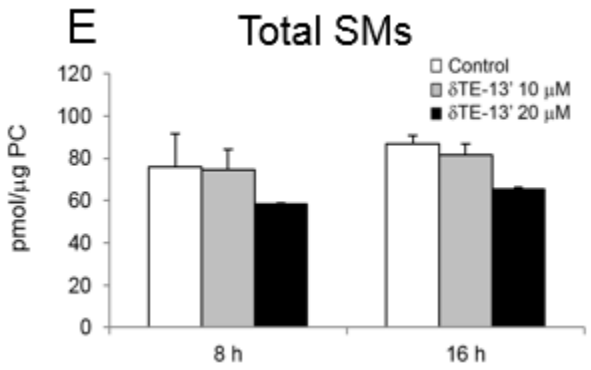

Figure 3.6 Effects of δTE-13'-COOH on sphingolipid metabolism in HCT-116 cells. HCT-116 cells were treated with 10 or 20 μM δTE-13'-COOH for 8 h or 16 h. The sphingolipid levels including (A) total dhCers, (B) $C_{16:0}$-dhCer, (C) dhSph, (D) $C_{16:0}$-Cer, $C_{18:0}$-Cer, $C_{24:1}$-Cer, and $C_{24:0}$-Cer and (E) total SMs were determined by LC-MS/MS. Results are shown as mean ± SD for two independent experiments.

3.4.4 13'-COOHs modulated *de novo* biosynthesis of sphingolipids

Since 13'-COOHs elevated dhCer and dhSph that are important sphingoid bases in *de novo* synthesis of sphingolipid pathway (Fig. 3.7A), we used $^{13}C_3$, ^{15}N-labeled L-serine, a substrate for making sphingolipids with palmitoyl-CoA, to trace the effect on the newly synthesized sphingolipids. We observed that δT-13'-COOH treatment induced a significant increase in labeled dhCers in a time-dependent manner (Fig. 3.7B) but resulted in decrease of Cers including $C_{16:0}$-, $C_{24:1}$- and $C_{24:0}$-Cers as early as 0.5 h to 2 h (Fig. 3.7C). δT-13'-COOH significantly suppressed *de novo* synthesis of $C_{16:0}$- and $C_{24:1}$-SMs (Fig. 3.7D). Despite elevation of newly-made dhCer, δT-13'-COOH significantly reduced the total amount of newly synthesized sphingolipids (Fig. 3.7E; Table 3.4) as a result of diminished synthesis of SM and Cer that are much more abundant than dhCer. These results thus indicate that δT-13'-COOH inhibits overall *de novo* biosynthesis of sphingolipids.

A *De novo* synthesis of sphingolipid

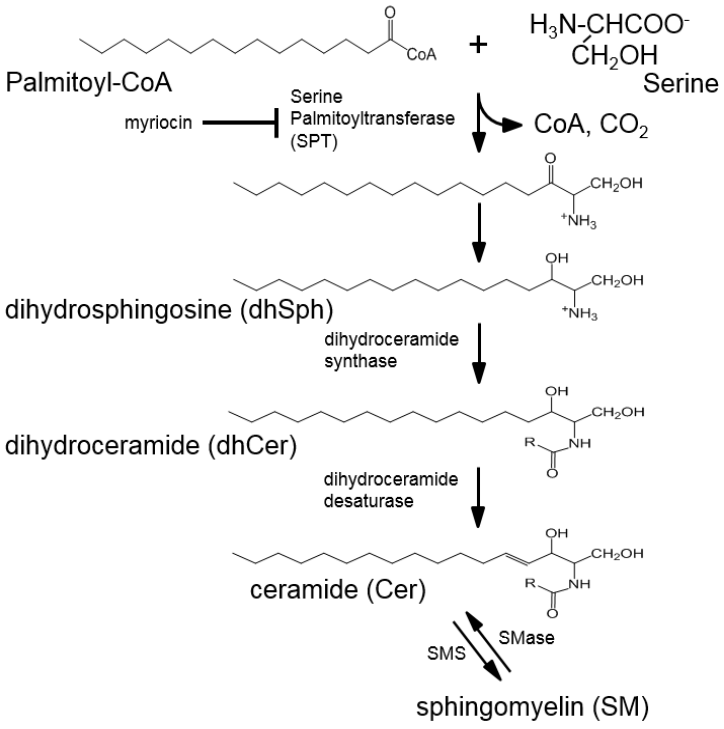

B

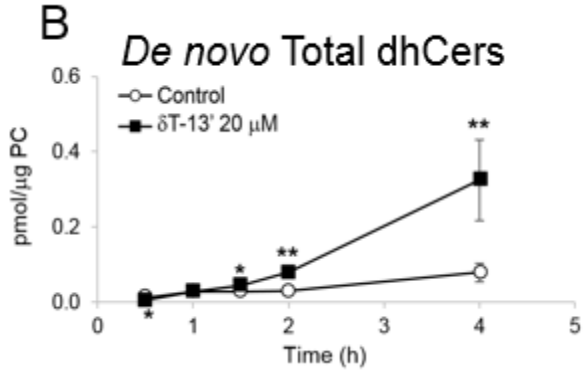

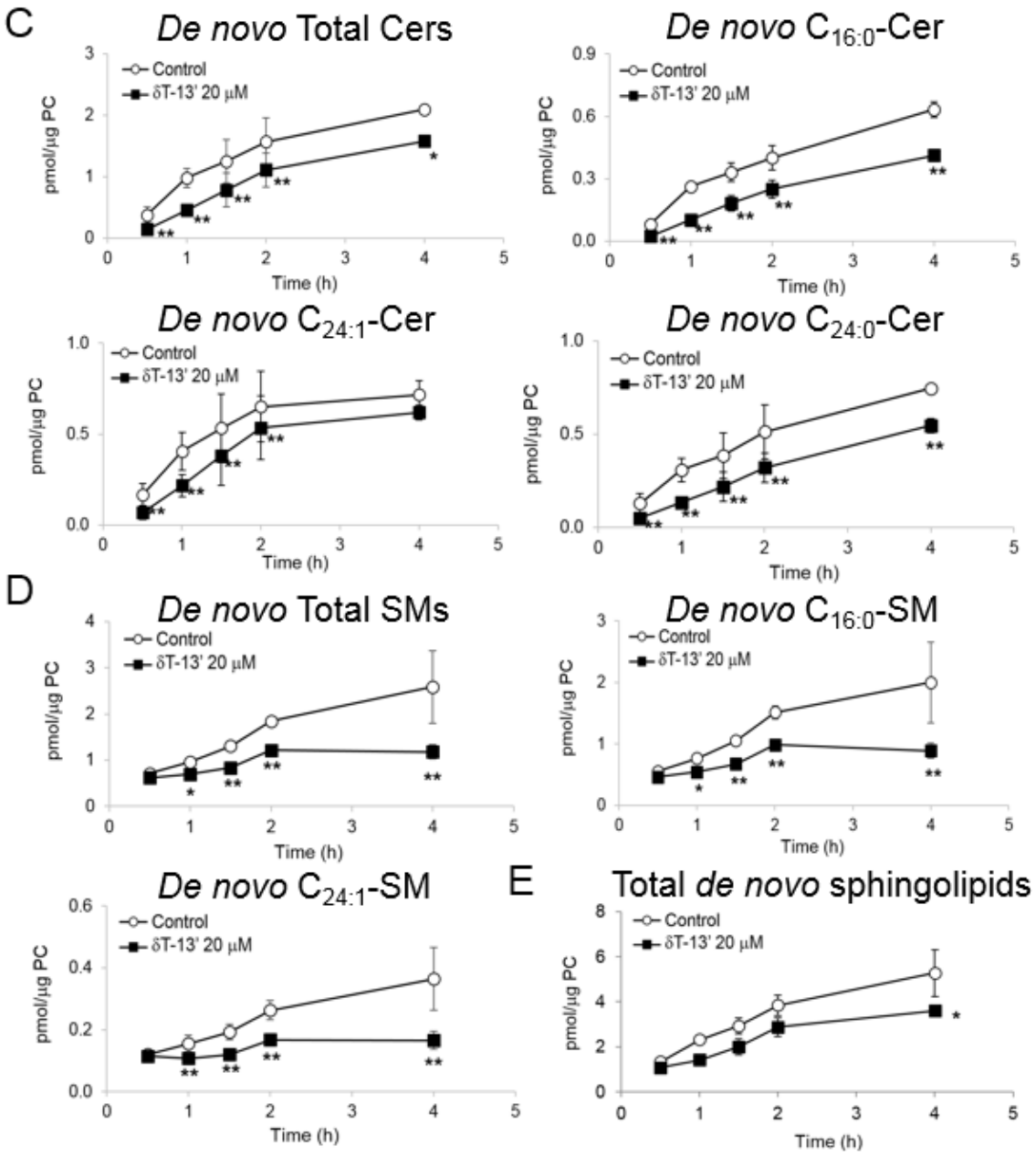

Figure 3.7 Effects of δT-13'-COOH on *de novo* sphingolipid biosynthesis in HCT-116 cells. (A) The *de novo* biosynthesis pathway of sphingolipids (SMS, sphingomyelin synthase; SMase, sphingomyelinase). HCT-116 cells were treated with either 400 μM $^{13}C_3$, ^{15}N-labeled L-serine alone as control or with a combination of 400 μM $^{13}C_3$, ^{15}N-labeled L-serine and 20 μM δT-13'-COOH for 0.5, 1, 1.5, 2, and 4 h. The amount of each labeled *de novo* sphingolipid including (B) total dhCers, (C) total, $C_{16:0}$-, $C_{24:1}$- and $C_{24:0}$-Cers, and (D) total, $C_{16:0}$- and $C_{24:1}$-SMs were determined by LC-MS/MS. (E) Total amounts of all the *de novo* synthesized sphingolipids were calculated. Results are shown as mean ± SEM for three independent experiments. *$p < 0.05$ and **$p < 0.01$ indicate a significant difference between treated and control cells.

3.4.5 13’-COOHs inhibited DEGS activity without affecting its protein expression

Based on the observation that δT-13’-COOH increased newly synthesized dhCers but decreased Cers, we reason that δT-13’-COOH likely inhibits the enzyme reaction or protein expression of dihydroceramide desaturase (DEGS), which is responsible for addition of the 4,5-*trans*-double bond of dhCer (Fig. 3.7A). The western blot data revealed that δT-13’-COOH had no effect on DEGS-1 protein expression in HCT-116 cells (Fig. 3.8A). We then examined potential effect of δT-13’-COOH on the DEGS enzyme activity. In the *in vitro* DEGS assay with cell homogenates, 1 or 2 h pre-incubation of δT-13’-COOH inhibited DEGS activity by about 38% or 47%, respectively. C8-CPPC, a known competitive inhibitor of DEGS (Triola et al., 2003), inhibited the enzyme activity by about 95% (Fig. 3.8B). On the other hand, δT-13’-COOH did not show the inhibition of DEGS enzyme activity in another *in vitro* DEGS assay using rat liver microsome (data not shown).

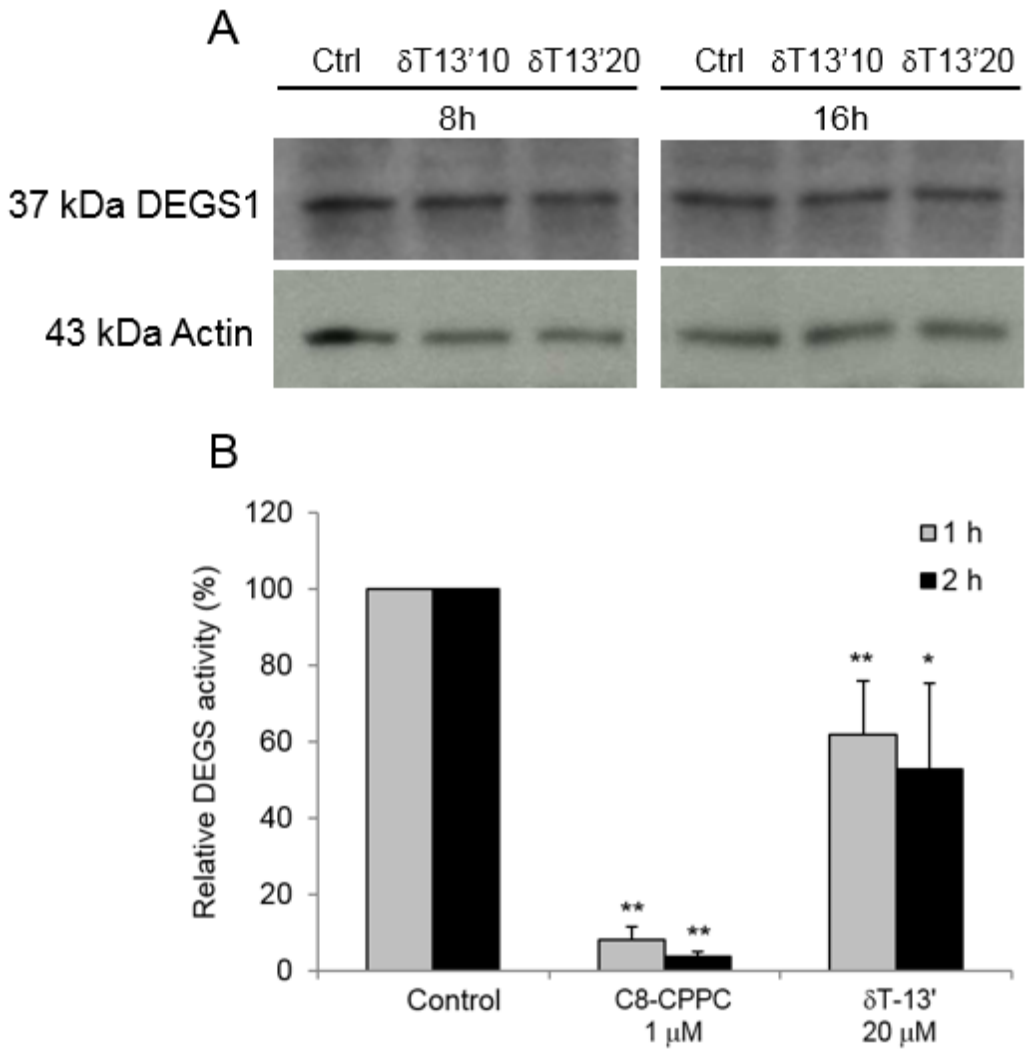

Figure 3.8 Effects of δT-13'-COOH on DEGS expression and activity. (A) HCT-116 cells were treated with 10 or 20 μM δT-13'-COOH for 8 or 16 h and the protein levels of DEGS-1 and actin as a loading control were detected by western blotting. (B) HCT-116 cells were treated with either 20 μM δT-13'-COOH or 1 μM C8-CPPC as a positive control for indirect *in vitro* DEGS assay. After 1 h or 2 h of treatment, cells were collected and homogenized. Using the homogenates, reaction was started for an hour in 37 °C followed by addition of $C_{8:0}$-dhCer as a substrate for DEGS with NADH. The levels of products which are $C_{8:0}$-sphingolipids were analyzed by using LC-MS/MS. The data are mean ± SD of three independent experiments. *$p < 0.05$ and **$p < 0.01$ indicate a significant difference between treated and control cells.

3.4.6 The role of sphingolipid modulation in 13'-COOH-induced cell death

Since 13'-COOHs induced accumulation of intracellular dhCer and dhSph, which are known to induce cell stress and/or death (Ahn and Schroeder, 2002; Jiang et al., 2012; Jiang et al., 2004), we used myriocin, a specific inhibitor of serine palmitoyltransferase, to block the increase of these sphingoid bases. Interestingly, co-treatment of cells with myriocin showed partial reversion of 13'-COOH-induced LC3-II expression (Fig. 3.9A), but had no effect on PARP-1 cleavage (data not shown). These data suggest that elevation of dhCer and dhSph may play a role in 13'-COOHs-induced autophagy.

Cers have been known to be potent inducer of apoptosis (Kolesnick, 2002; Radin, 2001; Woodcock, 2006). Because 13'-COOHs decreased Cers synthesis in the *de novo* pathway (Fig. 3.7C), we reason that the increase of Cers (Fig. 3.4D) after longer treatment is likely caused by hydrolysis of SM via sphingomyelinase (SMase). To establish the role of Cers from SMs in 13'-COOH-induced cancer cell death, we used desipramine and GW4869 to inhibit acid or neutral SMases, respectively. Co-treatment of GW4869 but not desipramine (data not shown) with 13'-COOHs partially counteracted anti-proliferation by 13'-COOHs (Fig. 3.9B). These data suggest that SM hydrolysis through the neutral SMase activation may in part contribute to 13'-COOHs-induced anticancer effects.

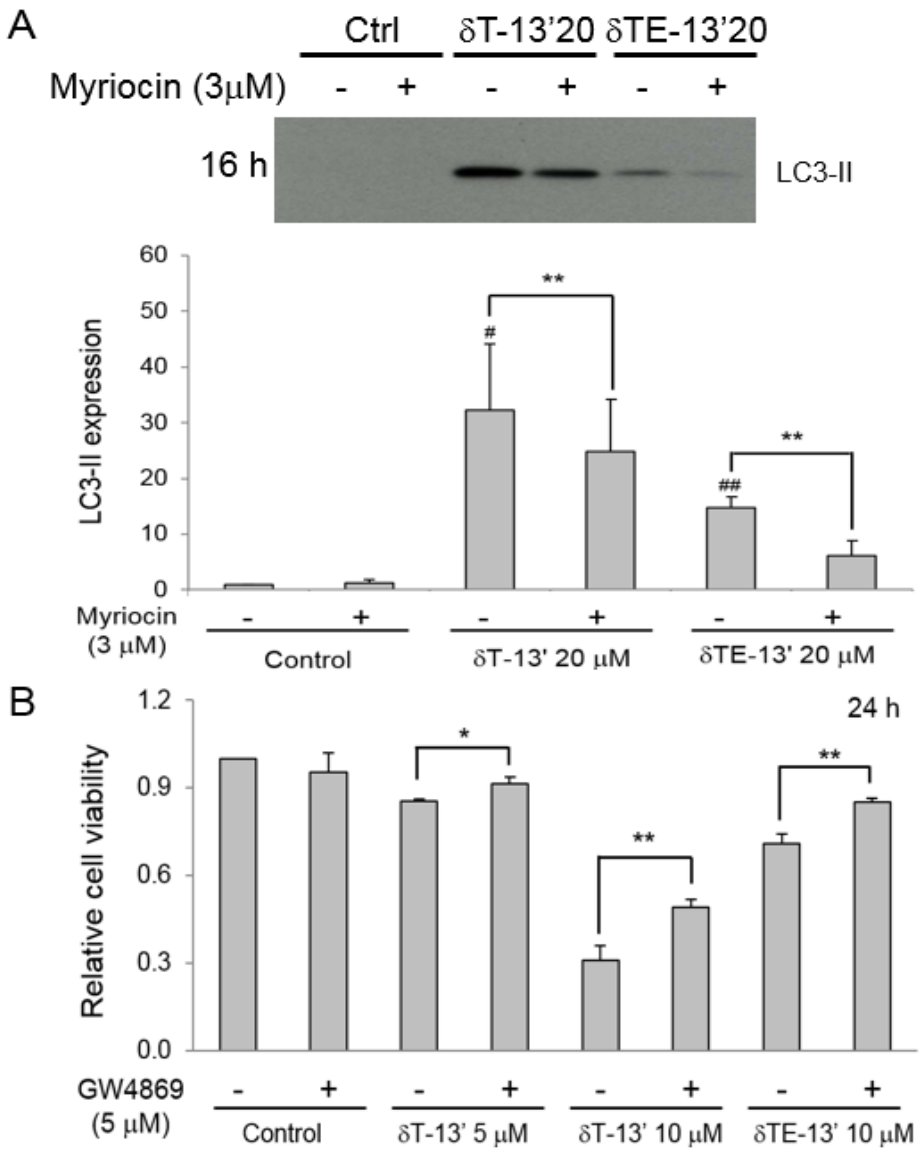

Figure 3.9 Protective effects of inhibitors of enzymes in sphingolipid metabolism on 13'-COOHs-induced cancer cell death. (A) HCT-116 cells were treated with 20 μM δT- or δTE-13'-COOH with or without 3 μM myriocin, a specific inhibitor of serine palmitoyltransferase to block the *de novo* sphingolipid pathway. After 16 h of treatment, the cells were collected and analyzed for detection of LC3-II expression. Western blots in this figure are representative of three or more independent experiments. LC3-II protein levels were quantified from the blots. The data are mean ± SEM of three or four independent experiments. *$p < 0.05$ and **$p < 0.01$; #$p < 0.05$ and ##$p < 0.01$ versus control indicate a significant difference. (B) HCT-116 cells were treated with 5 or 10 μM δT-13'-COOH or 10 μM δTE-13'-COOH with or without 5 μM GW4869, an inhibitor of neutral SMase for 24 h. Relative cell viability was measured by MTT assay compared with control. The data are mean ± SD of three independent experiments. *$p < 0.05$ and **$p < 0.01$ indicate a significant difference.

3.4.7 δTE-13'-COOH supplementation attenuated colon inflammation and inhibited tumorigenesis induced by AOM with two cycles of 1.5% DSS in mice

To examine whether the anticancer effect of 13'-COOH can be translated into whole body system, we investigated the effectiveness of δTE-13'-COOH supplementation against AOM-induced and DSS-promoted colon tumorigenesis in male Balb/c mice. The body weights and the amounts of food intake of AOM/DSS-treated δTE-13'-COOH-supplemented group were similar to those of the control diet group, and δTE-13'-COOH supplementation showed no apparent signs of toxicity throughout the experiment (Figs. 3.10B and C). δTE-13'-COOH supplementation attenuated colon inflammation induced by two-cycles of 1.5% DSS as indicated by significantly attenuated scores of rectal bleeding on day 6 of 2^{nd} cycle DSS administration (Fig. 3.10D), and significantly attenuated DSS-caused colon L/W ratio reduction compared with the control diet group (Fig. 3.10E). After 43 days, AOM/DSS-treated control diet group had 4.7 ± 0.3 tumors per mouse in the colon, but AOM/DSS-δTE-13'-COOH supplementation group showed beneficial effects with a significantly lower number of colon tumors (3.1 ± 0.3; $p < 0.01$; Fig. 3.10F) even the supplementation was started 7 days after AOM injection. Interestingly, when the tumors were categorized as small (< 2 mm^2) or large (> 2 mm^2) sizes, supplementation of δTE-13'-COOH after AOM/DSS treatment significantly decreased the number of large tumors by 58% ($p < 0.05$), which are closely associated with the development of malignancy, although it did not significantly decrease the number of small tumors. All these tumors were primarily found in the middle to rectal part of the distal colon.

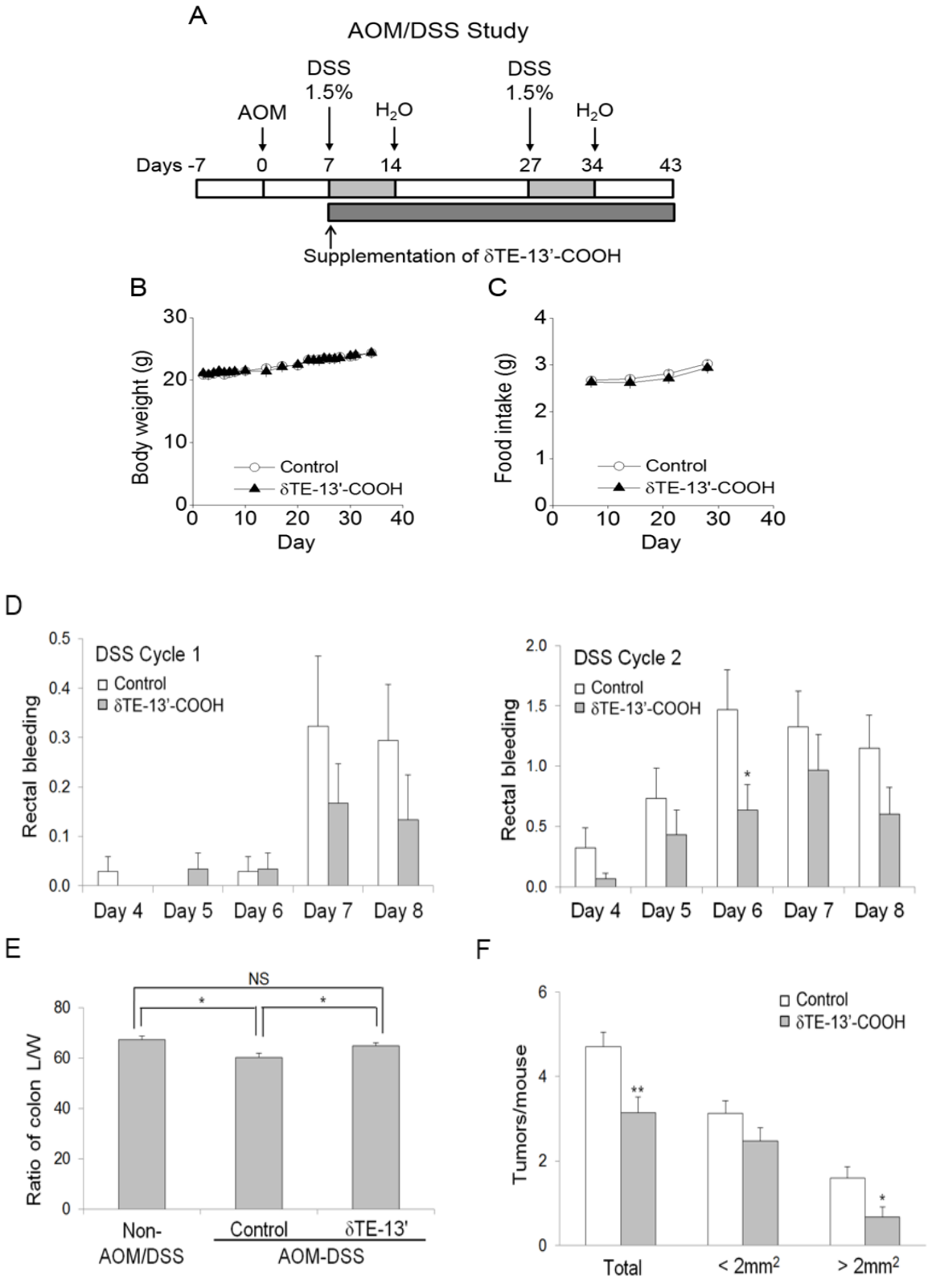
A
AOM/DSS Study
DSS 1.5%
DSS 1.5%
AOM
H2O
H2O
Days -7
0
7
14
27
34
43
Supplementation of δTE-13'-COOH
B
Body weight (g)
Control
δTE-13'-COOH
Day
C
Food intake (g)
Control
δTE-13'-COOH
Day
D
DSS Cycle 1
Control
δTE-13'-COOH
Rectal bleeding
Day 4
Day 5
Day 6
Day 7
Day 8
DSS Cycle 2
Control
δTE-13'-COOH
Rectal bleeding
Day 4
Day 5
Day 6
Day 7
Day 8
E
NS
Ratio of colon L/W
Non-AOM/DSS
Control
δTE-13'
AOM-DSS
F
Control
δTE-13'-COOH
Tumors/mouse
Total
< 2mm2
> 2mm2

Figure 3.10 Effects of δTE-13'-COOH on colon tumorigenesis induced by AOM with two cycles of 1.5% DSS. (A) The design of AOM/DSS study. (B) Body weight and (C) food intake of each group during the days after supplementation started. The effects of δTE-13'-COOH on (D) fecal scorings during DSS cycle 1 and 2, and (E) ratio of colon L/W. (F) The effects of δTE-13'-COOH on colon tumor multiplicity and polyps with sizes of < 2 mm^2 or > 2 mm^2 in the AOM/DSS study (mean ± SEM, n = 15-17). *p < 0.05 and **p < 0.01 differences between control and δTE-13'-COOH supplementation group.

3.4.8 δTE-13'-COOH supplementation attenuated colon inflammation induced by one cycle of 1.8% DSS in mice

We further examined whether δTE-13'-COOH has any direct effects on colon inflammation caused by one cycle of 1.8% DSS. Similar to the results from AOM/DSS study above, the body weights and the amount of food intake were not different between groups (Figs. 3.11B and C). Treatment with one cycle of 1.8% DSS resulted in colon bleeding and diarrhea, and δTE-13'-COOH supplementation significantly decreased this fecal scoring compared with the control-diet group (Figs. 3.11D-F), indicating that δTE-13'-COOH alleviated colon inflammation induced by DSS.

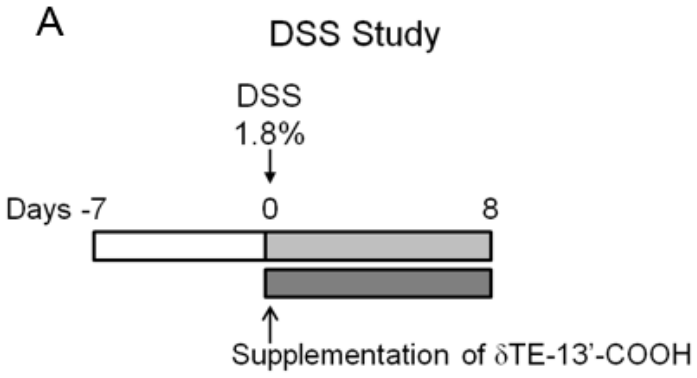

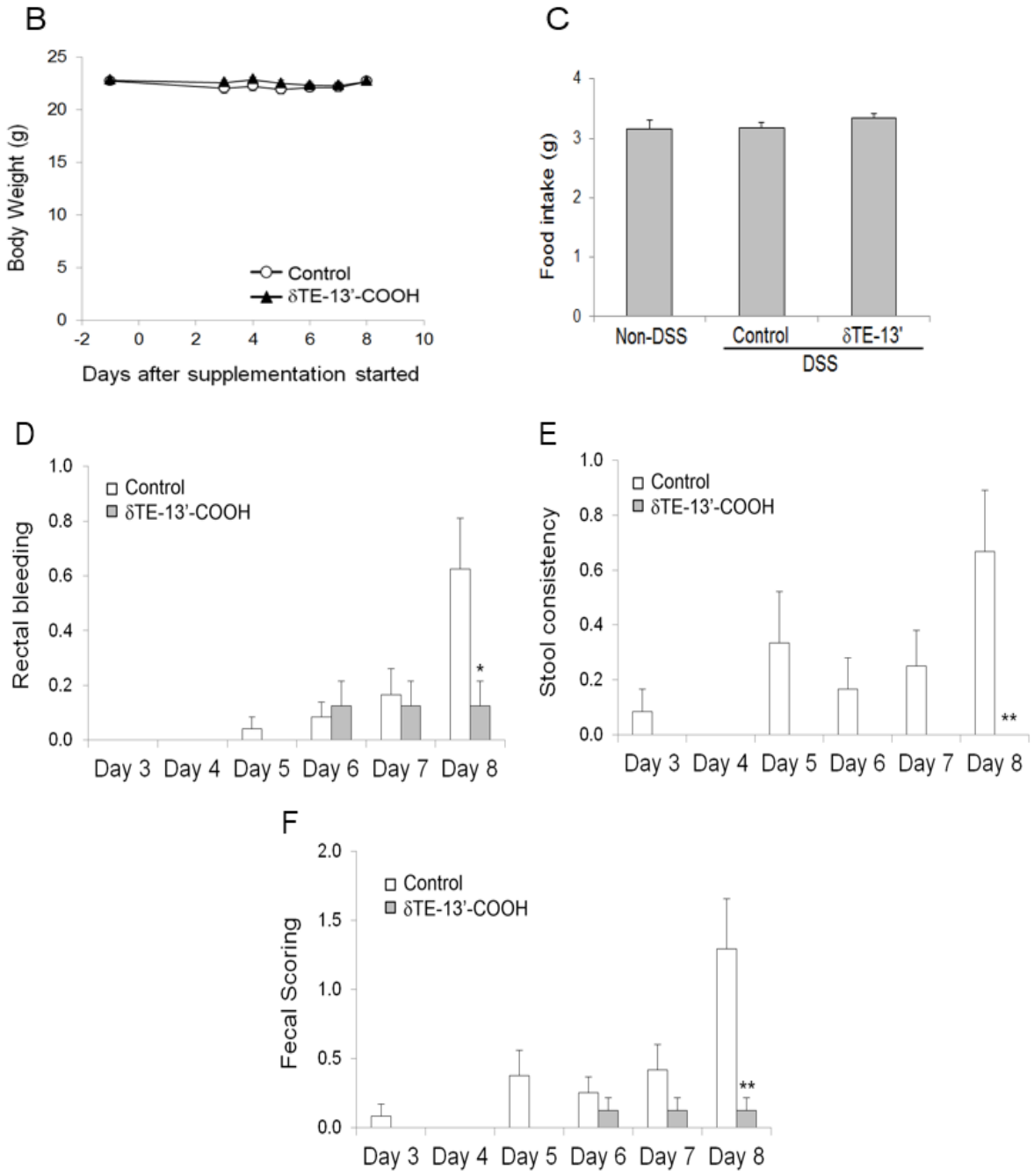

Figure 3.11 Effects of δTE-13'-COOH on colon inflammation induced by one cycle of 1.8% DSS. (A) The design of DSS study. (B) Body weight and (C) food intake of each group during the study. The effects of δTE-13'-COOH on (D) rectal bleeding, (E) stool consistency, and (F) total fecal scorings during the DSS study (mean ± SEM, n = 12). *$p < 0.05$ and **$p < 0.01$ differences between control and δTE-13'-COOH supplementation group.

3.4.9 Combined treatment of specific natural vitamin E forms with their long-chain metabolites exhibited synergistic or additive antiproliferative effects

Since parental vitamin E forms and their metabolites coexist in *in vivo* system, we evaluated whether the combined treatment of vitamin E forms and their long-chain metabolites has synergistic antiproliferative effects in colon cancer cells using MTT assay. Human colon HCT-116 cancer cells were treated with lower doses of δT or δT-13'-COOH alone or with their combination for 72 h. Treatment of cells with 5-10 μM δT or 2.5-5 μM δT-13'-COOH had no or little effect on cell growth, but combinded treatment of δT with δT-COOH induced a significant inhibition of cell growth in a dose-dependent manner (Fig. 3.12A). HCT-116 cells were also treated with lower doses of δTE or δTE-13'-COOH alone or with their combination for 72 h. Similar to the combined effects of δT and δT-13'-COOH, 2.5-5 μM δTE or 2.5-5μM had no effect on cell growth, but their combination exhibited a significant additive or synergistic antiproliferative effects (Fig. 3.12B).

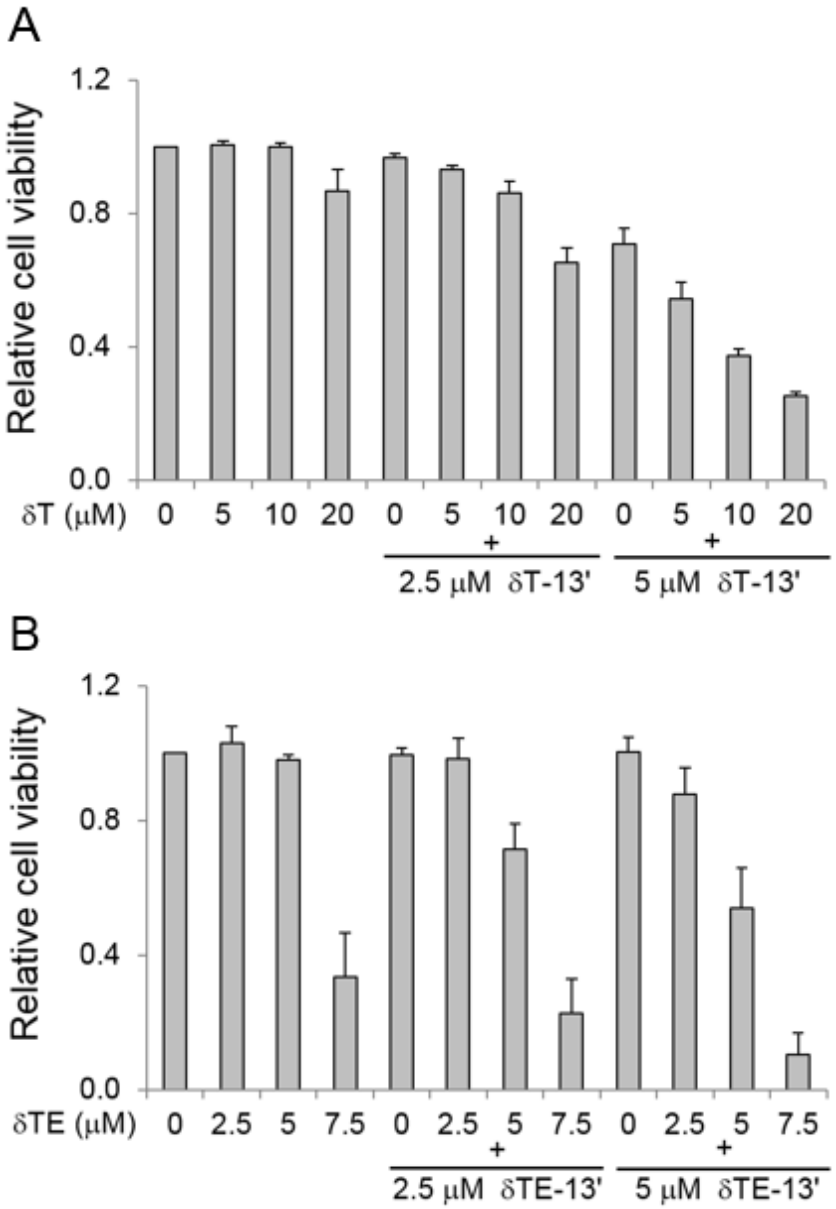

Figure 3.12 Effects of combined treatment of specific vitamin E forms with their long-chain metabolites on cancer cell growth. HCT-116 cells were treated with (A) δT, δT-13'-COOH, and their combination or (B) δTE, δTE-13'-COOH, and their combination for 72 h. Relative cell viability was measured after treatment with individual natural forms of vitamin E or their metabolites alone or with a combination at the stated concentrations by MTT assay compared with control. The data are mean ± SD for three independent experiments, each performed in duplicate.

Table 3.1 Effect of δT-13'-COOH on sphingolipid metabolism in HCT-116 cells. HCT-116 cells were treated with 10 or 20 μM δT-13'-COOH for 1, 2, 4, 8 and 16 h. The amount of each sphingolipid was determined by LC-MS/MS. Data are mean ± SEM of at least 3 independent experiments. *$p < 0.05$, **$p < 0.01$, significant difference between control and δT-13'-COOH-treated cells. Cer, ceramide; dhCer, dihydroceramide; Sph, sphingosine; dhSph, dihydrosphingosine; S1P, sphingosine-1-phosphate; SM, sphingomyelin; dhSM, dihydrosphingomyelin

Ceramides (pmol/μg PC)

$C_{16:0}$-Cer

Hours	**Control**	**δT-13' 10 μM**	**δT-13' 20 μM**
1	2.33 ± 0.40	1.96 ± 0.12	1.84 ± 0.15
2	3.04 ± 0.06	1.92 ± 0.10**	2.15 ± 0.13**
4	2.27 ± 0.26	1.81 ± 0.19**	2.36 ± 0.23
8	2.41 ± 0.18	2.00 ± 0.28*	2.76 ± 0.21*
16	2.91 ± 0.15	3.36 ± 0.05*	6.23 ± 0.47*

$C_{18:0}$-Cer

Hours	**Control**	**δT-13' 10 μM**	**δT-13' 20 μM**
1	0.061 ± 0.005	0.062 ± 0.007	0.076 ± 0.014
2	0.063 ± 0.004	0.052 ± 0.002	0.072 ± 0.004
4	0.051 ± 0.012	0.050 ± 0.013	0.079 ± 0.021**
8	0.041 ± 0.004	0.037 ± 0.003	0.064 ± 0.003**
16	0.040 ± 0.002	0.052 ± 0.001**	0.091 ± 0.005**

$C_{20:0}$-Cer

Hours	**Control**	**δT-13' 10 μM**	**δT-13' 20 μM**
1	0.043 ± 0.012	0.039 ± 0.007	0.044 ± 0.008
2	0.045 ± 0.006	0.038 ± 0.005**	0.059 ± 0.006**
4	0.036 ± 0.003	0.044 ± 0.017	0.085 ± 0.024**
8	0.028 ± 0.003	0.029 ± 0.002	0.063 ± 0.005**
16	0.028 ± 0.000	0.046 ± 0.002**	0.081 ± 0.005**

$C_{22:0}$-Cer

Hours	**Control**	**δT-13' 10 μM**	**δT-13' 20 μM**
1	0.45 ± 0.14	0.52 ± 0.096	0.60 ± 0.11
2	0.55 ± 0.074	0.56 ± 0.063	0.77 ± 0.069**
4	0.30 ± 0.092	0.58 ± 0.19**	0.83 ± 0.23**
8	0.27 ± 0.043	0.36 ± 0.027	0.53 ± 0.17
16	0.26 ± 0.010	0.51 ± 0.020**	0.78 ± 0.049**

$C_{24:1}$-Cer

Hours	**Control**	**δT-13' 10 μM**	**δT-13' 20 μM**
1	2.62 ± 0.55	2.13 ± 0.52**	2.35 ± 0.46
2	3.25 ± 1.28	2.13 ± 0.58	2.65 ± 0.59

4	1.06 ± 0.03	0.90 ± 0.07*	1.32 ± 0.07**
8	1.48 ± 0.40	1.03 ± 0.30**	1.87 ± 0.42**
16	2.00 ± 0.34	1.43 ± 0.27**	2.65 ± 0.42

$C_{24:0}$-Cer

Hours	**Control**	**δT-13' 10 μM**	**δT-13' 20 μM**
1	2.74 ± 0.50	2.64 ± 0.62	2.63 ± 0.55
2	3.48 ± 1.10	2.93 ± 0.73	2.81 ± 0.69
4	1.25 ± 0.16	1.66 ± 0.22**	1.24 ± 0.11
8	1.70 ± 0.29	2.20 ± 0.42**	1.51 ± 0.27
16	2.92 ± 0.28	3.59 ± 0.51*	2.11 ± 0.33*

$C_{26:1}$-Cer

Hours	**Control**	**δT-13' 10 μM**	**δT-13' 20 μM**
1	0.27 ± 0.044	0.22 ± 0.045**	0.23 ± 0.034
2	0.36 ± 0.13	0.23 ± 0.064**	0.27 ± 0.063
4	0.12 ± 0.013	0.11 ± 0.011	0.14 ± 0.012
8	0.15 ± 0.016	0.097 ± 0.015**	0.18 ± 0.017**
16	0.23 ± 0.009	0.13 ± 0.010**	0.29 ± 0.013

$C_{26:0}$-Cer

Hours	**Control**	**δT-13' 10 μM**	**δT-13' 20 μM**
1	0.14 ± 0.076	0.11 ± 0.064	0.12 ± 0.063
2	0.19 ± 0.12	0.12 ± 0.068	0.13 ± 0.072
4	0.11 ± 0.009	0.097 ± 0.009	0.098 ± 0.008
8	0.13 ± 0.016	0.11 ± 0.020**	0.12 ± 0.019
16	0.24 ± 0.005	0.13 ± 0.014**	0.16 ± 0.010**

Total Cers

Hours	**Control**	**δT-13' 10 μM**	**δT-13' 20 μM**
1	8.66 ± 0.71	7.68 ± 1.02	7.89 ± 0.84
2	10.97 ± 2.57	7.97 ±1.30**	8.91 ± 1.27
4	5.20 ± 0.57	5.25 ±0.71	6.16 ± 0.67**
8	6.21 ±0.90	5.87 ±1.03	7.08 ± 0.86**
16	8.63 ±0.78	9.24 ± 0.86	12.39 ± 0.84

Dihydroceramides (pmol/μg PC)

$C_{16:0}$-dhCer

Hours	**Control**	**δT-13' 10 μM**	**δT-13' 20 μM**
1	0.073 ± 0.009	0.092 ± 0.004	0.12 ± 0.017*
2	0.11 ± 0.004	0.13 ± 0.015	0.28 ± 0.031*
4	0.060 ± 0.005	0.13 ± 0.024*	0.33 ± 0.017**
8	0.087 ± 0.007	0.26 ± 0.031**	1.13 ± 0.092**
16	0.23 ± 0.022	1.04 ± 0.060**	3.40 ± 0.43**

$C_{18:0}$-dhCer

Hours	**Control**	**δT-13' 10 μM**	**δT-13' 20 μM**
1	0.0016 ± 0.0001	0.0017 ± 0.0003	0.0025 ± 0.0005
2	0.0016 ± 0.0001	0.0015 ± 0.0001	0.0035 ± 0.0003*
4	0.0016 ± 0.0003	0.0022 ± 0.0007	0.0041 ± 0.0005
8	0.0015 ± 0.0002	0.0023 ± 0.0004	0.011 ± 0.0024*
16	0.0017 ± 0.0003	0.0060 ± 0.0008**	0.027 ± 0.0024**

$C_{20:0}$-dhCer

Hours	**Control**	**δT-13' 10 μM**	**δT-13' 20 μM**
1	0.0008 ± 0.0003	0.0007 ± 0.0001	0.0012 ± 0.0005
2	0.0009 ± 0.0002	0.0012 ± 0.0003	0.0020 ± 0.0002
4	0.0006 ± 0.0001	0.0013 ± 0.0006	0.0038 ± 0.0009*
8	0.0006 ± 0.0001	0.0020 ± 0.0005*	0.143 ± 0.14
16	0.0011 ± 0.0000	0.0058 ± 0.0006**	0.013 ± 0.003**

$C_{22:0}$-dhCer

Hours	**Control**	**δT-13' 10 μM**	**δT-13' 20 μM**
1	0.0035 ± 0.0012	0.0035 ± 0.001	0.0059 ± 0.0012
2	0.0037 ± 0.001	0.0053 ± 0.001*	0.012 ± 0.0016**
4	0.0030 ± 0.001	0.0098 ± 0.004	0.032 ± 0.0084**
8	0.0034 ± 0.0002	0.014 ± 0.0024**	0.279 ± 0.23
16	0.0059 ± 0.001	0.048 ± 0.0060**	0.069 ± 0.011**

$C_{24:1}$-dhCer

Hours	**Control**	**δT-13' 10 μM**	**δT-13' 20 μM**
1	0.0065 ± 0.001	0.0058 ± 0.001	0.0079 ± 0.001
2	0.0080 ± 0.003	0.0068 ± 0.014	0.015 ± 0.003
4	0.0045 ± 0.001	0.0105 ± 0.001**	0.025 ± 0.001**
8	0.0079 ± 0.001	0.024 ± 0.004**	0.082 ± 0.007**
16	0.025 ± 0.004	0.071 ± 0.005*	0.15 ± 0.013**

$C_{24:0}$-dhCer

Hours	**Control**	**δT-13' 10 μM**	**δT-13' 20 μM**
1	0.0078 ± 0.001	0.0060 ± 0.0004	0.0067 ± 0.001
2	0.0080 ± 0.001	0.011 ± 0.003	0.017 ± 0.004
4	0.0056 ± 0.0004	0.020 ± 0.003*	0.025 ± 0.001**
8	0.011 ± 0.001	0.053 ± 0.009**	0.074 ± 0.004**
16	0.039 ± 0.005	0.22 ± 0.014**	0.13 ± 0.013**

$C_{26:1}$-dhCer

Hours	**Control**	**δT-13' 10 μM**	**δT-13' 20 μM**
1	0.00025 ± 0.0002	0.00016 ± 0.0002	0.00054 ± 0.0005
2	0.00022 ± 0.0002	0.00023 ± 0.0002	0.00054 ± 0.0005
4	0.00064 ± 0.0003	0.00060 ± 0.0004	0.0015 ± 0.001
8	0.00073 ± 0.0004	0.0017 ± 0.001	0.0088 ± 0.001
16	0.0041 ± 0.001	0.0080 ± 0.001	0.020 ± 0.003**

Total dhCers

Hours	Control	δT-13' 10 μM	δT-13' 20 μM
1	0.093 ± 0.009	0.11 ± 0.005	0.15 ± 0.021
2	0.13 ± 0.007	0.16 ± 0.017	0.33 ± 0.036*
4	0.075 ± 0.004	0.17 ± 0.033*	0.42 ± 0.027**
8	0.11 ± 0.008	0.35 ± 0.047**	1.73 ± 0.44**
16	0.31 ± 0.032	1.44 ± 0.10**	3.82 ± 0.47**

Sphingoid bases (pmol/μg PC)

Sph

Hours	Control	δT-13' 10 μM	δT-13' 20 μM
1	0.80 ± 0.10	1.00 ± 0.31	1.01 ± 0.33
2	1.03 ± 0.32	0.85 ± 0.22*	0.92 ± 0.29
4	0.63 ± 0.14	0.56 ± 0.14	0.62 ± 0.14
8	0.40 ± 0.057	0.38 ± 0.064	0.41 ± 0.035
16	0.43 ± 0.023	0.37 ± 0.027	0.45 ± 0.037

dhSph

Hours	Control	δT-13' 10 μM	δT-13' 20 μM
1	0.057 ± 0.017	0.068 ± 0.009	0.11 ± 0.032**
2	0.062 ± 0.008	0.067 ± 0.007*	0.12 ± 0.015
4	0.054 ± 0.012	0.064 ± 0.003	0.14 ± 0.016*
8	0.064 ± 0.003	0.060 ± 0.009	0.51 ± 0.18*
16	0.059 ± 0.005	0.12 ± 0.006**	1.90 ± 0.24**

S1P

Hours	Control	δT-13' 10 μM	δT-13' 20 μM
1	0.025 ± 0.007	0.019 ± 0.005	0.029 ± 0.008
2	0.016 ± 0.006	0.015 ± 0.004	0.019 ± 0.003
4	0.011 ± 0.002	0.0065 ± 0.001	0.012 ± 0.001
8	0.014 ± 0.005	0.021 ± 0.006	0.014 ± 0.004
16	0.013 ± 0.003	0.013 ± 0.002	0.015 ± 0.002

Sphingomyelins (pmol/μg PC)

$C_{16:0}$-SM

Hours	Control	δT-13' 10 μM	δT-13' 20 μM
1	54.41 ± 4.37	56.25 ± 5.70	54.49 ± 6.22
2	64.18 ± 6.12	55.41 ± 1.62	54.51 ± 2.77*
4	51.09 ± 3.76	52.39 ± 2.37	40.89 ± 2.23
8	64.19 ± 3.16	49.32 ± 5.61**	39.78 ± 2.80**
16	100.55 ± 13.49	58.11 ± 7.22**	48.45 ± 5.62**

$C_{18:0}$-SM

Hours	**Control**	**δT-13' 10 µM**	**δT-13' 20 µM**
1	0.69 ± 0.068	0.69 ± 0.079	0.66 ± 0.092
2	0.78 ± 0.079	0.68 ± 0.046	0.68 ± 0.062*
4	0.67 ± 0.037	0.66 ± 0.030	0.54 ± 0.009**
8	0.69 ± 0.025	0.59 ± 0.055*	0.53 ± 0.020**
16	0.74 ± 0.078	0.58 ± 0.043**	0.54 ± 0.083**

$C_{20:0}$-SM

Hours	**Control**	**δT-13' 10 µM**	**δT-13' 20 µM**
1	0.57 ± 0.092	0.60 ± 0.095*	0.56 ± 0.11
2	0.68 ± 0.089	0.62 ± 0.052	0.60 ± 0.068
4	0.62 ± 0.051	0.66 ± 0.046	0.55 ± 0.017
8	0.62 ± 0.029	0.57 ± 0.030	0.49 ± 0.040**
16	0.63 ± 0.047	0.53 ± 0.027*	0.46 ± 0.064*

$C_{22:0}$-SM

Hours	**Control**	**δT-13' 10 µM**	**δT-13' 20 µM**
1	3.31 ± 0.87	3.31 ± 0.75	3.21 ± 0.71
2	3.89 ± 0.73	3.56 ± 0.41	3.50 ± 0.52*
4	2.84 ± 0.35	3.28 ± 0.49*	2.56 ± 0.29*
8	2.73 ± 0.19	2.93 ± 0.32	2.23 ± 0.16*
16	3.11 ± 0.19	3.00 ± 0.02	2.32 ± 0.41*

$C_{24:1}$-SM

Hours	**Control**	**δT-13' 10 µM**	**δT-13' 20 µM**
1	15.13 ± 3.31	14.55 ± 3.49	14.25 ± 3.49
2	17.69 ± 3.23	15.92 ± 1.41	15.63 ± 2.12
4	14.94 ± 3.03	15.76 ± 3.46	12.65 ± 2.28**
8	12.66 ± 1.51	10.88 ± 1.47*	8.92 ± 1.22**
16	13.11 ± 1.24	9.16 ± 0.86**	7.43 ± 1.15**

$C_{26:1}$-SM

Hours	**Control**	**δT-13' 10 µM**	**δT-13' 20 µM**
1	0.79 ± 0.19	0.75 ± 0.19	0.72 ± 0.19
2	0.96 ± 0.15	0.82 ± 0.05	0.78 ± 0.07*
4	0.98 ± 0.27	1.09 ± 0.29	0.89 ± 0.21
8	0.76 ± 0.18	0.60 ± 0.14*	0.55 ± 0.13**
16	0.74 ± 0.11	0.45 ± 0.04**	0.46 ± 0.11**

Total SMs

Hours	**Control**	**δT-13' 10 µM**	**δT-13' 20 µM**
1	74.90 ± 8.79	76.16 ± 10.25	73.90 ± 10.75
2	88.18 ± 10.37	77.01 ± 3.10	75.69 ± 5.59*
4	71.14 ± 5.94	73.84 ± 4.43	58.09 ± 0.88
8	81.65 ± 1.86	64.89 ± 5.26**	52.50 ± 2.29**
16	118.88 ± 15.07	71.82 ± 8.03**	59.64 ± 7.39**

Dihydrosphingomyelins (pmol/μg PC)

$C_{16:0}$-dhSM

Hours	**Control**	**δT-13' 10 μM**	**δT-13' 20 μM**
1	6.60 ± 0.38	6.43 ± 0.27	6.53 ± 0.53
2	8.42 ± 1.63	7.60 ± 1.52**	7.59 ± 1.38*
4	8.12 ± 0.75	8.85 ± 1.61	7.57 ± 1.28
8	9.18 ± 1.04	9.68 ± 0.65	8.24 ± 0.91*
16	9.49 ± 0.98	10.73 ± 1.03	10.08 ± 1.68

$C_{18:0}$-dhSM

Hours	**Control**	**δT-13' 10 μM**	**δT-13' 20 μM**
1	0.14 ± 0.010	0.15 ± 0.012	0.14 ± 0.018
2	0.18 ± 0.027	0.17 ± 0.041	0.16 ± 0.027**
4	0.29 ± 0.078	0.28 ± 0.077	0.24 ± 0.071
8	0.26 ± 0.065	0.24 ± 0.044	0.22 ± 0.052
16	0.74 ± 0.078	0.58 ± 0.043	0.54 ± 0.083

$C_{20:0}$-dhSM

Hours	**Control**	**δT-13' 10 μM**	**δT-13' 20 μM**
1	0.13 ± 0.017	0.14 ± 0.025	0.14 ± 0.031
2	0.15 ± 0.015	0.14 ± 0.022	0.13 ± 0.020
4	0.22 ± 0.018	0.22 ± 0.032	0.20 ± 0.027
8	0.18 ± 0.035	0.18 ± 0.029	0.16 ± 0.037*
16	0.13 ± 0.032	0.16 ± 0.034**	0.14 ± 0.035

$C_{22:0}$-dhSM

Hours	**Control**	**δT-13' 10 μM**	**δT-13' 20 μM**
1	0.37 ± 0.067	0.39 ± 0.038	0.37 ± 0.039
2	0.47 ± 0.061	0.46 ± 0.069	0.44 ± 0.072
4	0.69 ± 0.12	0.67 ± 0.10	0.61 ± 0.11
8	0.49 ± 0.061	0.55 ± 0.078	0.49 ± 0.079
16	0.32 ± 0.051	0.59 ± 0.098**	0.50 ± 0.14

$C_{24:0}$-dhSM

Hours	**Control**	**δT-13' 10 μM**	**δT-13' 20 μM**
1	0.55 ± 0.13	0.49 ± 0.071	0.48 ± 0.071
2	0.71 ± 0.080	0.61 ± 0.081*	0.64 ± 0.12
4	1.05 ± 0.58	1.23 ± 0.71	0.89 ± 0.46
8	0.46 ± 0.13	0.50 ± 0.086	0.40 ± 0.11
16	0.45 ± 0.069	0.81 ± 0.12**	0.55 ± 0.18

$C_{26:0}$-dhSM

Hours	**Control**	**δT-13' 10 μM**	**δT-13' 20 μM**
1	0.07 ± 0.007	0.06 ± 0.004*	0.06 ± 0.006

2	0.08 ± 0.011	0.08 ± 0.020	0.08 ± 0.017
4	0.13 ± 0.061	0.13 ± 0.071	0.12 ± 0.057
8	0.05 ± 0.024	0.05 ± 0.016	0.05 ± 0.014
16	0.04 ± 0.010	0.12 ± 0.084	0.04 ± 0.013

Total dhSMs

Hours	**Control**	**δT-13' 10 μM**	**δT-13' 20 μM**
1	7.87 ± 0.61	7.65 ± 0.22	7.73 ± 0.51
2	10.02 ± 1.76	9.06 ± 1.73**	9.03 ± 1.61*
4	10.50 ± 1.01	11.38 ± 2.04	9.64 ± 1.40
8	10.63 ± 1.30	11.20 ± 0.78	9.56 ± 1.12*
16	10.58 ± 1.15	12.57 ± 1.29	11.49 ± 2.08

Table 3.2 Effect of δT-13'-COOH on sphingolipid metabolism in MCF-7 cells. MCF-7 cells were treated with 10 or 20 μM δT-13'-COOH for 4 and 8 h. The amount of each sphingolipid was determined by LC-MS/MS. Data are mean ± SEM of 2 independent experiments.

Ceramides (pmol/μg PC)

$C_{16:0}$-Cer

Hours	**Control**	**δT-13' 10 μM**	**δT-13' 20 μM**
4	1.49 ± 0.082	1.30 ± 0.17	1.56 ± 0.006
8	1.48 ± 0.14	1.23 ± 0.007	2.23 ± 0.23

$C_{18:0}$-Cer

Hours	**Control**	**δT-13' 10 μM**	**δT-13' 20 μM**
4	0.10 ± 0.015	0.084 ± 0.0004	0.086 ± 0.005
8	0.094 ± 0.001	0.071 ± 0.001	0.11 ± 0.001

$C_{20:0}$-Cer

Hours	**Control**	**δT-13' 10 μM**	**δT-13' 20 μM**
4	0.020 ± 0.0018	0.021 ± 0.0005	0.026 ± 0.0014
8	0.018 ± 0.0006	0.022 ± 0.0014	0.033 ± 0.0023

$C_{22:0}$-Cer

Hours	**Control**	**δT-13' 10 μM**	**δT-13' 20 μM**
4	0.056 ± 0.024	0.070 ± 0.051	0.068 ± 0.048
8	0.060 ± 0.038	0.079 ± 0.057	0.11 ± 0.096

$C_{24:1}$-Cer

Hours	**Control**	**δT-13' 10 μM**	**δT-13' 20 μM**
4	13.19 ± 1.19	12.21 ± 1.59	18.75 ± 1.51
8	13.57 ± 1.71	12.60 ± 1.26	25.52 ± 3.41

$C_{24:0}$-Cer

Hours	**Control**	**δT-13' 10 µM**	**δT-13' 20 µM**
4	2.34 ± 0.31	3.59 ± 0.24	2.56 ± 0.026
8	2.34 ± 0.20	5.34 ± 0.092	4.00 ± 0.082

$C_{26:1}$-Cer

Hours	**Control**	**δT-13' 10 µM**	**δT-13' 20 µM**
4	0.26 ± 0.10	0.41 ± 0.031	0.45 ± 0.019
8	0.27 ± 0.025	0.51 ± 0.0001	0.74 ± 0.035

Total Cers

Hours	**Control**	**δT-13' 10 µM**	**δT-13' 20 µM**
4	17..45 ± 1.67	17.68 ± 2.08	23.51 ± 1.56
8	17.84 ± 2.12	19.85 ± 1.41	32.75 ± 3.69

Dihydroceramides (pmol/µg PC)

$C_{16:0}$-dhCer

Hours	**Control**	**δT-13' 10 µM**	**δT-13' 20 µM**
4	0.093 ± 0.035	0.12 ± 0.027	0.14 ± 0.007
8	0.11 ± 0.022	0.13 ± 0.030	0.29 ± 0.018

$C_{18:0}$-dhCer

Hours	**Control**	**δT-13' 10 µM**	**δT-13' 20 µM**
4	0.0019 ± 0.0005	0.0028 ± 0.0007	0.004 ± 0.0006
8	0.0022 ± 0.0006	0.0036 ± 0.0009	0.0029 ± 0.0001

$C_{22:0}$-dhCer

Hours	**Control**	**δT-13' 10 µM**	**δT-13' 20 µM**
4	0.00051 ± 0.0003	0.0028 ± 0.0016	0.0039 ± 0.0012
8	0.0019 ± 0.0004	0.0044 ± 0.00001	0.0091 ± 0.0009

$C_{24:1}$-dhCer

Hours	**Control**	**δT-13' 10 µM**	**δT-13' 20 µM**
4	0.085 ± 0.0070	0.096 ± 0.018	0.24 ± 0.062
8	0.055 ± 0.0067	0.11 ± 0.036	0.41 ± 0.088

Total dhCers

Hours	**Control**	**δT-13' 10 µM**	**δT-13' 20 µM**
4	0.18 ± 0.029	0.22 ± 0.011	0.39 ± 0.053
8	0.16 ± 0.017	0.25 ± 0.0049	0.71 ± 0.071

Sphingoid bases (pmol/µg PC)

Sph

Hours	**Control**	**δT-13' 10 µM**	**δT-13' 20 µM**
4	0.51 ± 0.11	0.43 ± 0.017	0.49 ± 0.11
8	0.47 ± 0.0036	0.40 ± 0.045	0.46 ± 0.064

S1P

Hours	**Control**	**δT-13' 10 µM**	**δT-13' 20 µM**
4	0.010 ± 0.0004	0.016 ± 0.008	0.013 ± 0.001
8	0.013 ± 0.005	0.010 ± 0.0001	0.012 ± 0.004

Sphingomyelins (pmol/µg PC)

$C_{16:0}$-SM

Hours	**Control**	**δT-13' 10 µM**	**δT-13' 20 µM**
4	32.77 ± 4.04	31.70 ± 0.15	23.85 ± 0.34
8	34.30 ± 0.38	30.49 ± 0.09	23.92 ± 1.44

$C_{18:0}$-SM

Hours	**Control**	**δT-13' 10 µM**	**δT-13' 20 µM**
4	1.73 ± 0.33	1.73 ± 0.13	1.29 ± 0.10
8	1.79 ± 0.11	1.62 ± 0.17	1.25 ± 0.22

$C_{20:0}$-SM

Hours	**Control**	**δT-13' 10 µM**	**δT-13' 20 µM**
4	0.90 ± 0.18	0.93 ± 0.056	0.60 ± 0.019
8	0.92 ± 0.023	0.86 ± 0.11	0.62 ± 0.094

$C_{22:0}$-SM

Hours	**Control**	**δT-13' 10 µM**	**δT-13' 20 µM**
4	2.09 ± 0.67	2.06 ± 0.25	1.30 ± 0.068
8	1.92 ± 0.13	2.18 ± 0.30	1.43 ± 0.34

$C_{24:1}$-SM

Hours	**Control**	**δT-13' 10 µM**	**δT-13' 20 µM**
4	14.23 ± 3.11	12.96 ± 0.0033	8.88 ± 0.32
8	12.66 ± 0.61	11.89 ± 0.13	9.36 ± 0.66

$C_{26:1}$-SM

Hours	**Control**	**δT-13' 10 µM**	**δT-13' 20 µM**
4	3.26 ± 0.88	2.58 ± 0.016	1.72 ± 0.12
8	2.58 ± 0.12	2.51 ± 0.028	1.73 ± 0.13

Total SMs

Hours	**Control**	**δT-13' 10 µM**	**δT-13' 20 µM**
4	54.98 ± 9.21	51.96 ± 0.60	37.64 ± 0.082

8	54.17 ± 0.85	49.55 ± 0.64	38.35 ± 2.87

Dihydrosphingomyelins (pmol/μg PC)

$C_{16:0}$-dhSM

Hours	**Control**	**δT-13' 10 μM**	**δT-13' 20 μM**
4	3.84 ± 0.39	4.72 ± 0.027	3.30 ± 0.14
8	4.38 ± 0.14	4.96 ± 0.14	3.85 ± 0.21

$C_{18:0}$-dhSM

Hours	**Control**	**δT-13' 10 μM**	**δT-13' 20 μM**
4	0.24 ± 0.040	0.28 ± 0.021	0.18 ± 0.006
8	0.26 ± 0.010	0.30 ± 0.033	0.18 ± 0.026

$C_{20:0}$-dhSM

Hours	**Control**	**δT-13' 10 μM**	**δT-13' 20 μM**
4	0.18 ± 0.055	0.21 ± 0.020	0.12 ± 0.017
8	0.18 ± 0.0005	0.23 ± 0.035	0.12 ± 0.030

$C_{22:0}$-dhSM

Hours	**Control**	**δT-13' 10 μM**	**δT-13' 20 μM**
4	0.16 ± 0..054	0.18 ± 0.021	0.10 ± 0.0026
8	0.13 ± 0.0033	0.21 ± 0.024	0.12 ± 0.023

$C_{24:0}$-dhSM

Hours	**Control**	**δT-13' 10 μM**	**δT-13' 20 μM**
4	0.096 ± 0.029	0.11 ± 0.013	0.066 ± 0.0021
8	0.080 ± 0.0017	0.13 ± 0.016	0.076 ± 0.015

$C_{26:0}$-dhSM

Hours	**Control**	**δT-13' 10 μM**	**δT-13' 20 μM**
4	0.027 ± 0.0084	0.032 ± 0.0045	0.016 ± 0.0023
8	0.021 ± 0.0003	0.031 ± 0.0017	0.020 ± 0.0057

Total dhSMs

Hours	**Control**	**δT-13' 10 μM**	**δT-13' 20 μM**
4	4.54 ± 0.58	5.55 ± 0.052	3.79 ± 0.12
8	5.04 ± 0.13	5.86 ± 0.25	4.37 ± 0.31

Table 3.3 Effect of δTE-13'-COOH on sphingolipid metabolism in HCT-116 cells. HCT-116 cells were treated with 10 or 20 μM δTE-13'-COOH for 8 and 16 h. The amount of each sphingolipid was determined by LC-MS/MS. Data are mean ± SEM of 2 independent experiments.

Ceramides (pmol/μg PC)

$C_{16:0}$-Cer

Hours	Control	δTE-13' 10 μM	δTE-13' 20 μM
8	2.43 ± 0.036	1.79 ± 0.0047	2.20 ± 0.051
16	2.82 ± 0.080	1.69 ± 0.070	3.04 ± 0.26

$C_{18:0}$-Cer

Hours	Control	δTE-13' 10 μM	δTE-13' 20 μM
8	0.043 ± 0.003	0.035 ± 0.001	0.050 ± 0.002
16	0.039 ± 0.001	0.030 ± 0.002	0.066 ± 0.010

$C_{20:0}$-Cer

Hours	Control	δTE-13' 10 μM	δTE-13' 20 μM
8	0.025 ± 0.001	0.021 ± 0.002	0.052 ± 0.001
16	0.027 ± 0.001	0.018 ± 0.002	0.064 ± 0.012

$C_{22:0}$-Cer

Hours	Control	δTE-13' 10 μM	δTE-13' 20 μM
8	0.22 ± 0.016	0.24 ± 0.0004	0.49 ± 0.005
16	0.23 ± 0.005	0.21 ± 0.001	0.55 ± 0.049

$C_{24:1}$-Cer

Hours	Control	δTE-13' 10 μM	δTE-13' 20 μM
8	2.58 ± 0.27	1.92 ± 0.049	2.46 ± 0.12
16	2.68 ± 0.029	1.49 ± 0.010	2.26 ± 0.15

$C_{24:0}$-Cer

Hours	Control	δTE-13' 10 μM	δTE-13' 20 μM
8	2.64 ± 0.14	3.42 ± 0.22	3.12 ± 0.30
16	3.40 ± 0.007	4.15 ± 0.026	3.22 ± 0.26

$C_{26:1}$-Cer

Hours	Control	δTE-13' 10 μM	δTE-13' 20 μM
8	0.21 ± 0.007	0.17 ± 0.008	0.21 ± 0.014
16	0.27 ± 0.008	0.16 ± 0.008	0.21 ± 0.004

$C_{26:0}$-Cer

Hours	Control	δTE-13' 10 μM	δTE-13' 20 μM
8	0.16 ± 0.030	0.16 ± 0.003	0.16 ± 0.001
16	0.23 ± 0.001	0.19 ± 0.003	0.13 ± 0.011

Total Cers

Hours	Control	δTE-13' 10 μM	δTE-13' 20 μM
8	8.31 ± 0.49	7.76 ± 0.28	8.74 ± 0.48
16	9.70 ± 0.042	7.94 ± 0.098	9.55 ± 0.24

Dihydroceramides (pmol/μg PC)

$C_{16:0}$-dhCer

Hours	Control	δTE-13' 10 μM	δTE-13' 20 μM
8	0.19 ± 0.02	0.38 ± 0.03	0.85 ± 0.01
16	0.42 ± 0.002	0.52 ± 0.02	1.86 ± 0.22

$C_{18:0}$-dhCer

Hours	Control	δTE-13' 10 μM	δTE-13' 20 μM
8	0.0011 ± 0.0001	0.0017 ± 0.0004	0.0035 ± 0.00003
16	0.0020 ± 0.0006	0.0020 ± 0.0001	0.0087 ± 0.0005

$C_{20:0}$-dhCer

Hours	Control	δTE-13' 10 μM	δTE-13' 20 μM
8	0.0010 ± 0.0004	0.0010 ± 0.0002	0.0047 ± 0.0019
16	0.0004 ± 0.0001	0.0013 ± 0.0002	0.0086 ± 0.0009

$C_{22:0}$-dhCer

Hours	Control	δTE-13' 10 μM	δTE-13' 20 μM
8	0.0043 ± 0.0011	0.0076 ± 0.0013	0.022 ± 0.0019
16	0.0080 ± 0.0002	0.013 ± 0.0010	0.053 ± 0.0029

$C_{24:1}$-dhCer

Hours	Control	δTE-13' 10 μM	δTE-13' 20 μM
8	0.016 ± 0.001	0.035 ± 0.001	0.076 ± 0.010
16	0.043 ± 0.001	0.050 ± 0.005	0.14 ± 0.001

$C_{24:0}$-dhCer

Hours	Control	δTE-13' 10 μM	δTE-13' 20 μM
8	0.028 ± 0.007	0.083 ± 0.011	0.086 ± 0.007
16	0.066 ± 0.005	0.16 ± 0.011	0.21 ± 0.019

Total dhCers

Hours	Control	δTE-13' 10 μM	δTE-13' 20 μM
8	0.24 ± 0.033	0.51 ± 0.040	1.04 ± 0.007
16	0.54 ± 0.003	0.74 ± 0.018	2.28 ± 0.20

Sphingoid bases (pmol/μg PC)

Sph

Hours	Control	δTE-13' 10μM	δTE-13' 20μM
8	0.52 ± 0.067	0.42 ± 0.009	0.39 ± 0.097
16	0.37 ± 0.043	0.35 ± 0.008	0.39 ± 0.063

dhSph

Hours	Control	δTE-13' 10μM	δTE-13' 20μM
8	0.049 ± 0.006	0.054 ± 0.003	0.12 ± 0.00002
16	0.043 ± 0.005	0.074 ± 0.004	0.15 ± 0.013

S1P

Hours	Control	δTE-13' 10μM	δTE-13' 20μM
8	0.025 ± 0.007	0.025 ± 0.001	0.019 ± 0.003
16	0.013 ± 0.007	0.019 ± 0.002	0.011 ± 0.004

Sphingomyelins (pmol/μg PC)

$C_{16:0}$-SM

Hours	Control	δTE-13' 10μM	δTE-13' 20μM
8	55.88 ± 8.96	54.47 ± 4.88	44.53 ± 0.39
16	71.01 ± 2.01	60.66 ± 3.38	50.29 ± 2.19

$C_{18:0}$-SM

Hours	Control	δTE-13' 10μM	δTE-13' 20μM
8	0.69 ± 0.16	0.70 ± 0.092	0.58 ± 0.037
16	0.59 ± 0.060	0.65 ± 0.066	0.58 ± 0.043

$C_{20:0}$-SM

Hours	Control	δTE-13' 10μM	δTE-13' 20μM
8	0.60 ± 0.21	0.63 ± 0.19	0.53 ± 0.085
16	0.44 ± 0.037	0.57 ± 0.084	0.54 ± 0.094

$C_{22:0}$-SM

Hours	Control	δTE-13' 10μM	δTE-13' 20μM
8	2.52 ± 0.83	2.85 ± 0.74	2.08 ± 0.25
16	1.99 ± 0.25	2.97 ± 0.29	2.55 ± 0.27

$C_{24:1}$-SM

Hours	Control	δTE-13' 10μM	δTE-13' 20μM
8	9.52 ± 2.93	9.30 ± 2.02	6.70 ± 0.28
16	7.98 ± 0.68	8.85 ± 0.66	6.65 ± 0.29

$C_{26:1}$-SM

Hours	Control	δTE-13' 10μM	δTE-13' 20μM
8	0.55 ± 0.22	0.47 ± 0.14	0.33 ± 0.028
16	0.39 ± 0.049	0.43 ± 0.033	0.33 ± 0.038

Total SMs

Hours	Control	δTE-13' 10μM	δTE-13' 20μM
8	75.64 ± 15.77	74.35 ± 9.95	58.38 ± 0.62
16	86.85 ± 3.84	81.38 ± 5.36	65.20 ± 1.17

Dihydrosphingomyelins (pmol/μg PC)

$C_{16:0}$-dhSM

Hours	Control	δTE-13' 10μM	δTE-13' 20μM
8	6.71 ± 1.44	8.80 ± 1.08	7.44 ± 0.32
16	7.89 ± 1.63	13.28 ± 0.61	10.26 ± 0.60

$C_{18:0}$-dhSM

Hours	**Control**	**δTE-13' 10μM**	**δTE-13' 20μM**
8	0.14 ± 0.045	0.17 ± 0.034	0.15 ± 0.009
16	0.10 ± 0.019	0.18 ± 0.014	0.19 ± 0.023

$C_{20:0}$-dhSM

Hours	**Control**	**δTE-13' 10μM**	**δTE-13' 20μM**
8	0.11 ± 0..037	0.11 ± 0.029	0.10 ± 0.020
16	0.064 ± 0.011	0.14 ± 0.023	0.15 ± 0.026

$C_{22:0}$-dhSM

Hours	**Control**	**δTE-13' 10μM**	**δTE-13' 20μM**
8	0.31 ± 0.12	0.37 ± 0.14	0.27 ± 0.052
16	0.20 ± 0.039	0.60 ± 0.11	0.50 ± 0.080

$C_{24:0}$-dhSM

Hours	**Control**	**δTE-13' 10μM**	**δTE-13' 20μM**
8	0.37 ± 0.17	0.40 ± 0.15	0.24 ± 0.035
16	0.26 ± 0.061	0.78 ± 0.14	0.48 ± 0.018

$C_{26:0}$-dhSM

Hours	**Control**	**δTE-13' 10μM**	**δTE-13' 20μM**
8	0.030 ± 0.013	0.023 ± 0.0084	0.017 ± 0.0068
16	0.016 ± 0.0050	0.033 ± 0.0008	0.023 ± 0.0013

Total dhSMs

Hours	**Control**	**δTE-13' 10μM**	**δTE-13' 20μM**
8	8.55 ± 2.13	10.82 ± 1.68	8.90 ± 0.55
16	9.21 ± 1.88	16.10 ± 1.00	12.44 ± 0.80

Table 3.4 Effect of δT-13'-COOH on *de novo* sphingolipid biosynthesis in HCT-116 cells. HCT-116 cells were treated with either 400 μM $^{13}C_3$, ^{15}N-labeled L-serine alone as control or with a combination of 400 μM $^{13}C_3$, ^{15}N-labeled L-serine and 20 μM δT-13'-COOH for 0.5, 1, 1.5, 2, and 4 h. The amount of each labeled *de novo* sphingolipid was determined by LC-MS/MS. Data are mean ± SEM of 3 independent experiments. *p < 0.05, **p < 0.01, significant difference between control and δT-13'-COOH-treated cells.

Ceramides (pmol/μg PC)

***De novo* $C_{16:0}$-Cer**

Hours	**Control**	**δT-13' 20 μM**
0.5	0.081 ± 0.016	0.023 ± 0.010**
1	0.26 ± 0.015	0.10 ± 0.0074**
1.5	0.33 ± 0.046	0.18 ± 0.036**
2	0.40 ± 0.059	0.25 ± 0.044**

4	0.63 ± 0.038	0.41 ± 0.010**

***De novo* $C_{24:1}$-Cer**

Hours	**Control**	**δT-13' 20 µM**
0.5	0.17 ± 0.063	0.069 ± 0.038**
1	0.40 ± 0.11	0.22 ± 0.060**
1.5	0.53 ± 0.19	0.38 ± 0.16**
2	0.65 ± 0.19	0.53 ± 0.18**
4	0.72 ± 0.077	0.62 ± 0.041

***De novo* $C_{24:0}$-Cer**

Hours	**Control**	**δT-13' 20 µM**
0.5	0.13 ± 0.052	0.048 ± 0.020**
1	0.31 ± 0.064	0.13 ± 0.023**
1.5	0.38 ± 0.12	0.22 ± 0.079**
2	0.51 ± 0.15	0.32 ± 0.078**
4	0.75 ± 0.021	0.54 ± 0.038**

***De novo* total Cers**

Hours	**Control**	**δT-13' 20 µM**
0.5	0.37 ± 0.13	0.14 ± 0.068**
1	0.97 ± 0.15	0.45 ± 0.088**
1.5	1.25 ± 0.36	0.78 ± 0.28**
2	1.56 ± 0.39	1.11 ± 0.28**
4	2.09 ± 0.071	1.58 ± 0.068*

Dihydroceramides (pmol/µg PC)

***De novo* $C_{16:0}$-dhCer**

Hours	**Control**	**δT-13' 20 µM**
0.5	0.013 ± 0.0029	0.0058 ± 0.0014*
1	0.028 ± 0.0086	0.028 ± 0.010
1.5	0.029 ± 0.0038	0.045 ± 0.0024*
2	0.030 ± 0.0059	0.08 ± 0.0094**
4	0.056 ± 0.014	0.24 ± 0.065**

***De novo* total dhCers**

Hours	**Control**	**δT-13' 20 µM**
0.5	0.013 ± 0.0029	0.0058 ± 0.0014*
1	0.028 ± 0.0086	0.028 ± 0.010
1.5	0.029 ± 0.0038	0.045 ± 0.0024*
2	0.030 ± 0.0059	0.080 ± 0.0094**
4	0.079 ± 0.025	0.32 ± 0.11**

Sphingomyelins (pmol/μg PC)

***De novo* $C_{16:0}$-SM**

Hours	Control	δT-13' 20 μM
0.5	0.56 ± 0.049	0.47 ± 0.045
1	0.77 ± 0.034	0.55 ± 0.041*
1.5	1.05 ± 0.078	0.67 ± 0.092**
2	1.52 ± 0.11	0.99 ± 0.080**
4	2.00 ± 0.66	0.89 ± 0.12**

***De novo* $C_{18:0}$-SM**

Hours	Control	δT-13' 20 μM
0.5	0.017 ± 0.0043	0.026 ± 0.0092
1	0.026 ± 0.0077	0.023 ± 0.0078
1.5	0.027 ± 0.0078	0.022 ± 0.0046
2	0.031 ± 0.0034	0.031 ± 0.0057
4	0.030 ± 0.0038	0.026 ± 0.0014

***De novo* $C_{24:1}$-SM**

Hours	Control	δT-13' 20 μM
0.5	0.12 ± 0.016	0.11 ± 0.015
1	0.16 ± 0.028	0.11 ± 0.011**
1.5	0.19 ± 0.025	0.12 ± 0.007**
2	0.26 ± 0.031	0.17 ± 0.018**
4	0.36 ± 0.10	0.17 ± 0.029**

***De novo* total SMs**

Hours	Control	δT-13' 20 μM
0.5	0.71 ± 0.058	0.62 ± 0.061
1	0.97 ± 0.056	0.69 ± 0.025*
1.5	1.31 ± 0.052	0.84 ± 0.078**
2	1.85 ± 0.058	1.22 ± 0.062**
4	2.59 ± 0.79	1.18 ± 0.15**

Dihydrosphingomyelins (pmol/μg PC)

***De novo* $C_{16:0}$-dhSM**

Hours	Control	δT-13' 20 μM
0.5	0.76 ± 0.0084	0.077 ± 0.011
1	0.11 ± 0.012	0.090 ± 0.0031
1.5	0.14 ± 0.011	0.12 ± 0.013
2	0.17 ± 0.011	0.20 ± 0.014
4	0.23 ± 0.040	0.25 ± 0.025

***De novo* total dhSMs**

Hours	**Control**	**δT-13' 20 μM**
0.5	0.085 ± 0.010	0.086 ± 0.015
1	0.12 ± 0.0053	0.10 ± 0.0056
1.5	0.16 ± 0.0042	0.13 ± 0.012
2	0.19 ± 0.016	0.22 ± 0.0034
4	0.26 ± 0.050	0.29 ± 0.026

3.5 Discussion

We show that vitamin E long-chain metabolites, δT- and δTE-13'-COOH, inhibit the proliferation and induce apoptosis and autophagy in human colon, breast and pancreatic cancer cells. In these anticancer effects, δT-13'-COOH appears to be more potent than δTE-13'-COOH, and both 13'-COOHs are much stronger than tocopherols and slightly stronger than γTE. Using a lipidomic approach with LC-MS/MS, we demonstrate for the first time that 13'-COOHs profoundly modulate sphingolipid metabolism. Specifically, 13'-COOH treatment quickly increased dhCers and dhSph, subsequently enhanced Cers and decreased SMs. The importance of sphingolipid modulation in 13'-COOH-induced anticancer effects is supported by three lines of evidence. First, 13'-COOH-caused increase of dhCers and dhSph took place prior to any manifestation of cell death, and subsequent elevation of Cers occurred prior to and coinciding with LC3-II increase and PARP cleavage. Secondly, dhCers, dhSph and Cers, which are enhanced by 13'-COOHs, have been shown to induce antiproliferation, cell stress and death in different types of cancer cells (Jiang et al., 2012; Jiang et al., 2004;

Zheng et al., 2006). Furthermore, chemically blocking the increase of dhCers and dhSph by myriocin or Cers by suppressing SM hydrolysis partially reversed 13'-COOH-mediated cell death.

We identify DEGS in the *de novo* synthesis of sphingolipid pathway as an initial inhibitory target by 13'-COOHs based on their temporal modulation of endogenous and *newly* synthesized sphingolipids. Specifically, in the study with $^{13}C_3$, ^{15}N-labeled L-serine for tracing newly-made sphingolipids, 13'-COOHs caused rapid increase of dhCers, but profoundly decreased Cers like $C_{16:0}$- and C_{24}-Cers and SMs through *de novo* synthesis. This observation strongly suggests that DEGS-catalyzed conversion of dhCers to Cers is compromised. Consistently, the similar pattern of sphingolipid changes was reported in DEGS knockout model (Ruangsiriluk et al., 2012; Siddique et al., 2013). We further show that despite having no impact on DEGS protein expression, δT-13'-COOH inhibited the enzyme activity in an *in vitro* assay. On the other hand, we did not observe inhibition of DEGS when rat's microsome was used, which may be caused by limited access of 13'-COOHs to microsomal membrane under cell-free condition possibly due to lack of proper transportation.

DEGS was first proposed as a potential inhibitory target for γT that induced intracellular accumulation of dhCers and dhSph without changing total Cers in prostate cancer cells (Jiang et al., 2004). Similar effects on sphingolipids were observed by other known anticancer agents including γTE (Gopalan et al., 2012; Jiang et al., 2012), resveratrol (Signorelli et al., 2009), fenretinide (or 4-HPR) (Rahmaniyan et al., 2011) and celecoxib, a selective COX-2 inhibitor (Schiffmann et al., 2009b). Resveratrol and celecoxib have further been demonstrated to inhibit DEGS enzyme activity in cell

homogenates or intact cells, respectively (Schiffmann et al., 2009b; Signorelli et al., 2009). Recently, DEGS activity was found to be inhibited by hydrogen peroxide (Idkowiak-Baldys et al., 2010) or during hypoxia (Devlin et al., 2011). Interestingly, phenolic compounds are known to have prooxidant effects including presumably increasing hydrogen peroxide *in vitro* and the prooxidant activity can be counteracted by N-acetylcysteine (NAC) (Babich et al., 2009; Fujisawa et al., 2004). In our studies, we found that NAC did not reverse 13'-COOHs'-induced cell death (data not shown) or γTE-induced modulation of sphingolipids (Jang Y and Jiang Q, unpublished data). We therefore conclude that the modulation of dhCers and inhibition of DEGS is not likely caused by prooxidant activity, which is also supported by the inhibition of DEGS by celecoxib that is not a prooxidant.

The use of LC-MS/MS approach revealed that 13'-COOHs have differential effect on different forms of Cers. For instance, compared with controls, 13'-COOH initially decreased $C_{16:0}$-Cer but enhanced it after longer treatment, while caused a continuous increase of $C_{18:0}$-Cer. This is an intriguing observation because recent studies demonstrate that endogenous Cers with specific fatty acid chain lengths have distinct or sometimes opposed roles in proliferation and death (Hannun and Obeid, 2011; Senkal et al., 2010; Sentelle et al., 2012). For instance, $C_{16:0}$-Cer and $C_{18:0}$-Cer generated by Cer synthases 5/6 (CerS5/6) and CerS1 have been shown to have anti- and pro-apoptosis properties (Senkal et al., 2010), respectively. Besides proapoptotic, $C_{18:0}$-Cer has been found to induce lethal autophagy (Sentelle et al., 2012). The increase of $C_{18:0}$-Cer therefore may contribute to 13'-COOH-caused apoptosis and autophagy. In addition, the distinct effect on different Cer species suggests that 13'-COOH may have different

impact on CerS1 or CerS5/6 in addition to inhibition of DEGS. This is supported by an increase of dhSph, a key substrate of CerSs. Further investigation should be conducted to characterize the effect of 13'-COOH on these Cer synthases.

The observation that 13'-COOHs increased Cers and decreased SM during prolonged treatment is likely resulted from involvement of multi-pathways and enzymes. Cellular levels of Cers and SMs are determined by the balance between *de novo* synthesis and SM hydrolysis via SMases (Fig. 3.7A). Cers are *de novo* synthesized in the ER and then converted to SMs by SM synthases (SMS) in the Golgi. SMs are the most abundant sphingolipids located in membranes and can be hydrolyzed to regenerate Cers by acid or neutral SMases (Marchesini and Hannun, 2004). In the current study, given that 13'-COOHs inhibited DEGS and therefore led to decrease in *de novo* synthesized Cers, we reason that an increase of Cers in the prolonged treatment is likely caused by SMase-mediated SM hydrolysis, which resulted in further decrease of SMs in addition to the reduced synthesis via the *de novo* pathway. Acid SMases are known to be present in lysosomes and the outer membrane leaflet and have been shown to be activated by TNFα, oxidants, and UV radiation (Henry et al., 2013; Marchesini and Hannun, 2004; Zhang et al., 2001). Neutral SMases are found in the inner leaflet of the bilayer (Hannun and Obeid, 2008), and are stimulated by serum starvation (Jayadev et al., 1995), oxidative stress (Marchesini and Hannun, 2004), treatment of vitamin D (Okazaki et al., 1994) and curcumin (Abdel Shakor et al., 2014). Neutral SMase activation was also a necessary signaling event for the TNF-induced human MCF-7 breast cancer cell death (Luberto et al., 2002). Here we found that co-treatment with neutral SMase inhibitor GW4869 but not an acid SMase inhibitor significantly counteracted 13'-COOHs-induced cancer cell death,

suggesting that neutral SMase-catalyzed SM hydrolysis may be involved. However, we cannot completely rule out the possibility that SMS was inhibited by 13'-COOHs so that Cers were accumulated with simultaneous decrease of SMs.

Our finding that 13'-COOHs have potent anti-proliferation effect and induce cell death in various types of cancer cells has physiological implications. Previous studies have demonstrated that γT and mixed tocopherols are effective in suppression of colon tumorigenesis in preclinical mouse models (Jiang et al., 2013; Ju et al., 2009; Newmark et al., 2006). Interestingly, 13'-COOHs have been identified as a predominant fecal excreting vitamin E metabolite and found at relatively high levels in feces of mice fed γT or δT supplementation (Bardowell et al., 2012a; Bardowell et al., 2012b; Jiang et al., 2013). Since 13'-COOHs appear to be much stronger than un-metabolized tocopherols in induction of death in colon cancer cells, 13'-COOHs likely contribute to the anticancer effects of tocopherol supplements against colon cancer *in vivo*. Furthermore, given the anticancer and anti-inflammatory activities possessed by 13'-COOHs, these compounds are potentially excellent agents for chemoprevention. Consistently, our animal studies showed that δTE-13'-COOH effectively attenuated DSS-caused colon inflammation and AOM/DSS-induced tumor development in mice, which mimic colitis and colitis-promoted colon cancer, respectively.

In summary, we have demonstrated for the first time that 13'-COOHs, long-chain metabolites of vitamin E, induce apoptosis and autophagy by modulating sphingolipids in various types of cancer cells. Our results indicate that 13'-COOHs initially targets DEGS and subsequently activate SM hydrolysis possibly via neutral SMase during cell death process. This anticancer activity together with dual inhibition of COXs and 5-LOX

strongly suggest that 13'-COOHs likely play significant roles in the chemoprevention effect by vitamin E forms *in vivo* and that long-chain carboxychromanols may be novel preventative and therapeutic agents against cancer.

CHAPTER 4. TARGETING SPHINGOLIPID METABOLISM FOR THE ANTICANCER EFFECTS OF VARIOUS CHEMOPREVENTIVE COMPOUNDS

4.1 Abstract

Phytochemicals have been shown to exert anticancer activities, but the underlying mechanisms; in particular, the first important target has not been completely identified yet. We have earlier shown that specific vitamin E forms, phenolic compounds in various classes of phytochemicals, and 13'-carboxychromanols, long-chain vitamin E metabolites induced cancer cell death by modulation of sphingolipid metabolism as an initial primary target. In this study, we investigated whether other chemopreventive compounds including representative phytochemicals (curcumin, resveratrol, epigallocatechin gallate (EGCG), quercetin, sulforaphane), ER stress inducers (dithiothreitol, thapsigargin), and chemotherapeutic drugs (doxorubicin, camptothecin) also show anticancer effects by modulation of sphingolipid metabolism using a sphingolipidomic analysis via employing liquid chromatography tandem mass spectrometry (LC-MS/MS) in human colon cancer HCT-116 cells. We show that all the tested compounds modulated sphingolipid metabolism in HCT-116 cells. Specifically, while the effects of individual compounds on different Ceramide (Cer) species with distinct chain-length of fatty acyl-CoA were different, all tested compounds increased the levels of dihydroceramides (dhCers) compared with controls. For instance, curcumin increased C_{24}-Cers, but decreased $C_{16:0}$-

Cer, and resveratrol and DTT decreased the levels of all different species of Cers. On the other hand, while sulforaphane, quercentin, thapsigargin, doxorubicin and camptothecin increased all Cers, EGCG did not affect on the Cer levels during our tested treatment times. Moreover, we found that curcumin and quercetin significantly inhibited DEGS enzyme activities. Interestingly, these changes in sphingolipid metabolism by the tested compounds occurred quickly and prior to any manifestation of cell death. These data demonstrated that modulation of sphingolipid metabolism might be a general mechanism for the anticancer effects of various chemopreventive compounds against cancer, and inhibition of DEGS enzyme might be the initial primary target of their anticancer actions.

4.2 Introduction

Colon cancer is one of the leading causes of cancer-related deaths in the United States (Siegel et al., 2015). Since there are no effective treatment for advanced cancer, chemoprevention becomes a promising strategy to reduce cancer-caused death. Chemoprevention against cancer includes antiproliferation and induction of death in malignant cells, and therefore stops or delays the onset of metastasis. Epidemiological studies have consistently shown that intake of high levels of fruits and vegetables is inversely associated with cancer incidence (Block et al., 1992; Steinmetz and Potter, 1996). Recently, numerous dietary plant phytochemicals have been extensively studied and have exhibited cancer preventive activities through modulation of multiple signaling pathways and proteins, which are involved in cellular proliferation, differentiation, and apoptosis (Johnson, 2007; Lee et al., 2011; Surh, 2003). However, the underlying

mechanisms especially the first primary target of their anticancer effects is not understood yet.

Cellular metabolism, including sphingolipid metabolism, is emerging as promising targets as sphingolipids are closely associated with cell survival and death (Hannun and Obeid, 2008; Ryland et al., 2011; Zheng et al., 2006). Sphingolipids are structural components of cell membranes and play important roles in signal transduction. *De novo* sphingolipid biosynthesis starts in the endoplasmic reticulum with the condensation of palmitoyl-CoA and serine into 3-ketosphinganine by serine palmitoyltransferase, which rapidly reduced to dihydrosphingosine (dhSph) by 3-ketosphinganine reductase. A family of (dihydro)ceramide synthases (CerSs) attached fatty acyl-CoA with variable chain lengths to dhSph to generate the corresponding dihydroceramide (dhCer) subspecies. DhCer desaturase (DEGS) introduces a 4,5-*trans* double bond in dhCer, thus generating ceramide (Cer). The Cer is transported to the Golgi apparatus to generate more complex sphingolipids such as glycosyl-, or galactosyl-Cers and sphingomyelin (SM) by the actions of enzymes glucosyl-Cer synthase, Cer galactosyltransferase, or SM synthases, respectively (Hannun and Obeid, 2008).

DhCers were believed to be a non-signaling molecule and an inactive precursor of Cer, which is a well-known sphingolipid metabolite, especially involved in the regulation of apoptosis (Kolesnick, 2002; Radin, 2001; Woodcock, 2006). However, the potential effectiveness of dhCers has become recognized with the development of the new technology, LC-MS/MS, which can identify and distinguish the different species of Cer and dhCer. Since then, several recent studies reported that the increase of dhCers is related to the induction of cell cycle arrest (Kraveka et al., 2007), apoptosis (Gopalan et

al., 2012; Jiang et al., 2012; Stiban et al., 2006), and autophagy (Jiang et al., 2012; Signorelli et al., 2009; Zheng et al., 2006), and some compounds and environmental factors such as vitamin E forms (γT and γTE) (Gopalan et al., 2012; Jiang et al., 2012; Jiang et al., 2004), fenretinide (Rahmaniyan et al., 2011), resveratrol (Signorelli et al., 2009), celecoxib (Schiffmann et al., 2009b), oxidative stress (Idkowiak-Baldys et al., 2010), and hypoxia (Devlin et al., 2011) are known to induce accumulation of intracellular dhCers. In addition, the regulation of DEGS, an enzyme that converts dhCer into Cer, thus controls the levels of each sphingolipid metabolite became important, as genetic or chemical inhibition of DEGS was reported to induce accumulation of dhCer (Kraveka et al., 2007; Ruangsiriluk et al., 2012; Siddique et al., 2013).

We have previously shown that γTE and 13'-carboxychromanol, a long-chain vitamin E metabolite, induced colon cell death by inhibition of DEGS as an initial target, resulting in the accumulation of intracellular dhCers (Jang Y and Jiang Q, unpublished data). Therefore, the objectives of this study were to investigate whether like vitamin E forms, other chemopreventive compounds also modulate sphingolipid metabolism as a general pathway, and to determine whether this modulation is an initial primary target for their anticancer activities. Here, we demonstrated that various chemopreventive compounds (Fig. 4.1) including representative phytochemicals (curcumin, resveratrol, epigalloatecin gallate (EGCG), quercetin, sulforaphane), endoplasmic reticulum (ER) stress inducers (dithiothreitol (DTT), thapsigargin), and chemotherapeutic drugs (doxorubicin, camptothecin) induced increases of dhCers and modulation of Cers by interrupting *de novo* sphingolipid metabolism as their initial primary target.

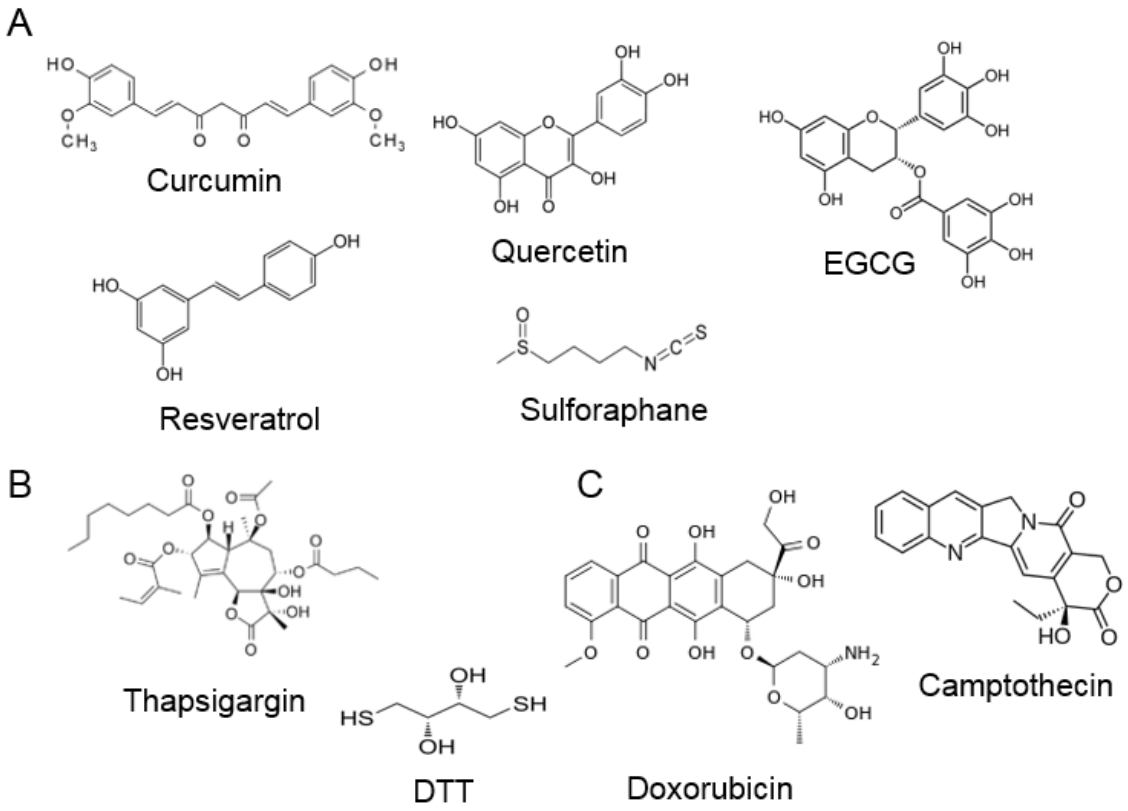

Figure 4.1 The structures of (A) representative phytochemicals, (B) ER stress inducers and (C) cancer chemotherapeutic drugs. (A) Representative phytochemicals: curcumin, resveratrol, quercetin, EGCG, and sulforaphane. (B) ER stress inducers: DTT and thapsigargin. (C) Cancer chemotherapeutic drugs: doxorubicin and camptothecin.

4.3 Materials and Methods

4.3.1 Materials and reagents

Curcumin (≥90%), resveratrol (≥98%), and epigallocatechin gallate (EGCG; ≥98%) were purchased from Sigma (St Louis, MO). Quercetin (≥95%), sulforaphane (≥90%), dithiothreitol (DTT; ≥99%), thapsigargin (≥98%), doxorubicin (98-102%), and camptothecin (≥90%) were purchased from Cayman Chemical (Ann Arbor, MI). All

sphingolipid standards were obtained from Avanti Polar Lipids (Alabaster, AL). C8-cyclopropenylceramide (C8-CPPC) was purchased from Matreya LLC (Pleasant Gap, PA). $^{13}C_3$, ^{15}N-labeled L-serine, Dimethyl sulfoxide (DMSO), [3-(4,5)-dimethylthiazol-2-yl]-2,5-diphenyl tetrazolium bromide] (MTT), and all other chemicals were from Sigma.

4.3.2 Cell culture and treatment

Human colon cancer HCT-116 cells were obtained from American Type Culture Collection (Manassas, VA). Cells were routinely cultured in McCoy's 5A modified growth medium containing 10% fetal bovine serum (FBS) at 37 °C in 5% CO_2. For experiments, cells were seeded in the growth medium with 10% FBS either at a density of 4 x 10^4 cells/well in 24-well plates or at a density of 7-8 x 10^5 cells in 10-cm dishes. After overnight attachment, media were replaced with fresh Dulbecco's modified eagle medium (DMEM) containing 1% FBS with tested compounds. All the treatment solutions were freshly prepared for each experiment. All the tested compounds were dissolved in DMSO and the same amount of DMSO was added to control group.

4.3.3 MTT assay

Cell viability was examined by the estimation of mitochondrial dehydrogenase activity that reduces MTT to form formazan which was dissolved in DMSO and measured the absorbance at 570 nm by using a microplate reader (SpectraMax 190, Molecular Devices, Sunnyvale, CA) (Mosmann, 1983).

4.3.4 Lipid extraction

Lipids were extracted according to a previously published method (Merrill et al., 2005). Briefly, cell pellets were resuspended in methanol/chloroform/water (10:5:1 [v/v/v]), after the addition of internal standard mixture containing 0.5 nmol of $C_{12:0}$-Cer, $C_{25:0}$-Cer, C_{17}-sphingosine, C_{17}-dhSph, and $C_{12:0}$-SM (Avanti Polar Lipids, Alabaster, AL). The suspension was tip sonicated and then incubated overnight at 48 °C. A total of 100 µL of suspension was used to determine the amount of total choline-containing phospholipids by an enzymatic colorimetric assay (Wako chemicals, Osaka, Japan) (Jiang et al., 2004) 75 µL of 1M KOH in methanol was added to the rest of the suspension and sonicated for 30 min. Samples were incubated at 37 °C for 2 h and evaporated under a stream of nitrogen.

4.3.5 Measurement of sphingolipids using liquid chromatography tandem mass spectrometry (LC-MS/MS)

Immediately before the LC-MS/MS analyses, the prepared samples above were resolved in methanol, sonicated, and then briefly centrifuged. The LC-MS/MS analyses were performed using the Agilent 6460 triple quadrupole mass spectrometer coupled with the Agilent 1200 Rapid Resolution HPLC (Agilent Technologies, Santa Clara, CA) with identification of each sphingolipid in positive mode by multiple reaction monitoring (MRM) technique (Merrill et al., 2005). The HPLC mobile phases consisted of methanol-H_2O-formic acid (74:25:1, v/v/v; RA) and methanol-formic acid (99:1, v/v; RB); both RA and RB contain 5 mM ammonium formate. For measurement of Cers and sphingoid bases, Agilent column XDB-C18 (4.6 x 50 mm) with particle size of 1.8 µm, was used

with isocratic run (100% B) or gradient (0-1 min, 20% B, 10-13 min, 100% B and 15-20 min at 20% B), respectively. For measurement of SMs, Agilent Zorbax XDB-C8 (2.1 x 50 mm) with particle size of 3.5 μm, was used with gradient (0-1 min, 20% B, 10-20 min, 100% B, 22-30 min, 20% B). The MS/MS parameters were as follows: gas temperature, 325-350 °C; gas flow rate, 7-10 L/min; nebulizer pressure, 45-50 psi; capillary voltage, 3500 V; The fragmentor voltage was 100 V and collision energy was 12-20 V. Precursor-to-product ion transitions for each sphingolipid were used according to the method of Merrill *et al.* (Merrill et al., 2005).

4.3.6 *De novo* sphingolipids anlaysis

HCT-116 cells were treated with either 400 μM $^{13}C_3$, ^{15}N-labeled L-serine alone or with a combination of 400 μM $^{13}C_3$, ^{15}N-labeled L-serine and 10 μM of curcumin for 20, 30, 60 and 90 min. Lipids were extracted and *de novo* synthesized sphingolipids were measured using LC-MS/MS.

4.3.7 Dihydroceramide desaturase (DEGS) assays

In Vitro DEGS assay - HCT-116 cells were treated with either a tested compound or 1 μM C8-CPPC as a positive control for 1 or 2 h. Cells were collected and homogenized in a buffer (5 mM Hepes, pH 7.4, containing 50 mM sucrose) followed by 10 min incubation on ice. The cell homogenate was centrifuged at 250 x g for 5 min at 4 °C to remove unbroken cells. Reaction was started by addition of $C_{8:0}$-dihydroceramide ($C_{8:0}$-dhCer) as a non-physiological substrate for the DEGS enzyme and NADH as a

cofactor at 37 °C for an hour. Immediately after the reaction, lipids were extracted and the products ($C_{8:0}$-Cer and $C_{8:0}$-SM) were quantified by LC-MS/MS.

In Situ DEGS assay - HCT-116 cells were pretreated with either a tested compound or C8-CPPC, and then added 10 μM of $C_{8:0}$-dhCer as a substrate for the DEGS enzyme, followed by 1h incubation. The cells were collected and lipids were extracted. The levels of products ($C_{8:0}$-Cer and $C_{8:0}$-SM) were measured by LC-MS/MS.

4.3.8 Statistics

Statistical significance was determined using a Student's t-test. $P < 0.05$ was considered statistically significant.

4.4 Results

4.4.1 Curcumin increased dhCers, dhSph, and C_{24}-Cers, but decreased $C_{16:0}$-Cer by DEGS inhibition

We first investigated the effects of curcumin, which is a polyphenolic compound isolated from a rhizome of the plant *Curcuma longa* and a promising phytochemical for cancer chemoprevention and therapy, on sphingolipid metabolism using LC-MS/MS in human colon HCT-116 cancer cells. HCT-116 cells were treated with 10 μM of curcumin for 1, 2, and 4 hours. During the treatment times, curcumin caused significant increases of dhCers including $C_{16:0}$-, $C_{24:1}$-, and $C_{24:0}$-dhCers, and dhSph, compared with controls (Fig. 4.2B). While $C_{16:0}$-Cer was significantly decreased as early as 1 h incubation with curcumin, C_{24}-Cers were increased compared with controls (Fig. 4.2C). Meanwhile, there

were no apparent changes of SM and dhSM species after 4 h incubation with curcumin (Fig. 4.2D; Table 4.1). Since treatment of curcumin induced accumulations of dhCers and dhSph, which are important sphingolipid metabolites in the *de novo* sphingolipid biosynthesis pathway (Fig. 4.3A), we used $^{13}C_3$, ^{15}N-labeled L-serine to only trace the effect of curcumin on *de novo* synthesized sphingolipids. Curcumin treatment induced significant increases in labeled dhCers, but decreases in $C_{16:0}$-Cer as early as 20 min to 90 min (Figs. 4.3C and D), without affecting the amount of total *de novo*-syntheized sphingolipids (Fig. 4.3B; Table 4.2). The increases of *de novo* dhCers but decreases of *de novo* Cers suggest the inhibition of DEGS-catalyzed reaction by curcumin treatment. Therefore, we next examined the effect of curcumin on the DEGS enzyme activity. In the *in vitro* DEGS assay with cell homogenates, 1 h incubation with 10 or 20 μM of curcumin showed ~76% and ~92% inhibition of DEGS enzyme activity, respectively (Fig. 4.4A). In another assay, *in situ* DEGS assay also showed significant inhibition of DEGS activity with 10 or 20 μM of curcumin after 2-3 hours incubation, though the inhibitory effects in this assay were much lower than those in the *in vitro* assay (Fig. 4.4B). In both assays, C8-CPPC, a known competitive inhibitor of DEGS (Triola et al., 2003), inhibited the enzyme activity by about 85~95%. Interestingly, these all modulation of sphingolipid metabolism was occurred prior to any signs of cell death determined by MTT cell viability assay (data not shown).

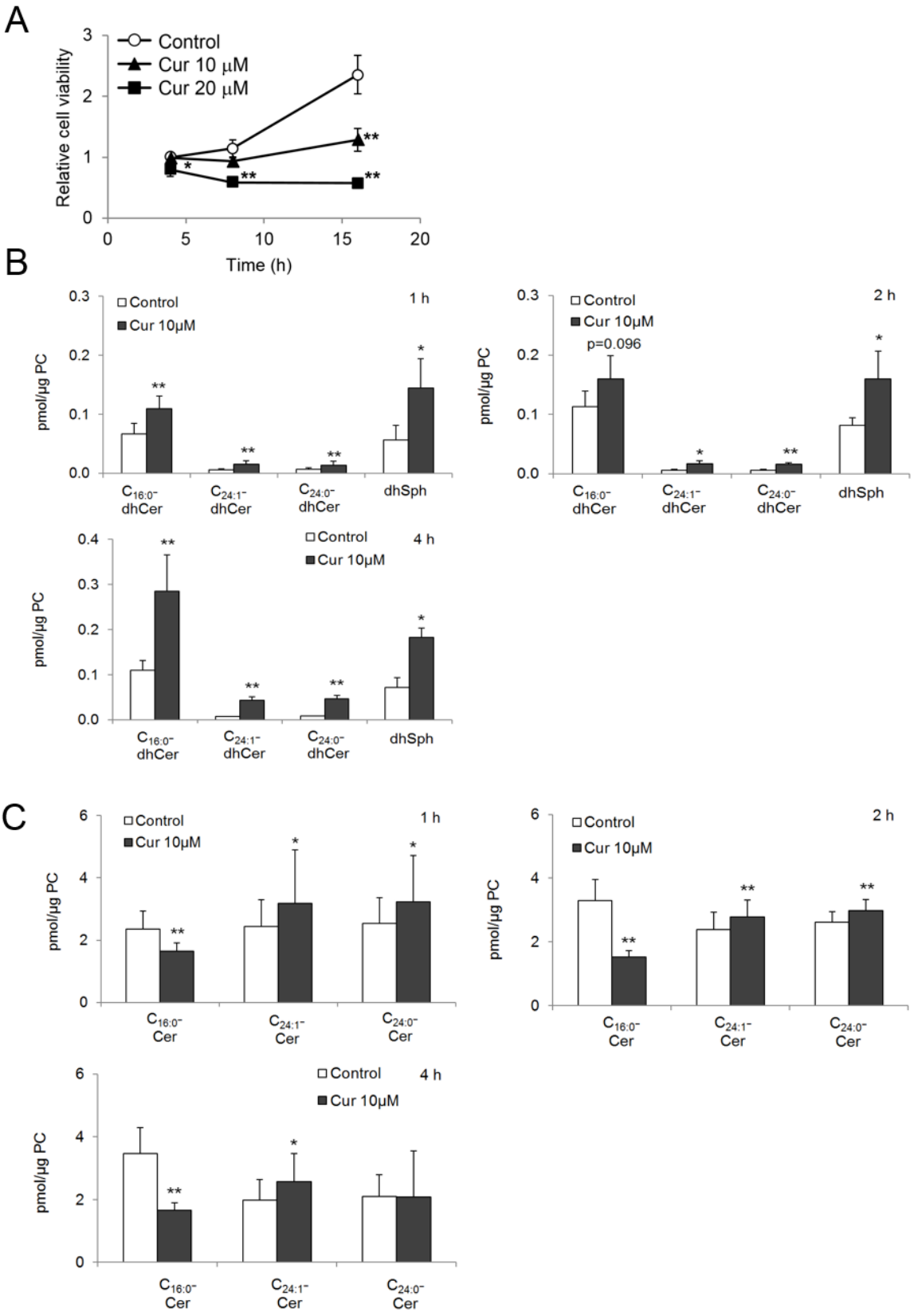
A
Relative cell viability
Time (h)
Control
Cur 10 μM
Cur 20 μM
B
pmol/μg PC
Control
Cur 10μM
1 h
2 h
4 h
p=0.096
C16:0- dhCer
C24:1- dhCer
C24:0- dhSph
dhSph
C
pmol/μg PC
C16:0- Cer
C24:1- Cer
C24:0- Cer

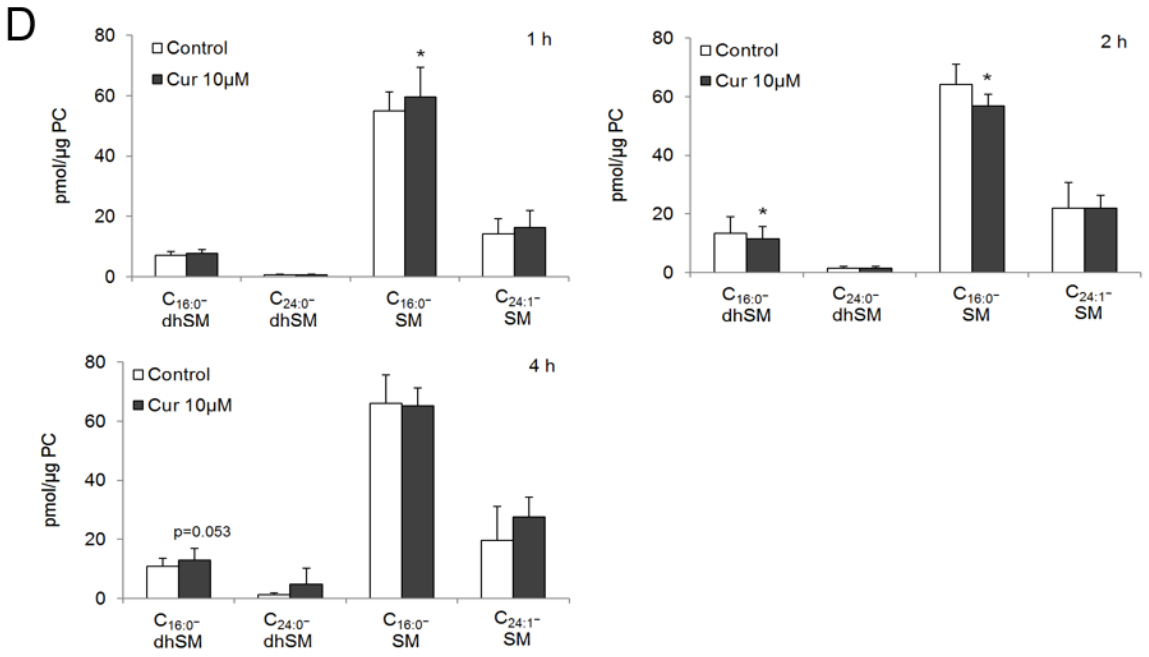

Figure 4.2 Effects of curcumin on sphingolipid metabolism in HCT-116 cells. (A) The anti-proliferative effects of curcumin on human colon HCT-116 cancer cells. Relative cell viability was measured after treatment with curcumin at the stated concentrations and time by MTT assay compared with control. The data are mean ± SD for 3 independent experiments, each performed in duplicate. HCT-116 cells were treated with 10 μM of curcumin for 1, 2, and 4 hours. The sphingolipid levels including (B) dhCers; $C_{16:0}$-, $C_{24:1}$-, and $C_{24:0}$-dhCers and dhSph, (C) Cers; $C_{16:0}$-, $C_{24:1}$-, and $C_{24:0}$-Cers, (D) dhSM; $C_{16:0}$- and $C_{24:0}$-dhSMs, and SMs; $C_{16:0}$- and $C_{24:1}$-SMs were determined by LC-MS/MS. Results are shown as mean ± SD for 3-4 independent experiments. *$p < 0.05$ and **$p < 0.01$ indicate a significant difference between treated and control cells.

A *De novo* synthesis of sphingolipid

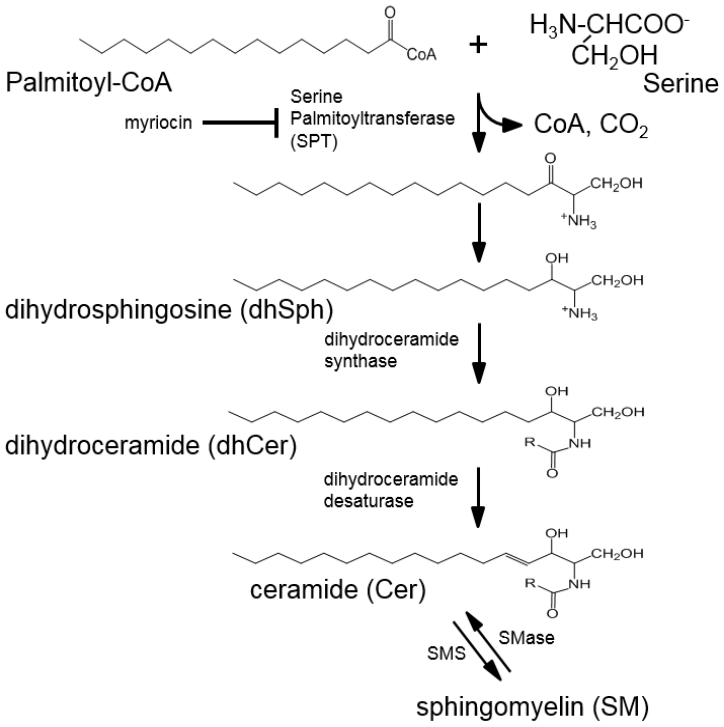

B Total *de novo* sphingolipids

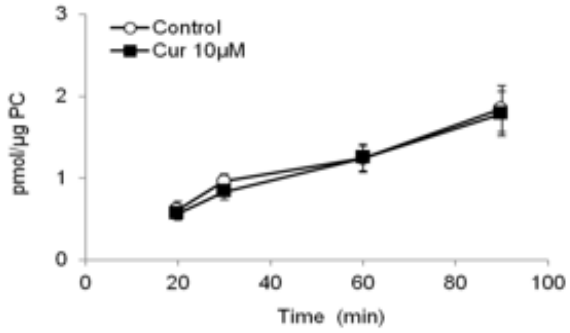

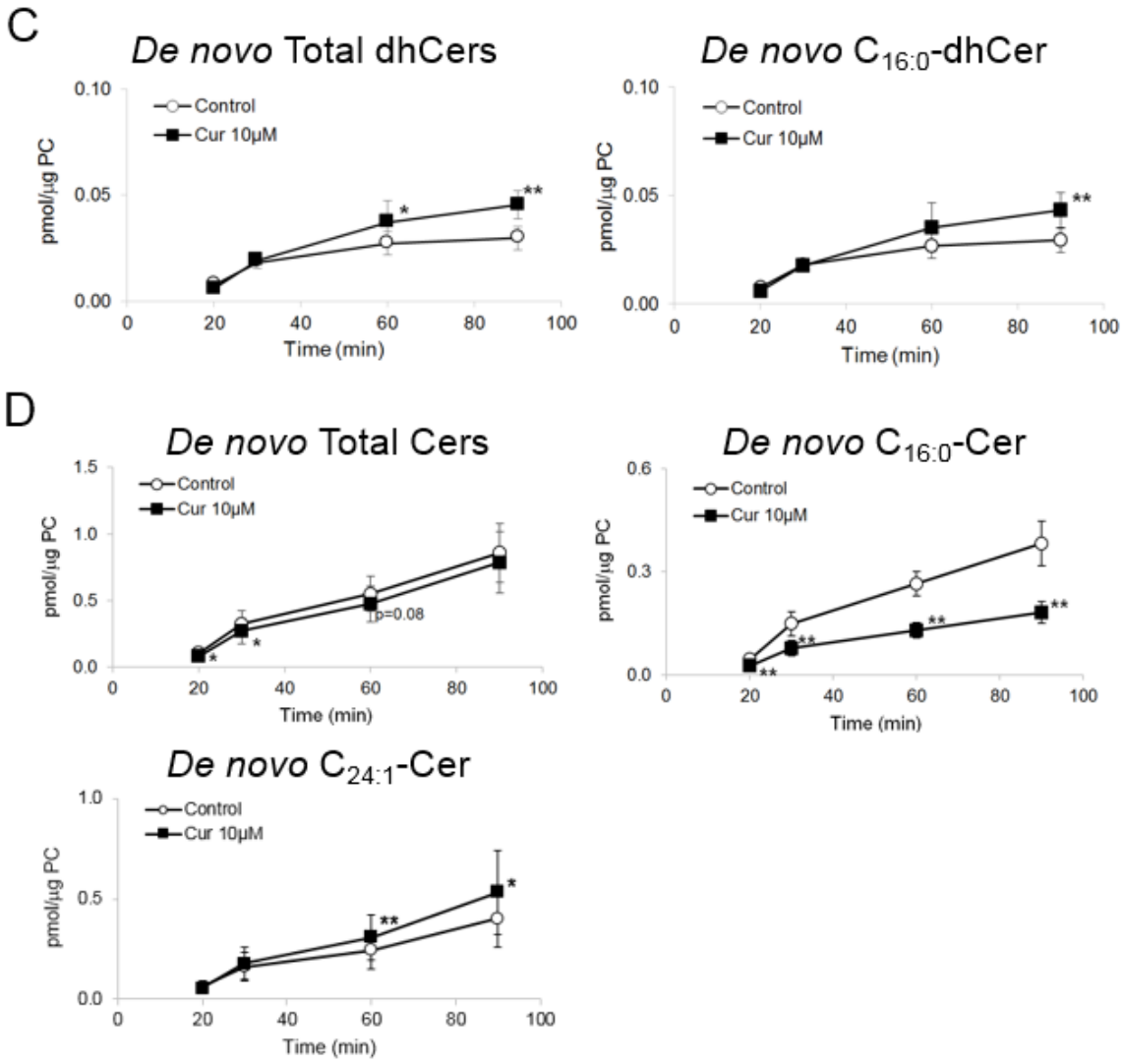

Figure 4.3 Effects of curcumin on *de novo* sphingolipid biosynthesis in HCT-116 cells. (A) The *de novo* biosynthesis pathway of sphingolipids (SMS, sphingomyelin synthase; SMase, sphingomyelinase). HCT-116 cells were treated with either 400 μM $^{13}C_3$, ^{15}N-labeled L-serine alone as control or with a combination of 400 μM $^{13}C_3$, ^{15}N-labeled L-serine and 10 μM curcumin for 20, 30, 60, and 90 min. The amount of each labeled *de novo* sphingolipid including (B) total amounts of all the *de novo* synthesized sphingolipids, (C) *de novo* total dhCer and *de novo* $C_{16:0}$-dhCer, (D) *de novo* total Cers, *de novo* $C_{16:0}$-Cer, and *de novo* $C_{24:1}$-Cer were determined by LC-MS/MS. Results are shown as mean ± SEM for 3-4 independent experiments. $*p < 0.05$ and $**p < 0.01$ indicate a significant difference between treated and control cells.

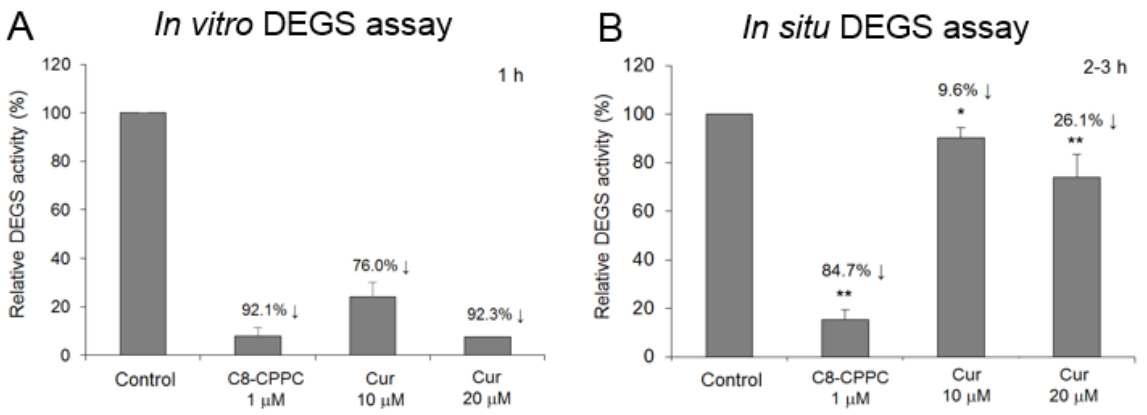

Figure 4.4 Effects of curcumin on DEGS activity. HCT-116 cells were treated with either 10 or 20 μM curcumin or 1 μM C8-CPPC as a positive control. (A) *In vitro* DEGS assay: After 1 h of treatment, cells were collected and homogenized. Using the homogenates, reaction was started by addition of $C_{8:0}$-dhCer as a substrate for DEGS with NADH for an hour in 37 °C. The levels of products which are $C_{8:0}$-sphingolipids were analyzed by using LC-MS/MS. The data are mean ± SD of 1-2 independent experiments. (B) *In situ* DEGS assay: After 1-2 hours of pretreatment, cells were incubated with 10 μM $C_{8:0}$-dhCer as a substrate for DEGS for additional 1 h. The cells were collected and the levels of products which are $C_{8:0}$-sphingolipids were analyzed by using LC-MS/MS. The data are mean ± SD of three independent experiments. *$p < 0.05$ and **$p < 0.01$ indicate a significant difference between treated and control cells.

4.4.2 Resveratrol and DTT increased dhCers, dhSph, but decreased $C_{16:0}$-Cer and C_{24}-Cers

We next examined the modulation of sphingolipid using another naturally occurring, well-recognized cancer chemopreventive polyphenolic compound, resveratrol, found in grapes and wine. Reseveratrol has been shown to induce autophagy by inhibition of DEGS activity followed by dhCer accumulation in gastric cancer cells (Signorelli et al., 2009). Consistently, 50 μM of resveratrol treatment for 2-4 hours significantly enhanced intracelluar levels of dhCers and dhSph (Fig. 4.5B). Compared with controls, resveratrol treatment induced decreases in $C_{16:0}$- and $C_{24:1}$-Cers (Fig. 4.5C). While $C_{16:0}$-SM was decreased, $C_{16:0}$-dhSM was increased by 4 h incubation with resveratrol (Fig. 4.5D; Table 4.3).

In addition, we tested the effects of ER stress inducers including DTT and thapsigargin on sphingolipid metabolism. Since *de novo* synthesis pathway occurs in the ER, we hypothesized that disruption of ER environment by ER stress induction may also induce interruption of sphingolipid metabolism. As we expected, similar to resveratrol, 2 mM of DTT treatment for 2-4 hours elevated dhCers and dhSph, but decreased in $C_{16:0}$- and C_{24}-Cers (Figs. 4.6A and B). DTT treatment also tends to decrease in $C_{16:0}$-SM but increase in $C_{16:0}$-dhSM as compared with controls (Fig. 4.6C; Table 4.4).

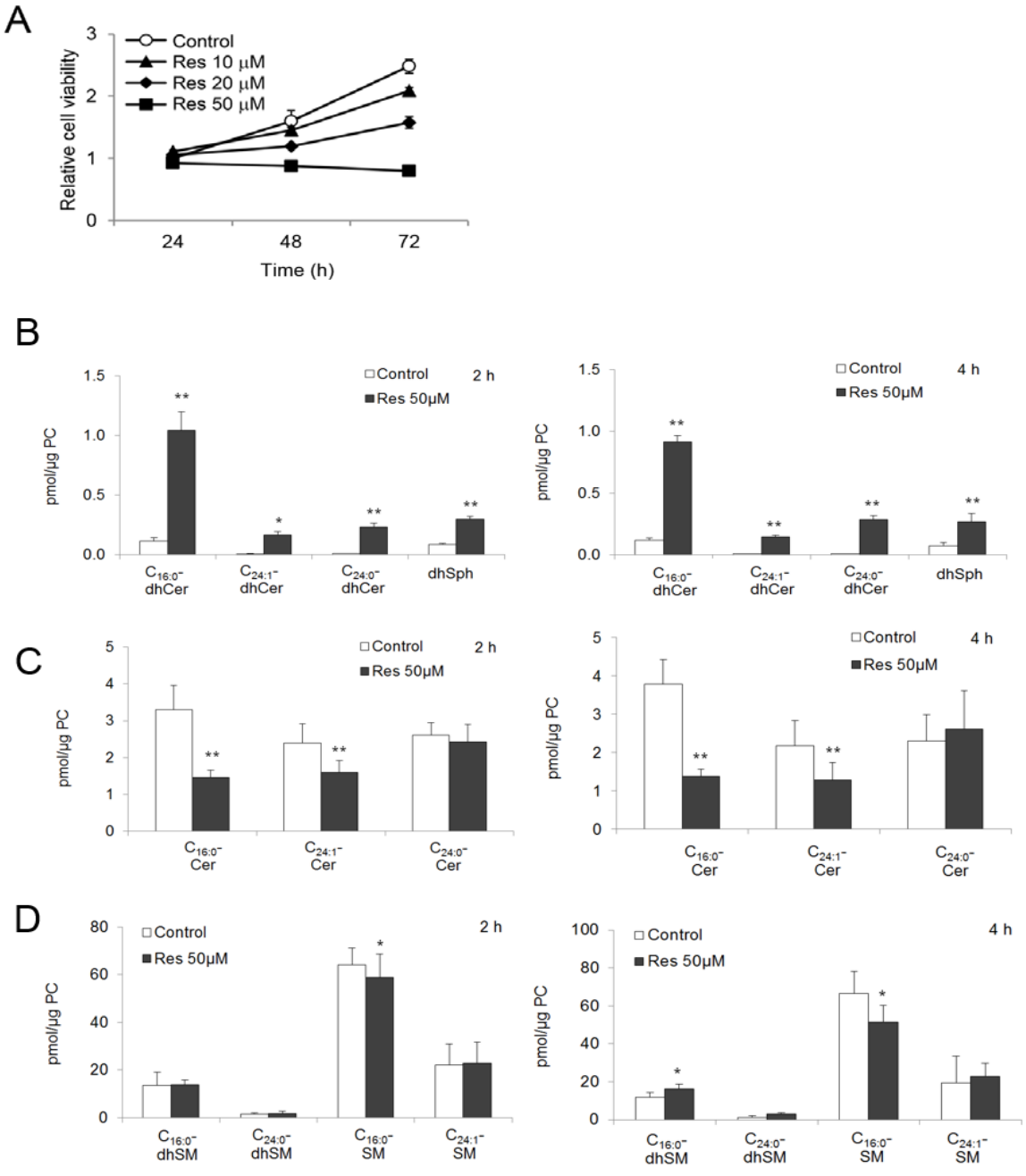

Figure 4.5 Effects of resveratrol on sphingolipid metabolism in HCT-116 cells. (A) The anti-proliferative effects of resveratrol on human colon HCT-116 cancer cells. Relative cell viability was measured after treatment with resveratrol at the stated concentrations and time by MTT assay compared with control. The data are mean ± SD for 1 duplicate experiment. HCT-116 cells were treated with 50 μM of resveratrol for 2 and 4 hours. The sphingolipid levels including (B) dhCers; $C_{16:0}$-, $C_{24:1}$-, and $C_{24:0}$-dhCers and dhSph, (C) Cers; $C_{16:0}$-, $C_{24:1}$-, and $C_{24:0}$-Cers, (D) dhSM; $C_{16:0}$- and $C_{24:0}$-dhSMs, and SMs; $C_{16:0}$-

and $C_{24:1}$-SMs were determined by LC-MS/MS. Results are shown as mean ± SD for three independent experiments. *$p < 0.05$ and **$p < 0.01$ indicate a significant difference between treated and control cells.

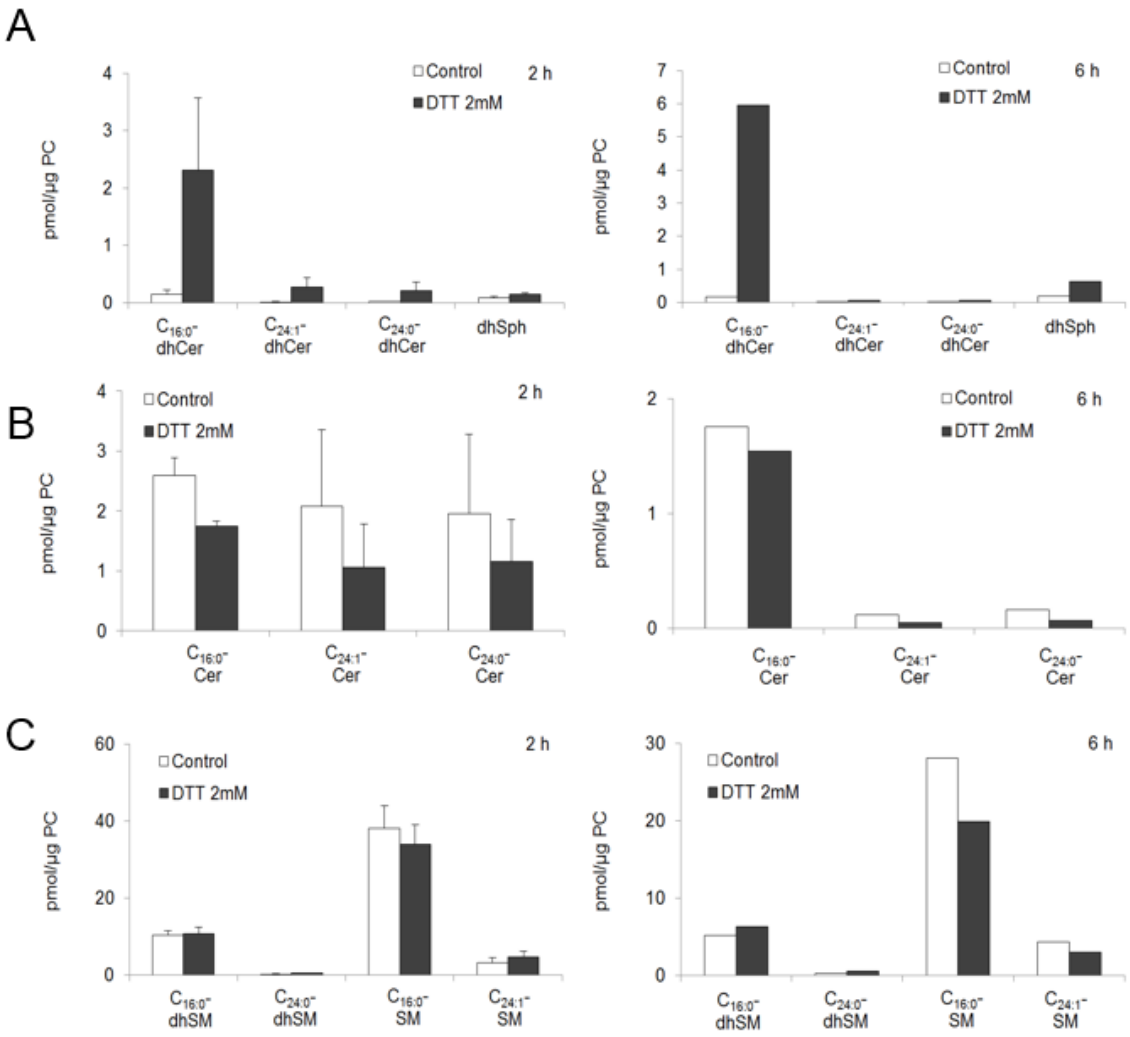

Figure 4.6 Effects of DTT on sphingolipid metabolism in HCT-116 cells. HCT-116 cells were treated with 2 mM of DTT for 2 and 6 hours. The sphingolipid levels including (A) dhCers; $C_{16:0}$-, $C_{24:1}$-, and $C_{24:0}$-dhCers and dhSph, (B) Cers; $C_{16:0}$-, $C_{24:1}$-, and $C_{24:0}$-Cers, (C) dhSM; $C_{16:0}$- and $C_{24:0}$-dhSMs, and SMs; $C_{16:0}$- and $C_{24:1}$-SMs were determined by LC-MS/MS. Results are shown as mean ± SD for 1 (6 h) or 2 (2 h) independent experiments.

4.4.3 Sulforaphane, quercetin, thapsigargin, doxorubicin and camptothecin increased Cers and dhCers

We then investigated to see whether sulforaphane also modulates sphingolipid metabolism as it belongs to a class of organosulfur compounds in phytochemical groups. Different with phenolic compounds that contain one or more hydroxyl groups attached to one or more aromatic rings, organosulfur compounds contain sulfur in their structure. Treatment of cells with 20 μM of sulforaphane for 2-4 hours also modulated sphingolipid metabolism by increasing the levels of Cers as well as the levels of dhCers compared with controls (Fig. 4.7; Table 4.5). Another phenolic compound, quercetin modulated the levels of sphingolipid metabolites as similar way with sulforaphane (Fig. 4.8; Table 4.6). Since 20 μM of quercetin elevated not only dhCers, but also Cers, we tested the effects of quercetin on DEGS enzyme activity. In the *in situ* DEGS assay, incubation of cells with 20 μM of quercetin for 2-3 hours significantly inhibited the DEGS activity by 42% (Fig. 4.8E). Interestingly, thapsigargin, another ER stress inducer, also induced accumulation of intracellular $C_{16:0}$-dhCer after 6 h treatment with 1 μM concentration, but different with DTT, it did not decrease the levels of Cers (Fig. 4.9; Table 4.7).

Furthermore, to evaluate whether cancer chemotherapeutic drugs modulate sphingolipid metabolism or not, we used two well-known drugs, doxorubicin and camptothecin. Treatment of cells with 5 μM of doxorubicin or 1 μM of camptothecin both enhanced $C_{16:0}$-dhCer and Cers after 24 h incubation (Fig 4.10; Table 4.8).

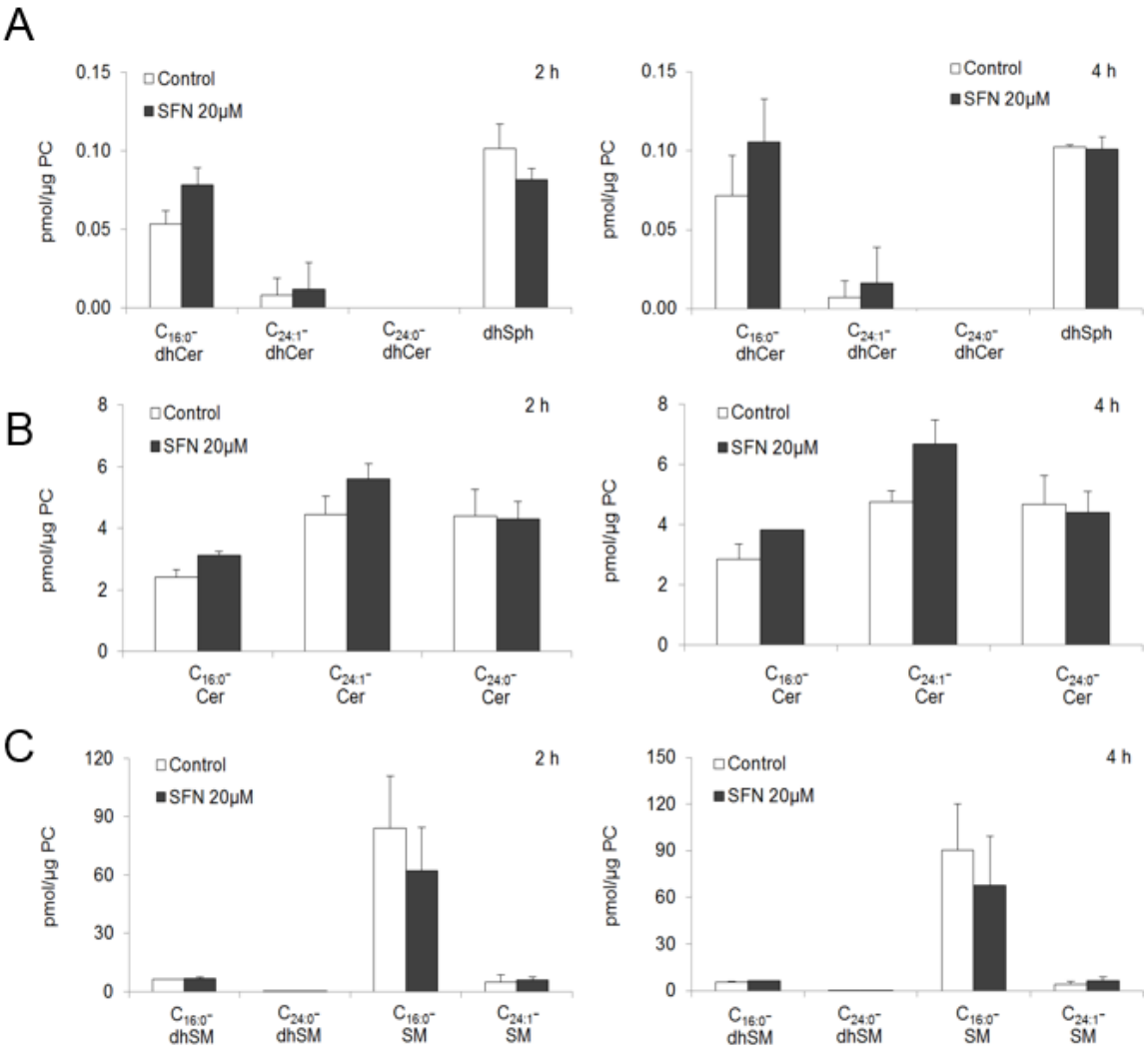

Figure 4.7 Effects of sulforaphane on sphingolipid metabolism in HCT-116 cells. HCT-116 cells were treated with 20 μM of sulforaphane for 2 and 4 hours. The sphingolipid levels including (A) dhCers; $C_{16:0}$-, $C_{24:1}$-, and $C_{24:0}$-dhCers and dhSph, (B) Cers; $C_{16:0}$-, $C_{24:1}$-, and $C_{24:0}$-Cers, (C) dhSM; $C_{16:0}$- and $C_{24:0}$-dhSMs, and SMs; $C_{16:0}$- and $C_{24:1}$-SMs were determined by LC-MS/MS. Results are shown as mean ± SD for two independent experiments.

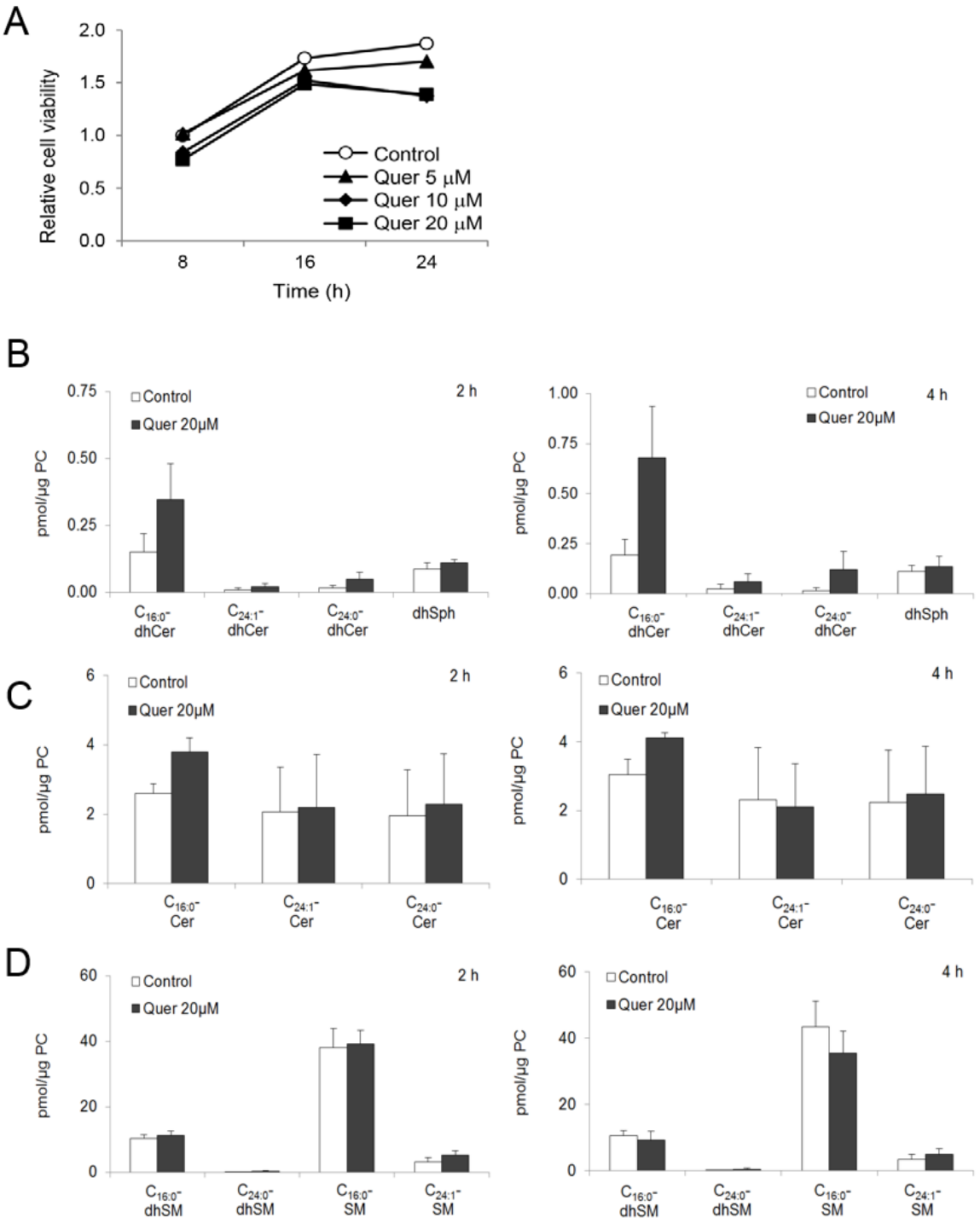
A
Relative cell viability
2.0
1.5
1.0
0.5
0.0
8
16
24
Time (h)
Control
Quer 5 μM
Quer 10 μM
Quer 20 μM
B
pmol/μg PC
0.75
0.50
0.25
0.00
Control
Quer 20μM
2 h
C16:0- dhCer
C24:1- dhCer
C24:0- dhCer
dhSph
1.00
0.75
0.50
0.25
0.00
4 h
C
6
4
2
0
C16:0- Cer
C24:1- Cer
C24:0- Cer
D
60
40
20
0
C16:0- dhSM
C24:0- dhSM
C16:0- SM
C24:1- SM

E

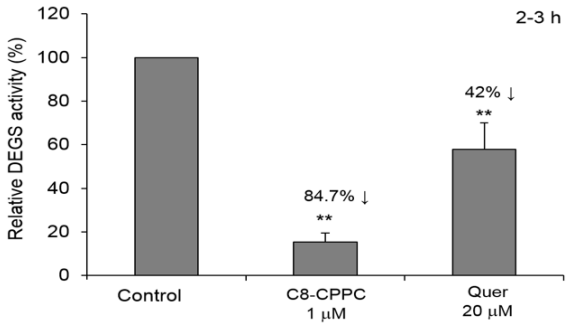

Figure 4.8 Effects of quercetin on sphingolipid metabolism in HCT-116 cells. (A) The anti-proliferative effects of quercetin on human colon HCT-116 cancer cells. Relative cell viability was measured after treatment with quercetin at the stated concentrations and time by MTT assay compared with control. The data are mean ± SD for 1 duplicate experiment. HCT-116 cells were treated with 20 μM of quercetin for 2 and 4 hours. The sphingolipid levels including (B) dhCers; $C_{16:0}$-, $C_{24:1}$-, and $C_{24:0}$-dhCers and dhSph, (C) Cers; $C_{16:0}$-, $C_{24:1}$-, and $C_{24:0}$-Cers, (D) dhSM; $C_{16:0}$- and $C_{24:0}$-dhSMs, and SMs; $C_{16:0}$- and $C_{24:1}$-SMs were determined by LC-MS/MS. Results are shown as mean ± SD for two independent experiments. (E) The effect of quercetin on DEGS activity was measured by *in situ* assay. HCT-116 cells were preincubated with either 20 μM quercetin or 1 μM C8-CPPC for 2-3 hours followed by 10 μM $C_{8:0}$-dhCer treatment for 1 h. The cells were collected and the levels of products which are $C_{8:0}$-sphingolipids were analyzed by using LC-MS/MS. The data are mean ± SD of three independent experiments. *$p < 0.05$ and **$p < 0.01$ indicate a significant difference between treated and control cells.

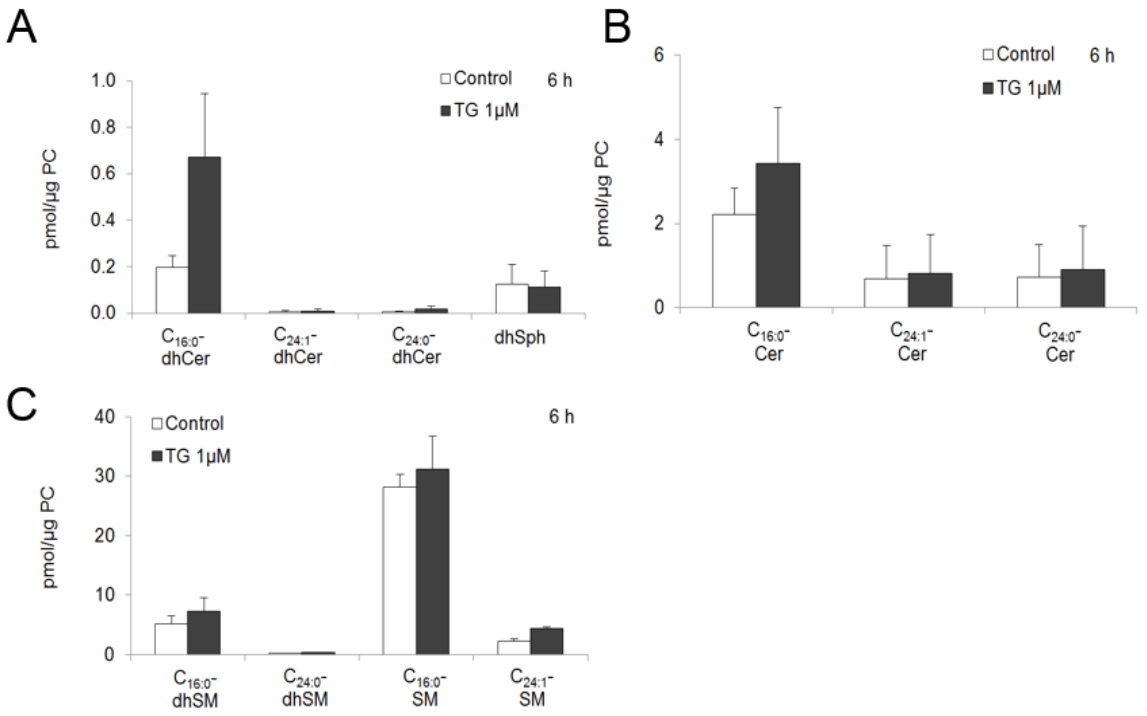

Figure 4.9 Effects of thapsigargin on sphingolipid metabolism in HCT-116 cells. HCT-116 cells were treated with 1 μM of thapsigargin for 6 hours. The sphingolipid levels including (A) dhCers; $C_{16:0}$-, $C_{24:1}$-, and $C_{24:0}$-dhCers and dhSph, (B) Cers; $C_{16:0}$-, $C_{24:1}$-, and $C_{24:0}$-Cers, (C) dhSM; $C_{16:0}$- and $C_{24:0}$-dhSMs, and SMs; $C_{16:0}$- and $C_{24:1}$-SMs were determined by LC-MS/MS. Results are shown as mean ± SD for two independent experiments.

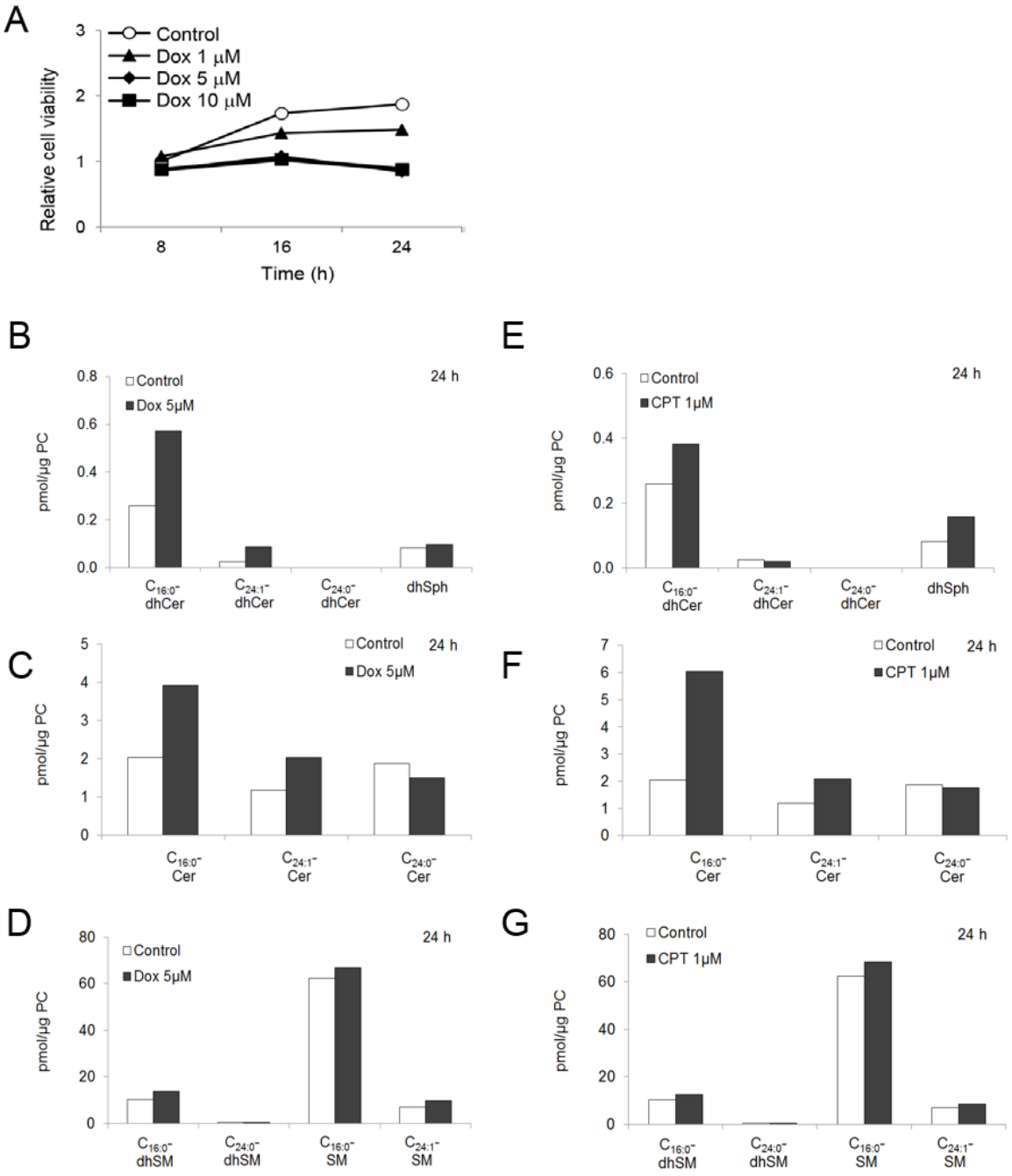

Figure 4.10 Effects of cancer chemotherapeutic drugs (doxorubicin and camptothecin) on sphingolipid metabolism in HCT-116 cells. (A) The anti-proliferative effects of doxorubicin on human colon HCT-116 cancer cells. Relative cell viability was measured after treatment with doxorubicin at the stated concentrations and time by MTT assay compared with control. The data are mean ± SD for 1 duplicate experiment. HCT-116 cells were treated with 5 μM of doxorubicin or 1 μM of camptothecin for 24 hours. The sphingolipid levels including (B and E) dhCers; $C_{16:0}$-, $C_{24:1}$-, and $C_{24:0}$-dhCers and

dhSph, (C and F) Cers; $C_{16:0}$-, $C_{24:1}$-, and $C_{24:0}$-Cers, (D and G) dhSM; $C_{16:0}$- and $C_{24:0}$-dhSMs, and SMs; $C_{16:0}$- and $C_{24:1}$-SMs were determined by LC-MS/MS. Results are shown as mean ± SD for one independent experiment.

4.4.4 EGCG increased dhCer, but did not affect other sphingolipids

The effects of EGCG, the major polyphenolic compound found in green tea, on sphingolipid metabolism were investigated in human colon HCT-116 cancer cells. Treatment of cells with 50 μM of EGCG for 4 h elevated dhCers including $C_{16:0}$-, $C_{24:1}$-, and $C_{24:0}$-dhCers compared with controls, but not in 2 h incubation with EGCG (Fig. 4.11B). Even in 4 h incubation, EGCG did not change the levels of Cer species (Fig. 4.11C). While EGCG tends to increase $C_{24:1}$-SM at 2 h, it did not affect SM and dhSM levels in 4 h incubation (Fig. 4.11D; Table 4.9).

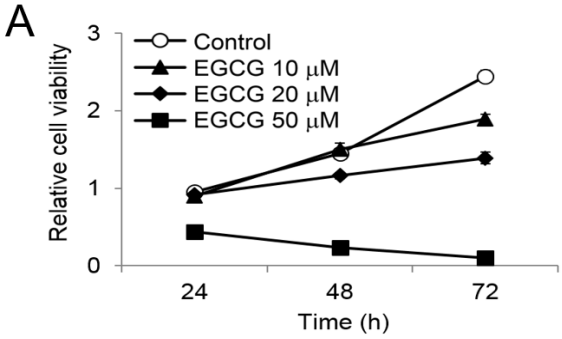

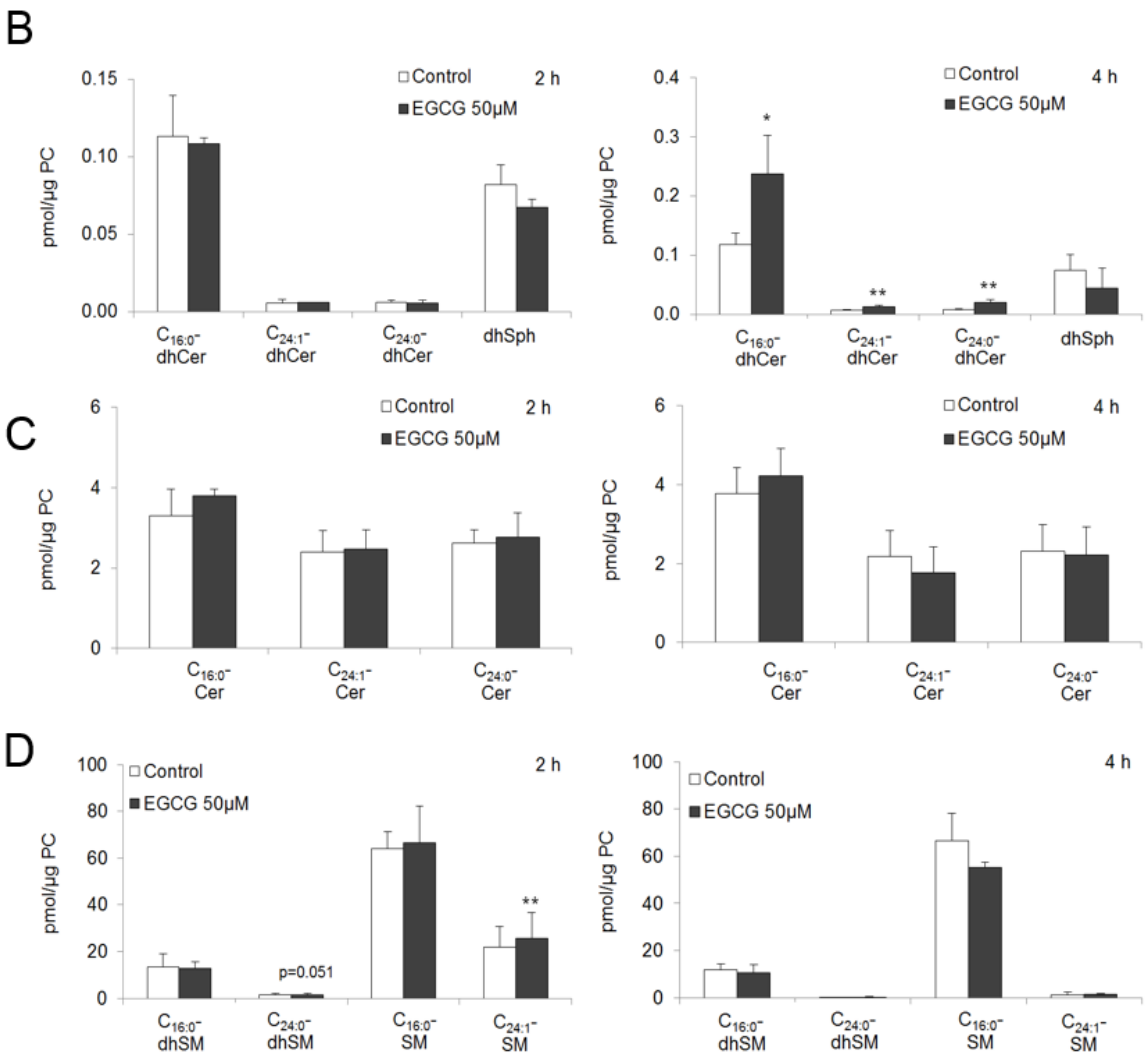

Figure 4.11 Effects of EGCG on sphingolipid metabolism in HCT-116 cells. (A) The anti-proliferative effects of EGCG on human colon HCT-116 cancer cells. Relative cell viability was measured after treatment with EGCG at the stated concentrations and time by MTT assay compared with control. The data are mean ± SD for 1 duplicate experiment. HCT-116 cells were treated with 50 μM of EGCG for 2 and 4 hours. The sphingolipid levels including (B) dhCers; $C_{16:0}$-, $C_{24:1}$-, and $C_{24:0}$-dhCers and dhSph, (C) Cers; $C_{16:0}$-, $C_{24:1}$-, and $C_{24:0}$-Cers, (D) dhSM; $C_{16:0}$- and $C_{24:0}$-dhSMs, and SMs; $C_{16:0}$- and $C_{24:1}$-SMs were determined by LC-MS/MS. Results are shown as mean ± SD for three independent experiments. *$p < 0.05$ and **$p < 0.01$ indicate a significant difference between treated and control cells.

Table 4.1 Effect of curcumin on sphingolipid metabolism in HCT-116 cells. HCT-116 cells were treated with 10 μM curcumin for 1, 2, and 4 h. The amount of each sphingolipid was determined by LC-MS/MS. Data are mean ± SEM of 3-4 independent experiments. *p < 0.05, **p < 0.01, significant difference between control and curcumin-treated cells. Cer, ceramide; dhCer, dihydroceramide; Sph, sphingosine; dhSph, dihydrosphingosine; S1P, sphingosine-1-phosphate; SM, sphingomyelin; dhSM, dihydrosphingomyelin

Ceramides (pmol/μg PC)

$C_{16:0}$-Cer

Hours	**Control**	**Cur 10 μM**
1	2.36 ± 0.29	1.65 ± 0.13**
2	3.29 ± 0.38	1.53 ± 0.11**
4	3.46 ± 0.42	1.66 ± 0.12**

$C_{18:0}$-Cer

Hours	**Control**	**Cur 10 μM**
1	0.069 ± 0.008	0.10 ± 0.020
2	0.083 ± 0.009	0.093 ± 0.011
4	0.084 ± 0.019	0.11 ± 0.022*

$C_{20:0}$-Cer

Hours	**Control**	**Cur 10 μM**
1	0.046 ± 0.009	0.072 ± 0.013**
2	0.057 ± 0.006	0.080 ± 0.008*
4	0.058 ± 0.016	0.099 ± 0.026**

$C_{22:0}$-Cer

Hours	**Control**	**Cur 10 μM**
1	0.49 ± 0.11	0.71 ± 0.13*
2	0.64 ± 0.032	0.87 ± 0.092
4	0.58 ± 0.15	1.03 ± 0.20**

$C_{24:1}$-Cer

Hours	**Control**	**Cur 10 μM**
1	2.43 ± 0.43	3.18 ± 0.85*
2	2.39 ± 0.31	2.77 ± 0.31**
4	1.98 ± 0.33	2.57 ± 0.45*

$C_{24:0}$-Cer

Hours	**Control**	**Cur 10 μM**
1	2.54 ± 0.41	3.23 ± 0.74*
2	2.61 ± 0.19	2.97 ± 0.21**
4	2.11 ± 0.34	2.08 ± 0.72

$C_{26:1}$-Cer

Hours	**Control**	**Cur 10 µM**
1	0.24 ± 0.041	0.45 ± 0.11**
2	0.24 ± 0.026	0.45 ± 0.052**
4	0.20 ± 0.029	0.50 ± 0.089**

$C_{26:0}$-Cer

Hours	**Control**	**Cur 10 µM**
1	0.14 ± 0.054	0.21 ± 0.088**
2	0.19 ± 0.019	0.28 ± 0.030**
4	0.15 ± 0.024	0.32 ± 0.060**

Total Cers

Hours	**Control**	**Cur 10 µM**
1	8.32 ± 0.61	9.61 ± 1.55
2	9.51 ± 0.88	9.05 ± 0.80
4	8.61 ± 0.96	8.36 ± 0.94

Dihydroceramides (pmol/µg PC)

$C_{16:0}$-dhCer

Hours	**Control**	**Cur 10 µM**
1	0.067 ± 0.009	0.11 ± 0.011**
2	0.11 ± 0.015	0.16 ± 0.023
4	0.11 ± 0.011	0.29 ± 0.039**

$C_{18:0}$-dhCer

Hours	**Control**	**Cur 10 µM**
1	0.0016 ± 0.0001	0.0035 ± 0.0006*
2	0.0020 ± 0.0004	0.0035 ± 0.0006**
4	0.0019 ± 0.0004	0.0071 ± 0.0012**

$C_{20:0}$-dhCer

Hours	**Control**	**Cur 10 µM**
1	0.00080 ± 0.0002	0.0021 ± 0.0004
2	0.0011 ± 0.0001	0.0017 ± 0.0001**
4	0.0012 ± 0.0002	0.0054 ± 0.0014**

$C_{22:0}$-dhCer

Hours	**Control**	**Cur 10 µM**
1	0.0036 ± 0.001	0.009 ± 0.003**
2	0.0037 ± 0.001	0.011 ± 0.002
4	0.0049 ± 0.001	0.03 ± 0.007**

$C_{24:1}$-dhCer

Hours	**Control**	**Cur 10 µM**
1	0.0055 ± 0.001	0.015 ± 0.003**
2	0.0055 ± 0.001	0.017 ± 0.003
4	0.0069 ± 0.043	0.043 ± 0.004**

$C_{24:0}$-dhCer

Hours	**Control**	**Cur 10 µM**
1	0.0069 ± 0.001	0.014 ± 0.003**
2	0.0060 ± 0.0009	0.016 ± 0.002**
4	0.0081 ± 0.0003	0.046 ± 0.004**

$C_{26:1}$-dhCer

Hours	**Control**	**Cur 10 µM**
1	0.00041 ± 0.0002	0.0012 ± 0.0007
2	0.00081 ± 0.0001	0.0020 ± 0.0006
4	0.00085 ± 0.0002	0.0060 ± 0.0005**

Total dhCers

Hours	**Control**	**Cur 10 µM**
1	0.085 ± 0.010	0.15 ± 0.014**
2	0.13 ± 0.019	0.21 ± 0.030
4	0.13 ± 0.010	0.42 ± 0.044**

Sphingoid bases (pmol/µg PC)

Sph

Hours	**Control**	**Cur 10 µM**
1	0.94 ± 0.16	1.25 ± 0.30
2	1.40 ± 0.15	1.27 ± 0.17
4	1.02 ± 0.25	1.03 ± 0.17

dhSph

Hours	**Control**	**Cur 10 µM**
1	0.057 ± 0.012	0.14 ± 0.025**
2	0.082 ± 0.007	0.16 ± 0.027*
4	0.071 ± 0.011	0.18 ± 0.010*

S1P

Hours	**Control**	**Cur 10 µM**
1	0.022 ± 0.006	0.025 ± 0.013
2	0.018 ± 0.004	0.011 ± 0.001
4	0.017 ± 0.005	0.0091 ± 0.003

Sphingomyelins (pmol/µg PC)

$C_{16:0}$-SM

Hours	Control	Cur 10 µM
1	54.91 ± 3.13	59.54 ± 4.97*
2	64.14 ± 4.06	56.92 ± 2.24*
4	66.1 ± 4.76	65.24 ± 3.01

$C_{18:0}$-SM

Hours	Control	Cur 10 µM
1	0.69 ± 0.048	0.81 ± 0.064*
2	1.06 ± 0.14	1.02 ± 0.076
4	0.90 ± 0.075	1.42 ± 0.11*

$C_{20:0}$-SM

Hours	Control	Cur 10 µM
1	0.57 ± 0.065	0.70 ± 0.076**
2	1.04 ± 0.24	1.12 ± 0.18
4	0.95 ± 0.21	1.49 ± 0.18

$C_{22:0}$-SM

Hours	Control	Cur 10 µM
1	3.19 ± 0.62	3.77 ± 0.61*
2	4.77 ± 0.93	4.95 ± 0.55
4	4.06 ± 1.15	6.49 ± 1.01

$C_{24:1}$-SM

Hours	Control	Cur 10 µM
1	14.09 ± 2.57	16.35 ± 2.76
2	22.00 ± 5.07	21.88 ± 2.62
4	19.56 ± 5.76	28.11 ± 4.06

$C_{26:1}$-SM

Hours	Control	Cur 10 µM
1	0.72 ± 0.15	0.89 ± 0.17
2	1.41 ± 0.37	1.42 ± 0.25
4	1.23 ± 0.42	1.78 ± 0.39

Total SMs

Hours	Control	Cur 10 µM
1	74.16 ± 6.26	82.05 ± 8.59*
2	94.42 ± 10.73	87.31 ± 5.17
4	92.81 ± 7.20	107.21 ± 5.95*

Dihydrosphingomyelins (pmol/µg PC)

$C_{16:0}$-dhSM

Hours	**Control**	**Cur 10 µM**
1	7.14 ± 0.60	7.63 ± 0.68
2	13.42 ± 3.22	11.47 ± 2.39*
4	10.91 ± 1.33	12.06 ± 2.32

$C_{18:0}$-dhSM

Hours	**Control**	**Cur 10 µM**
1	0.16 ± 0.018	0.19 ± 0.029
2	0.38 ± 0.10	0.37 ± 0.089
4	0.31 ± 0.033	0.54 ± 0.083**

$C_{20:0}$-dhSM

Hours	**Control**	**Cur 10 µM**
1	0.14 ± 0.012	0.18 ± 0.033
2	0.32 ± 0.083	0.34 ± 0.092
4	0.25 ± 0.054	0.46 ± 0.050

$C_{22:0}$-dhSM

Hours	**Control**	**Cur 10 µM**
1	0.38 ± 0.047	0.46 ± 0.057
2	0.84 ± 0.15	0.86 ± 0.15
4	0.78 ± 0.16	1.37 ± 0.14

$C_{24:0}$-dhSM

Hours	**Control**	**Cur 10 µM**
1	0.56 ± 0.094	0.67 ± 0.11
2	1.44 ± 0.30	1.44 ± 0.32
4	1.24 ± 0.32	5.63 ± 3.20

$C_{26:0}$-dhSM

Hours	**Control**	**Cur 10 µM**
1	0.067 ± 0.006	0.075 ± 0.010
2	0.19 ± 0.058	0.19 ± 0.070
4	0.14 ± 0.052	0.17 ± 0.011

Total dhSMs

Hours	**Control**	**Cur 10 µM**
1	8.44 ± 0.71	9.21 ± 0.83
2	16.58 ± 3.55	14.66 ± 2.93
4	13.63 ± 0.98	20.23 ± 5.73

Table 4.2 Effect of curcumin on *de novo* sphingolipid biosynthesis in HCT-116 cells. HCT-116 cells were treated with either 400 µM $^{13}C_3$, ^{15}N-labeled L-serine alone as control or with a combination of 400 µM $^{13}C_3$, ^{15}N-labeled L-serine and 10 µM curcumin

for 20, 30, 60, and 90 min. The amount of each labeled *de novo* sphingolipid was determined by LC-MS/MS. Data are mean ± SEM of 3-4 independent experiments. *p < 0.05, **p < 0.01, significant difference between control and curcumin-treated cells.

Ceramides (pmol/μg PC)

***De novo* $C_{16:0}$-Cer**

Minutes	**Control**	**Cur 10 μM**
20	0.045 ± 0.014	0.027 ± 0.008**
30	0.15 ± 0.035	0.078 ± 0.022**
60	0.27 ± 0.035	0.13 ± 0.023**
90	0.38 ± 0.065	0.18 ± 0.031**

***De novo* $C_{24:1}$-Cer**

Minutes	**Control**	**Cur 10 μM**
20	0.063 ± 0.032	0.056 ± 0.029
30	0.16 ± 0.070	0.18 ± 0.082
60	0.25 ± 0.094	0.31 ± 0.11**
90	0.40 ± 0.15	0.53 ± 0.21*

***De novo* total Cers**

Minutes	**Control**	**Cur 10 μM**
20	0.11 ± 0.046	0.082 ± 0.038*
30	0.33 ± 0.10	0.27 ± 0.10*
60	0.55 ± 0.13	0.47 ± 0.14
90	0.86 ± 0.22	0.79 ± 0.23

Dihydroceramides (pmol/μg PC)

***De novo* $C_{16:0}$-dhCer**

Minutes	**Control**	**Cur 10 μM**
20	0.0076 ± 0.002	0.0059 ± 0.001
30	0.018 ± 0.003	0.019 ± 0.001
60	0.027 ± 0.005	0.037 ± 0.010
90	0.030 ± 0.005	0.045 ± 0.007**

Sphingomyelins (pmol/μg PC)

***De novo* $C_{16:0}$-SM**

Minutes	**Control**	**Cur 10 μM**
20	0.26 ± 0.043	0.27 ± 0.051
30	0.34 ± 0.025	0.31 ± 0.040
60	0.42 ± 0.056	0.40 ± 0.032

90	0.64 ± 0.052	0.56 ± 0.033

***De novo* $C_{18:0}$-SM**

Minutes	**Control**	**Cur 10 µM**
20	0.0095 ± 0.007	0.0038 ± 0.002
30	0.024 ± 0.019	0.028 ± 0.024
60	0.018 ± 0.015	0.045 ± 0.038
90	0.018 ± 0.009	0.018 ± 0.009

***De novo* $C_{24:1}$-SM**

Minutes	**Control**	**Cur 10 µM**
20	0.14 ± 0.073	0.13 ± 0.076
30	0.15 ± 0.054	0.11 ± 0.052**
60	0.13 ± 0.048	0.17 ± 0.058
90	0.18 ± 0.076	0.21 ± 0.066

***De novo* total SMs**

Minutes	**Control**	**Cur 10 µM**
20	0.41 ± 0.079	0.41 ± 0.061
30	0.51 ± 0.043	0.45 ± 0.049
60	0.57 ± 0.077	0.62 ± 0.064
90	0.83 ± 0.12	0.79 ± 0.070

Dihydrosphingomyelins (pmol/µg PC)

***De novo* $C_{16:0}$-dhSM**

Minutes	**Control**	**Cur 10 µM**
20	0.094 ± 0.019	0.071 ± 0.005
30	0.11 ± 0.012	0.088 ± 0.008
60	0.094 ± 0.004	0.11 ± 0.010
90	0.12 ± 0.005	0.17 ± 0.023

Table 4.3 Effect of resveratrol on sphingolipid metabolism in HCT-116 cells. HCT-116 cells were treated with 50 µM resveratrol for 2 and 4 h. The amount of each sphingolipid was determined by LC-MS/MS. Data are mean ± SEM of 3 independent experiments. *p < 0.05, **p < 0.01, significant difference between control and resveratrol-treated cells.

Ceramides (pmol/µg PC)

$C_{16:0}$-Cer

Hours	**Control**	**Res 50 µM**
2	3.29 ± 0.38	1.46 ± 0.11**
4	3.78 ± 0.37	1.37 ± 0.11**

$C_{18:0}$-Cer

Hours	Control	Res 50 µM
2	0.083 ± 0.009	0.068 ± 0.005**
4	0.098 ± 0.018	0.069 ± 0.003*

$C_{20:0}$-Cer

Hours	Control	Res 50 µM
2	0.057 ± 0.006	0.049 ± 0.004
4	0.069 ± 0.016	0.049 ± 0.006*

$C_{22:0}$-Cer

Hours	Control	Res 50 µM
2	0.64 ± 0.032	0.64 ± 0.067
4	0.70 ± 0.13	0.78 ± 0.046

$C_{24:1}$-Cer

Hours	Control	Res 50 µM
2	2.39 ± 0.31	1.60 ± 0.18**
4	2.18 ± 0.38	1.29 ± 0.26**

$C_{24:0}$-Cer

Hours	Control	Res 50 µM
2	2.61 ± 0.19	2.43 ± 0.27
4	2.31 ± 0.39	2.62 ± 0.58

$C_{26:1}$-Cer

Hours	Control	Res 50 µM
2	0.24 ± 0.026	0.24 ± 0.036
4	0.22 ± 0.034	0.25 ± 0.043

$C_{26:0}$-Cer

Hours	Control	Res 50 µM
2	0.19 ± 0.019	0.19 ± 0.023
4	0.17 ± 0.023	0.21 ± 0.035*

Total Cers

Hours	Control	Res 50 µM
2	9.51 ± 0.88	6.66 ± 0.65**
4	9.52 ± 0.44	6.64 ± 0.92*

Dihydroceramides (pmol/µg PC)

$C_{16:0}$-dhCer

Hours	Control	Res 50 µM
2	0.11 ± 0.015	1.04 ± 0.090**

4	0.12 ± 0.011	0.92 ± 0.029**

$C_{18:0}$-dhCer

Hours	**Control**	**Res 50 µM**
2	0.0020 ± 0.0004	0.012 ± 0.0005**
4	0.0021 ± 0.0005	0.011 ± 0.002**

$C_{20:0}$-dhCer

Hours	**Control**	**Res 50 µM**
2	0.0011 ± 0.0001	0.014 ± 0.0003
4	0.0014 ± 0.0003	0.013 ± 0.0035**

$C_{22:0}$-dhCer

Hours	**Control**	**Res 50 µM**
2	0.0037 ± 0.001	0.14 ± 0.011**
4	0.0055 ± 0.002	0.17 ± 0.028**

$C_{24:1}$-dhCer

Hours	**Control**	**Res 50 µM**
2	0.0055 ± 0.0014	0.16 ± 0.016*
4	0.0069 ± 0.0004	0.15 ± 0.0058**

$C_{24:0}$-dhCer

Hours	**Control**	**Res 50 µM**
2	0.0060 ± 0.0009	0.23 ± 0.019**
4	0.0083 ± 0.0002	0.29 ± 0.019**

$C_{26:1}$-dhCer

Hours	**Control**	**Res 50 µM**
2	0.00081 ± 0.0001	0.022 ± 0.0034
4	0.0010 ± 0.0002	0.020 ± 0.0003

Total dhCers

Hours	**Control**	**Res 50 µM**
2	0.13 ± 0.019	1.62 ± 0.12**
4	0.14 ± 0.008	1.56 ± 0.007**

Sphingoid bases (pmol/µg PC)

Sph

Hours	**Control**	**Res 50 µM**
2	1.40 ± 0.15	1.24 ± 0.10
4	1.17 ± 0.27	0.91 ± 0.17*

dhSph

Hours	**Control**	**Res 50 µM**

2	0.082 ± 0.007	0.29 ± 0.014**
4	0.074 ± 0.016	0.27 ± 0.040**

S1P

Hours	**Control**	**Res 50 µM**
2	0.018 ± 0.004	0.018 ± 0.004
4	0.020 ± 0.006	0.013 ± 0.002

Sphingomyelins (pmol/µg PC)

$C_{16:0}$-SM

Hours	**Control**	**Res 50 µM**
2	64.14 ± 4.06	58.89 ± 5.65*
4	66.68 ± 6.68	51.39 ± 5.09*

$C_{18:0}$-SM

Hours	**Control**	**Res 50 µM**
2	1.06 ± 0.14	0.93 ± 0.13
4	0.92 ± 0.10	0.83 ± 0.11*

$C_{20:0}$-SM

Hours	**Control**	**Res 50 µM**
2	1.04 ± 0.24	1.05 ± 0.25
4	0.96 ± 0.30	1.02 ± 0.19

$C_{22:0}$-SM

Hours	**Control**	**Res 50 µM**
2	4.77 ± 0.93	5.07 ± 1.06*
4	4.01 ± 1.62	5.43 ± 0.99

$C_{24:1}$-SM

Hours	**Control**	**Res 50 µM**
2	22.00 ± 5.07	22.84 ± 5.11
4	19.51 ± 8.14	22.94 ± 3.91

$C_{26:1}$-SM

Hours	**Control**	**Res 50 µM**
2	1.41 ± 0.37	1.49 ± 0.41
4	1.30 ± 0.58	1.57 ± 0.31

Total SMs

Hours	**Control**	**Res 50 µM**
2	94.42 ± 10.73	90.27 ± 12.59
4	93.38 ± 10.16	83.17 ± 10.59**

Dihydrosphingomyelins (pmol/μg PC)

$C_{16:0}$-dhSM

Hours	Control	Res 50 μM
2	13.42 ± 3.22	13.73 ± 1.23
4	11.70 ± 1.52	16.18 ± 1.52*

$C_{18:0}$-dhSM

Hours	Control	Res 50 μM
2	0.38 ± 0.10	0.45 ± 0.087
4	0.34 ± 0.019	0.64 ± 0.023**

$C_{20:0}$-dhSM

Hours	Control	Res 50 μM
2	0.32 ± 0.083	0.43 ± 0.11*
4	0.28 ± 0.069	0.65 ± 0.076

$C_{22:0}$-dhSM

Hours	Control	Res 50 μM
2	0.84 ± 0.15	1.48 ± 0.30**
4	0.79 ± 0.22	2.70 ± 0.23

$C_{24:0}$-dhSM

Hours	Control	Res 50 μM
2	1.44 ± 0.30	1.79 ± 0.44
4	1.19 ± 0.44	3.15 ± 0.33

$C_{26:0}$-dhSM

Hours	Control	Res 50 μM
2	0.19 ± 0.058	0.22 ± 0.057*
4	0.15 ± 0.071	0.35 ± 0.034

Total dhSMs

Hours	Control	Res 50 μM
2	16.58 ± 3.55	18.11 ± 1.65
4	14.44 ± 0.77	23.67 ± 0.91**

Table 4.4 Effect of DTT on sphingolipid metabolism in HCT-116 cells. HCT-116 cells were treated with 2 mM DTT for 2 and 6 h. The amount of each sphingolipid was determined by LC-MS/MS. Data are mean ± SEM of 1 (6 h) or 2 (2 h) independent experiments.

Ceramides (pmol/μg PC)

$C_{16:0}$-Cer

Hours	**Control**	**DTT 2 mM**
2	2.59 ± 0.20	1.75 ± 0.059
6	1.76	1.55

$C_{18:0}$-Cer

Hours	**Control**	**DTT 2 mM**
2	0.055 ± 0.002	0.043 ± 0.004
6	0.038	0.036

$C_{20:0}$-Cer

Hours	**Control**	**DTT 2 mM**
2	0.034 ± 0.0001	0.027 ± 0.0007
6	0.029	0.023

$C_{22:0}$-Cer

Hours	**Control**	**DTT 2 mM**
2	0.27 ± 0.002	0.15 ± 0.007
6	0.10	0.059

$C_{24:1}$-Cer

Hours	**Control**	**DTT 2 mM**
2	2.07 ± 0.90	1.05 ± 0.51
6	0.12	0.054

$C_{24:0}$-Cer

Hours	**Control**	**DTT 2 mM**
2	1.95 ± 0.94	1.15 ± 0.49
6	0.17	0.069

$C_{26:1}$-Cer

Hours	**Control**	**DTT 2 mM**
2	0.22 ± 0.069	0.11 ± 0.046
6	0.019	0.0076

Total Cers

Hours	**Control**	**DTT 2 mM**
2	7.20 ± 2.12	4.28 ± 1.11
6	2.23	1.80

Dihydroceramides (pmol/μg PC)

$C_{16:0}$-dhCer

Hours	**Control**	**DTT 2 mM**
2	0.15 ± 0.049	2.30 ± 0.89
6	0.16	5.95

$C_{18:0}$-dhCer

Hours	Control	DTT 2 mM
2	0.00066 ± 0.0007	0.0052 ± 0.0052
6	0.0018	0.028

$C_{22:0}$-dhCer

Hours	Control	DTT 2 mM
2	0.0017	0.023
6	0.0022	0.096

$C_{24:1}$-dhCer

Hours	Control	DTT 2 mM
2	0.0080 ± 0.006	0.27 ± 0.12
6	0.0018	0.063

$C_{24:0}$-dhCer

Hours	Control	DTT 2 mM
2	0.015 ± 0.007	0.22 ± 0.10
6	0.0040	0.070

Total dhCers

Hours	Control	DTT 2 mM
2	0.17 ± 0.034	2.81 ± 0.64
6	0.17	6.23

Sphingoid bases (pmol/μg PC)

Sph

Hours	Control	DTT 2 mM
2	0.68 ± 0.059	0.56 ± 0.068
6	1.69	1.06

dhSph

Hours	Control	DTT 2 mM
2	0.088 ± 0.016	0.15 ± 0.018
6	0.19	0.62

S1P

Hours	Control	DTT 2 mM
2	0.042 ± 0.003	0.035 ± 0.005
6	0.037	0.020

Sphingomyelins (pmol/μg PC)

$C_{16:0}$-SM

Hours	**Control**	**DTT 2 mM**
2	38.08 ± 4.13	33.91 ± 3.57
6	28.09	19.89

$C_{18:0}$-SM

Hours	**Control**	**DTT 2 mM**
2	1.54 ± 0.091	0.64 ± 0.075
6	0.53	0.40

$C_{20:0}$-SM

Hours	**Control**	**DTT 2 mM**
2	0.33 ± 0.054	0.49 ± 0.015
6	0.64	0.44

$C_{22:0}$-SM

Hours	**Control**	**DTT 2 mM**
2	0.90 ± 0.29	1.41 ± 0.33
6	0.77	0.55

$C_{24:1}$-SM

Hours	**Control**	**DTT 2 mM**
2	3.16 ± 0.89	4.68 ± 1.02
6	4.29	2.99

$C_{26:1}$-SM

Hours	**Control**	**DTT 2 mM**
2	0.68 ± 0.017	0.28 ± 0.10
6	0.43	0.33

Total SMs

Hours	**Control**	**DTT 2 mM**
2	44.69 ± 5.47	41.41 ± 5.08
6	34.75	24.59

Dihydrosphingomyelins (pmol/μg PC)

$C_{16:0}$-dhSM

Hours	**Control**	**DTT 2 mM**
2	10.36 ± 0.79	10.76 ± 1.18
6	5.15	6.30

$C_{18:0}$-dhSM

Hours	**Control**	**DTT 2 mM**
2	0.27 ± 0.005	0.35 ± 0.022
6	0.18	0.18

$C_{20:0}$-dhSM

Hours	**Control**	**DTT 2 mM**
2	0.11 ± 0.002	0.30 ± 0.010
6	0.17	0.20

$C_{22:0}$-dhSM

Hours	**Control**	**DTT 2 mM**
2	0.19 ± 0.090	0.37 ± 0.029
6	0.12	0.23

$C_{24:0}$-dhSM

Hours	**Control**	**DTT 2 mM**
2	0.20 ± 0.045	0.41 ± 0.054
6	0.27	0.57

Total dhSMs

Hours	**Control**	**DTT 2 mM**
2	11.13 ± 0.91	12.20 ± 1.30
6	5.96	7.61

Table 4.5 Effect of sulforaphane on sphingolipid metabolism in HCT-116 cells. HCT-116 cells were treated with 20 μM sulforaphane for 2 and 4 h. The amount of each sphingolipid was determined by LC-MS/MS. Data are mean ± SEM of 2 independent experiments.

Ceramides (pmol/μg PC)

$C_{16:0}$-Cer

Hours	**Control**	**SFN 20 μM**
2	2.40 ± 0.18	3.13 ± 0.073
4	2.85 ± 0.36	3.83 ± 0.010

$C_{18:0}$-Cer

Hours	**Control**	**SFN 20 μM**
2	0.038 ± 0.001	0.054 ± 0.009
4	0.042 ± 0.0002	0.061 ± 0.006

$C_{20:0}$-Cer

Hours	**Control**	**SFN 20 μM**
2	0.022 ± 0.003	0.035 ± 0.006
4	0.025 ± 0.002	0.042 ± 0.010

$C_{22:0}$-Cer

Hours	**Control**	**SFN 20 μM**
2	0.19 ± 0.017	0.26 ± 0.024

4	0.21 ± 0.0003	0.30 ± 0.025

$C_{24:1}$-Cer

Hours	**Control**	**SFN 20 µM**
2	4.45 ± 0.42	5.61 ± 0.35
4	4.76 ± 0.26	6.68 ± 0.58

$C_{24:0}$-Cer

Hours	**Control**	**SFN 20 µM**
2	4.41 ± 0.59	4.31 ± 0.40
4	4.67 ± 0.67	4.41 ± 0.50

$C_{26:1}$-Cer

Hours	**Control**	**SFN 20 µM**
2	0.37 ± 0.051	0.47 ± 0.017
4	0.43 ± 0.037	0.47 ± 0.024

Total Cers

Hours	**Control**	**SFN 20 µM**
2	11.88 ± 1.23	13.87 ± 0.65
4	12.99 ± 1.32	15.79 ± 1.04

Dihydroceramides (pmol/µg PC)

$C_{16:0}$-dhCer

Hours	**Control**	**SFN 20 µM**
2	0.053 ± 0.006	0.078 ± 0.007
4	0.072 ± 0.018	0.11 ± 0.019

$C_{24:1}$-dhCer

Hours	**Control**	**SFN 20 µM**
2	0.0078 ± 0.008	0.012 ± 0.012
4	0.0074 ± 0.007	0.016 ± 0.016

Total dhCers

Hours	**Control**	**SFN 20 µM**
2	0.061 ± 0.002	0.090 ± 0.004
4	0.079 ± 0.011	0.12 ± 0.003

Sphingoid bases (pmol/µg PC)

Sph

Hours	**Control**	**SFN 20 µM**
2	0.57 ± 0.018	0.50 ± 0.013
4	0.53 ± 0.025	0.61 ± 0.055

dhSph

Hours	**Control**	**SFN 20 µM**
2	0.10 ± 0.011	0.081 ± 0.005
4	0.10 ± 0.001	0.10 ± 0.006

S1P

Hours	**Control**	**SFN 20 µM**
2	0.013 ± 0.007	0.016 ± 0.003
4	0.010 ± 0.002	0.014 ± 0.004

Sphingomyelins (pmol/µg PC)

$C_{16:0}$-SM

Hours	**Control**	**SFN 20 µM**
2	83.97 ± 19.12	62.22 ± 15.81
4	90.58 ± 20.91	67.94 ± 22.24

$C_{18:0}$-SM

Hours	**Control**	**SFN 20 µM**
2	1.59 ± 0.26	0.65 ± 0.17
4	1.61 ± 0.13	0.60 ± 0.14

$C_{20:0}$-SM

Hours	**Control**	**SFN 20 µM**
2	0.37 ± 0.17	0.50 ± 0.13
4	0.28 ± 0.084	0.50 ± 0.13

$C_{22:0}$-SM

Hours	**Control**	**SFN 20 µM**
2	1.32 ± 0.63	1.77 ± 0.29
4	1.03 ± 0.33	1.84 ± 0.47

$C_{24:1}$-SM

Hours	**Control**	**SFN 20 µM**
2	4.80 ± 2.52	5.98 ± 1.14
4	3.86 ± 1.53	6.31 ± 1.74

$C_{26:1}$-SM

Hours	**Control**	**SFN 20 µM**
2	2.12 ± 0.12	0.25 ± 0.040
4	2.15 ± 0.048	0.27 ± 0.064

Total SMs

Hours	**Control**	**SFN 20 µM**
2	94.16 ± 22.83	71.37 ± 17.57

4	99.51 ± 23.04	77.45 ± 24.79

Dihydrosphingomyelins (pmol/μg PC)

$C_{16:0}$-dhSM

Hours	**Control**	**SFN 20 μM**
2	6.22 ± 0.15	6.78 ± 0.46
4	5.50 ± 0.42	6.24 ± 0.12

$C_{18:0}$-dhSM

Hours	**Control**	**SFN 20 μM**
2	0.11 ± 0.019	0.16 ± 0.005
4	0.082 ± 0.016	0.13 ± 0.008

$C_{20:0}$-dhSM

Hours	**Control**	**SFN 20 μM**
2	0.033 ± 0.005	0.078 ± 0.016
4	0.025 ± 0.011	0.068 ± 0.007

$C_{22:0}$-dhSM

Hours	**Control**	**SFN 20 μM**
2	0.081 ± 0.006	0.17 ± 0.034
4	0.053 ± 0.026	0.15 ± 0.004

$C_{24:0}$-dhSM

Hours	**Control**	**SFN 20 μM**
2	0.063 ± 0.010	0.12 ± 0.026
4	0.045 ± 0.029	0.11 ± 0.012

$C_{26:0}$-dhSM

Hours	**Control**	**SFN 20 μM**
2	0.0052 ± 0.001	0.010 ± 0.002
4	0.0036 ± 0.002	0.011 ± 0.003

Total dhSMs

Hours	**Control**	**SFN 20 μM**
2	6.51 ± 1.16	7.30 ± 0.17
4	5.71 ± 0.00002	6.71 ± 0.84

Table 4.6 Effect of quercetin on sphingolipid metabolism in HCT-116 cells. HCT-116 cells were treated with 20 μM quercetin for 2 and 4 h. The amount of each sphingolipid was determined by LC-MS/MS. Data are mean ± SEM of 2 independent experiments.

Ceramides (pmol/μg PC)

$C_{16:0}$-Cer

Hours	**Control**	**Quer 20 µM**
2	2.59 ± 0.20	3.79 ± 0.29
4	3.04 ± 0.32	4.10 ± 0.11

$C_{18:0}$-Cer

Hours	**Control**	**Quer 20 µM**
2	0.055 ± 0.002	0.082 ± 0.003
4	0.058 ± 0.009	0.085 ± 0.004

$C_{20:0}$-Cer

Hours	**Control**	**Quer 20 µM**
2	0.034 ± 0.0001	0.052 ± 0.001
4	0.038 ± 0.005	0.050 ± 0.003

$C_{22:0}$-Cer

Hours	**Control**	**Quer 20 µM**
2	0.27 ± 0.002	0.32 ± 0.022
4	0.25 ± 0.025	0.32 ± 0.010

$C_{24:1}$-Cer

Hours	**Control**	**Quer 20 µM**
2	2.07 ± 0.90	2.19 ± 1.08
4	2.31 ± 1.07	2.10 ± 0.89

$C_{24:0}$-Cer

Hours	**Control**	**Quer 20 µM**
2	1.95 ± 0.94	2.28 ± 1.03
4	2.23 ± 1.07	2.48 ± 0.98

$C_{26:1}$-Cer

Hours	**Control**	**Quer 20 µM**
2	0.22 ± 0.069	0.17 ± 0.10
4	0.21 ± 0.085	0.16 ± 0.086

Total Cers

Hours	**Control**	**Quer 20 µM**
2	7.20 ± 2.12	8.88 ± 2.52
4	8.14 ± 2.59	9.30 ± 2.06

Dihydroceramides (pmol/µg PC)

$C_{16:0}$-dhCer

Hours	**Control**	**Quer 20 µM**
2	0.15 ± 0.049	0.34 ± 0.10

4	0.19 ± 0.055	0.68 ± 0.18

$C_{24:1}$-dhCer

Hours	**Control**	**Quer 20 µM**
2	0.0080 ± 0.006	0.020 ± 0.008
4	0.025 ± 0.015	0.060 ± 0.029

$C_{24:0}$-dhCer

Hours	**Control**	**Quer 20 µM**
2	0.015 ± 0.007	0.048 ± 0.020
4	0.016 ± 0.009	0.12 ± 0.063

Total dhCers

Hours	**Control**	**Quer 20 µM**
2	0.17 ± 0.034	0.42 ± 0.064
4	0.24 ± 0.028	0.87 ± 0.081

Sphingoid bases (pmol/µg PC)

Sph

Hours	**Control**	**Quer 20 µM**
2	0.68 ± 0.059	1.13 ± 0.31
4	0.75 ± 0.029	0.77 ± 0.017

dhSph

Hours	**Control**	**Quer 20 µM**
2	0.088 ± 0.016	0.11 ± 0.008
4	0.11 ± 0.021	0.14 ± 0.037

S1P

Hours	**Control**	**Quer 20 µM**
2	0.042 ± 0.003	0.039 ± 0.001
4	0.033 ± 0.008	0.026 ± 0.019

Sphingomyelins (pmol/µg PC)

$C_{16:0}$-SM

Hours	**Control**	**Quer 20 µM**
2	38.08 ± 4.13	39.18 ± 2.96
4	43.38 ± 5.40	35.33 ± 4.79

$C_{18:0}$-SM

Hours	**Control**	**Quer 20 µM**
2	1.54 ± 0.091	0.68 ± 0.021
4	1.69 ± 0.078	0.59 ± 0.15

$C_{20:0}$-SM

Hours	**Control**	**Quer 20 µM**
2	0.33 ± 0.054	0.51 ± 0.069
4	0.33 ± 0.092	0.60 ± 0.070

$C_{22:0}$-SM

Hours	**Control**	**Quer 20 µM**
2	0.90 ± 0.29	1.55 ± 0.23
4	0.93 ± 0.30	1.33 ± 0.40

$C_{24:1}$-SM

Hours	**Control**	**Quer 20 µM**
2	3.16 ± 0.89	5.24 ± 0.92
4	3.25 ± 1.13	4.77 ± 1.25

$C_{26:1}$-SM

Hours	**Control**	**Quer 20 µM**
2	0.68 ± 0.017	0.34 ± 0.083
4	0.78 ± 0.099	0.30 ± 0.065

Total SMs

Hours	**Control**	**Quer 20 µM**
2	44.69 ± 5.47	47.51 ± 4.28
4	50.37 ± 7.10	42.93 ± 6.72

Dihydrosphingomyelins (pmol/µg PC)

$C_{16:0}$-dhSM

Hours	**Control**	**Quer 20 µM**
2	10.36 ± 0.79	11.25 ± 0.92
4	10.56 ± 1.01	9.13 ± 1.95

$C_{18:0}$-dhSM

Hours	**Control**	**Quer 20 µM**
2	0.27 ± 0.005	0.40 ± 0.012
4	0.36 ± 0.11	0.33 ± 0.072

$C_{20:0}$-dhSM

Hours	**Control**	**Quer 20 µM**
2	0.11 ± 0.002	0.21 ± 0.054
4	0.087 ± 0.010	0.17 ± 0.021

$C_{22:0}$-dhSM

Hours	**Control**	**Quer 20 µM**
2	0.19 ± 0.090	0.36 ± 0.048

4	0.17 ± 0.046	0.32 ± 0.095

$C_{24:0}$-dhSM

Hours	**Control**	**Quer 20 µM**
2	0.20 ± 0.045	0.35 ± 0.046
4	0.16 ± 0.004	0.38 ± 0.18

Total dhSMs

Hours	**Control**	**Quer 20 µM**
2	11.13 ± 1.72	12.56 ± 1.73
4	11.34 ± 1.62	10.33 ± 3.30

Table 4.7 Effect of thapsigargin on sphingolipid metabolism in HCT-116 cells. HCT-116 cells were treated with 1 µM thapsigargin for 6 h. The amount of each sphingolipid was determined by LC-MS/MS. Data are mean ± SEM of 2 independent experiments.

Ceramides (pmol/µg PC)

$C_{16:0}$-Cer

Hours	**Control**	**TG 1 µM**
6	2.21 ± 0.45	3.43 ± 0.93

$C_{18:0}$-Cer

Hours	**Control**	**TG 1 µM**
6	0.045 ± 0.007	0.088 ± 0.020

$C_{20:0}$-Cer

Hours	**Control**	**TG 1 µM**
6	0.031 ± 0.003	0.059 ± 0.004

$C_{22:0}$-Cer

Hours	**Control**	**TG 1 µM**
6	0.16 ± 0.059	0.31 ± 0.15

$C_{24:1}$-Cer

Hours	**Control**	**TG 1 µM**
6	0.68 ± 0.56	0.81 ± 0.66

$C_{24:0}$-Cer

Hours	**Control**	**TG 1 µM**
6	0.72 ± 0.55	0.90 ± 0.73

Total Cers

Hours	**Control**	**TG 1 µM**
6	3.92 ± 1.68	5.71 ± 2.57

Dihydroceramides (pmol/μg PC)

$C_{16:0}$-dhCer

Hours	Control	TG 1 μM
6	0.20 ± 0.035	0.67 ± 0.19

$C_{24:1}$-dhCer

Hours	Control	TG 1 μM
6	0.0059 ± 0.0041	0.0094 ± 0.0068

$C_{24:0}$-dhCer

Hours	Control	TG 1 μM
6	0.0054 ± 0.0015	0.017 ± 0.010

Total dhCers

Hours	Control	TG 1 μM
6	0.21 ± 0.038	0.71 ± 0.20

Sphingoid bases (pmol/μg PC)

Sph

Hours	Control	TG 1 μM
6	1.12 ± 0.56	1.03 ± 0.27

dhSph

Hours	Control	TG 1 μM
6	0.13 ± 0.060	0.11 ± 0.048

S1P

Hours	Control	TG 1 μM
6	0.032 ± 0.005	0.030 ± 0.003

Sphingomyelins (pmol/μg PC)

$C_{16:0}$-SM

Hours	Control	TG 1 μM
6	28.09 ± 1.52	31.20 ± 3.89

$C_{18:0}$-SM

Hours	Control	TG 1 μM
6	1.60 ± 0.023	0.63 ± 0.085

$C_{20:0}$-SM

Hours	Control	TG 1 μM
6	0.35 ± 0.12	0.58 ± 0.10

$C_{22:0}$-SM		
Hours	**Control**	**TG 1 μM**
6	0.40 ± 0.12	1.03 ± 0.25
$C_{24:1}$-SM		
Hours	**Control**	**TG 1 μM**
6	2.25 ± 0.25	4.32 ± 0.17
$C_{26:1}$-SM		
Hours	**Control**	**TG 1 μM**
6	0.85 ± 0.089	0.41 ± 0.10
Total SMs		
Hours	**Control**	**TG 1 μM**
6	33.54 ± 1.16	38.18 ± 3.85

Dihydrosphingomyelins (pmol/μg PC)

$C_{16:0}$-dhSM		
Hours	**Control**	**TG 1 μM**
6	5.15 ± 0.97	7.23 ± 1.63
$C_{18:0}$-dhSM		
Hours	**Control**	**TG 1 μM**
6	0.20 ± 0.021	0.24 ± 0.070
$C_{20:0}$-dhSM		
Hours	**Control**	**TG 1 μM**
6	0.17 ± 0.003	0.19 ± 0.014
$C_{22:0}$-dhSM		
Hours	**Control**	**TG 1 μM**
6	0.12 ± 0.059	0.19 ± 0.059
$C_{24:0}$-dhSM		
Hours	**Control**	**TG 1 μM**
6	0.14 ± 0.038	0.29 ± 0.045
Total dhSMs		
Hours	**Control**	**TG 1 μM**
6	5.86 ± 0.98	8.21 ± 1.78

Table 4.8 Effect of cancer chemotherapeutic drugs (doxorubicin and camptothecin) on sphingolipid metabolism in HCT-116 cells. HCT-116 cells were treated with 5 μM doxorubicin or 1 μM camptothecin for 24 h. The amount of each sphingolipid was determined by LC-MS/MS. Data are results of 1 experiment.

Ceramides (pmol/μg PC)

$C_{16:0}$-Cer

Hours	**Control**	**Dox 5 μM**	**CPT 1 μM**
24	2.03	3.93	6.04

$C_{18:0}$-Cer

Hours	**Control**	**Dox 5 μM**	**CPT 1 μM**
24	0.025	0.064	0.094

$C_{20:0}$-Cer

Hours	**Control**	**Dox 5 μM**	**CPT 1 μM**
24	0.022	0.039	0.062

$C_{22:0}$-Cer

Hours	**Control**	**Dox 5 μM**	**CPT 1 μM**
24	0.16	0.24	0.27

$C_{24:1}$-Cer

Hours	**Control**	**Dox 5 μM**	**CPT 1 μM**
24	1.18	2.03	2.08

$C_{24:0}$-Cer

Hours	**Control**	**Dox 5 μM**	**CPT 1 μM**
24	1.87	1.51	1.75

$C_{26:1}$-Cer

Hours	**Control**	**Dox 5 μM**	**CPT 1 μM**
24	0.16	0.11	0.22

$C_{26:0}$-Cer

Hours	**Control**	**Dox 5 μM**	**CPT 1 μM**
24	0.15	0.11	0.24

Total Cers

Hours	**Control**	**Dox 5 μM**	**CPT 1 μM**
24	5.60	8.03	10.77

Dihydroceramides (pmol/μg PC)

$C_{16:0}$-dhCer

Hours	**Control**	**Dox 5 μM**	**CPT 1 μM**
24	0.26	0.57	0.38

$C_{24:1}$-dhCer

Hours	**Control**	**Dox 5 μM**	**CPT 1 μM**

24	0.024	0.088	0.021

Total dhCers

Hours	**Control**	**Dox 5 µM**	**CPT 1 µM**
24	0.28	0.66	0.40

Sphingoid bases (pmol/µg PC)

Sph

Hours	**Control**	**Dox 5 µM**	**CPT 1 µM**
24	0.88	0.96	2.10

dhSph

Hours	**Control**	**Dox 5 µM**	**CPT 1 µM**
24	0.08	0.10	0.16

S1P

Hours	**Control**	**Dox 5 µM**	**CPT 1 µM**
24	0.011	0.029	0.034

Sphingomyelins (pmol/µg PC)

$C_{16:0}$-SM

Hours	**Control**	**Dox 5 µM**	**CPT 1 µM**
24	62.19	66.74	68.25

$C_{18:0}$-SM

Hours	**Control**	**Dox 5 µM**	**CPT 1 µM**
24	0.51	0.65	0.68

$C_{20:0}$-SM

Hours	**Control**	**Dox 5 µM**	**CPT 1 µM**
24	0.45	0.55	0.55

$C_{22:0}$-SM

Hours	**Control**	**Dox 5 µM**	**CPT 1 µM**
24	1.58	1.99	1.94

$C_{24:1}$-SM

Hours	**Control**	**Dox 5 µM**	**CPT 1 µM**
24	7.02	9.60	8.38

$C_{26:1}$-SM

Hours	**Control**	**Dox 5 µM**	**CPT 1 µM**
24	0.37	0.57	0.48

Total SMs

Hours	**Control**	**Dox 5 µM**	**CPT 1 µM**
24	72.12	80.11	80.28

Dihydrosphingomyelins (pmol/µg PC)

$C_{16:0}$-dhSM

Hours	**Control**	**Dox 5 µM**	**CPT 1 µM**
24	10.19	13.65	12.52

$C_{18:0}$-dhSM

Hours	**Control**	**TG 1 µM**	**CPT 1 µM**
24	0.23	0.38	0.38

$C_{20:0}$-dhSM

Hours	**Control**	**TG 1 µM**	**CPT 1 µM**
24	0.15	0.26	0.24

$C_{22:0}$-dhSM

Hours	**Control**	**TG 1 µM**	**CPT 1 µM**
24	0.26	0.42	0.38

$C_{24:0}$-dhSM

Hours	**Control**	**TG 1 µM**	**CPT 1 µM**
24	0.31	0.50	0.38

$C_{26:0}$-dhSM

Hours	**Control**	**TG 1 µM**	**CPT 1 µM**
24	0.03	0.06	0.06

Total dhSMs

Hours	**Control**	**TG 1 µM**	**CPT 1 µM**
24	11.17	15.26	13.96

Table 4.9 Effect of EGCG on sphingolipid metabolism in HCT-116 cells. HCT-116 cells were treated with 50 µM EGCG for 2 and 4 h. The amount of each sphingolipid was determined by LC-MS/MS. Data are mean ± SEM of 3 independent experiments. *$p < 0.05$, **$p < 0.01$, significant difference between control and EGCG-treated cells.

Ceramides (pmol/µg PC)

$C_{16:0}$-Cer

Hours	**Control**	**EGCG 50 µM**
2	3.29 ± 0.38	3.80 ± 0.10
4	3.78 ± 0.37	4.22 ± 0.40

$C_{18:0}$-Cer

Hours	Control	EGCG 50 µM
2	0.083 ± 0.009	0.080 ± 0.008
4	0.098 ± 0.018	0.085 ± 0.009

$C_{20:0}$-Cer

Hours	Control	EGCG 50 µM
2	0.057 ± 0.006	0.058 ± 0.006
4	0.069 ± 0.016	0.064 ± 0.008

$C_{22:0}$-Cer

Hours	Control	EGCG 50 µM
2	0.64 ± 0.032	0.63 ± 0.069
4	0.70 ± 0.13	0.59 ± 0.031

$C_{24:1}$-Cer

Hours	Control	EGCG 50 µM
2	2.39 ± 0.31	2.47 ± 0.28
4	2.18 ± 0.38	1.76 ± 0.38

$C_{24:0}$-Cer

Hours	Control	EGCG 50 µM
2	2.61 ± 0.19	2.76 ± 0.35
4	2.31 ± 0.39	2.21 ± 0.42

$C_{26:1}$-Cer

Hours	Control	EGCG 50 µM
2	0.24 ± 0.026	0.22 ± 0.036
4	0.22 ± 0.034	0.16 ± 0.028*

$C_{26:0}$-Cer

Hours	Control	EGCG 50 µM
2	0.19 ± 0.019	0.17 ± 0.026
4	0.17 ± 0.023	0.15 ± 0.022

Total Cers

Hours	Control	EGCG 50 µM
2	9.51 ± 0.88	10.18 ± 0.86
4	9.52 ± 0.44	9.24 ± 0.87

Dihydroceramides (pmol/µg PC)

$C_{16:0}$-dhCer

Hours	Control	EGCG 50 µM
2	0.11 ± 0.015	0.11 ± 0.002

4	0.12 ± 0.011	0.24 ± 0.037*

$C_{18:0}$-dhCer

Hours	**Control**	**EGCG 50 µM**
2	0.0020 ± 0.0004	0.0019 ± 0.0002
4	0.0021 ± 0.0005	0.0037 ± 0.0004*

$C_{20:0}$-dhCer

Hours	**Control**	**EGCG 50 µM**
2	0.0011 ± 0.0001	0.00092 ± 0.0001
4	0.0014 ± 0.0003	0.0019 ± 0.0002

$C_{22:0}$-dhCer

Hours	**Control**	**EGCG 50 µM**
2	0.0037 ± 0.0006	0.0034 ± 0.0007
4	0.0055 ± 0.0019	0.012 ± 0.0027*

$C_{24:1}$-dhCer

Hours	**Control**	**EGCG 50 µM**
2	0.0055 ± 0.0014	0.0058 ± 0.0002
4	0.0069 ± 0.0004	0.013 ± 0.0011**

$C_{24:0}$-dhCer

Hours	**Control**	**EGCG 50 µM**
2	0.0060 ± 0.0009	0.0056 ± 0.0010
4	0.0083 ± 0.0002	0.020 ± 0.0025**

$C_{26:1}$-dhCer

Hours	**Control**	**EGCG 50 µM**
2	0.00081 ± 0.0001	0.0009 ± 0.0001
4	0.0010 ± 0.0002	0.0015 ± 0.0002

Total dhCers

Hours	**Control**	**EGCG 50 µM**
2	0.13 ± 0.019	0.13 ± 0.003
4	0.14 ± 0.008	0.29 ± 0.041*

Sphingoid bases (pmol/µg PC)

Sph

Hours	**Control**	**EGCG 50 µM**
2	1.40 ± 0.15	1.24 ± 0.16
4	1.17 ± 0.27	0.96 ± 0.20*

dhSph

Hours	**Control**	**EGCG 50 µM**

2	0.082 ± 0.007	0.067 ± 0.003
4	0.074 ± 0.016	0.045 ± 0.019

S1P

Hours	**Control**	**EGCG 50 µM**
2	0.018 ± 0.004	0.022 ± 0.003
4	0.020 ± 0.006	0.017 ± 0.004

Sphingomyelins (pmol/µg PC)

$C_{16:0}$-SM

Hours	**Control**	**EGCG 50 µM**
2	64.14 ± 4.06	66.62 ± 9.12
4	66.68 ± 6.68	55.12 ± 1.34

$C_{18:0}$-SM

Hours	**Control**	**EGCG 50 µM**
2	1.06 ± 0.14	1.34 ± 0.25
4	0.92 ± 0.10	0.99 ± 0.088*

$C_{20:0}$-SM

Hours	**Control**	**EGCG 50 µM**
2	1.04 ± 0.24	1.30 ± 0.37
4	0.96 ± 0.30	1.05 ± 0.12

$C_{22:0}$-SM

Hours	**Control**	**EGCG 50 µM**
2	4.77 ± 0.93	5.90 ± 1.51
4	4.01 ± 1.62	4.99 ± 0.55

$C_{24:1}$-SM

Hours	**Control**	**EGCG 50 µM**
2	22.00 ± 5.07	25.67 ± 6.43**
4	19.51 ± 8.14	23.25 ± 2.37

$C_{26:1}$-SM

Hours	**Control**	**EGCG 50 µM**
2	1.41 ± 0.37	1.65 ± 0.47**
4	1.30 ± 0.58	1.53 ± 0.15

Total SMs

Hours	**Control**	**EGCG 50 µM**
2	94.42 ± 10.73	102.48 ± 17.82
4	93.38 ± 10.16	86.92 ± 4.56

Dihydrosphingomyelins (pmol/μg PC)

$C_{16:0}$-dhSM

Hours	**Control**	**EGCG 50 μM**
2	13.42 ± 3.22	12.75 ± 1.58
4	11.70 ± 1.52	10.46 ± 2.02

$C_{18:0}$-dhSM

Hours	**Control**	**EGCG 50 μM**
2	0.38 ± 0.10	0.44 ± 0.10
4	0.34 ± 0.019	0.40 ± 0.044

$C_{20:0}$-dhSM

Hours	**Control**	**EGCG 50 μM**
2	0.32 ± 0.083	0.40 ± 0.11
4	0.28 ± 0.069	0.35 ± 0.031

$C_{22:0}$-dhSM

Hours	**Control**	**EGCG 50 μM**
2	0.84 ± 0.15	1.08 ± 0.22**
4	0.79 ± 0.22	1.08 ± 0.12

$C_{24:0}$-dhSM

Hours	**Control**	**EGCG 50 μM**
2	1.44 ± 0.30	1.62 ± 0.34
4	1.19 ± 0.44	1.65 ± 0.16

$C_{26:0}$-dhSM

Hours	**Control**	**EGCG 50 μM**
2	0.19 ± 0.058	0.22 ± 0.059*
4	0.15 ± 0.071	0.27 ± 0.059

Total dhSMs

Hours	**Control**	**EGCG 50 μM**
2	16.58 ± 3.55	16.51 ± 2.07
4	14.44 ± 0.77	14.21 ± 2.25

4.5 Discussion

We show that various anticancer compounds including representative chemopreventive phytochemicals against cancer (phenolics: curcumin, resveratrol, quercetin, EGCG; organosulfur compound: sulforaphane), ER stress inducers (DTT, thapsigargin), and cancer chemotherapeutic drugs (doxorubicin, camptothecin), all modulated sphingolipid metabolism in human colon HCT-116 cancer cells. Specifically, while the effects of individual compounds on Cer species with specific fatty acid chain lengths were different, all tested compounds increased the levels of dhCers compared with controls. For instance, curcumin increased C_{24}-Cers, but decreased $C_{16:0}$-Cer, and resveratrol and DTT decreased the levels of all different species of Cers. On the other hand, while sulforaphane, quercentin, thapsigargin, doxorubicin and camptothecin increased all Cers, EGCG did not affect on the Cer levels during our tested treatment times. Moreover, we found that curcumin and quercetin significantly inhibited DEGS enzyme activities. Interestingly, these changes of sphingolipid by the tested compounds occurred quickly and took place prior to any manifestation of cell death. These data demonstrated that modulation of sphingolipid metabolism might be a general mechanism for the anticancer effects of chemopreventive compounds against cancer, and inhibition of DEGS enzyme might be the initial primary target of their anticancer actions.

We suggests DEGS in the *de novo* sphingolipid biosynthesis pathway as an initial inhibitory target of various cancer chemopreventive compounds based on the quick increase of intracellular dhCers after treatment of all the tested compounds in human colon HCT-116 cancer cells. DEGS is a key enzyme, which is responsible for addition of

a double bond in dhCer, thus regulating the levels of dhCer as well as Cer in the cell. As well as the elevation of dhCers, various compounds seem to have different effects on the regulation of individual Cer species. Recent studies have shown that individual Cers with specific fatty acid chain lengths have distinct roles in cell proliferation and death (Hannun and Obeid, 2011; Ryland et al., 2011). For instance, $C_{18:0}$-Cer generated by CerS1 has been found to induce apoptosis (Senkal et al., 2010) or lethal autophagy (Sentelle et al., 2012). The roles of $C_{16:0}$-Cer generated by CerS5/6 are still debatable as it has shown anti- or pro-apoptotic properties (Mullen et al., 2011; Schiffmann et al., 2009b; Senkal et al., 2010; White-Gilbertson et al., 2009). In this study, in contrast to dhCer, the effects of various cancer chemopreventive or chemotherapeutic compounds on Cer varied with treatment time and specific Cer species. Therefore, further studies are needed to verify their specific effects on CerS enzymes and the roles of individual Cers in the regulation of cell fate.

Plant-derived phytochemicals were thought to act as only antioxidants to exhibit their chemopreventive effects against cancer. However, interestingly, these compounds have been found to show dual roles as pro-oxidants as well as antioxidants depending on various environmental factors. They can generate reactive oxygen species and cause oxidative stress (Babich et al., 2011; Fujisawa et al., 2004; Galati et al., 2002). Recently, DEGS activity was found to be inhibited by hydrogen peroxide (Idkowiak-Baldys et al., 2010). The mechanism whether the inhibition of DEGS and modulation of sphingolipid metabolism by our tested compounds are caused by their pro-oxidant effects is not understood, which warrants further investigation. In addition, the concentrations of several compounds that we used in this study are not physiological as their low

bioavailability due to rapid metabolism and excretion. Although many studies reported anticancer effects of phytochemicals *in vitro* and *in vivo*, the effects of phytochemicals in humans will need to be assessed in the future studies.

The current results also showed that ER stress inducers, DTT and thapsigargin, modulated sphingolipid metabolism in cancer cells. The ER is an important organelle that plays roles in the folding and maturation of newly synthesized transmembrane and secretory proteins. Disruption of ER function causes an accumulation of unfolded and misfolded proteins in the ER lumen, a condition termed ER stress, which then activates unfolded protein response (UPR) to recover the condition. However, the excessive and unresolvable ER stress induces apoptosis of the cell (Sano and Reed, 2013). DTT is an ER stress inducer as it is a strong reducing compound and blocks disulfide-bond formation. Thapsigargin is another well-known ER stress inducer and it acts as a specific inhibitor of the sarcoplasmic/ER Ca^{2+}-ATPase (SERCA), resulting in a decrease in calcium levels in the ER. The decreased calcium levels in the ER lead to the accumulation of unfolded protein followed by ER stress induction due to the loss of activities of calcium-dependent ER chaperones (Oslowski and Urano, 2011). Since the *de novo* sphingolipid biosynthesis pathway occurs in the ER, we hypothesized that ER stress inducers may interrupt this sphingolipid metabolism. We found that both ER stress inducers, DTT and thapsigargin enhanced dhCers and modulated sphingolipid metabolism. Their mechanism of actions on sphingolipid metabolism is not completely identified yet, but DTT has been shown to strongly inhibit DEGS activity, probably by elevating cellular thiol contents or/and interfering with disulfide bonds in enzyme, leading to impaired protein stability and catalytic activity (Michel et al., 1997).

In summary, we have shown that various compounds with cancer preventive or therapeutic properties all induced accumulation of dhCers and modulation of sphingolipid metabolism in human colon HCT-116 cancer cells. Our results indicate that these compounds initially target DEGS and induce subsequent increase of dhCer species as these responses took place very quickly and prior to any signs of cell death. Although further studies to identify the clear mechanisms and the different effects of chemopreventive compounds on individual CerSs are needed, we have demonstrated that sphingolipid metabolism is the initial primary target of anticancer effects of various compounds.

CHAPTER 5. SUMMARY AND FUTURE DIRECTION

5.1 Effects and Mechanisms of γTE on Sphingolipid Metabolism

Sphingolipids are structural components of cell membranes and play important roles in cellular signal transduction. Using sphingolipidomic approach by LC-MS/MS, we demonstrated that γTE, a vitamin E form abundant in palm oil, modulated sphingolipid metabolism as an initial primary target and led to induction of apoptosis, autophagy and death of cancer cells. Specifically, γTE induced accumulation of intracellular dhCers and dhSph, which are important sphingolipid intermediates in the *de novo* biosynthesis pathway and appear to mediate cell death, but decreased in total Cers during the initial phase. In the study with $^{13}C_3$, ^{15}N-labeled L-serine for tracing newly-synthesized sphingolipids, γTE caused rapid increase of dhCers, but decreases of Cers, suggesting that DEGS-catalyzed reaction is likely inhibited by γTE. Consistently, we found the inhibition of DEGS activity by γTE, but not the expression. In addition, γTE treatment caused increases of endogenous Cer levels with still lower levels of *de novo* Cers during prolonged incubation, suggesting hydrolysis of SM via SMases activation by γTE treatment. Blocking the γTE-induced increases of dhCers/dhSph or Cers from SM by using myriocin (a specific inhibitor of the first enzyme in the *de novo* sphingolipid pathway) or desipramine (an inhibitor of acid SMase), repectively, partially but

significantly reversed the γTE-induced cancer cell death. Overall, our results indicate that γTE modulated enzyme activities in sphingolipid metabolism, specifically by inhibition of DEGS as an initial target and activation of SM hydrolysis, and this modulation of sphingolipid plays an important role in γTE-induced cancer cell death.

We showed that γTE also modulated Cer levels, although the effects of γTE on individual Cers were varied in cancer cells. For instance, γTE treatment led to significant decrease in $C_{16:0}$-Cer during the initial phase, but increase in the longer time treatment. While γTE caused an increase in $C_{18:0}$-Cer, it led to continuous decreases in $C_{24:1}$- and $C_{24:0}$-Cers. Interestingly, emerging results suggest that endogenous Cers with different fatty acyl-chain lengths appear to have distinct bioactivities. $C_{18:0}$-Cer generated by CerS1 has been found to induce apoptosis and lethal autophagy (Senkal et al., 2010; Sentelle et al., 2012). However, the roles of $C_{16:0}$-Cer and C_{24}-Cers in the regulation of cell death are still debatable. $C_{16:0}$-Cer generated by CerS5/6 have been proposed to have antiapoptotic roles (Senkal et al., 2010), but several other studies found that this Cer also plays important roles in apoptotic cell death (Mullen et al., 2011; Schiffmann et al., 2009b; White-Gilbertson et al., 2009). Therefore, further investigation should be conducted to determine the role of individual Cer species and to characterize the effects of γTE on individual CerSs and Cers.

Although our study provided a mechanistic explanation of anticancer activity of γTE, the underlying mechanisms by which γTE modulates sphingolipid metabolism are not completely understood. Since sphingolipid metabolism is a dynamic and complex process, we need to consider many possible aspects that control this process. Specifically,

it remains to be investigated regarding how γTE inhibits DEGS enzyme activity and activates acid SMase. In addition, whether this mechanistic study can be translated in preclinical models also warrants further investigation.

5.2 Anticancer Effects and Mechanisms of 13'-carboxychromanols, Long-chain Metabolites of Vitamin E

Cancer is one of the leading causes of death worldwide. Natural forms of vitamin E are potentially good chemoprevention agents as they are known to be safe and specific forms of vitamin E have been shown to have cancer prevention effects. Among them, αT, which is the predominant vitamin E form in tissues, is the most extensively studied in relation to prevention of cancer. However, the human clinical studies as well as numerous animal studies of αT in cancer prevention resulted in inconsistent and disappointing outcomes. On the other hand, recent mechanistic and preclinical studies using preclinical animal models have demonstrated that other forms of vitamin E appear to have different and stronger biological properties for cancer prevention and therapy compared with αT. Despite these exciting findings, the anticancer effects may not directly be rooted in non-αT form of vitamin E *per se* because most vitamin E forms are readily metabolized *in vivo*. Recently, long-chain carboxychromanols are found at high levels in feces from mice fed diet supplemented with γT or δT, and 13'-carboxychromanols (13'-COOHs) were major fecal excreted carboxychromanols (Bardowell et al., 2012a; Bardowell et al., 2012b; Jiang et al., 2007; Jiang et al., 2013). Interestingly, 13'-COOHs appear to have superior anti-inflammatory properties over their vitamin E precursor by showing dual

inhibitory effects toward COXs and LOX activities (Jiang et al., 2008; Jiang et al., 2011). Since chronic inflammation has been recognized to be an important risk factor in cancer development, 13'-COOHs could be potential cancer preventive agents due to their strong anti-inflammatory properties. Birringer *et al.* recently found that 13'-COOHs metabolized from αT or δT induced apoptosis in human liver cells, but the underlying mechanism was not completely understood (Birringer et al., 2010).

We showed that 13'-COOHs derived from δT or δTE inhibited the growth and induced apoptosis and autophagy in human colon, breast, and pancreatic cancer cells. In these activities, 13'-COOHs were much stronger than natural forms of vitamin E. Using LC-MS/MS method, we found that δT-13'-COOH increased intracellular dhSph and dhCers but decreased $C_{16:0}$-Cer within 2 h treatment. During longer treatment, δT-13'-COOH enhanced all sphingoid bases including Cers while decreased SMs. Modulation of sphingolipids by 13'-COOHs was observed prior to or coinciding with biochemical manifestation of cell death including PARP cleavage and LC3-II increase. The importance of sphingolipid modulation was supported by the observation that pharmaceutically blocking the increase of these sphingolipids partially counteracted 13'-COOH-induced cell death. Further mechanistic studies indicated that 13'-COOH inhibited DEGS without affecting its protein expression and may activate SM hydrolysis to enhance Cers. In agreement with these cell-based studies, δTE-13'-COOH significantly decreased colon tumor multiplicity induced by AOM with two cycles of 1.5% DSS without any apparent toxicity even when the dietary supplementation was started after AOM injection. Our study demonstrates that 13'-COOHs have potent

anticancer effects by modulating enzyme activities in sphingolipid metabolism in cancer cells.

Current study demonstrated that 13'-COOHs have potent anticancer effects in various human cancer cells, even stronger than their unmetabolized vitamin E forms. However, as 13'-COOHs are relatively newly found compounds, studies to investigate the effects and mechanisms of 13'-COOHs are scarce. Therefore, many further studies are needed to understand the properties of these compounds using cell culture studies, animal models and human studies. First of all, although our study provides mechanistic insight into 13'-COOHs-mediated anticancer effects, underlying mechanisms by which 13'-COOHs modulate enzyme activities in sphingolipid metabolism and exert anticancer effects are not completely understood. Moreover, investigation and comparison of the anticancer effects of other 13'-COOHs would be interesting. Second, in our AOM-DSS colon cancer animal study, supplementation of δTE-13'-COOH significantly attenuated DSS-caused colon inflammation and decreased the number of large-sized tumors. To better understand the underlying mechanisms of the anticancer effects of 13'-COOHs, we can analyze other cancer biomarkers such as β-catenin and Ki67 as a proliferation marker as well as inflammatory markers such as PGE_2 and LTB_4 from plasma. Further measurement of the levels of 13'-COOHs in plasma, feces, and other tissues also needed to be conducted. In addition, further researches are needed to investigate bioavailability of 13'-COOHs in animals and humans. Although we know that relative high levels of 13'-COOHs can be found in feces after vitamin E supplementation and we can speculate that 13'-COOHs may exert their anticancer effects when they pass through the colon tissue, the bioavailability information of these metabolites in other tissues is lacking.

Therefore, future studies are needed to investigate their anticancer effects and underlying mechanisms as well as bioavailability in other cancer tissues.

5.3 Phytochemicals as Chemopreventive Agents

Carcinogenesis is generally recognized as a multistep process including tumor initiation, promotion and progression, and cancer cell growth is driven by multiple altered signaling pathways to gain unlimited growth potential. Therefore, blocking only one signaling transduction pathway might not be sufficient to suppress the growth of cancer cells.

Dietary phytochemicals have been used for the prevention as well as treatment of cancer for a long time due to their safety and general availability. Chemopreventive phytochemicals can block or reverse the multistep carcinogenesis by targeting multiple signaling pathways and proteins. Despite their beneficial properties against cancers, the underlying mechanisms are not completely understood. Although many studies have shown the multiple targets of chemopreventive phytochemicals, if we can find the initial primary target of their anticancer effects, it would be more useful information to understand their mechanism.

We demonstrate that various representative phytochemicals including curcumin, resveratrol, EGCG, quercetin and sulforaphane show anticancer effects by modulation of sphingolipid metabolism using LC-MS/MS technology. Specifically, while the effects of individual compounds on different Cer species with distinct chain-length of fatty acyl-CoA were different, all the tested compounds increased the levels of dhCers compared

with controls. Interestingly, these changes of sphingolipids by the tested phytochemicals occurred quickly and took place prior to any signs of cell death. These data demonstrated that modulation of sphingolipid metabolism might be a general mechanism for the anticancer effects of various chemopreventive compounds against cancer, and inhibition of DEGS enzyme might be the initial primary target of their anticancer actions.

Although several phytochemicals have been extensively studied and have exhibited potent anticancer activities through alteration of various mechanisms, and our study demonstrates the modulation of sphingolipid metabolism as an initial and primary target for anticancer activity of them, there are still a number of key weaknesses and further researches to be conducted. First weakness of the current researches of phytochemicals is that most studies have been conducted *in vitro* and little is known about the bioavailability of the compounds. Although numerous cell-culture studies have evaluated and defined the anticancer effects and mechanisms of several phytochemicals, most *in vitro* studies used supraphysiological concentrations, which might not be achievable when the phytochemicals are administered as a diet. In addition, phytochemicals generally show very low bioavailability as the small proportion of these compounds is absorbed and it further has extensive metabolism before going to target organs. Moreover, their bioavailability might become further lower as they are present as glycosides or converted to other conjugated forms after absorption. Finally, although many reports have suggested health benefits and molecular targets of dietary phytochemicals in cell culture and animal models, the effects of phytochemicals in humans will need to be assessed. In order to apply phytochemicals as cancer preventive

agents in humans, further investigations of pharmacokinetics and bioavailability, and the anticancer effects and mechanisms of the compounds should be conducted carefully.

5.4 Dietary Vitamin E in Colon Cancer Prevention

Colon cancer is one of the leading causes of cancer-related deaths in the US (Siegel et al., 2015). Because advanced colon cancer is a devastating disease for patients, intervening before the development of tumor can prevent cancer-associated deaths. Early detection of dysplasia and prevention of colon cancer progression in high-risk population as secondary prevention, which is the treatment for patients who already have developed risk factors or disease, will be a key strategy to reduce its incidence. Given that chronic inflammation has been directly associated with the malignant transformation and development of colon cancer, patients with long-standing inflammatory bowel disease (IBD), which can be divided into two major disorders such as ulcerative colitis and Chrohn's disease, have an increased risk of developing colon cancer and have been known to be a high-risk population for colon cancer. Although IBD-associated colon cancer accounts for only about 1~2% of all cases of colon cancer, patients with IBD are six times more likely to develop colon cancer than the general population (Lennard-Jones et al., 1983). Thus, secondary prevention must be considered in this population to prevent the risk.

The ideal chemopreventive agent would be safe, inexpensive, and effective. In this regard, natural forms of vitamin E are considered as potentially promising chemopreventive agents. Recent studies by others and us have shown that vitamin E

forms such as γT and γTE, and δT-13'-COOH, a long-chain metabolite of δT exert anti-inflammatory activities (Jiang, 2014; Jiang et al., 2000; Wang and Jiang, 2013; Wang et al., 2015). In addition, results from previous studies in our lab and this study have demonstrated that supplementation of vitamin E forms (Jiang et al., 2013) or its long-chain metabolite results in a significant reduction of carcinogen-induced colon tumor incidence or the fecal scores in AOM-DSS colon cancer model and DSS colitis model in mice, respectively, suggesting that vitamin E may play important roles in preventing colon tumorigenesis.

Although the doses of vitamin E used in the current study had no adverse effects in mice, more researches are needed to translate the dose of vitamin E and the timing to begin vitamin E supplementation in animal studies into clinical trials in humans. Overall, our data from the *in vivo* studies as well as *in vitro* studies support that dietary vitamin E reduces the risk of colon tumorigenesis and may contribute to the establishment of dietary recommendation for vitamin E to prevent colon cancer.

LIST OF REFERENCES

LIST OF REFERENCES

Abdel Shakor, A.B., M. Atia, I.A. Ismail, A. Alshehri, H. El-Refaey, K. Kwiatkowska, and A. Sobota. 2014. Curcumin induces apoptosis of multidrug-resistant human leukemia HL60 cells by complex pathways leading to ceramide accumulation. *Biochim Biophys Acta*. 1841:1672-1682.

Agarwal, B., and J.A. Baur. 2011. Resveratrol and life extension. *Ann N Y Acad Sci*. 1215:138-143.

Ahmad, N., D.K. Feyes, A.L. Nieminen, R. Agarwal, and H. Mukhtar. 1997. Green tea constituent epigallocatechin-3-gallate and induction of apoptosis and cell cycle arrest in human carcinoma cells. *J Natl Cancer Inst*. 89:1881-1886.

Ahn, E.H., and J.J. Schroeder. 2002. Sphingoid bases and ceramide induce apoptosis in HT-29 and HCT-116 human colon cancer cells. *Exp Biol Med (Maywood)*. 227:345-353.

Amtmann, E. 1996. The antiviral, antitumoural xanthate D609 is a competitive inhibitor of phosphatidylcholine-specific phospholipase C. *Drugs Exp Clin Res*. 22:287-294.

Babich, H., N.J. Ackerman, F. Burekhovich, H.L. Zuckerbraun, and A.G. Schuck. 2009. Gingko biloba leaf extract induces oxidative stress in carcinoma HSC-2 cells. *In* Toxicol In Vitro. Vol. 23, England. 992-999.

Babich, H., A.G. Schuck, J.H. Weisburg, and H.L. Zuckerbraun. 2011. Research strategies in the study of the pro-oxidant nature of polyphenol nutraceuticals. *J Toxicol*. 2011:467305.

Balkwill, F., and A. Mantovani. 2001. Inflammation and cancer: back to Virchow? *Lancet*. 357:539-545.

Bardowell, S.A., X. Ding, and R.S. Parker. 2012a. Disruption of P450-mediated vitamin E hydroxylase activities alters vitamin E status in tocopherol supplemented mice and reveals extra-hepatic vitamin E metabolism. *J Lipid Res*. 53:2667-2676.

Bardowell, S.A., F. Duan, D. Manor, J.E. Swanson, and R.S. Parker. 2012b. Disruption of mouse cytochrome p450 4f14 (Cyp4f14 gene) causes severe perturbations in vitamin E metabolism. *J Biol Chem*. 287:26077-26086.

Behrens, W.A., and R. Madere. 1986. Alpha- and gamma tocopherol concentrations in human serum. *J Am Coll Nutr*. 5:91-96.

Bharti, A.C., N. Donato, S. Singh, and B.B. Aggarwal. 2003. Curcumin (diferuloylmethane) down-regulates the constitutive activation of nuclear factor-kappa B and IkappaBalpha kinase in human multiple myeloma cells, leading to suppression of proliferation and induction of apoptosis. *Blood*. 101:1053-1062.

Bielawska, A., H.M. Crane, D. Liotta, L.M. Obeid, and Y.A. Hannun. 1993. Selectivity of ceramide-mediated biology. Lack of activity of erythro-dihydroceramide. *J Biol Chem*. 268:26226-26232.

Bieri, J.G., and R.P. Evarts. 1974. Vitamin E activity of gamma-tocopherol in the rat, chick and hamster. *J Nutr*. 104:850-857.

Birringer, M., D. Lington, S. Vertuani, S. Manfredini, D. Scharlau, M. Glei, and M. Ristow. 2010. Proapoptotic effects of long-chain vitamin E metabolites in HepG2 cells are mediated by oxidative stress. *Free Radic Biol Med*. 49:1315-1322.

Bishayee, A. 2009. Cancer prevention and treatment with resveratrol: from rodent studies to clinical trials. *Cancer Prev Res (Phila)*. 2:409-418.

Block, G., B. Patterson, and A. Subar. 1992. Fruit, vegetables, and cancer prevention: a review of the epidemiological evidence. *Nutr Cancer*. 18:1-29.

Blot, W.J., J.Y. Li, P.R. Taylor, W. Guo, S. Dawsey, G.Q. Wang, C.S. Yang, S.F. Zheng, M. Gail, G.Y. Li, and et al. 1993. Nutrition intervention trials in Linxian, China: supplementation with specific vitamin/mineral combinations, cancer incidence, and disease-specific mortality in the general population. *J Natl Cancer Inst*. 85:1483-1492.

Bode, A.M., and Z. Dong. 2009. Cancer prevention research - then and now. *Nat Rev Cancer*. 9:508-516.

Brigelius-Flohe, R., and M.G. Traber. 1999. Vitamin E: function and metabolism. *Faseb j*. 13:1145-1155.

Britton, G. 1995. Structure and properties of carotenoids in relation to function. *Faseb j*. 9:1551-1558.

Burton, G.W., M.G. Traber, R.V. Acuff, D.N. Walters, H. Kayden, L. Hughes, and K.U. Ingold. 1998. Human plasma and tissue alpha-tocopherol concentrations in response to supplementation with deuterated natural and synthetic vitamin E. *Am J Clin Nutr*. 67:669-684.

Campbell, S.E., W.L. Stone, S. Lee, S. Whaley, H. Yang, M. Qui, P. Goforth, D. Sherman, D. McHaffie, and K. Krishnan. 2006. Comparative effects of RRR-alpha- and RRR-gamma-tocopherol on proliferation and apoptosis in human colon cancer cell lines. *BMC Cancer*. 6:13.

Catarzi, S., E. Giannoni, F. Favilli, E. Meacci, T. Iantomasi, and M.T. Vincenzini. 2007. Sphingosine 1-phosphate stimulation of NADPH oxidase activity: relationship with platelet-derived growth factor receptor and c-Src kinase. *Biochim Biophys Acta*. 1770:872-883.

Chatelain, E., D.O. Boscoboinik, G.M. Bartoli, V.E. Kagan, F.K. Gey, L. Packer, and A. Azzi. 1993. Inhibition of smooth muscle cell proliferation and protein kinase C activity by tocopherols and tocotrienols. *Biochim Biophys Acta*. 1176:83-89.

Chen, C., R. Yu, E.D. Owuor, and A.N. Kong. 2000. Activation of antioxidant-response element (ARE), mitogen-activated protein kinases (MAPKs) and caspases by major green tea polyphenol components during cell survival and death. *Arch Pharm Res*. 23:605-612.

Clarke, J.D., R.H. Dashwood, and E. Ho. 2008. Multi-targeted prevention of cancer by sulforaphane. *Cancer Lett*. 269:291-304.

Clement, M., and J.M. Bourre. 1997. Graded dietary levels of RRR-gamma-tocopherol induce a marked increase in the concentrations of alpha- and gamma-tocopherol in nervous tissues, heart, liver and muscle of vitamin-E-deficient rats. *Biochim Biophys Acta*. 1334:173-181.

Cooney, R.V., A.A. Franke, P.J. Harwood, V. Hatch-Pigott, L.J. Custer, and L.J. Mordan. 1993. Gamma-tocopherol detoxification of nitrogen dioxide: superiority to alpha-tocopherol. *Proc Natl Acad Sci U S A*. 90:1771-1775.

Coward, J., G. Ambrosini, E. Musi, J.P. Truman, A. Haimovitz-Friedman, J.C. Allegood, E. Wang, A.H. Merrill, Jr., and G.K. Schwartz. 2009. Safingol (L-threo-sphinganine) induces autophagy in solid tumor cells through inhibition of PKC and the PI3-kinase pathway. *Autophagy*. 5:184-193.

Cuvillier, O. 2002. Sphingosine in apoptosis signaling. *Biochim Biophys Acta*. 1585:153-162.

D'Angelo, G., E. Polishchuk, G. Di Tullio, M. Santoro, A. Di Campli, A. Godi, G. West, J. Bielawski, C.C. Chuang, A.C. van der Spoel, F.M. Platt, Y.A. Hannun, R. Polishchuk, P. Mattjus, and M.A. De Matteis. 2007. Glycosphingolipid synthesis requires FAPP2 transfer of glucosylceramide. *Nature*. 449:62-67.

Das, R., G.H. Mahabeleshwar, and G.C. Kundu. 2003. Osteopontin stimulates cell motility and nuclear factor kappaB-mediated secretion of urokinase type plasminogen activator through phosphatidylinositol 3-kinase/Akt signaling pathways in breast cancer cells. *J Biol Chem*. 278:28593-28606.

Dashwood, W.M., G.A. Orner, and R.H. Dashwood. 2002. Inhibition of beta-catenin/Tcf activity by white tea, green tea, and epigallocatechin-3-gallate (EGCG): minor contribution of H(2)O(2) at physiologically relevant EGCG concentrations. *Biochem Biophys Res Commun*. 296:584-588.

Devlin, C.M., T. Lahm, W.C. Hubbard, M. Van Demark, K.C. Wang, X. Wu, A. Bielawska, L.M. Obeid, M. Ivan, and I. Petrache. 2011. Dihydroceramide-based response to hypoxia. *J Biol Chem*. 286:38069-38078.

Erdreich-Epstein, A., L.B. Tran, N.N. Bowman, H. Wang, M.C. Cabot, D.L. Durden, J. Vlckova, C.P. Reynolds, M.F. Stins, S. Groshen, and M. Millard. 2002. Ceramide signaling in fenretinide-induced endothelial cell apoptosis. *J Biol Chem*. 277:49531-49537.

Evans, H.M., and K.S. Bishop. 1922. ON THE EXISTENCE OF A HITHERTO UNRECOGNIZED DIETARY FACTOR ESSENTIAL FOR REPRODUCTION. *Science*. 56:650-651.

Freiser, H., and Q. Jiang. 2009. Gamma-tocotrienol and gamma-tocopherol are primarily metabolized to conjugated 2-(beta-carboxyethyl)-6-hydroxy-2,7,8-trimethylchroman and sulfated long-chain carboxychromanols in rats. *J Nutr*. 139:884-889.

Fujisawa, S., T. Atsumi, M. Ishihara, and Y. Kadoma. 2004. Cytotoxicity, ROS-generation activity and radical-scavenging activity of curcumin and related compounds. *Anticancer Res*. 24:563-569.

Gable, K., H. Slife, D. Bacikova, E. Monaghan, and T.M. Dunn. 2000. Tsc3p is an 80-amino acid protein associated with serine palmitoyltransferase and required for optimal enzyme activity. *J Biol Chem*. 275:7597-7603.

Galati, G., O. Sabzevari, J.X. Wilson, and P.J. O'Brien. 2002. Prooxidant activity and cellular effects of the phenoxyl radicals of dietary flavonoids and other polyphenolics. *Toxicology*. 177:91-104.

Gault, C.R., L.M. Obeid, and Y.A. Hannun. 2010. An overview of sphingolipid metabolism: from synthesis to breakdown. *Adv Exp Med Biol*. 688:1-23.

Gaziano, J.M., R.J. Glynn, W.G. Christen, T. Kurth, C. Belanger, J. MacFadyen, V. Bubes, J.E. Manson, H.D. Sesso, and J.E. Buring. 2009. Vitamins E and C in the prevention of prostate and total cancer in men: the Physicians' Health Study II randomized controlled trial. *Jama*. 301:52-62.

Goldkorn, T., K.A. Dressler, J. Muindi, N.S. Radin, J. Mendelsohn, D. Menaldino, D. Liotta, and R.N. Kolesnick. 1991. Ceramide stimulates epidermal growth factor receptor phosphorylation in A431 human epidermoid carcinoma cells. Evidence that ceramide may mediate sphingosine action. *J Biol Chem*. 266:16092-16097.

Gong, L., Y. Li, A. Nedeljkovic-Kurepa, and F.H. Sarkar. 2003. Inactivation of NF-kappaB by genistein is mediated via Akt signaling pathway in breast cancer cells. *Oncogene*. 22:4702-4709.

Gonzalez-Vallinas, M., M. Gonzalez-Castejon, A. Rodriguez-Casado, and A. Ramirez de Molina. 2013. Dietary phytochemicals in cancer prevention and therapy: a complementary approach with promising perspectives. *Nutr Rev*. 71:585-599.

Gopalan, A., W. Yu, Q. Jiang, Y. Jang, B.G. Sanders, and K. Kline. 2012. Involvement of de novo ceramide synthesis in gamma-tocopherol and gamma-tocotrienol-induced apoptosis in human breast cancer cells. *Mol Nutr Food Res*. 56:1803-1811.

Guan, F., G. Li, A.B. Liu, M.J. Lee, Z. Yang, Y.K. Chen, Y. Lin, W. Shih, and C.S. Yang. 2012. delta- and gamma-tocopherols, but not alpha-tocopherol, inhibit colon carcinogenesis in azoxymethane-treated F344 rats. *Cancer Prev Res (Phila)*. 5:644-654.

Guthrie, N., A. Gapor, A.F. Chambers, and K.K. Carroll. 1997. Inhibition of proliferation of estrogen receptor-negative MDA-MB-435 and -positive MCF-7 human breast cancer cells by palm oil tocotrienols and tamoxifen, alone and in combination. *J Nutr*. 127:544s-548s.

Hanada, K. 2003. Serine palmitoyltransferase, a key enzyme of sphingolipid metabolism. *Biochim Biophys Acta*. 1632:16-30.

Hanada, K., K. Kumagai, S. Yasuda, Y. Miura, M. Kawano, M. Fukasawa, and M. Nishijima. 2003. Molecular machinery for non-vesicular trafficking of ceramide. *Nature*. 426:803-809.

Handelman, G.J., L.J. Machlin, K. Fitch, J.J. Weiter, and E.A. Dratz. 1985. Oral alpha-tocopherol supplements decrease plasma gamma-tocopherol levels in humans. *J Nutr*. 115:807-813.

Hannun, Y.A., C.R. Loomis, A.H. Merrill, Jr., and R.M. Bell. 1986. Sphingosine inhibition of protein kinase C activity and of phorbol dibutyrate binding in vitro and in human platelets. *J Biol Chem*. 261:12604-12609.

Hannun, Y.A., and L.M. Obeid. 2008. Principles of bioactive lipid signalling: lessons from sphingolipids. *Nat Rev Mol Cell Biol*. 9:139-150.

Hannun, Y.A., and L.M. Obeid. 2011. Many ceramides. *J Biol Chem*. 286:27855-27862.

Hayes, J.D., and M. McMahon. 2001. Molecular basis for the contribution of the antioxidant responsive element to cancer chemoprevention. *Cancer Lett*. 174:103-113.

Heart, P.g. 2002. MRC/BHF Heart Protection Study of antioxidant vitamin supplementation in 20,536 high-risk individuals: a randomised placebo-controlled trial. *Lancet*. 360:23-33.

Heinonen, O.P., D. Albanes, J. Virtamo, P.R. Taylor, J.K. Huttunen, A.M. Hartman, J. Haapakoski, N. Malila, M. Rautalahti, S. Ripatti, H. Maenpaa, L. Teerenhovi, L. Koss, M. Virolainen, and B.K. Edwards. 1998. Prostate cancer and supplementation with alpha-tocopherol and beta-carotene: incidence and mortality in a controlled trial. *J Natl Cancer Inst*. 90:440-446.

Helzlsouer, K.J., H.Y. Huang, A.J. Alberg, S. Hoffman, A. Burke, E.P. Norkus, J.S. Morris, and G.W. Comstock. 2000. Association between alpha-tocopherol, gamma-tocopherol, selenium, and subsequent prostate cancer. *J Natl Cancer Inst*. 92:2018-2023.

Henry, B., R. Ziobro, K.A. Becker, R. Kolesnick, and E. Gulbins. 2013. Acid sphingomyelinase. *Handb Exp Pharmacol*:77-88.

Heo, K., K.A. Park, Y.H. Kim, S.H. Kim, Y.S. Oh, I.H. Kim, S.H. Ryu, and P.G. Suh. 2009. Sphingosine 1-phosphate induces vascular endothelial growth factor expression in endothelial cells. *BMB Rep*. 42:685-690.

Hercberg, S., P. Galan, P. Preziosi, S. Bertrais, L. Mennen, D. Malvy, A.M. Roussel, A. Favier, and S. Briancon. 2004. The SU.VI.MAX Study: a randomized, placebo-controlled trial of the health effects of antioxidant vitamins and minerals. *Arch Intern Med*. 164:2335-2342.

Hiura, Y., H. Tachibana, R. Arakawa, N. Aoyama, M. Okabe, M. Sakai, and K. Yamada. 2009. Specific accumulation of gamma- and delta-tocotrienols in tumor and their antitumor effect in vivo. *J Nutr Biochem*. 20:607-613.

Holmes-McNary, M., and A.S. Baldwin, Jr. 2000. Chemopreventive properties of trans-resveratrol are associated with inhibition of activation of the IkappaB kinase. *Cancer Res*. 60:3477-3483.

Huang, H.C., T. Nguyen, and C.B. Pickett. 2002. Phosphorylation of Nrf2 at Ser-40 by protein kinase C regulates antioxidant response element-mediated transcription. *J Biol Chem*. 277:42769-42774.

Huitema, K., J. van den Dikkenberg, J.F. Brouwers, and J.C. Holthuis. 2004. Identification of a family of animal sphingomyelin synthases. *Embo j*. 23:33-44.

Idkowiak-Baldys, J., A. Apraiz, L. Li, M. Rahmaniyan, C.J. Clarke, J.M. Kraveka, A. Asumendi, and Y.A. Hannun. 2010. Dihydroceramide desaturase activity is modulated by oxidative stress. *Biochem J*. 427:265-274.

Itoh, K., N. Wakabayashi, Y. Katoh, T. Ishii, K. Igarashi, J.D. Engel, and M. Yamamoto. 1999. Keap1 represses nuclear activation of antioxidant responsive elements by Nrf2 through binding to the amino-terminal Neh2 domain. *Genes Dev*. 13:76-86.

Jarvis, W.D., F.A. Fornari, R.S. Traylor, H.A. Martin, L.B. Kramer, R.K. Erukulla, R. Bittman, and S. Grant. 1996. Induction of apoptosis and potentiation of ceramide-mediated cytotoxicity by sphingoid bases in human myeloid leukemia cells. *J Biol Chem*. 271:8275-8284.

Jayadev, S., B. Liu, A.E. Bielawska, J.Y. Lee, F. Nazaire, M. Pushkareva, L.M. Obeid, and Y.A. Hannun. 1995. Role for ceramide in cell cycle arrest. *J Biol Chem*. 270:2047-2052.

Jemal, A., F. Bray, M.M. Center, J. Ferlay, E. Ward, and D. Forman. 2011. Global cancer statistics. *In* CA Cancer J Clin. Vol. 61, United States. 69-90.

Jiang, Q. 2014. Natural forms of vitamin E: metabolism, antioxidant, and anti-inflammatory activities and their role in disease prevention and therapy. *Free Radic Biol Med*. 72:76-90.

Jiang, Q., and B.N. Ames. 2003. Gamma-tocopherol, but not alpha-tocopherol, decreases proinflammatory eicosanoids and inflammation damage in rats. *Faseb j*. 17:816-822.

Jiang, Q., S. Christen, M.K. Shigenaga, and B.N. Ames. 2001. gamma-tocopherol, the major form of vitamin E in the US diet, deserves more attention. *Am J Clin Nutr*. 74:714-722.

Jiang, Q., I. Elson-Schwab, C. Courtemanche, and B.N. Ames. 2000. gamma-tocopherol and its major metabolite, in contrast to alpha-tocopherol, inhibit cyclooxygenase activity in macrophages and epithelial cells. *Proc Natl Acad Sci U S A*. 97:11494-11499.

Jiang, Q., H. Freiser, K.V. Wood, and X. Yin. 2007. Identification and quantitation of novel vitamin E metabolites, sulfated long-chain carboxychromanols, in human A549 cells and in rats. *J Lipid Res*. 48:1221-1230.

Jiang, Q., Z. Jiang, Y.J. Hall, Y. Jang, P.W. Snyder, C. Bain, J. Huang, A. Jannasch, B. Cooper, Y. Wang, and M. Moreland. 2013. Gamma-tocopherol attenuates moderate but not severe colitis and suppresses moderate colitis-promoted colon tumorigenesis in mice. *Free Radic Biol Med*. 65:1069-1077.

Jiang, Q., X. Rao, C.Y. Kim, H. Freiser, Q. Zhang, Z. Jiang, and G. Li. 2012. Gamma-tocotrienol induces apoptosis and autophagy in prostate cancer cells by increasing intracellular dihydrosphingosine and dihydroceramide. *International journal of cancer. Journal international du cancer*. 130:685-693.

Jiang, Q., J. Wong, H. Fyrst, J.D. Saba, and B.N. Ames. 2004. gamma-Tocopherol or combinations of vitamin E forms induce cell death in human prostate cancer cells by interrupting sphingolipid synthesis. *Proc Natl Acad Sci U S A*. 101:17825-17830.

Jiang, Q., X. Yin, M.A. Lill, M.L. Danielson, H. Freiser, and J. Huang. 2008. Long-chain carboxychromanols, metabolites of vitamin E, are potent inhibitors of cyclooxygenases. *Proc Natl Acad Sci U S A*. 105:20464-20469.

Jiang, Z., X. Yin, and Q. Jiang. 2011. Natural forms of vitamin E and 13'-carboxychromanol, a long-chain vitamin E metabolite, inhibit leukotriene generation from stimulated neutrophils by blocking calcium influx and suppressing 5-lipoxygenase activity, respectively. *J Immunol*. 186:1173-1179.

Joe, A.K., H. Liu, M. Suzui, M.E. Vural, D. Xiao, and I.B. Weinstein. 2002. Resveratrol induces growth inhibition, S-phase arrest, apoptosis, and changes in biomarker expression in several human cancer cell lines. *Clin Cancer Res*. 8:893-903.

Johnson, I.T. 2007. Phytochemicals and cancer. *Proc Nutr Soc*. 66:207-215.

Ju, J., X. Hao, M.J. Lee, J.D. Lambert, G. Lu, H. Xiao, H.L. Newmark, and C.S. Yang. 2009. A gamma-tocopherol-rich mixture of tocopherols inhibits colon inflammation and carcinogenesis in azoxymethane and dextran sulfate sodium-treated mice. *In* Cancer Prev Res (Phila). Vol. 2, United States. 143-152.

Kamal-Eldin, A., and L.A. Appelqvist. 1996. The chemistry and antioxidant properties of tocopherols and tocotrienols. *Lipids*. 31:671-701.

Karahatay, S., K. Thomas, S. Koybasi, C.E. Senkal, S. Elojeimy, X. Liu, J. Bielawski, T.A. Day, M.B. Gillespie, D. Sinha, J.S. Norris, Y.A. Hannun, and B. Ogretmen. 2007. Clinical relevance of ceramide metabolism in the pathogenesis of human head and neck squamous cell carcinoma (HNSCC): attenuation of C(18)-ceramide in HNSCC tumors correlates with lymphovascular invasion and nodal metastasis. *Cancer Lett*. 256:101-111.

Khan, N., F. Afaq, M. Saleem, N. Ahmad, and H. Mukhtar. 2006. Targeting multiple signaling pathways by green tea polyphenol (-)-epigallocatechin-3-gallate. *Cancer Res*. 66:2500-2505.

Kitatani, K., J. Idkowiak-Baldys, and Y.A. Hannun. 2008. The sphingolipid salvage pathway in ceramide metabolism and signaling. *Cell Signal*. 20:1010-1018.

Kitatani, K., K. Sheldon, V. Anelli, R.W. Jenkins, Y. Sun, G.A. Grabowski, L.M. Obeid, and Y.A. Hannun. 2009. Acid beta-glucosidase 1 counteracts p38delta-dependent induction of interleukin-6: possible role for ceramide as an anti-inflammatory lipid. *J Biol Chem*. 284:12979-12988.

Kolesnick, R. 2002. The therapeutic potential of modulating the ceramide/sphingomyelin pathway. *J Clin Invest*. 110:3-8.

Koybasi, S., C.E. Senkal, K. Sundararaj, S. Spassieva, J. Bielawski, W. Osta, T.A. Day, J.C. Jiang, S.M. Jazwinski, Y.A. Hannun, L.M. Obeid, and B. Ogretmen. 2004. Defects in cell growth regulation by C18:0-ceramide and longevity assurance gene 1 in human head and neck squamous cell carcinomas. *J Biol Chem*. 279:44311-44319.

Kraveka, J.M., L. Li, Z.M. Szulc, J. Bielawski, B. Ogretmen, Y.A. Hannun, L.M. Obeid, and A. Bielawska. 2007. Involvement of dihydroceramide desaturase in cell cycle progression in human neuroblastoma cells. *J Biol Chem*. 282:16718-16728.

Kroesen, B.J., B. Pettus, C. Luberto, M. Busman, H. Sietsma, L. de Leij, and Y.A. Hannun. 2001. Induction of apoptosis through B-cell receptor cross-linking occurs via de novo generated C16-ceramide and involves mitochondria. *J Biol Chem*. 276:13606-13614.

Kumar, K.S., M. Raghavan, K. Hieber, C. Ege, S. Mog, N. Parra, A. Hildabrand, V. Singh, V. Srinivasan, R. Toles, P. Karikari, G. Petrovics, T. Seed, S. Srivastava, and A. Papas. 2006. Preferential radiation sensitization of prostate cancer in nude mice by nutraceutical antioxidant gamma-tocotrienol. *Life Sci*. 78:2099-2104.

Kunnumakkara, A.B., B. Sung, J. Ravindran, P. Diagaradjane, A. Deorukhkar, S. Dey, C. Koca, V.R. Yadav, Z. Tong, J.G. Gelovani, S. Guha, S. Krishnan, and B.B. Aggarwal. 2010. {Gamma}-tocotrienol inhibits pancreatic tumors and sensitizes them to gemcitabine treatment by modulating the inflammatory microenvironment. *Cancer Res*. 70:8695-8705.

Laviad, E.L., L. Albee, I. Pankova-Kholmyansky, S. Epstein, H. Park, A.H. Merrill, Jr., and A.H. Futerman. 2008. Characterization of ceramide synthase 2: tissue distribution, substrate specificity, and inhibition by sphingosine 1-phosphate. *J Biol Chem*. 283:5677-5684.

Lee, H.J., J. Ju, S. Paul, J.Y. So, A. DeCastro, A. Smolarek, M.J. Lee, C.S. Yang, H.L. Newmark, and N. Suh. 2009. Mixed tocopherols prevent mammary tumorigenesis by inhibiting estrogen action and activating PPAR-gamma. *Clin Cancer Res*. 15:4242-4249.

Lee, I.M., N.R. Cook, J.M. Gaziano, D. Gordon, P.M. Ridker, J.E. Manson, C.H. Hennekens, and J.E. Buring. 2005. Vitamin E in the primary prevention of cardiovascular disease and cancer: the Women's Health Study: a randomized controlled trial. *Jama*. 294:56-65.

Lee, K.W., A.M. Bode, and Z. Dong. 2011. Molecular targets of phytochemicals for cancer prevention. *Nat Rev Cancer*. 11:211-218.

Lennard-Jones, J.E., B.C. Morson, J.K. Ritchie, and C.B. Williams. 1983. Cancer surveillance in ulcerative colitis. Experience over 15 years. *Lancet*. 2:149-152.

Li, Q., and I.M. Verma. 2002. NF-kappaB regulation in the immune system. *Nat Rev Immunol*. 2:725-734.

Li, Y., and F.H. Sarkar. 2002. Inhibition of nuclear factor kappaB activation in PC3 cells by genistein is mediated via Akt signaling pathway. *Clin Cancer Res*. 8:2369-2377.

Libby, P., P.M. Ridker, and A. Maseri. 2002. Inflammation and atherosclerosis. *Circulation*. 105:1135-1143.

Lippman, S.M., E.A. Klein, P.J. Goodman, M.S. Lucia, I.M. Thompson, L.G. Ford, H.L. Parnes, L.M. Minasian, J.M. Gaziano, J.A. Hartline, J.K. Parsons, J.D. Bearden, 3rd, E.D. Crawford, G.E. Goodman, J. Claudio, E. Winquist, E.D. Cook, D.D. Karp, P. Walther, M.M. Lieber, A.R. Kristal, A.K. Darke, K.B. Arnold, P.A. Ganz, R.M. Santella, D. Albanes, P.R. Taylor, J.L. Probstfield, T.J. Jagpal, J.J. Crowley, F.L. Meyskens, Jr., L.H. Baker, and C.A. Coltman, Jr. 2009. Effect of selenium and vitamin E on risk of prostate cancer and other cancers: the Selenium and Vitamin E Cancer Prevention Trial (SELECT). *Jama*. 301:39-51.

Liu, R.H. 2004. Potential synergy of phytochemicals in cancer prevention: mechanism of action. *J Nutr*. 134:3479s-3485s.

Loganathan, R., K.R. Selvaduray, K. Nesaretnam, and A.K. Radhakrishnan. 2013. Tocotrienols promote apoptosis in human breast cancer cells by inducing poly(ADP-ribose) polymerase cleavage and inhibiting nuclear factor kappa-B activity. *Cell Prolif*. 46:203-213.

Lonn, E., J. Bosch, S. Yusuf, P. Sheridan, J. Pogue, J.M. Arnold, C. Ross, A. Arnold, P. Sleight, J. Probstfield, and G.R. Dagenais. 2005. Effects of long-term vitamin E supplementation on cardiovascular events and cancer: a randomized controlled trial. *Jama*. 293:1338-1347.

Luberto, C., D.F. Hassler, P. Signorelli, Y. Okamoto, H. Sawai, E. Boros, D.J. Hazen-Martin, L.M. Obeid, Y.A. Hannun, and G.K. Smith. 2002. Inhibition of tumor necrosis factor-induced cell death in MCF7 by a novel inhibitor of neutral sphingomyelinase. *J Biol Chem*. 277:41128-41139.

MacDonald, B.T., K. Tamai, and X. He. 2009. Wnt/beta-catenin signaling: components, mechanisms, and diseases. *Dev Cell*. 17:9-26.

Mahmoud, N.N., A.M. Carothers, D. Grunberger, R.T. Bilinski, M.R. Churchill, C. Martucci, H.L. Newmark, and M.M. Bertagnolli. 2000. Plant phenolics decrease intestinal tumors in an animal model of familial adenomatous polyposis. *Carcinogenesis*. 21:921-927.

Maiani, G., M.J. Caston, G. Catasta, E. Toti, I.G. Cambrodon, A. Bysted, F. Granado-Lorencio, B. Olmedilla-Alonso, P. Knuthsen, M. Valoti, V. Bohm, E. Mayer-Miebach, D. Behsnilian, and U. Schlemmer. 2009. Carotenoids: actual knowledge on food sources, intakes, stability and bioavailability and their protective role in humans. *Mol Nutr Food Res*. 53 Suppl 2:S194-218.

Maloney, D.J., and S.M. Hecht. 2005. A stereocontrolled synthesis of delta-trans-tocotrienoloic acid. *Organic letters*. 7:4297-4300.

Manor, D., and S. Morley. 2007. The alpha-tocopherol transfer protein. *Vitam Horm*. 76:45-65.

Marchesini, N., and Y.A. Hannun. 2004. Acid and neutral sphingomyelinases: roles and mechanisms of regulation. *Biochem Cell Biol*. 82:27-44.

McLaughlin, P.J., and J.L. Weihrauch. 1979. Vitamin E content of foods. *J Am Diet Assoc*. 75:647-665.

Merrill, A.H., Jr. 2002. De novo sphingolipid biosynthesis: a necessary, but dangerous, pathway. *J Biol Chem*. 277:25843-25846.

Merrill, A.H., Jr., A.M. Sereni, V.L. Stevens, Y.A. Hannun, R.M. Bell, and J.M. Kinkade, Jr. 1986. Inhibition of phorbol ester-dependent differentiation of human promyelocytic leukemic (HL-60) cells by sphinganine and other long-chain bases. *J Biol Chem*. 261:12610-12615.

Merrill, A.H., Jr., M.C. Sullards, J.C. Allegood, S. Kelly, and E. Wang. 2005. Sphingolipidomics: high-throughput, structure-specific, and quantitative analysis of sphingolipids by liquid chromatography tandem mass spectrometry. *Methods*. 36:207-224.

Merrill, A.H., Jr., M.C. Sullards, E. Wang, K.A. Voss, and R.T. Riley. 2001. Sphingolipid metabolism: roles in signal transduction and disruption by fumonisins. *Environ Health Perspect*. 109 Suppl 2:283-289.

Michel, C., G. van Echten-Deckert, J. Rother, K. Sandhoff, E. Wang, and A.H. Merrill, Jr. 1997. Characterization of ceramide synthesis. A dihydroceramide desaturase introduces the 4,5-trans-double bond of sphingosine at the level of dihydroceramide. *J Biol Chem*. 272:22432-22437.

Mizutani, Y., A. Kihara, and Y. Igarashi. 2006. LASS3 (longevity assurance homologue 3) is a mainly testis-specific (dihydro)ceramide synthase with relatively broad substrate specificity. *Biochem J*. 398:531-538.

Moriarty, R.M., R. Naithani, and B. Surve. 2007. Organosulfur compounds in cancer chemoprevention. *Mini Rev Med Chem*. 7:827-838.

Mosmann, T. 1983. Rapid colorimetric assay for cellular growth and survival: application to proliferation and cytotoxicity assays. *J Immunol Methods*. 65:55-63.

Moya-Camarena, S.Y., and Q. Jiang. 2012. The role of vitamin E forms in cancer prevention and therapy - studies in human intervention trials and animal models. N.a.C.N.Y. Springer, editor. 323-354.

Mullen, T.D., R.W. Jenkins, C.J. Clarke, J. Bielawski, Y.A. Hannun, and L.M. Obeid. 2011. Ceramide synthase-dependent ceramide generation and programmed cell death: involvement of salvage pathway in regulating postmitochondrial events. *J Biol Chem*. 286:15929-15942.

Murakami, A., H. Ashida, and J. Terao. 2008. Multitargeted cancer prevention by quercetin. *Cancer Lett*. 269:315-325.

Newmark, H.L., M.T. Huang, and B.S. Reddy. 2006. Mixed tocopherols inhibit azoxymethane-induced aberrant crypt foci in rats. *Nutr Cancer*. 56:82-85.

Ohanian, J., and V. Ohanian. 2001. Sphingolipids in mammalian cell signalling. *Cell Mol Life Sci*. 58:2053-2068.

Ohrvall, M., G. Sundlof, and B. Vessby. 1996. Gamma, but not alpha, tocopherol levels in serum are reduced in coronary heart disease patients. *J Intern Med*. 239:111-117.

Ohta, H., E.A. Sweeney, A. Masamune, Y. Yatomi, S. Hakomori, and Y. Igarashi. 1995. Induction of apoptosis by sphingosine in human leukemic HL-60 cells: a possible endogenous modulator of apoptotic DNA fragmentation occurring during phorbol ester-induced differentiation. *Cancer Res*. 55:691-697.

Okamoto, T. 2005. Safety of quercetin for clinical application (Review). *Int J Mol Med*. 16:275-278.

Okazaki, T., A. Bielawska, N. Domae, R.M. Bell, and Y.A. Hannun. 1994. Characteristics and partial purification of a novel cytosolic, magnesium-independent, neutral sphingomyelinase activated in the early signal transduction of 1 alpha,25-dihydroxyvitamin D3-induced HL-60 cell differentiation. *J Biol Chem*. 269:4070-4077.

Oslowski, C.M., and F. Urano. 2011. Measuring ER stress and the unfolded protein response using mammalian tissue culture system. *Methods Enzymol*. 490:71-92.

Packer, L., S.U. Weber, and G. Rimbach. 2001. Molecular aspects of alpha-tocotrienol antioxidant action and cell signalling. *J Nutr*. 131:369s-373s.

Park, S.K., B.G. Sanders, and K. Kline. 2010. Tocotrienols induce apoptosis in breast cancer cell lines via an endoplasmic reticulum stress-dependent increase in extrinsic death receptor signaling. *Breast Cancer Res Treat*. 124:361-375.

Parker, R.A., B.C. Pearce, R.W. Clark, D.A. Gordon, and J.J. Wright. 1993. Tocotrienols regulate cholesterol production in mammalian cells by post-transcriptional suppression of 3-hydroxy-3-methylglutaryl-coenzyme A reductase. *J Biol Chem*. 268:11230-11238.

Pewzner-Jung, Y., S. Ben-Dor, and A.H. Futerman. 2006. When do Lasses (longevity assurance genes) become CerS (ceramide synthases)?: Insights into the regulation of ceramide synthesis. *J Biol Chem*. 281:25001-25005.

Pianetti, S., S. Guo, K.T. Kavanagh, and G.E. Sonenshein. 2002. Green tea polyphenol epigallocatechin-3 gallate inhibits Her-2/neu signaling, proliferation, and transformed phenotype of breast cancer cells. *Cancer Res*. 62:652-655.

Plummer, S.M., K.A. Holloway, M.M. Manson, R.J. Munks, A. Kaptein, S. Farrow, and L. Howells. 1999. Inhibition of cyclo-oxygenase 2 expression in colon cells by the chemopreventive agent curcumin involves inhibition of NF-kappaB activation via the NIK/IKK signalling complex. *Oncogene*. 18:6013-6020.

Pyne, S., and N.J. Pyne. 2000. Sphingosine 1-phosphate signalling in mammalian cells. *Biochem J*. 349:385-402.

Radin, N.S. 2001. Killing cancer cells by poly-drug elevation of ceramide levels: a hypothesis whose time has come? *In* Eur J Biochem. Vol. 268, Germany. 193-204.

Rahmaniyan, M., R.W. Curley, Jr., L.M. Obeid, Y.A. Hannun, and J.M. Kraveka. 2011. Identification of dihydroceramide desaturase as a direct in vitro target for fenretinide. *J Biol Chem*. 286:24754-24764.

Riebeling, C., J.C. Allegood, E. Wang, A.H. Merrill, Jr., and A.H. Futerman. 2003. Two mammalian longevity assurance gene (LAG1) family members, trh1 and trh4, regulate dihydroceramide synthesis using different fatty acyl-CoA donors. *J Biol Chem*. 278:43452-43459.

Rimando, A.M., and N. Suh. 2008. Biological/chemopreventive activity of stilbenes and their effect on colon cancer. *Planta Med*. 74:1635-1643.

Ruangsiriluk, W., S.E. Grosskurth, D. Ziemek, M. Kuhn, S.G. des Etages, and O.L. Francone. 2012. Silencing of enzymes involved in ceramide biosynthesis causes distinct global alterations of lipid homeostasis and gene expression. *J Lipid Res*. 53:1459-1471.

Ryland, L.K., T.E. Fox, X. Liu, T.P. Loughran, and M. Kester. 2011. Dysregulation of sphingolipid metabolism in cancer. *Cancer Biol Ther*. 11:138-149.

Sano, R., and J.C. Reed. 2013. ER stress-induced cell death mechanisms. *Biochim Biophys Acta*. 1833:3460-3470.

Scarlatti, F., C. Bauvy, A. Ventruti, G. Sala, F. Cluzeaud, A. Vandewalle, R. Ghidoni, and P. Codogno. 2004. Ceramide-mediated macroautophagy involves inhibition of protein kinase B and up-regulation of beclin 1. *J Biol Chem*. 279:18384-18391.

Schiffmann, S., J. Sandner, K. Birod, I. Wobst, C. Angioni, E. Ruckhaberle, M. Kaufmann, H. Ackermann, J. Lotsch, H. Schmidt, G. Geisslinger, and S. Grosch. 2009a. Ceramide synthases and ceramide levels are increased in breast cancer tissue. *Carcinogenesis*. 30:745-752.

Schiffmann, S., J. Sandner, R. Schmidt, K. Birod, I. Wobst, H. Schmidt, C. Angioni, G. Geisslinger, and S. Grosch. 2009b. The selective COX-2 inhibitor celecoxib modulates sphingolipid synthesis. *J Lipid Res*. 50:32-40.

Senkal, C.E., S. Ponnusamy, J. Bielawski, Y.A. Hannun, and B. Ogretmen. 2010. Antiapoptotic roles of ceramide-synthase-6-generated C16-ceramide via selective regulation of the ATF6/CHOP arm of ER-stress-response pathways. *Faseb j*. 24:296-308.

Sentelle, R.D., C.E. Senkal, W. Jiang, S. Ponnusamy, S. Gencer, S.P. Selvam, V.K. Ramshesh, Y.K. Peterson, J.J. Lemasters, Z.M. Szulc, J. Bielawski, and B. Ogretmen. 2012. Ceramide targets autophagosomes to mitochondria and induces lethal mitophagy. *Nat Chem Biol*. 8:831-838.

Shankar, S., and R.K. Srivastava. 2007. Involvement of Bcl-2 family members, phosphatidylinositol 3'-kinase/AKT and mitochondrial p53 in curcumin (diferulolylmethane)-induced apoptosis in prostate cancer. *Int J Oncol*. 30:905-918.

Shehzad, A., F. Wahid, and Y.S. Lee. 2010. Curcumin in cancer chemoprevention: molecular targets, pharmacokinetics, bioavailability, and clinical trials. *Arch Pharm (Weinheim)*. 343:489-499.

Shibata, A., K. Nakagawa, P. Sookwong, T. Tsuduki, S. Oikawa, and T. Miyazawa. 2009. delta-Tocotrienol suppresses VEGF induced angiogenesis whereas alpha-tocopherol does not. *J Agric Food Chem*. 57:8696-8704.

Siddique, M.M., Y. Li, L. Wang, J. Ching, M. Mal, O. Ilkayeva, Y.J. Wu, B.H. Bay, and S.A. Summers. 2013. Ablation of dihydroceramide desaturase 1, a therapeutic target for the treatment of metabolic diseases, simultaneously stimulates anabolic and catabolic signaling. *Mol Cell Biol*. 33:2353-2369.

Siegel, R.L., K.D. Miller, and A. Jemal. 2015. Cancer statistics, 2015. *CA Cancer J Clin*. 65:5-29.

Signorelli, P., J.M. Munoz-Olaya, V. Gagliostro, J. Casas, R. Ghidoni, and G. Fabrias. 2009. Dihydroceramide intracellular increase in response to resveratrol treatment mediates autophagy in gastric cancer cells. *Cancer Lett*. 282:238-243.

Siskind, L.J. 2005. Mitochondrial ceramide and the induction of apoptosis. *J Bioenerg Biomembr*. 37:143-153.

Sjoholm, A., P.O. Berggren, and R.V. Cooney. 2000. gamma-tocopherol partially protects insulin-secreting cells against functional inhibition by nitric oxide. *Biochem Biophys Res Commun*. 277:334-340.

Slover, H.T. 1971. Tocopherols in foods and fats. *Lipids*. 6:291-296.

Smolarek, A.K., J.Y. So, B. Burgess, A.N. Kong, K. Reuhl, Y. Lin, W.J. Shih, G. Li, M.J. Lee, Y.K. Chen, C.S. Yang, and N. Suh. 2012. Dietary administration of delta- and gamma-tocopherol inhibits tumorigenesis in the animal model of estrogen receptor-positive, but not HER-2 breast cancer. *Cancer Prev Res (Phila)*. 5:1310-1320.

Snider, A.J., K.A. Orr Gandy, and L.M. Obeid. 2010. Sphingosine kinase: Role in regulation of bioactive sphingolipid mediators in inflammation. *Biochimie*. 92:707-715.

Solomon, J.C., K. Sharma, L.X. Wei, T. Fujita, and Y.F. Shi. 2003. A novel role for sphingolipid intermediates in activation-induced cell death in T cells. *Cell Death Differ*. 10:193-202.

Sontag, T.J., and R.S. Parker. 2002. Cytochrome P450 omega-hydroxylase pathway of tocopherol catabolism. Novel mechanism of regulation of vitamin E status. *J Biol Chem*. 277:25290-25296.

Spiegel, S., and A.H. Merrill, Jr. 1996. Sphingolipid metabolism and cell growth regulation. *Faseb j*. 10:1388-1397.

Steinmetz, K.A., and J.D. Potter. 1996. Vegetables, fruit, and cancer prevention: a review. *J Am Diet Assoc*. 96:1027-1039.

Stiban, J., D. Fistere, and M. Colombini. 2006. Dihydroceramide hinders ceramide channel formation: Implications on apoptosis. *Apoptosis*. 11:773-780.

Suh, N., S. Paul, H.J. Lee, Y. Ji, M.J. Lee, C.S. Yang, B.S. Reddy, and H.L. Newmark. 2007. Mixed tocopherols inhibit N-methyl-N-nitrosourea-induced mammary tumor growth in rats. *Nutr Cancer*. 59:76-81.

Sun, Y., T. Fox, G. Adhikary, M. Kester, and E. Pearlman. 2008. Inhibition of corneal inflammation by liposomal delivery of short-chain, C-6 ceramide. *J Leukoc Biol*. 83:1512-1521.

Surh, Y.J. 2003. Cancer chemoprevention with dietary phytochemicals. *Nat Rev Cancer*. 3:768-780.

Swanson, J.E., R.N. Ben, G.W. Burton, and R.S. Parker. 1999. Urinary excretion of 2,7, 8-trimethyl-2-(beta-carboxyethyl)-6-hydroxychroman is a major route of elimination of gamma-tocopherol in humans. *J Lipid Res*. 40:665-671.

Takahashi, S., K. Takeshita, A. Seeni, S. Sugiura, M. Tang, S.Y. Sato, H. Kuriyama, M. Nakadate, K. Abe, Y. Maeno, M. Nagao, and T. Shirai. 2009. Suppression of prostate cancer in a transgenic rat model via gamma-tocopherol activation of caspase signaling. *Prostate*. 69:644-651.

Tan, H.L., J.M. Thomas-Ahner, E.M. Grainger, L. Wan, D.M. Francis, S.J. Schwartz, J.W. Erdman, Jr., and S.K. Clinton. 2010. Tomato-based food products for prostate cancer prevention: what have we learned? *Cancer Metastasis Rev*. 29:553-568.

Tang, L., G. Li, L. Song, and Y. Zhang. 2006. The principal urinary metabolites of dietary isothiocyanates, N-acetylcysteine conjugates, elicit the same anti-proliferative response as their parent compounds in human bladder cancer cells. *Anticancer Drugs*. 17:297-305.

Tasinato, A., D. Boscoboinik, G.M. Bartoli, P. Maroni, and A. Azzi. 1995. d-alpha-tocopherol inhibition of vascular smooth muscle cell proliferation occurs at physiological concentrations, correlates with protein kinase C inhibition, and is independent of its antioxidant properties. *Proc Natl Acad Sci U S A*. 92:12190-12194.

Terashima, K., T. Shimamura, M. Tanabayashi, l.M. Aqui, J. Akinniyi, and M. Niwa. 1997. Constituents of the seeds of Garcinia kola: Two new antioxidants, Garcinoic acid and Garcinal. *Heterocycles*. 45:1559-1566.

Terashima, K., Y. Takaya, and M. Niwa. 2002. Powerful antioxidative agents based on garcinoic acid from Garcinia kola. *Bioorg Med Chem*. 10:1619-1625.

Ternes, P., S. Franke, U. Zahringer, P. Sperling, and E. Heinz. 2002. Identification and characterization of a sphingolipid delta 4-desaturase family. *J Biol Chem*. 277:25512-25518.

Thudichum, J.L.W. 1884. A Treatise on the chemical constitution of brain. Bailliere, Tindall and Cox, London.

Traber, M.G. 2007. Vitamin E regulatory mechanisms. *Annu Rev Nutr*. 27:347-362.

Traber, M.G., and J.F. Stevens. 2011. Vitamins C and E: beneficial effects from a mechanistic perspective. *Free Radic Biol Med*. 51:1000-1013.

Triola, G., G. Fabrias, J. Casas, and A. Llebaria. 2003. Synthesis of cyclopropene analogues of ceramide and their effect on dihydroceramide desaturase. *J Org Chem*. 68:9924-9932.

Triola, G., G. Fabrias, M. Dragusin, L. Niederhausen, R. Broere, A. Llebaria, and G. van Echten-Deckert. 2004. Specificity of the dihydroceramide desaturase inhibitor N-[(1R,2S)-2-hydroxy-1-hydroxymethyl-2-(2-tridecyl-1-cyclopropenyl)ethyl]octanami de (GT11) in primary cultured cerebellar neurons. *Mol Pharmacol*. 66:1671-1678.

Vagni, S., F. Saccone, L. Pinotti, and A. Baldi. 2011. Vitamin E Bioavailability: Past and Present Insights. *Food and Nutrition Sciences*. 2:1088-1096.

Vane, J.R. 1976. Prostaglandins as mediators of inflammation. *Adv Prostaglandin Thromboxane Res*. 2:791-801.

Venkataraman, K., C. Riebeling, J. Bodennec, H. Riezman, J.C. Allegood, M.C. Sullards, A.H. Merrill, Jr., and A.H. Futerman. 2002. Upstream of growth and differentiation factor 1 (uog1), a mammalian homolog of the yeast longevity assurance gene 1 (LAG1), regulates N-stearoyl-sphinganine (C18-(dihydro)ceramide) synthesis in a fumonisin B1-independent manner in mammalian cells. *J Biol Chem*. 277:35642-35649.

Wadsworth, J.M., D.J. Clarke, S.A. McMahon, J.P. Lowther, A.E. Beattie, P.R. Langridge-Smith, H.B. Broughton, T.M. Dunn, J.H. Naismith, and D.J. Campopiano. 2013. The chemical basis of serine palmitoyltransferase inhibition by myriocin. *J Am Chem Soc*. 135:14276-14285.

Wan Nazaimoon, W.M., and B.A. Khalid. 2002. Tocotrienols-rich diet decreases advanced glycosylation end-products in non-diabetic rats and improves glycemic control in streptozotocin-induced diabetic rats. *Malays J Pathol*. 24:77-82.

Wang, D., and R.N. Dubois. 2010. Eicosanoids and cancer. *Nat Rev Cancer*. 10:181-193.

Wang, H., A.G. Charles, A.J. Frankel, and M.C. Cabot. 2003. Increasing intracellular ceramide: an approach that enhances the cytotoxic response in prostate cancer cells. *Urology*. 61:1047-1052.

Wang, H., B.J. Maurer, C.P. Reynolds, and M.C. Cabot. 2001. N-(4-hydroxyphenyl)retinamide elevates ceramide in neuroblastoma cell lines by coordinate activation of serine palmitoyltransferase and ceramide synthase. *Cancer Res*. 61:5102-5105.

Wang, Y., and Q. Jiang. 2013. gamma-Tocotrienol inhibits lipopolysaccharide-induced interlukin-6 and granulocyte colony-stimulating factor by suppressing C/EBPbeta and NF-kappaB in macrophages. *J Nutr Biochem*. 24:1146-1152.

Wang, Y., N.Y. Park, Y. Jang, A. Ma, and Q. Jiang. 2015. Vitamin E gamma-Tocotrienol Inhibits Cytokine-Stimulated NF-kappaB Activation by Induction of Anti-Inflammatory A20 via Stress Adaptive Response Due to Modulation of Sphingolipids. *J Immunol*. 195:126-133.

Watson, P., and D.J. Stephens. 2005. ER-to-Golgi transport: form and formation of vesicular and tubular carriers. *Biochim Biophys Acta*. 1744:304-315.

Watts, J.D., M. Gu, S.D. Patterson, R. Aebersold, and A.J. Polverino. 1999. On the complexities of ceramide changes in cells undergoing apoptosis: lack of evidence for a second messenger function in apoptotic induction. *Cell Death Differ*. 6:105-114.

White-Gilbertson, S., T. Mullen, C. Senkal, P. Lu, B. Ogretmen, L. Obeid, and C. Voelkel-Johnson. 2009. Ceramide synthase 6 modulates TRAIL sensitivity and nuclear translocation of active caspase-3 in colon cancer cells. *Oncogene*. 28:1132-1141.

Wilson, E., M.C. Olcott, R.M. Bell, A.H. Merrill, Jr., and J.D. Lambeth. 1986. Inhibition of the oxidative burst in human neutrophils by sphingoid long-chain bases. Role of protein kinase C in activation of the burst. *J Biol Chem*. 261:12616-12623.

Wong, R.S., and A.K. Radhakrishnan. 2012. Tocotrienol research: past into present. *Nutr Rev*. 70:483-490.

Woodcock, J. 2006. Sphingosine and ceramide signalling in apoptosis. *In* IUBMB Life. Vol. 58, England. 462-466.

Xu, W.L., J.R. Liu, H.K. Liu, G.Y. Qi, X.R. Sun, W.G. Sun, and B.Q. Chen. 2009. Inhibition of proliferation and induction of apoptosis by gamma-tocotrienol in human colon carcinoma HT-29 cells. *Nutrition*. 25:555-566.

Yang, F., H.S. Oz, S. Barve, W.J. de Villiers, C.J. McClain, and G.W. Varilek. 2001. The green tea polyphenol (-)-epigallocatechin-3-gallate blocks nuclear factor-kappa B activation by inhibiting I kappa B kinase activity in the intestinal epithelial cell line IEC-6. *Mol Pharmacol*. 60:528-533.

Yap, W.N., N. Zaiden, S.Y. Luk, D.T. Lee, M.T. Ling, Y.C. Wong, and Y.L. Yap. 2010. In vivo evidence of gamma-tocotrienol as a chemosensitizer in the treatment of hormone-refractory prostate cancer. *Pharmacology*. 85:248-258.

Yu, R., W. Lei, S. Mandlekar, M.J. Weber, C.J. Der, J. Wu, and A.N. Kong. 1999a. Role of a mitogen-activated protein kinase pathway in the induction of phase II detoxifying enzymes by chemicals. *J Biol Chem*. 274:27545-27552.

Yu, W., L. Jia, S.K. Park, J. Li, A. Gopalan, M. Simmons-Menchaca, B.G. Sanders, and K. Kline. 2009. Anticancer actions of natural and synthetic vitamin E forms: RRR-alpha-tocopherol blocks the anticancer actions of gamma-tocopherol. *Mol Nutr Food Res*. 53:1573-1581.

Yu, W., L. Jia, P. Wang, K.A. Lawson, M. Simmons-Menchaca, S.K. Park, L. Sun, B.G. Sanders, and K. Kline. 2008a. In vitro and in vivo evaluation of anticancer actions of natural and synthetic vitamin E forms. *Mol Nutr Food Res*. 52:447-456.

Yu, W., S.K. Park, L. Jia, R. Tiwary, W.W. Scott, J. Li, P. Wang, M. Simmons-Menchaca, B.G. Sanders, and K. Kline. 2008b. RRR-gamma-tocopherol induces human breast cancer cells to undergo apoptosis via death receptor 5 (DR5)-mediated apoptotic signaling. *Cancer Lett*. 259:165-176.

Yu, W., M. Simmons-Menchaca, A. Gapor, B.G. Sanders, and K. Kline. 1999b. Induction of apoptosis in human breast cancer cells by tocopherols and tocotrienols. *Nutr Cancer*. 33:26-32.

Zhang, W., and H.T. Liu. 2002. MAPK signal pathways in the regulation of cell proliferation in mammalian cells. *Cell Res*. 12:9-18.

Zhang, Y., P. Mattjus, P.C. Schmid, Z. Dong, S. Zhong, W.Y. Ma, R.E. Brown, A.M. Bode, and H.H. Schmid. 2001. Involvement of the acid sphingomyelinase pathway in uva-induced apoptosis. *J Biol Chem*. 276:11775-11782.

Zheng, W., J. Kollmeyer, H. Symolon, A. Momin, E. Munter, E. Wang, S. Kelly, J.C. Allegood, Y. Liu, Q. Peng, H. Ramaraju, M.C. Sullards, M. Cabot, and A.H. Merrill, Jr. 2006. Ceramides and other bioactive sphingolipid backbones in health and disease: lipidomic analysis, metabolism and roles in membrane structure, dynamics, signaling and autophagy. *Biochim Biophys Acta*. 1758:1864-1884.

VITA

VITA

Yumi Jang

Graduate School, Purdue University

Education

- Ph.D., Nutrition Science, 2015, Purdue University, West Lafayette, Indiana, USA
- M.S., Food and Nutrition, 2009, Seoul National University, Seoul, Republic of Korea
- B.S., Food and Nutrition, 2007, Pusan National University, Pusan, Republic of Korea

Awards and Honors

- Purdue Research Foundation (PRF) Fellowship 2014-2015
- Travel Award from Cancer Research Center (2014)
- Poster Presentation Award (2014) at Health and Disease: Science, Culture and Policy Research Poster Session at Purdue University
- Poster Presentation Honorable Mention (2014) at Interdepartmental Nutrition Program (INP) Poster Session at Purdue University
- Poster Presentation Award (2013) at Chronic Disease Research Poster Session sponsored by the College of Health and Human Sciences at Purdue University

Teaching Experience

- Fall 2013: Teaching Assistant for course NUTR43800, Micronutrient Metabolism in Human Health and Disease at Purdue University
- 2007-2008: Teaching Assistant for courses of Biochemistry and Nutrition at Seoul National University

Research Experience

- 2010-2015 Research Assistant in Dr. Qing Jiang's Lab at Purdue University
- 2007-2010 Research Assistant in Dr. Young Hye Kwon's Lab at Seoul National University

PUBLICATIONS

PUBLICATIONS

1. **Yumi Jang**, Agnetha Rostgaard-Hansen, Jianjie Huang, and Qing Jiang. (2015) 13'-Carboxychromanols, long-chain vitamin E metabolites, induced apoptosis and autophagy by modulating sphingolipid metabolism in different types of cancer cells. (in preparation)
2. **Yumi Jang**, Xiayu Rao, and Qing Jiang. (2015) Sphingolipid metabolism is the initial primary target of gamma-tocotrienol and plays a role in cell death induction. (in preparation)
3. **Yumi Jang** and Qing Jiang. (2015) Targeting sphingolipid metabolism for the anticancer effects of various chemopreventive compounds. (in preparation)
4. Yun Wang, Na Young Park, **Yumi Jang**, Averil Ma, and Qing Jiang. (2015) Vitamin E γ-tocotrienol inhibits cytokine-stimulated NF-κB activation by induction of anti-inflammatory A20 via stress adaptive response due to modulation of sphingolipids. *The Journal of Immunology*, 195:126-133
5. Qing Jiang, Ziying Jiang, Yava Jones-Hall, **Yumi Jang**, Paul W. Snyder, Carol Bain, Jianjie Huang, Amber Jannasch, Bruce Cooper, Yun Wang, and Michelle Moreland. (2013) Gamma-tocopherol attenuates moderate but not severe colitis and suppresses moderate colitis-promoted colon tumorigenesis in mice. *Free Radical Biology and Medicine*, 65:1069-1077
6. Archana Gopalan, Weiping Yu, Qing Jiang, **Yumi Jang**, Bob G. Sanders and Kimberly Kline. (2012) Involvement of de novo ceramide synthesis in gamma-tocopherol and gamma-tocotrienol induced apoptosis in human breast cancer cells. *Molecular Nutrition & Food Research*, 56:1803-1811
7. Youn-Jin Park, Je Won Ko, **Yumi Jang** and Young Hye Kwon. (2012) Activation of AMP-activated protein kinase alleviates homocysteine-mediated neurotoxicity in SH-SY5Y cells. *Neurochemical Research*, 38:1561-1571
8. Juhae Kim, Youn-jin Park, **Yumi Jang**, and Young Hye Kwon. (2011) AMPK activation inhibits apoptosis and tau hyperphosphorylation mediated by palmitate in SH-SY5Y cells. *Brain Research*, 1418:42-51
9. Youn-Jin Park, **Yu-mi Jang** and Young Hye Kwon. (2009) Isoflavones prevent endoplasmic reticulum stress-mediated neuronal degeneration by inhibiting tau hyperphosphorylation in SH-SY5Y cells. *Journal of Medicinal Food,* 12:528-535
10. Hyang-ki Cho, Jin-young Lee, **Yu-mi Jang** and Young Hye Kwon. (2008) Involvement of endoplasmic reticulum stress in palmitate-induced apoptosis in HepG2 cells. *Official Journal of Korean Society of Toxicology,* 24:129-135

11. Hyun-Jung Kim, **Yu-mi Jang**, Harriet Kim and Young Hye Kwon. (2007) Apoptotic effect of IP6 was not enhanced by co-treatment with myo-inositol in prostate carcinoma PC3 cells, *Nutrition Research and Practice*, 1:195-199

Presentations:

1. **Yumi Jang** and Qing Jiang. (2014) Lipidomic analysis reveals that gamma-tocotrienol exerts anticancer effects by inhibition of dihydroceramide desaturase and activation of sphingomyelin hydrolysis. *Experimental Biology meeting 2014*, San Diego, CA
2. **Yumi Jang**, Soo Yee Kuah and Qing Jiang. (2013) 13'-Carboxychromanol, a long-chain metabolite of δ-tocopherol, has potent anti-cancer effects by interrupting de novo sphingolipid synthesis in human cancer cells. *Experimental Biology meeting 2013*, Boston, MA
3. **Yumi Jang**, Xiayu Rao and Qing Jiang. (2012) Vitamin E forms and 13'-carboxychromanol, a long-chain metabolite of δ-tocopherol, induce cell death by interrupting de novo sphingolipid synthesis in human cancer cells. *AACR annual meeting 2012*, Chicago, IL